2018

Human metabolic allometry from basal to maximal ambulatory states, including load carriage and its distribution

Heather Marie Bowes
University of Wollongong

HUMAN METABOLIC ALLOMETRY FROM BASAL TO MAXIMAL AMBULATORY STATES, INCLUDING LOAD CARRIAGE AND ITS DISTRIBUTION

A thesis submitted in fulfilment of the requirements for the award of the degree

DOCTOR OF PHILOSOPHY

from

UNIVERSITY OF WOLLONGONG

by

HEATHER MARIE BOWES, BSc. (Hons), MRes.

SCHOOL OF MEDICINE

2018

CERTIFICATION

I, Heather M. Bowes, declare that this thesis, submitted in fulfilment of the requirements for the award of Doctor of Philosophy, in the School of Medicine, University of Wollongong, is wholly my own work unless otherwise referenced or acknowledged. The document has not been submitted for qualifications at any other academic institution.

_____

Heather M. Bowes

ABSTRACT

Whole-body metabolic rate is strongly linked with body size, as it is primarily determined by both the number of cells within the body and their tissue-specific metabolic rates. For these reasons alone there will always be some inter-individual variations in metabolism, at any given metabolic intensity. While variations in body mass can explain the majority of these differences between individuals, it still remains difficult to remove the effect of body mass from metabolic data, as the relationship between both variables does not scale by a one-to-one ratio. Accordingly, the ubiquitous mass-normalisation approach is ineffective at this task ($mL.kg^{-1}.min^{-1}$). Therefore, an alternative scaling method was required so that metabolic rate can be both described and analysed with minimal error.

In animals, basal metabolic rate scales by a non-linear, allometric regression against body mass, and can be described using the body-mass exponent, $mass_{body}^{0.67}$. However, in humans, the nature[1] of the scaling relationship remains unconfirmed, with both linear (first-order polynomial) and non-linear (allometric) scaling approaches used by researchers. An often overlooked issue with this situation is that the predictive error between both models increases as the mass range widens. Accordingly, the primary aim within this series of investigation was to determine which scaling model was more appropriate to describe the relationship between metabolic rate and body mass in humans.

To achieve this aim, a large sample of men were recruited across a broad mass range (N=72; 81.2 kg: 56.0-117.1 kg), who were controlled for morphological and physiological variables that might influence metabolic rate, beyond what would be expected with a change in body mass. To evaluate the effect of a change in body mass and metabolic intensity, participants completed 18 separate trials within five research phases (Chapters 2-6). Throughout those trials, the scaling relationship was evaluated across the physiological range of bipedal metabolic intensity (basal [Chapter 2] through to peak exercise [running: Chapter 3]), also with the addition of ambulatory

[1] The term nature has been solely used to refer to the shape, or steepness, of the scaling relationship between whole-body metabolic rate and body mass, without indicating whether it is linear or nonlinear.

gradient (±5%: Chapter 4) and load carriage (Chapters 5 and 6). Participants acted as their own controls throughout those trials, wearing standardised clothing (t-shirt, combat trousers and their own sports shoes) and foot masses (500 g per foot). Oxygen consumption was measured continuously using open-circuit indirect respirometry. Both linear and non-linear regression models were applied to those datasets and systematically analysed to determine which was more appropriate during each metabolic intensity, and whether or not there was an effect of intensity on that relationship.

The first experiment (Chapter 2) was aimed at determining the shape of the scaling model during basal and standing (resting) conditions. Due to the strictly-controlled nature of basal testing, the scaling relationship derived during this state could be used as a baseline, from which the effect of all other stimuli could be compared. Oxygen consumption and deep-body temperature data were collected during a 60-min period where participants lay motionless in a low-stimulus and normothermic environment (~23°C; ~50% relative humidity). Those data were used to approximate basal metabolic rate and to evaluate the efficacy of adjusting those data to a common deep-body temperature before analyses (36.2°C). After the basal stage, participants completed a 10-min standing (rest) stage, so that a change of posture on the scaling model could be evaluated.

During both metabolic intensities, it was more appropriate to scale metabolic data (and oxygen consumption) using a non-linear, allometric regression. The mass exponent derived for those basal metabolic data (kJ.day-1) was significantly smaller than the value applied to animal data within comparative physiology (humans: $mass_{body}^{0.55}$; animals: $mass_{body}^{0.67}$; $P<0.05$). And, unlike animal data, normalising those human data to a common deep-body temperature did not modify that body-mass exponent ($P>0.05$). Accordingly, humans-specific basal metabolic data should not be compared using the animal value of $mass_{body}^{0.67}$, however it is possible that this value is still more appropriate when scaling metabolic data across animal species.

The change in posture from a supine (basal) to standing condition significantly increased mean oxygen consumption (supine: 0.27 $L.min^{-1}$ [$\pm<0.01$]; standing: 0.33

$L.min^{-1}$ [$\pm < 0.01$]; $P < 0.05$]). However, that increase in metabolic rate did not result in any change to the body-mass exponent ($P > 0.05$). Therefore, the mass exponent remained constant during the resting states. This was most likely because standing is relatively passive, with the body's mass being supported by the skeletal structure. Accordingly, both values could be scaled against the basal oxygen consumption exponent of $mass_{body}^{0.54}$. That value was selected as it represented the scaling relationship least influenced by additional variables and data transformations.

The next two experimental phases (Chapter 3 and 4) were designed to determine whether or not there was an interaction effect between the scaling model and metabolic intensity. For these trials, participants attended the laboratory over three separate days, with the start time matched ± 1 h. During each visit, participants completed one of three, 15-min treadmill walks (4.8 $km.h^{-1}$): level, uphill (5%), downhill (-5%). After each walking trial, participants then completed a treadmill ramp test (wearing their own sports clothing). In this way, by the third laboratory visit, participants were familiarised to complete the peak exercise test. During exercise, non-linear scaling remained the more appropriate model to describe the relationship between oxygen consumption and body mass. All four exercise states scaled by a significantly larger mass exponent than observed during rest ($P < 0.05$). However, no difference in the mass exponent was found among those exercise intensities ($P > 0.05$). Accordingly, during bipedal states where the body supports its own mass, the relationship between oxygen consumption and body mass could be described using a single mass exponent. The peak-exercise exponent was selected for this, as it was a relative state across all participants and represented the maximum likely scaling exponent for humans.

The final two experimental phases were aimed to extend the steady-state walking outcome to loaded states. During these trials, loads were individually carried on the torso (25-kg weight vest: Chapter 5), head (1.38-kg helmet: Chapter 6), hands (2-kg wrist weights [each arm]: Chapter 6) and feet (2 kg each foot: Chapter 6). These trials were conducted during the same days that participants attended at the laboratory for the experimental themes investigated in Chapters 3 and 4. So, to minimised the potential effect of repeated testing on the oxygen consumption data collected, trial

orders were balanced using a Latin Square Design. Again, no effect of ambulatory gradient was observed between the loaded body-mass exponents.($P > 0.05$). However, during both torso and foot loading conditions, the body-mass exponent significantly decreased compared with the unloaded trials ($P < 0.05$). This outcome was due to the body-mass response in nett oxygen consumption during fixed-load carriage. Thus, when scaling fixed-mass loaded oxygen consumption to body mass, if that load causes a sufficient physiological stain, it will likely result in a modified scaling exponent.

Nevertheless, it was possible to remove that effect of load carriage in all but two conditions by scaling oxygen consumption data against the total mass carried (body mass plus all external loads worn), rather than the body mass alone. The derived mass exponents for these states were statistically similar to those observed during the same within-gradient unloaded test ($P > 0.05$). The only exceptions to this outcome were during head- and foot-loaded downhill walking, whereby walking efficiency increased with body mass, significantly reducing the total-mass exponent ($P < 0.05$). Regardless of the result from those two conditions, a consistent relationship was otherwise demonstrated between a change in total mass (growth or external load) and oxygen consumption, for, when scaling against the total mass carried, both unloaded and loaded trials could be described using the same scaling model. Accordingly, total mass was considered the more appropriate morphological variable to scale against during steady-state walking.

Consequently, from this series of investigations, non-linear regression was the more appropriate scaling model to describe the relationship between oxygen consumption (metabolic rate) and body mass in humans. Throughout the physiological range of resting and bipedal metabolic intensities, four unique scaling exponents were established for that non-linear model: $mass_{body}^{0.54}$ (rest), $mass_{total}^{0.66}$ (head- and foot-loaded downhill walking), $mass_{total}^{0.80}$ (unloaded and all other loaded steady-state exercise, $mass_{body}^{0.80}$ (peak exercise).

ACKNOWLEDGEMENTS

Firstly, I'd like to express my sincerest gratitude to my supervisor, Nigel Taylor. I am honoured to have had the privilege to study under him for the past 4.5 years. The level of support and guidance he provided during that time has been truly exceptional, and only second to the warm environment that he fosters within the research team. Thank you for sharing your infectious passion for research (and good humour) with all of us. I would also like to extend my thanks to both Catriona Burdon and Greg Peoples for their additional guidance and encouragement, particularly throughout this last year.

A big thank you to past and present friends and colleagues here in Wollongong, you have made my time here feel like a home away from home and kept a smile on my face. I am lucky to know you all.

A special thank you to my participants, who spent many hours covered in velcro in the laboratory while walking towards a white square. Your patience and humour with the process was fantastic. I cannot thank you enough.

Finally, I'd like to thank my friends and family for their patience and support while I have been completing my studies, so far away from home. I am most grateful for the unconditional support I have received from my wife, Tiff. You have forever changed my life for the better, I would not be here without you.

TABLE OF CONTENTS

ABSTRACT . . . . . *ii*

ACKNOWLEDGEMENTS . . . . . *vi*

TABLE OF CONTENTS . . . . . *vii*

LIST OF FIGURES . . . . . *xiv*

LIST OF TABLES . . . . . **xviii**

CHAPTER 1: INTRODUCTION **1**

1.1 CONCEPTUAL INTRODUCTION 1

1.2 REFERENCES 11

CHAPTER 2: SCALING OXYGEN CONSUMPTION DURING BASAL AND RESTING STATES IN ADULT MALES **16**

2.1 INTRODUCTION 16

2.1.1 Methods for quantifying basal metabolic rate 17

2.1.1.1 Direct calorimetry 17

2.1.1.2 Respirometry 19

2.1.2 Scaling whole-body, basal metabolic rate 21

2.1.2.1 Linear scaling 24

2.1.2.2 Non-linear scaling 26

2.1.3 Postural changes and energy expenditure 30

2.1.4 Aims and hypotheses 32

2.2 METHODS 33

2.2.1 Considerations for subject recruitment 33

2.2.1.1 Metabolic and compositional changes with age and gender 33

2.2.1.2 Controlling for variations in body adiposity 36

2.2.1.3 Determining the body-mass range and sample size . .37

2.2.2 Subjects 40
2.2.3 Procedural overview 40
2.2.3.1 Measuring basal and standing oxygen consumption . 44
2.2.4 Experimental standardisation 44
2.2.5 Experimental measurements 45
2.2.5.1 Oxygen consumption 45
2.2.5.2 Deep-body temperature 46
2.2.5.3 Cardiac frequency 48
2.2.5.4 Anthropometric measures 49
Height-adjusted adiposity and body mass 49
2.2.6 Design and analysis 53
2.2.6.1 Experimental design 53
2.2.6.2 Data analysis 55
Determining the sample homogeneity 55
Determining the shape of the scaling models 55
Comparing differences between scaling models 60
Evaluating the model-specific normalised metabolic data 61
Comparing mean physiological variables 62
Dealing with outliers 62
2.3 RESULTS 63
2.3.1 Pre-experimental standardisation 63
2.3.1.1 Evaluating the sample morphometry 63
2.3.1.2 Validating the basal data 65
2.3.2 Scaling whole-body basal metabolic rate with body mass . . . 67
2.3.2.1 Normalising the basal metabolic dataset 72
2.3.2.2 Adjusting basal metabolic rate to deep-body temperature 75
2.3.2.3 Comparing the human and animal body-mass exponents 76
2.3.3 The effect of posture change when scaling oxygen consumption 80

2.3.3.1 Exploratory investigation: scaling mass-supported standing 80
2.3.3.2 Scaling oxygen consumption during unaided standing 85
2.4 DISCUSSION 91
2.4.1 Scaling basal metabolic rate in humans. 91
2.4.2 Evaluating non-linear scaling for human basal metabolism . . 97
2.4.2.1 The effect of adjusting data to a common deep-body temperature 97
2.4.2.2 Comparing the human mass exponent against mass$^{0.67}$ 98
2.4.3 The effect of postural change on the scaling relationship . . . 102
2.5 CONCLUSION 103
2.6 REFERENCES 105

CHAPTER 3: SCALING AMBULATORY OXYGEN CONSUMPTION DATA DURING STEADY STATE AND MAXIMAL EXERCISE 123
3.1 INTRODUCTION 123
3.1.1 Scaling steady-state oxygen consumption 128
3.1.2 Scaling peak oxygen consumption 130
3.1.3 Aims and hypotheses 131
3.2 METHODS 132
3.2.1 Subjects 132
3.2.2 Procedural overview 133
3.2.2.1 Experimental standardisation 135
3.2.2.2 Measuring steady-state (walking) oxygen consumption 135
3.2.2.3 Measuring mass-supported, walking oxygen consumption 137
3.2.2.4 Measuring peak oxygen consumption 137
3.2.4 Experimental measurements 138
3.2.5 Design and analysis 140
3.2.5.1 Experimental design 140

3.2.5.2 Data analysis 140
3.3 RESULTS 143
3.3.1 Pre-experimental standardisation 143
3.3.1.1 Evaluating the sample morphometry 143
3.3.2 Scaling oxygen consumption against body mass 144
3.3.3 Assessing the effect of metabolic intensity on the scaling relationship 152
3.3.3.1 Oxygen consumption during mass-supported walking 157
Evaluating whether non-linear regression was appropriate to describe the dataset 157
The effect of body support, movement and load carriage on the scaling regression 160
3.4 DISCUSSION 164
3.4.1 Determining the shape of the scaling regression during exercise 166
3.4.2 The pitfalls of scaling to lean body mass 171
3.5 CONCLUSION 175
3.6 REFERENCES 177

CHAPTER 4: SCALING STEADY-STATE OXYGEN CONSUMPTION DURING WALKING ON DIFFERENT GRADIENTS 188
4.1 INTRODUCTION 188
4.2 METHODS 190
4.2.1 Subjects 190
4.2.2 Procedural overview 192
4.2.2.1 Measuring oxygen consumption during steady-state walking 193
4.2.3 Experimental standardisation 193
4.2.4 Experimental measurements 193
4.2.5 Design and analysis 194
4.2.5.1 Experimental design 194
4.2.5.2 Data analysis 194

4.3 RESULTS 198
4.3.1 Pre-experimental standardisation 198
4.3.2 Comparing the effect of walking gradient on the scaling relationships 199
4.4 DISCUSSION 201
4.5 CONCLUSION 208
4.6 REFERENCES 210

CHAPTER 5: THE EFFECT OF TORSO-BORNE LOAD CARRIAGE WHEN SCALING STEADY-STATE, AMBULATORY OXYGEN CONSUMPTION 216
5.1 INTRODUCTION 216
5.2 METHODS 221
5.2.1 Subjects 221
5.2.2 Procedural overview 221
5.2.2.1 Measuring oxygen consumption 224
5.2.3 Experimental standardisation 225
5.2.4 Experimental measurements 225
5.2.5 Design and analysis 226
5.2.5.1 Experimental design 226
5.2.5.2 Data analysis 226
5.3 RESULTS 228
5.3.1 Pre-experimental standardisation 228
5.3.2 Assessing the regression assumptions 230
5.3.3 Comparing the effect of load carriage on the scaling relationship 233
5.3.3.1 Comparing the effect of gradient 233
5.3.3.2 Scaling oxygen consumption against total mass . . . 238
5.4 DISCUSSION 240
5.4.1 The effect of torso loading during a steady state 241
5.4.2 Scaling oxygen consumption against body mass during loaded walking 241

5.4.3 Scaling oxygen consumption against total mass during loaded walking 243
5.4.4 The effect of ambulatory gradient during loaded walking. . . 244
5.5 CONCLUSION 246
5.6 REFERENCES 247

CHAPTER 6: THE EFFECT OF LOAD DISTRIBUTION WHEN SCALING STEADY-STATE, AMBULATORY OXYGEN CONSUMPTION . . . 254
6.1 INTRODUCTION 254
6.2 METHODS 258
6.2.1 Subjects 258
6.2.2 Procedural overview 258
6.2.2.1 Experimental procedure 261
6.2.3 Experimental standardisation 261
6.2.4 Experimental measures 261
6.2.5 Design and analysis 262
6.2.5.1 Experimental design 262
6.2.5.2 Data analysis 262
6.3 RESULTS 265
6.3.1 Pre-experimental standardisation 265
6.3.2 Effect of load position 267
6.3.2.1 The effect of load placement on the scaling regressions 270
6.4 DISCUSSION 274
6.4.1 The effect of carrying loads on the head 277
6.4.2 The effect of carrying loads on the hands 279
6.4.3 The effect of carrying loads on the feet 281
6.5 CONCLUSION 283
6.6 REFERENCES 285

CHAPTER 7: CONCLUSIONS AND RECOMMENDATIONS 290
7.1 CONCLUSIONS 290
7.1.1 Concluding remarks 299

7.2 FUTURE RESEARCH RECOMMENDATIONS 300
7.2.1 The effect of heavy load carriage on the scaling relationship between oxygen consumption and body mass in adult humans 300
7.2.2 The effect of steep gradients on the scaling relationship during unloaded and loaded steady-state walking 302
7.2.3 The effect of non-locomotive exercise on the scaling relationship between oxygen consumption and body mass 304
7.3 REFERENCES 307

LIST OF FIGURES

Figure 1.1: Scatter plot of the error between linear and ratiometric models when applied to a basal metabolic dataset (A) and the mass-specific residuals for those data (B). 3

Figure 1.2: Schematic of the project design for experimental Chapters 2-6 9

Figure 2.1: Scatter plot of the error between linear and non-linear models applied to the scaling relationship between body mass and basal metabolic rate. 23

Figure 2.2: *A priori* test to predict the standard error of the mean for mass exponents from variations in sample size. 39

Figure 2.3: Mass distribution of participants completing the resting trials 42

Figure 2.4: Experimental setup for the basal (A) and standing (B) conditions. Example auditory canal thermistor fitting (C) 43

Figure 2.5: Schematic representation of the six skinfold locations (A) and the calliper measurement technique (B) 50

Figure 2.6: Schematic of a standard-nine distribution and the corresponding height-adjusted adiposity range for the sample 52

Figure 2.7: Schematic of the experimental design for Chapter 2. 54

Figure 2.8: Decision-making flow chart for the scaling model. 57

Figure 2.9: Visual representation of a $\log_{10}$-transformation outcome for a non-linear dataset. 59

Figure 2.10: Body-mass group differences in raw (A) and height-adjusted body masses (B). Scatter plot of the individual height-adjusted body-mass data points (C) 64

Figure 2.11: Body-mass group differences in raw (A) and height-adjusted body skinfold thicknesses (B). Scatter plot of the individual height-adjusted skinfold data points (C). 66

Figure 2.12: Histogram distributions for raw and log10-transformed body mass and basal metabolic rata data. 69

Figure 2.13: Scatter (A) and residual plots (B) of the basal data, used to assess linearity and homeoscedasticity. 71

Figure 2.14: Error between the linear (first-order polynomial with a positive intercept), non-linear and ratiometric models.. 73

Figure 2.15: Remaining mass relationships between the fitted and predicted metabolic residuals for the ratiometric (A), intercept-adjusted (B), intercept and variance adjusted (C) and allometrically adjusted (D) normalised basal data 74
Figure 2.16: Histogram (A), scatter (B) and residual (C) plots for the temperature-adjusted basal metabolic dataset. 77
Figure 2.17: Difference between the unadjusted and temperature-adjusted body-mass exponents for the basal scaling models 79
Figure 2.18: Scatter plots used to assess linearity in the mass-supported standing exploratory dataset 82
Figure 2.19: Residual plots used to assess homeoscedasticity in the mass-supported standing exploratory dataset 84
Figure 2.20: Body-mass exponent differences for the mass-supported standing trials (A) and the respective variations in cardiac frequency. 86
Figure 2.21: Untransformed (A) and $\log_{10}$-transformed (B) histogram distributions for standing oxygen consumption. 88
Figure 2.22: Scatter and residual plots for oxygen consumption during standing to assess the assumptions of linearity and homeoscedasticity 90
Figure 2.23: Difference between the supine and standing body-mass exponents. . 92
Figure 2.24: Linear and non-linear models applied to the scaling relationship between basal metabolic rate and body mass, across the entire human mass range . .96
Figure 2.25: Correlation between deep-body temperature and body mass (A) and basal metabolic rate (B) 99
Figure 2.26: A comparison between human-only and human and primate scaling models for basal metabolic rate. 101
Figure 3.1: Mass distribution of participants completing the exercise-intensity trials 134
Figure 3.2: Clothing ensemble worn by participants (A) and ankle weights used to standardise loading at the feet (B). 136
Figure 3.3: A schematic of the experimental design for Chapters 2 and 3. 141
Figure 3.4: Frequency histogram plots of the untransformed (A, C) and $\log_{10}$-transformed (B, D) regression variables measured during the walking trial. 145

Figure 3.5: Frequency histogram plots of the untransformed (A, C) and $\log_{10}$-transformed (B, D) regression variables measured during the peak-exercise trial. 146
Figure 3.6: Scatter (A, C) and residual (B, D) plots to assess linearity and homeoscedasticity for the relationship between walking oxygen consumption and body mass. 149
Figure 3.7: Scatter (A, C) and residual (B, D) plots to assess linearity and homeoscedasticity for the relationship between peak oxygen consumption and body mass. 150
Figure 3.8: A comparison between linear and non-linear model fits for the scaling relationship between oxygen consumption and body mass during walking (A) and peak exercise (B) intensities. 151
Figure 3.9: The remaining mass-relationship among the walking (A) and peak exercise data (B) after non-linear normalisation. 153
Figure 3.10: Scatter plot displaying the differences in shape among the four non-linear scaling models (A) and the differences among the respective mass exponents (B). 155
Figure 3.11: Frequency histogram plots of the $\log_{10}$-transformed regression variables used, in the scaling analyses of the exploratory investigation to assess for a normal distribution 158
Figure 3.12: Scatter (A, B, C) and residual plots (D, E, F) of the $\log_{10}$-transformed scaling relationships for standing, mass-supported walking and unaided walking. 161
Figure 3.13: Allometric (A) and $\log_{10}$-transformed regressions (B) of the three exploratory datasets: standing, mass-supported walking and unaided walking 162
Figure 4.1: Mass distribution of participants who completed the gradient walking trails 191
Figure 4.2: A schematic of the experimental design for Chapters 2 and 4. 195
Figure 4.3: Mass-dependent differences in oxygen consumption between level and downhill walking 200

Figure 4.4: Allometric (A) and $\log_{10}$-transformed (B) scaling models comparing level, uphill and downhill oxygen consumption, and the respective differences in body-mass exponents (C). 202
Figure 4.5: Remaining mass relationship among the normalised gradient walking data 204
Figure 5.1: Mass distribution of participants completed the torso-loaded walking 222
Figure 5.2: Torso-load configuration (A) and ankle weights used to standardise shoe masses (B) 223
Figure 5.3: A schematic of the experimental design for Chapters 2 and 5. 227
Figure 5.4: Scatter plots used to assess linearity during standing (A), level walking (B), uphill walking (C) and downhill walking (D) while wearing the torso-loaded trials. 231
Figure 5.5: Residual plots used to assess homeoscedasticity of the $\log_{10}$-transformed scaling models for standing (A) and level (B), uphill (C) and downhill walking (D) while torso loaded. 232
Figure 5.6: Allometric (A) and $\log_{10}$-transformed (B) scaling unloaded and torso-loaded scaling models, and the respective differences in body-mass exponents (C). 236
Figure 5.7: Percentage increase in oxygen consumption during load carriage across gradients and body-mass groups 237
Figure 5.8: Mass-dependent percentage decreases in oxygen consumption between level and downhill walking, with and without torso loading. 239
Figure 6.1: Mass distribution of participants completed the loaded-distribution trials 259
Figure 6.2: Loading configurations: head (A), hands (B), feet (C) and the control standardisation of shoe masses (D) 260
Figure 6.3: A schematic of the experimental design for Chapters 2 and 6. 263
Figure 6.4: Comparison of the effect of load distribution and a change in gradient on the body- and total-mass exponents 273

LIST OF TABLES

Table 1.1: Distribution of research themes across the experimental Chapters . . . 10

Table 2.1: Variations in tissue-specific metabolic rates and their proportional differences within ageing humans, for both a reference adult and neonate 34

Table 2.2: Morphological and physiological sample characteristics 41

Table 2.3: Normality and autocorrelation assumptions for basal metabolic rate. . 70

Table 2.4: Normality and autocorrelation assumptions for temperature-adjusted basal metabolic rate. 78

Table 2.5: Normality and autocorrelation assumptions for mass-supported walking exploratory trial 83

Table 2.6: Normality and autocorrelation assumptions for standing oxygen consumption. 89

Table 2.7: Summary table of the derived regression equations in Chapter 2 93

Table 3.1: Literature review of previous investigations where peak scaling has been performed 124

Table 3.2: Peak oxygen consumption for the familiarisation pilot testing 139

Table 3.3: Normality and autocorrelation assumptions for steady-state walking and peak exercise oxygen consumption. 148

Table 3.4: Summary table for the scaling models derived in Chapters 2 and 3 . . 156

Table 3.5: Normality and autocorrelation assumptions for oxygen consumption during mass-supported walking 159

Table 3.6: Bootstrapped regression coefficients for the exploratory investigation: mass-supported walking 163

Table 4.1: Summary table of the scaling models derived within Chapter 4 203

Table 5.1: Summary table of the scaling models derive in Chapters 2-4. 229

Table 5.2: Mean effects of load carriage on oxygen consumption and cardiac frequency during standing and steady-state walking (-5%, 0%, 5%). . . . 234

Table 5.3: Summary of all body- and total-mass scaling models derived during Chapters 2-5. 235

Table 6.1: Linear regression equations derived during walking with distally-placed loads. 266

Table 6.2: Raw and $\log_{10}$-transformed equations for the scaling relationship between oxygen consumption and body mass during all walking trials.. 268
Table 6.3: Mean oxygen consumption and cardiac frequency responses during walking with and without loads 269
Table 6.4: Raw and $\log_{10}$-transformed equations for the scaling relationship between oxygen consumption and total mass during all walking trials.. 272
Table 6.5: Mean oxygen consumption data, collected during level walking with all five load configurations, normalised to $mass_{body}^{0.80}$, $mass_{total}^{0.80}$ and $mass^{-1}$ 275

CHAPTER 1: INTRODUCTION

1.1 CONCEPTUAL INTRODUCTION

To sustain life, animals must take energy in from external sources. This energy is transformed within the body through chemical reactions that can be classified into one of two processes. Catabolism, the breakdown of stored chemical energy from ingested foods and internal energy reserves, and anabolism, the utilisation of these smaller compounds, created during catabolism, for the building and repair of tissue structures within the body. Collectively, the sum of energy transformed during these processes is known as the metabolic rate of an animal (Guyton and Hall, 2006). From these processes, there are two measurable consequences of metabolism that can be used to approximate the rate of whole-body energy transformation for an animal: exothermic heat production, a by-product of energy transformation, and oxygen consumption, inspired atmospheric molecules necessary for sustained cellular respiration. Throughout this series of investigations, the latter will be used to approximate metabolic rate.

At a cellular level (cellular respiration), the rate of metabolism varies depending upon the tissue type, number of cells and metabolic intensity (Elia, 1992). Accordingly, whole-body metabolism is influenced by both an organism's tissue composition and body size (mass; Sarrus and Rameaux, 1839; Taylor *et al.,* 1970; Müller *et al.,* 2013). Indeed, it is logical that larger animals, having a greater number of cells, will also have a greater absolute whole-body metabolic rate. In humans, this relationship accounts for approximately 80% of the inter-individual variation in metabolic rate across individuals (Elia, 1992; Johnstone *et al.,* 2005; Müller *et al.,* 2013). However, a consequence of that mass-dependent relationship is that absolute data cannot be directly compared among individuals of varying body masses. Therefore, it is necessary to normalise metabolic data for the effect of body mass before performing such comparisons.

Despite its ubiquitous use, that mass relationship can rarely be removed by simply dividing absolute metabolic rate by body mass (Tanner, 1949; Packard and Boardman, 1988; Albrect *et al.,* 1993). To use that approach, a one-to-one (ratiometric) relationship is assumed between both variables; however, this seldom

occurs within a metabolic dataset (see Figure 1.1). As a result, the application of this normalisation method often over-corrects the mass relationship present among such data and leaves a systematic mass bias among the normalised residuals (Atchley *et al.,* 1976; Packard and Boardman, 1988; Albrect *et al.,* 1993; see Figure 1.1). Consequently, a different normalisation approach is required. The normalisation approach should be based upon the shape of the regression between both variables, referred to as the scaling relationship. To date, the shape of this relationship in humans remains unconfirmed (Schofield, 1985; Harris and Benedict, 1919; Markovic *et al.,* 2007).

Since the invention of the first calorimeter[2] by Lavoisier in 1780 (Lavoisier and DeLaPlace, 1994), the inter- and intra-subject variations in metabolic rate have been of interest to researchers. The scaling of metabolic rate was initially explored in the field of comparative physiology during basal[3] conditions (Sarrus and Rameaux, 1839; Rubner, 1883; Kleiber, 1932). Continued today, an analysis of the basal metabolic rate of mammals, over five orders of magnitude mass range, provides evidence for a non-linear, allometric[4] relationship between metabolism and body mass ($mass^{0.67}$: White and Seymour, 2003). Meaning that, per kilogram of mass (mass-specific), larger animals use less energy during basal conditions than smaller animals.

In contrast, for humans, that scaling relationship has been described in some fields

[2] A calorimeter is a device used to approximate the metabolic rate of an organism by quantifying the rate of thermal energy exchange with the surrounding environment (see Section 2.1.1.1 for details).

[3] Basal metabolic rate is the minimum amount of energy required to sustain basic life processes within an organism. It is tested during fasted, well-rested, thermoneutral and resting conditions.

[4] An allometric (power) regression is defined by the equation $y = ax^b$, where y is the dependent, physiological variable (metabolic rate), a is the multiplicative constant, x is the independent morphological variable (body mass) and b is the mass exponent.

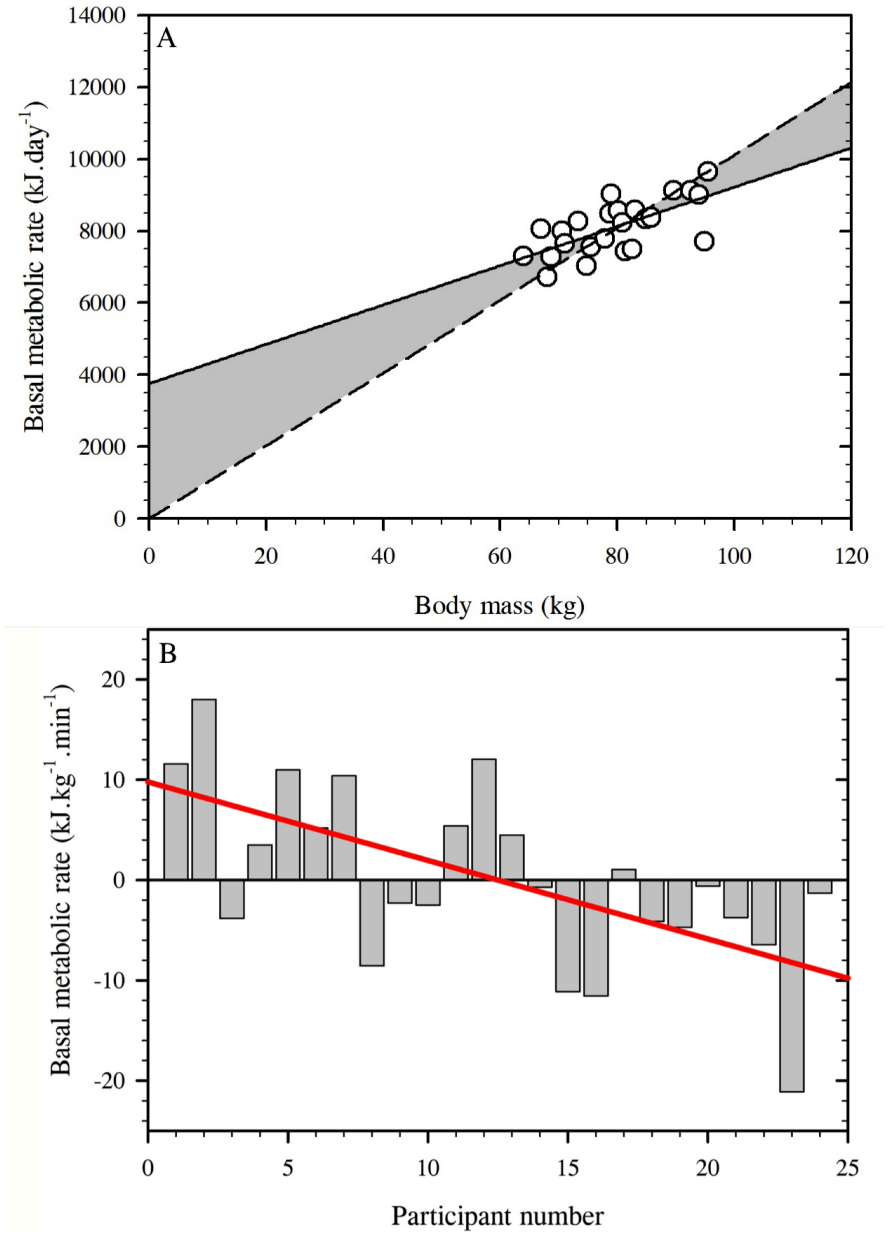

Figure 1.1: (Figure 1.1A) A scatter plot of the relationship between basal metabolic rate and body mass in 24 adult males. Both an ordinary least squares (solid line: intercept=3758.81 kJ.day^{-1}, r^2=0.45, P<0.05) and ratiometric (dashed line) regression have been applied to the dataset to demonstrate the error between both methods. Figure 1.1B displays the systematic error present among those data when normalised using a ratiometric approach (kJ.kg^{-1}.day^{-1}). That remaining mass relationship is evident when participants are ordered from lightest to heaviest across the abscissa, as above (r=-0.65).

using a linear[5] model (first-order polynomial), starting with the first basal metabolic study on a healthy cohort (Benedict *et al.,* 1914; Benedict, 1915). Within that series of investigations, it was concluded that those human data did not fit the aforementioned non-linear scaling shape observed in the animal kingdom ($mass^{0.67}$). However, those data were not analysed to determine whether an alternative exponent should be applied instead, rather a linear regression was deemed more appropriate and was adopted. That conclusion led to a cascade of work where a similar, linear analysis approach was adopted for human basal metabolic data (Schofield, 1985; Harris and Benedict, 1919; Cole and Henry, 2005).

Nevertheless, it has been argued that any scaling model applied to a biological dataset must be both statistically and biologically appropriate (Sholl, 1948). That is, the chosen model must be theoretically defensible using biological mechanisms. Thus, for metabolic scaling, this statement challenges the use of linear models that utilise a non-origin intercept (*i.e.* Harris and Benedict, 1919; Schofield, 1985). In such instances, the extrapolated regression will lead to erroneously high predictions of metabolic rate at very light body masses (see Figure 1.1A). Indeed, it is physiologically impossible to have any metabolic rate at a body mass of zero. Accordingly, the use of linear modelling to describe the scaling relationship of metabolic data in humans was challenged within this project. In contrast, it was anticipated that humans, as a species, would scale by a similar relationship against body mass as observed within other mammals: non-linear, allometric scaling.

While testing the scaling relationship using a controlled sample during a basal state provides a unique opportunity to determine a baseline relationship free from other influential covariates, the body is rarely in a basal state. Therefore, it was of interest to ascertain whether the shape of that scaling relationship was modified by a change in metabolic intensity. Accordingly, within this project, the effect of metabolic intensity on the scaling relationship was evaluated throughout the physiological range, from the basal state through to maximal exercise (running).

---

[5] Linear scaling is commonly performed using ordinary least squares regression, and applying a first-order polynomial equation to a dataset: $y = ax + c$, where y is the dependent, physiological variable (metabolic rate), a is the multiplicative constant, x is the independent morphological variable (body mass) and c is the intercept constant for the physiological variable.

Absolute metabolic rate increases stepwise with metabolic intensity. At a cellular level, that relationship coincides with a shift in metabolic pathways and changes the body from an oxygen-demand (basal) to oxygen-supply (maximal) limiting state. The theorised outcome from that response being a stepwise increase in the steepness of the regression for the scaling relationship (Allometric cascade theory: Darveau *et al.,* 2002; Hochachka *et al.,* 2003; Suarez *et al.,* 2004). At a whole-body level, a non-uniform, mass-dependent increase in absolute metabolic rate occurs at any fixed velocity. Indeed, to cover the same horizontal distance, a heavier animal requires a greater amount of energy to both support its structure and move its mass (Mahadeva *et al.,* 1952; Taylor *et al.,* 1970). Accordingly, this response was also likely to result in a steepening of the regression shape with metabolic intensity. However, while that outcome could be anticipated, whether it had a meaningful effect on the shape of the scaling relationship in humans remained unclear.

Within animal research, the shape of the scaling relationship remains non-linear during exercise intensities but is reported to scale by a steeper regression slope than that observed during a basal condition (Kleiber, 1961; Taylor *et al.,* 1970; McMahon, 1975). In contrast, while a similar relationship has been observed between metabolic intensity and the regression steepness in humans (Rogers *et al.,* 1995; Markovic *et al.,* 2007), both linear (Durnin and Passmore, 1967; Goldman and Iampietro, 1962; Mahadeva *et al.,* 1952) and non-linear (Bergh *et al.,* 1991; Nevill *et al.,* 1992; Rogers *et al.,* 1995) scaling relationships have been used to describe those data. As a result, no definitive outcome has been identified for the effect of metabolic intensity on the scaling regression shape (linear or non-linear) or steepness that can be used to accurately predict or normalise metabolic data in humans. Moreover, the magnitude increase in metabolic rate necessary to significantly change the scaling relationship compared with that observed during a basal condition was also unknown. To address these issues, the scaling relationship was evaluated during three non-basal states within this project: standing, steady-state walking and maximal running.

In addition to an increase in locomotive intensity, it was considered that the scaling relationship might also be influenced by other related variables. For this reason, the effects of gravity and load carriage on the shape of the scaling relationship were also

evaluated, both independently and together. To the author's best knowledge, this was the first investigation where the effect either variable on the scaling relationship had been assessed in humans.

During gradient walking, absolute metabolic rate changes relative to the gradient direction; metabolism increases linearly with an increase in gradient from horizontal (Bobbert, 1960), and decreases by a curvilinear relationship with a decrease in gradient (Margaria, 1938). That response is influenced by the effect of gravity on the cost of movement: mechanical work (concentric muscle contractions) increases during uphill walking, relative to the gain in potential energy, and decreases during downhill walking as that potential energy is released into the gait cycle (Minetti *et al.,* 1993, 1994). However, at steeper downhill gradients, the gait is typically shortened, and step frequency increased, to increase stability (Sheehan and Gottschall, 2012, 2014; Padulo *et al.,* 2013), resulting in the curvilinear response. To date, this relationship has been studied through a wide gradient range (±45%: Minetti *et al.,* 2002), with data often reported as absolute means or in mass-specific units (Goldman and Iampietro, 1962; Johnson *et al.,* 2002; Minetti *et al.,* 2002), despite the long-known presence of a body-mass response (Seltzer, 1940). That response is likely an effect of the proportional relationship between mass and the metabolic cost of vertical ascent, which is relatively uniform per kilogram per vertical metre (Zuntz, 1897; Slowtzoff, 1903; Taylor *et al.,* 1972). Accordingly, in humans, gradient may have a similar effect on the scaling relationship as that anticipated for a change in metabolic intensity. While that response has been observed in animals during uphill locomotion, it was uncertain whether a similar response would be observed across the narrower human mass range.

So far metabolic rate has been considered in relation to body mass during unloaded conditions. During such conditions, absolute metabolism increases with body mass, thus, favouring lighter individuals. In contrast, during load carriage, the metabolic rate of an individual increases proportionally to the total mass change (Goldman and Iampietro, 1962; Taylor *et al.,* 1980; Maloiy, 1986). Accordingly, when carrying a fixed-mass, a lighter individual will experience a greater relative increase in metabolic rate, because that external load comprises a greater percentage of their body mass and

therefore poses a greater physiological burden. In this instance, despite the increase in absolute metabolic rate, the regression slope may, in fact, flatten. Such a response would be atypical of the expected relationship between metabolic intensity and the steepness of the regression slope. Moreover, if it were to occur, it would indicate the potential requirement for task-specific scaling models, rather than a purely intensity-driven approach. For this reason, load carriage was included as an exploratory variable within this project.

Within that research theme, it was considered possible that the location on the body that the load would be carried might result in a further modification to the shape of the scaling relationship. That was presumed due to the relationship between the metabolic burden of load carriage and its distance from the body's centre of mass (Lind and McNicol 1968; Soule and Goldman 1969; Legg and Mahanty 1986). For instance, loads placed distally on the legs increase the propulsion and braking forces of the leg swing during walking (Myers and Steudel 1985) while also increasing the moment of inertia about the hip (Browning *et al.,* 2007), thus, increasing total energy expenditure. Accordingly, it was anticipated that the effect of load carriage on the scaling relationship would be magnified when loads are carried away from the body's centre of mass, further flattening the regression slope relative to the loading factor[6] of each load location. To test this assumption, the scaling relationship was evaluated with loads carried at the head, torso, hands and feet.

In summary, the shape of the scaling relationship between metabolic rate and body mass remains unconfirmed in humans, with researchers using both linear and non-linear scaling models to describe that relationship. As a result, no uniform method has been established to predict and normalise metabolic data that also minimises error. In addition, it was likely that the scaling shape will be modified by a change in metabolic intensity, gradient and load carriage. Accordingly, it was possible that unique scaling models would be required to predict and normalise metabolic data, depending upon the specific test conditions. To explore that possibility, this project was based on a

[6] The term loading factor is used to define the multiplicative metabolic burden of a load carriage location relative to the same mass carried about the torso. For instance, load carriage at the feet has a loading factor of ~5.8x that of torso loading during walking at 4.8 $km.h^{-1}$ (Soule and Goldman, 1969).

five by nine by five factorial design (Figure 1.2) split across five experimental Chapters (2-6), with five levels of the first factor (body mass: extra-small, small, medium, large, extra-large), nine levels of the second factor (metabolic intensity: basal, 100% mass-supported standing [exploratory investigation], 50% mass-supported standing [exploratory investigation], standing, 50% mass-supported walking [exploratory investigation], level walking, uphill walking, downhill walking and peak exercise [running]) and five levels of the third factor (load configuration: unloaded, head, torso, hands and feet). The distribution of those experimental phases across the project is detailed in Table 1.1. The project was based upon a repeated-measures design with a sample of participants, who were morphologically and physiologically homogeneous except for variations in body mass, acting as their own controls.

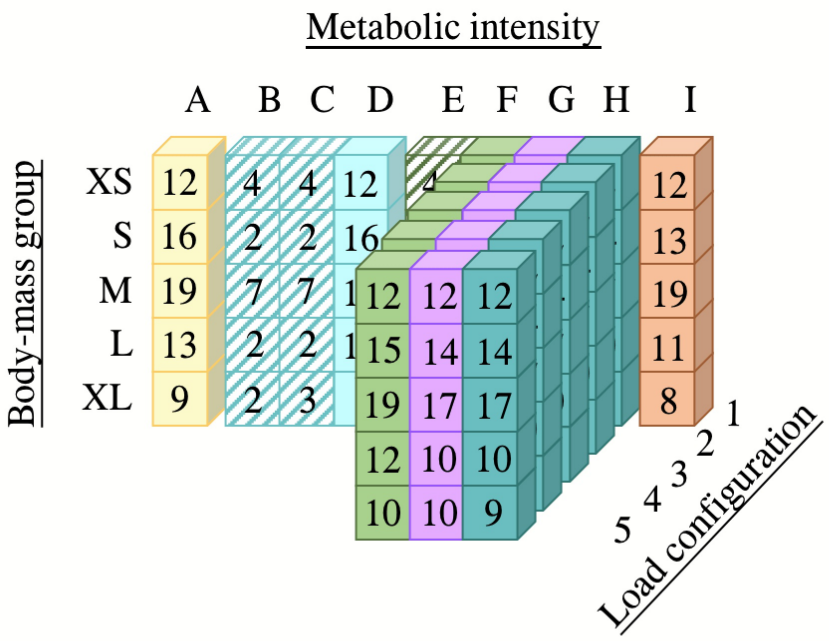

Figure 1.2: A schematic of the experimental design used within this project (Chapters 2-6). Exploratory trials are identified by the hashed fills. Sample sizes are identified within each cell. The project consisted of a three-way factorial design. The first factor (body mass) had five levels: extra-small (XS: $<$65 kg); small (S: 66-76 kg); medium (M: 77-87 kg); large (L: 88-98 kg); and extra-large (XL: $>$99 kg). The second factor (metabolic intensity) had nine levels: supine (A: basal, rest); 100% mass-supported standing (B: exploratory investigation); 50% mass-supported standing (C: exploratory investigation); standing (D); 50% mass-supported walking (E: exploratory investigation); level walking (F); uphill walking (G); downhill walking (H); peak exercise (I). The third factor (load configuration) had five levels: unloaded (1), head (2: 1.38-kg helmet), torso (3: 25-kg weighted vest), hands (4: 2 kg each hand) and feet (5: 2 kg each foot) loads.

Table 1.1: Breakdown of the metabolic intensities explored within this project and their corresponding experimental Chapters.

Experimental Chapter	**Metabolic intensities explored**
Chapter 2	Basal (supine) and standing (resting)
Exploratory phase	100% and 50% Mass-supported standing
Chapter 3	Level walking and peak exercise (running)
Exploratory phase	50% mass-supported, level walking
Chapter 4	Uphill (5%) and downhill (-5%) walking
Chapter 5	Torso-borne load carriage during level, uphill and downhill walking
Chapter 6	Load distribution on the head, hands and feet, during level, uphill and downhill walking

1.2 REFERENCES

Albrecht, G.H., Gelvin, B.R., and Hartman, S.E. (1993). Ratios as a size adjustment in morphometrics. *American Journal of Physical Anthropology*. 91(4):441-468.

Atchley, W.R., Gaskins, C.T., and Anderson, D. (1976). Statistical properties of ratios. I. Empirical results. *Systematic Zoology*. 25(2):137-148.

Benedict, F.G. (1915). Factors affecting basal metabolism. *Journal of Biological Chemistry*. 20(3):263-299.

Benedict, F.G., Emmes, L.E., Roth, P., and Smith, H.M. (1914). The basal, gaseous metabolism of normal men and women. *Journal of Biological Chemistry*. 18(2):139-155.

Bergh, U., Sjödin, B., Forsberg, A., and Svedenhag, J. (1991). The relationship between body mass and oxygen uptake during running in humans. *Medicine and Science in Sports and Exercise*. 23(2):205-211.

Bobbert, A.C. (1960). Energy expenditure in level and grade walking. *Journal of Applied Physiology*. 15(6):1015-1021.

Browning, R.C., Modica, J.R., Kram, R., and Goswami, A. (2007). The effects of adding mass to the legs on the energetics and biomechanics of walking. *Medicine and Science in Sports and Exercise*. 39(3):515-525.

Cole, T.J., and Henry, C.J.K. (2005). The Oxford Brookes basal metabolic rate database – a reanalysis. *Public Health Nutrition*. 8(7A):1202-12.

Darveau, C.A., Suarez, R.K., Andrews, R.D., and Hochachka, P.W. (2002). Allometric cascade as a unifying principle of body mass effects on metabolism. *Nature*. 417(6885):166-170.

Durnin, J.V.G.A. and Passmore, R. (1967). *Energy, work and leisure*. Heinemann Educational Books Ltd., London.

Elia, M. (1992). Organ and tissue contribution to metabolic rate. In: Kinney J.M., and Tucker H.N. (Ed.). *Energy metabolism: Tissue determinants and cellular corollaries*. Raven Press, New York. Pp. 61-80.

Goldman, R.F., and Iampietro, P.F. (1962). Energy cost of load carriage. *Journal of Applied Physiology*. 17(4):675-676.

Guyton, A.C., and Hall, J.E. (2006). *Textbook of Medical physiology*. Elsevier, Pennsylvania.

Harris, J.A., and Benedict, F.G. (1919). *A Biometric Study of Basal Metabolism in Man*. Carnegie Institution, Washington.

Hochachka, P.W., Darveau, C.A., Andrews, R.D., and Suarez, R.K. (2003). Allometric cascade: a model for resolving body mass effects on metabolism. *Comparative Biochemistry and Physiology Part A: Molecular and Integrative Physiology*. 134(4):675-91.

Johnson, A.T., Benjamin, M.B., and Silverman, N. (2002). Oxygen consumption, heat production, and muscular efficiency during uphill and downhill walking. *Applied Ergonomics*. 33(5):485-491.

Johnstone, A.M., Murison, S.D., Duncan, J.S., Rance, K.A., and Speakman, J.R. (2005). Factors influencing variation in basal metabolic rate include fat-free mass, fat mass, age, and circulating thyroxine but not sex, circulating leptin, or triiodothyronine. *The American Journal of Clinical Nutrition*. 82(5):941-948.

Kleiber, M. (1932). Body size and metabolism. *The Journal of Agricultural Science*. 6(11):315-353.

Kleiber, M. (1961). *The Fire of Life. An Introduction to Animal Energetics*. Wiley, New York.

Lavoisier, A.L., and DeLaplace, P.S. (1994). Memoir on Heat Read to the Royal Academy of Sciences, 28 June 1783. *Obesity research*. 2(2):189-202.

Legg, S.J., and Mahanty, A. (1986). Energy cost of backpacking in heavy boots. *Ergonomics*. 29(3):433-438.

Lind, A.R., and McNicol, G.W. (1968). Cardiovascular responses to holding and carrying weights by hand and by shoulder harness. *Journal of Applied Physiology*. 25(3):261-267.

Mahadeva, K., Passmore, R., and Woolf, B. (1952). Individual variations in the metabolic cost of standardized exercises: the effects of food, age, sex and race. *The Journal of Physiology*. 121(2):225-231.

Maloiy, G.M.O., Heglund, N.C., Prager, L.M., Cavagna, G.A., and Taylor, C.R. (1986). Energetic cost of carrying loads: have African women discovered an economic way? *Nature*. 319(6055):668-669.

Margaria, R. (1938). Sulla fisiologia e specialmente sul consumo energetico della marcia e della corsa a varie velocità ed inclinazioni del terreno. *Atti della Accademia Nazionale dei Lincei Memorie*. 7:299-368.

Markovic, G., Vucetic, V., and Nevill, A.M. (2007). Scaling behaviour of in athletes and untrained individuals. *Annals of Human Biology*. 34(3):315-328.

McMahon, T.A. (1975). Using body size to understand the structural design of animals: quadrupedal locomotion. *Journal of Applied Physiology*. 39(4):619-627.

Minetti, A.E., Ardigo, L.P., and Saibene, F. (1993). Mechanical determinants of gradient walking energetics in man. *The Journal of Physiology*. 472(1):725-35.

Minetti, A.E., Ardigo, L.P., and Saibene, F. (1994). Mechanical determinants of the minimum energy cost of gradient running in humans. *Journal of Experimental Biology*. 195(1):211-225.

Minetti, A.E., Moia, C., Roi, G.S., Susta, D., and Ferretti, G. (2002). Energy cost of walking and running at extreme uphill and downhill slopes. *Journal of Applied Physiology*. 93(3):1039-1046.

Müller, M.J., Wang, Z., Heymsfield, S.B., Schautz, B., and Bosy-Westphal, A. (2013). Advances in the understanding of specific metabolic rates of major organs and tissues in humans. *Current Opinion in Clinical Nutrition and Metabolic Care*. 16(5):501-508.

Myers, M.J., and Steudel, K. (1985). Effect of limb mass and its distribution on the energetic cost of running. *Journal of Experimental Biology*. 116(1):363-373.

Nevill, A.M., Ramsbottom, R., and Williams, C. (1992). Scaling physiological measurements for individuals of different body size. *European Journal of Applied Physiology and Occupational Physiology*. 65(2):110-117.

Packard, G.C., and Boardman, T.J. (1988). The misuse of ratios, indices, and percentages in ecophysiological research. *Physiological Zoology*. 61(1):1-9.

Padulo, J., Annino, G., Tihanyi, J., Calcagno, G., Vando, S., Smith, L., Vernillo, G., La Torre, A., and D'Ottavio, S. (2013). Uphill racewalking at iso-efficiency speed. *The Journal of Strength and Conditioning Research*. 27(7):1964-1973.

Rogers, D.M., Olson, B.L., and Wilmore, J.H. (1995). Scaling for the $\dot{V}O_2$-to-body size relationship among children and adults. *Journal of Applied Physiology*. 79(3):958-967.

Rubner, M. (1883). Über den Einfluss der körpergrösse auf stoffund kaftwechsel. *Zeitschrift für Biologie*. 19:535-562.

Sarrus, F., and Rameaux, J.F. (1839). Mathématique appliquée à la physiologie. *Bulletin de l'Academie Royale de Medicine de Paris*. 3:1094-100.

Schofield, W.N. (1985). Predicting basal metabolic rate, new standards and review of previous work. *Human Nutrition. Clinical Nutrition*. 39C(S1):5-41.

Seltzer, C.C. (1940). Body build and oxygen metabolism at rest and during exercise. *American Journal of Physiology-Legacy Content*. 129(1):1-13.

Sheehan, R.C., and Gottschall, J.S. (2012). At similar angles, slope walking has a greater fall risk than stair walking. *Applied Ergonomics*. 43(3):473-478.

Sheehan, R.C., and Gottschall, J.S. (2014). Segment lengths influence hill walking strategies. *Journal of Biomechanics*. 47(11):2611-2617.

Sholl, D. (1948). The quantitative investigation of the vertebrate brain and the applicability of allometric formulae to its study. *Proceedings of the Royal Society B: Biological Sciences*. 135(879):243-258.

Slowtzoff, B. (1903). Über die Beziehungen zwischen Körpergröße und Stoffverbrauch der Hunde bei Ruhe und Arbeit. *Pflügers Archiv European Journal of Physiology*. 95(3):158-191.

Soule, R.G., and Goldman, R.F. (1969). Energy cost of loads carried on the head, hands, or feet. *Journal of Applied Physiology*. 27(5):687-690.

Suarez, R.K., Darveau, C.A., and Childress, J.J. (2004). Metabolic scaling: a many-splendoured thing. *Comparative Biochemistry and Physiology Part B: Biochemistry and Molecular Biology*. 139(3):531-541.

Tanner, J.M. (1949). Fallacy of per-weight and per-surface area standards, and their relation to spurious correlation. *Journal of Applied Physiology*. 2(1):1-15.

Taylor, C.R., Caldwell, S.L., and Rowntree, V.J. (1972). Running up and down hills: some consequences of size. *Science*. 178(4065):1096-1097.

Taylor, C.R., Heglund, N.C., McMahon, T.A., and Looney, T.R. (1980). Energetic cost of generating muscular force during running. *Journal of Experimental Biology*. 86(1):9-18.

Taylor, C.R., Schmidt-Nielsen, K., and Raab, J.L. (1970). Scaling of energetic cost of running to body size in mammals. *American Journal of Physiology*. 219(4):1104-1107.

White, C.R., and Seymour, R.S. (2003). Mammalian basal metabolic rate is proportional to body mass$^{2/3}$. *Proceedings of the National Academy of Sciences*. 100(7):4046-4049.

Zuntz, N. (1897). Über den Stoffverbrauch des Hundes bei Muskelarbeit. *Pflügers Archiv European Journal of Physiology*. 68(5):191-211.

CHAPTER 2: SCALING OXYGEN CONSUMPTION DURING BASAL AND RESTING STATES IN ADULT MALES

2.1 INTRODUCTION

Basal metabolic rate is the minimum energy expenditure of an organism necessary to conserve life (Mitchell, 1962). This includes the energy consumed by ion-transport systems (Himms-Hagen, 1976), the energy required for growth and repair (Garrow, 1985), the mechanical work performed by the cardiovascular and respiratory systems and the energy expended during the conversion of metabolic substrates (Zuntz, 1901), all of which are tightly linked to the size of an organism. Therefore, even at the lowest metabolic intensity, absolute metabolic rate increases with body size. As a result, in studies where large body-mass ranges are tested, regardless of the metabolic intensity, it becomes important to normalise absolute data for changes in body mass, so that the impact of this size-dependent nature[7] is minimised.

To generate such mass-independent data, it is first necessary to understand how those data scale against body mass. Some assume that human basal metabolism scales linearly (first-order polynomial with an intercept) against body mass (Harris and Benedict, 1919; Schofield, 1985; Cole and Henry, 2005), however, it is more probable that those data follow a similar trend to that seen in other mammals, for which a non-linear, allometric approach best fits those data (White and Seymour, 2003). Since the nature (exponent[8]) of that relationship can vary depending on the number and type of species tested (Heusner, 1982; White and Seymour, 2003), the exponent used to describe human data, if that relationship is indeed correct, cannot be assumed directly from animal studies and must be calculated from a relevant sample. As yet, the scaling of human basal metabolism has not been explored using a population sample that is wide in its mass range, but otherwise homogeneous for factors that may independently influence metabolic rate. Therefore a direct

[7] The term nature has been solely used to refer to the shape, or steepness, of the scaling relationship between whole-body metabolic rate and body mass, without indicating whether it is linear or nonlinear.

[8] An allometric, power, regression is described using the equation $y = ax^b$, where y is metabolic rate, a is the multiplicative constant, x is body mass and b is the mass exponent. For such relationships, the mass exponent primarily dictates the regression shape. Therefore, differences in that regression coefficient can be used to identify unique scaling relationships between species and other metabolic intensities.

comparison between both scaling models (linear and non-linear) using an appropriate sample is required to address this issue.

Within this experimental phase, the scaling of both basal and resting (standing) oxygen consumption was explored in humans. By first testing during a basal state, it was possible to establish a baseline for that relationship, from which the effects of an increase in metabolic intensity, during both unloaded and loaded states, could be compared in the subsequent Chapters (2-5). In this way, a staged approach was taken, with each step used to build a layered understanding of this relationship. Throughout those stages, it was necessary to accurately quantify the rate of energy transformation, for which direct calorimetry and respirometry are the appropriate experimental methods (Atwater and Rosa, 1899).

2.1.1 Methods for quantifying metabolic rate

Direct calorimetry and respirometry can both be used to accurately estimate the rate of cellular respiration (Atwater and Rosa, 1899). While neither method is capable of permitting a direct measurement of the rate of adenosine triphosphate synthesis within the body, both methods quantify the magnitude of reactants consumed or products created during this reaction. For example, direct calorimetry is the measurement of metabolic heat emitted from the body, while respirometry is the measurement of respiratory flows and the changes in the gaseous fractions of the respired air. Accordingly, both methods measure components from the same stoichiometric reaction. Thus, estimations of whole-body metabolic rate made using either method are similar ($<1\%$; Atwater and Rosa, 1899).

2.1.1.1 Direct calorimetry

Direct calorimetry is considered the most accurate method to estimate metabolic rate (Kenny and Jay, 2013), and was therefore the preferable measurement technique for this project. The method is based on the physical laws of energy conservation (First Law of Thermodynamics: von Mayer, 1845) and mass and energy equivalence (Einstein, 1905). That is, energy can be neither created nor destroyed, only change form and concentration. The movement of that energy is predictable, travelling down gradients from areas of high to low energy content (Carnot, 1824; Clausius, 1850,

1854; Thomson, 1853; Carathéodory, 1909; Planck, 1927). Thus, if the total energy of the system (enthalpy) remains constant, the rate of energy received must be equal to the rate of energy emitted ($kJ.min^{-1}$). Regarding metabolism, the process of cellular respiration in humans is inefficient, with about 80% of the energy liberated being released as heat (thermal energy; Whipp and Wasserman, 1969). Assuming that ratio remains constant, it is possible to estimate whole-body metabolism by measuring the rate of heat production.

To reduce the impact of unregulated hyperthermia, the body has evolved complex thermoregulatory mechanisms to remove excess thermal energy. This heat loss is controlled by the preoptic anterior hypothalamus (Boulant, 1981) through changes in blood flow (vasomotion) and sweating (Neilsen, 1938; Lind 1963; Kerslake, 1972; Edholm and Weiner, 1981). Those mechanisms control heat loss via evaporative and dry (convective, conductive and radiative) heat loss pathways, and in doing so, regulate mean body temperature. For example, in mammals and other endothermic species, areas of high thermal energy lose heat through both convective (e.g. vascular and pulmonary pumping) and conductive processes, with heat being transferred to cooler tissues. Once at the skin's surface, excess thermal energy is emitted to the environment, predominantly through evaporative, convective and radiative pathways. For this reason, if mean body temperature[9] remains stable, the amount of thermal energy being transferred to the environment must be equal to that being produced during metabolism.

In healthy humans, mean body temperature is regulated within a narrow range, and is an outcome of the balance between metabolic heat production and the heat flux around the body's tissues, and between the body and its surrounding environment (Piironen, 1970; Baker *et al.,* 1972). During conditions where metabolic heat production is greater than heat loss, mean body temperature will increase with tissues storing this excess thermal energy, thus, heat loss will no longer be equal to metabolic heat production. Therefore, changes in mean body temperature should also be considered

[9] Mean body temperature is calculated from a weighted average of deep-body and mean-skin temperature (Burton, 1935). The weighting used for both measurements is variable depending upon the surrounding environmental condition: hot, comfortable and cold.

when quantifying whole-body metabolic rate in this way.

During a basal state, non-evaporative heat losses account for ~80% of the total thermal energy transfer. The remaining 20% is lost through insensible pathways: transepidermally (Taylor and Machado-Moreira, 2013) and the respiratory tract (Jéquier, 1986; Levine, 2005). Therefore, to ensure an accurate quantification of metabolic rate, all heat loss pathways must be measured.

Non-evaporative heat losses were first quantified in animals by Lavoisier and Laplace (1780) using an ice calorimeter, with the volume of thawed ice representing the total heat emitted from the animal. Technology has since advanced, with modern devices working on the principles of flow and gradient layer calorimetry. Within these devices, the changes in temperature (or electrical current) between inlet and outlet values are assessed to quantify the magnitude of non-evaporative heat transferred from the body to the environment (Webb, 1985; Kaiyala and Ramsay, 2011; Kenny and Jay, 2013). Evaporative heat losses can be measured by making small modifications to these devices to quantify changes in water vapour pressure. In this way, all heat transfer from the body can be quantified.

Through the ability to quantify all heat generated by the body, direct calorimetry is often the preferred method for studying metabolism (Kenny and Jay, 2013). That method, however, was not available at the host laboratory. Therefore, the alternative method of respirometry was adopted for the current series of projects.

2.1.1.2 Respirometry

Respirometry can be used to approximate whole-body energy expenditure in the absence of a direct heat measurement. Unlike direct calorimetry, which measures heat production, indirect respirometry measures changes in the gaseous fractions of carbon dioxide and oxygen between the inspired and expired air and ventilatory flows (minute ventilation) to estimate energy production from approximations of substrate utilisation. Substrate utilisation is estimated using the respiratory exchange ratio (volume of carbon dioxide produced divided by the volume of oxygen consumed), for which known macronutrient calorific constants exist (Zuntz, 1901; Magnus-Levy,

1893; Livesey and Elia, 1988). Each mole of carbohydrate or fat (non-esterified, free fatty acids) is broken down using a fixed number of oxygen molecules to liberate a fixed amount of energy (adenosine triphosphate), carbon dioxide and heat[10]. Accordingly, both metabolic measurement methods are inherently linked, and therefore generate equivalent estimates of whole-body energy expenditure ($<1\%$ error using a room calorimeter and respirometer: Atwater and Rosa, 1899; Atwater and Benedict, 1905; Benedict and Carpenter, 1910). Those expired gas fractions and air flows can be measured using a mouthpiece, covered hood (both open circuit) or sealed room or system (closed circuit).

The energy in protein is not liberated through the same metabolic processes. The transamination of amino acids liberates the anime group before the remaining structure enters the metabolic pathways, the urea and kreb cycles, after which, it is excreted from the body in the form of urea. The metabolic determination of urinary nitrogen (Lusk, 1928) made it possible to estimate whole-body energy expenditure using respirometry, including daily basal metabolic rate (Weir, 1949). At rest, the energy contribution from amino acids is considered relatively stable. Therefore, it is possible to substitute protein energy contributions with a constant when calculating metabolism. In healthy participants, this method only increases the error by 2% (Weir, 1949), and thus, estimates of energy expenditure can be made without the measurement of urinary nitrogen. This method is considered a reliable and more immediate approximation of energy expenditure (Weir, 1949; Turell and Alexander, 1964; Westenskow *et al.,* 1988; Mansell and MacDonald, 1990), and by utilising this method, it is possible to estimate basal metabolic rate within this project.

The Haldane transformation (1892; Geppert and Zuntz, 1888) made it possible to perform indirect respirometry without using a closed-loop system (closed-circuit respirometry). This open-circuit method enabled the creation of smaller and more portable gas analysis systems, increasing the feasibility of measuring energy expenditure during exercising states. Moreover, respirometry can overcome some of

[10] Metabolic stoichiometric equations for carbohydrate (i) and fat (ii):
(i) $C_6H_{12}O_6 + 6O_2 \rightarrow 6CO_2 + 6H_2O$
(ii) $C_{57}H_{104}O_6 - 6H_2O + 80O_2 \rightarrow 57CO_2 + 46H_2O$

the limitations of direct calorimetry for exercising conditions, with faster metabolic response times (1-2 min to steady state: Kenny *et al.,* 2008) and an easier ability to quantify the work of exercise, since some of this heat is often stored within the body initially (Kenny, 2017; Schoffelen, 2017). Nonetheless, the method of respirometry is not without its limits, and requires a number of conditions to be met before data can be assumed accurate. Some of these include: the attainment of a steady state, accurate gas, flow, temperature and pressure readings, a correct pre-test calibration and no leaks anywhere between the participant's airways and the gas analysis system (Archiza *et al.,* 2017; Shephard, 2017). Thus, providing the testing assumptions are satisfied, modern respirometry devices permit researchers the flexibility to test during a wide range of activity conditions, such as those explored in future Chapters (Chapters 2-5).

There is an alternative method to calculate whole-body energy expenditure within clinical settings, whereby blood, rather than respiratory, gas fractions are measured. These values can be used to approximate oxygen consumption by rearranging the Fick equation (Fick, 1870); the so-called direct Fick method. The formula was initially created to estimate cardiac output, however, by accounting for haemoglobin and oxygen saturation, oxygen consumption can be estimated from measures of cardiac output and the oxygen concentration of arterial and venous blood (Liggett *et al.,*1987). While this method permits the measurement of oxygen delivery rates, it does not measure oxygen consumption at the lungs and has thus been shown to consistently underestimate energy expenditure compared with respirometry (Levinson *et al.,* 1987; Stock *et al.,* 1992; Williams and Fuenning, 1991; Flancbaum *et al.,* 1999). Moreover, with advances in technology increasing the speed and accuracy of respirometry, respirometry, rather than the use of arterial catheters, has become the preferred method to estimate metabolic rate even within the clinical setting (Levinson *et al.,* 1987; Takala *et al.,* 1989).

2.1.2 Scaling whole-body, basal metabolic rate

During a basal state, a wide variance in metabolic rate can be observed across an adult, human population (Quenouille *et al.,* 1951; Cole and Henry, 2005). Differences in body mass explain approximately 70-80% of this variation (Elia, 1992;

Johnstone *et al.,* 2005; Müller *et al.,* 2013). Indeed, it is intuitive that the possession of more cells must be accompanied by a greater absolute metabolic rate. However, because of that relationship it is difficult to compare absolute metabolic data obtained from individuals of varying body sizes. To permit such comparisons, the effect of body size must first be removed from those metabolic data.

Mass-independent metabolic data are typically generated by normalising data to a chosen index of body size (for example, body mass). To successfully achieve this outcome, the normalisation approach must reflect the nature of the scaling relationship between body mass and metabolic rate. In addition, once that relationship is understood, it becomes possible to not only normalise data but to also predict the metabolic rate for individuals who have yet to be tested. However, a consensus on how to best describe the scaling relationship between oxygen consumption and body mass in humans is yet to emerge. As a result, two opposing scaling approaches are concurrently used within the literature when describing human metabolic data: linear (first-order polynomial regression: Harris and Benedict, 1919; Schofield, 1985; Cole and Henry, 2005) and non-linear (allometric [power] regression: Boothby and Sandiford, 1922; Rogers *et al.,* 1995; Markovic *et al.,* 2007) scaling. Due to the long-standing use of these two scaling approaches within the human-metabolic literature, both have been selected for analysis within this series of investigations to evaluate their appropriateness for describing human metabolic data both individually and against one another.

A concern with the use of both models is that the predictive error between them increases with the distance from the mean, particularly when data are less than the mean. That outcome is demonstrated by the shaded area in Figure 2.1. This response is particularly important to consider when a model might be used to predict data at the extremes of, or beyond its measured range. Moreover, when no alternative is available, that model might also be used to predict metabolic responses across other human populations *i.e.* women, children and the elderly, despite population-specific differences in metabolism. Therefore, extrapolated data must remain realistic. As a result, the applicability of both models is questioned when evaluating metabolic data across a broad mass range. Consequently, the primary aim within this experimental

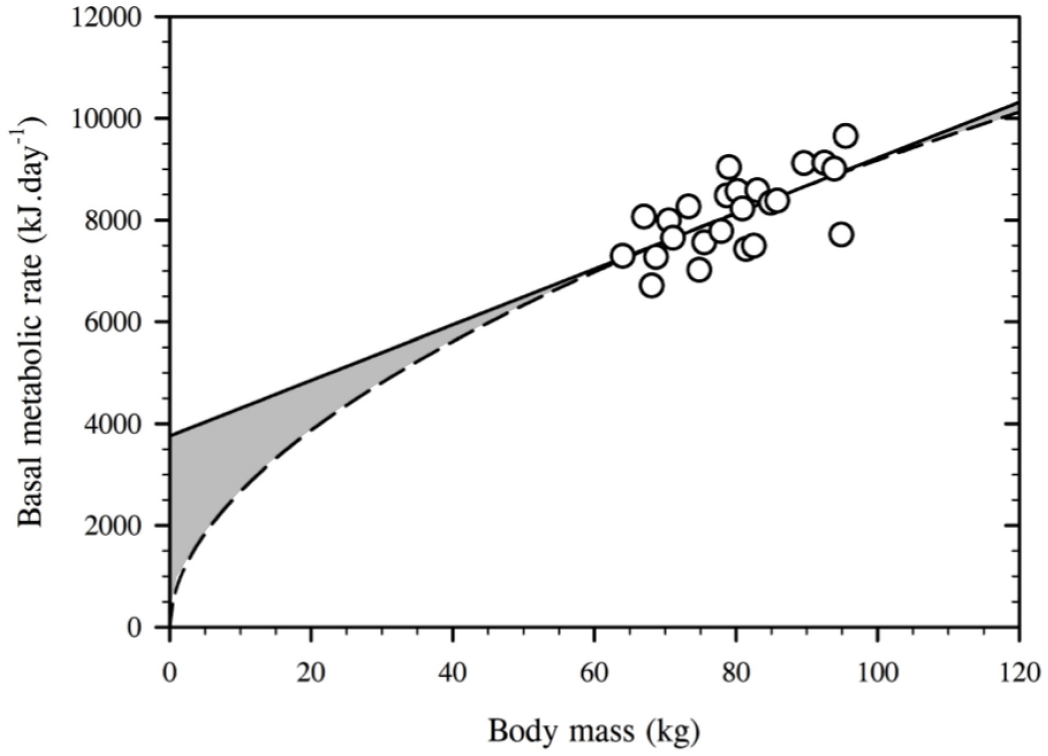

Figure 2.1: A scatter plot of the relationship between body mass (kg) and metabolic rate (kJ.day^{-1}) in 24 adult males (64.0 - 95.5 kg). Two least-squares regressions were applied to the data and extrapolated to zero mass: a linear (solid line: $y = 54.64x + 3758.81$; $P < 0.05$) and a power model (dashed line: $y = 774.68x^{-0.537}$; $P < 0.05$). Both models fit the data with a similar accuracy. However, as indicated by the shaded area, an increasing predictive error is evident as those models extend away from, and particularly below the mean (8115.66 kJ.day^{-1}; 79.74 kg), demonstrating that, for the same dataset, only one model can accurately describe the relationship between the two variables.

phase was to determine which scaling method is more appropriate to use when analysing the mass dependency of human metabolic data.

2.1.2.1 Linear scaling

Morphometric scaling is used to define the structural and functional consequences of a change in size. One method of choice, linear scaling, assumes a proportional relationship between metabolic rate and body mass. In its simplest form, isometry or ratiometric scaling, linear scaling can be used to describe the change in size among geometrically similar shapes. Consider a cube. A change in the size of any cube is brought about by equal increments in the length of its sides. Thus, the scaling relationship reveals a one-to-one (proportional) ratio between its size variables. As a consequence, the regression model that describes this relationship must pass through the origin, and can be described mathematically as: $y=ax$. Moreover, for such datasets, the mass relationship can be simply removed by dividing the absolute metabolic data by body mass, to generate mass-specific units: $kJ.kg^{-1}.day^{-1}$ (Tanner, 1949; Albrect *et al.,* 1993).

Alternatively, in instances where the relationship is linear but does not pass through the origin, a non-zero intercept (c) must be applied to the regression equation (first-order polynomial: $y= ax + c$; Figure 1.1A). This approach is more commonly observed when a linear regression is applied to a human metabolic dataset (Harris and Benedict, 1919; Schofield, 1985; Cole and Henry, 2005). However, the addition of this intercept constant produces two noticeable effects on the scaling model. Firstly, it becomes non-viable to normalise data using a ratiometric approach (Tanner, 1949; Katch, 1973; Packard and Boardman, 1988), despite its ubiquitous use. Indeed, the difference between the measured (solid line: Figure 1.1A) and assumed regression slopes generates a systematic bias among the mass-specific, normalised residuals (Figure 1.1B).

While other normalisation methods do exist to effectively remove that body-mass relationship in a linear dataset, such as an Analysis of Covariance (Packard and Boardman, 1999; Karp *et al.,* 2012) or by rearranging the regression formula ($k= [y-c]/ax$; where, $k=$ normalised metabolic data, $y=$ measured metabolic rate, $c=$

intercept constant, a= coefficient [slope], x= body mass; Albrect *et al.,* 1993), these are often overlooked. Therefore, although it is not a new argument, the effect of ratiometric normalisation for a metabolic dataset will be briefly explored within this experimental phase to demonstrate the consequences of its use.

Secondly, the presence of a non-zero intercept reduces the predictive capacity of a metabolic scaling model (Tanner, 1949; Packard and Boardman, 1988; Albrecht *et al.,* 1993). That is, it is physiologically impossible to have a non-zero metabolic rate at zero mass. As a result, unrealistically large metabolic rates would be predicted at very low body masses, and, at heavier mass ranges, metabolic rates would be under predicted (Figure 1.1A). Consequently, for the regression model to be biologically appropriate across a broad mass range, it must intercept the origin (ratiometric regression).

Nevertheless, despite these constraints, linear scaling has sometimes been applied without appropriate consideration for the implications of violating these obligations. Indeed, some often-cited, large-scale studies contain regression models with a non-zero intercept (Harris and Benedict, 1919; Schofield, 1985; Cole and Henry, 2005). However, extrapolated data would increase in predictive error with its distance from the mean. Not considering the non-uniform rates of growth during childhood (Holliday, 1971), such a response could produce discrepancies in predicted metabolism for individuals nearing age-specific model thresholds and, thus, also introduce normalisation errors. Consequently, such a model would only have predictive validity within the mass and age ranges tested.

It is possible to overcome those intercept constraints by forcing the regression through the origin, thus artificially generating a ratiometric model. However, if the original ordinate-intercept was significantly different from zero, this approach would generate a reversed systematic error to that observed if using mass-specific normalisation on a non-ratiometric relationship (Tanner, 1949; Figure 1.1B). Indeed, this would lead to an over-prediction of metabolism in individuals heavier than the mean mass and an under-prediction in those lighter (Atchley *et al.,* 1978; Karp *et al.,* 2012). Therefore, this method must be used with caution.

In summary, linear scaling is not suitable for all biological datasets. Before applying that method, it is important to consider both the statistical and biological assumptions. To apply linear scaling, it is assumed that the relationship is linear, that it is normally distributed, that the residuals have a constant variance of error (homeoscedasticity) and that no autocorrelation exists between the variables (Poole and O'Farrell, 1971). In addition, when applying this scaling approach to human data, it is necessary to consider the variables measured, for these will exert further model constraints. Specifically, when scaling against body mass an origin intercept is necessary to accurately describe those data, particularly at lower mass ranges. In instances where these assumptions are not met, an alternative approach might be to apply a non-linear regression to these data, and the principle objective of this research stage was to evaluate that possibility.

2.1.2.2 Non-linear scaling

In circumstances where the assumptions of linear scaling are violated, it is often more suitable with biological datasets to fit data with a power curve (Schmidt-Nielsen, 1984). This type of non-linear scaling is often referred to as allometry and can be applied when the dependent variable increases disproportionately with an increase in the independent variable. The assumptions of a non-linear power-model are more flexible than those used in linear regressions for instances of heteroscedasticity are accepted. A normal distribution is not required within the data. While it would help to reduce the model error, it is more common for biological datasets to have a positive skew, increasing in distribution as the mass range becomes heavier (Kleiber, 1932; Benedict, 1938, White and Seymour, 2003).

Perhaps the most commonly used power model when describing basal metabolic data is that which describes the geometric relationship between surface area and volume. Consider a cube once more, its surface area can be calculated by squaring its length and, by the same concept, its volume equals its length cubed. With both surface area and volume now expressed within the same units it becomes clear that the cube's surface area is two-thirds of the value of its volume ($volume^{2/3}$). This relationship results in an increase in surface area by only two-thirds for every whole increase in volume, or mass.

Within basal metabolic research in animals, the earliest scaling regression equation applied to data was nonlinear, against mass$^{0.67}$ (Sarrus and Rameaux, 1839). The concept of scaling a geometric surface area was likened to this metabolic scaling model and combined with Bergmann's (1848) rule, that body size dictates heat loss and habitat, and Allen's rule (1877), that surface area dictates heat loss, to form what has today become known as Sarrus and Rameaux's "surface law" (Rubner, 1883; Richet, 1889; Voit, 1901). It is theorised within the surface law that metabolic heat production is limited by the potential for heat loss from an animal, which at the time was believed limited by the animal's surface area, or mass$^{0.67}$. For if metabolic heat was produced faster than it could be lost (through the skin's surface), then the cumulative heat storage within the body would eventually lead to a lethal state of hyperthermia. The adoption of this theoretical approach within the literature has led to the common use of surface area (mass$^{0.67}$) as a morphological unit when reporting basal metabolic data.

However, it is now understood that the rate of thermal energy transfer in homoeotherms is not solely proportional to changes in external temperatures and thus the temperature gradient between the body and surrounding environment is not only determined by the geometric shape (, 1888). As discussed (Section 2.1.1.1), thermal energy transfer is governed by both passive structures (body mass, composition and surface area) and active thermoregulatory mechanisms (vasomotion, sudomotion, and behaviourally). Furthermore, at rest, neither the thermoregulatory system nor heat production are maximal (Fortney and Vroman, 1985; Krustrup *et al.,* 2001), for metabolic rate is primarily dictated by the energy demands of the organs rather than a limiting variable in the metabolic pathway (Elia, 1992). Together, these facts make it difficult to infer that heat loss through the body's surface area is the limiting factor to the rate of metabolism, despite the fact that the scaling relationship could be described by plotting metabolic data again mass$^{0.67}$.

The discrepancy between the exponent value and theoretical explanation behind the surface law has divided researchers for the better part of a century, and led to some researchers reinvestigating the relationship and promoting the use of a new, higher scaling exponent (mass$^{0.75}$: Kleiber, 1932; West *et al.,* 1997). However, a reappraisal

of this new scaling value suggests that it may be artificially inflated due to the inclusion of large ruminant animals within the datasets analysed (McNab, 1997), as these animals are unlikely to reach a post-absorptive state. Nevertheless, the debate as to which value to use when scaling animal basal metabolism still continues today (West *et al.,* 1997; Dodds *et al.,* 2001; Darveau *et al.,* 2002; White and Seymour, 2003; White and Kearney, 2014). Though, regardless of the discrepancy over the exponent value, it is important to note that the fact that basal metabolism can be described as a power function of body mass has remained undisputed both within and across species in animals. For this reason, it was assumed that, if non-linear, human metabolic data would scale by a similar, allometric approach.

While in animals the reappraisal of the $mass^{0.67}$ scaling exponent led to the use of an additional non-linear model ($mass^{0.75}$), in human research the scaling method was split between non-linear (Harris and Benedict, 1918, 1919 [use of surface area for normalisation]; Boothby and Sandiford, 1922; Durnin, 1981) and linear approaches (Section 2.1.2.1: Harris and Benedict, 1919; Schofield, 1985; Cole and Henry, 2005). This stemmed from an early publication that supported the use of linear modelling to describe human metabolic data (Harris and Benedict, 1919), despite the fact that no comparisons to non-linear methods were intentionally performed within the original article (Harris and Benedict, 1919, p.87). It is possible that this linear approach was favoured either for its ease of statistical analyses or because the human mass range tested provided little visual confirmation of a non-linear relationship. After that article, some model comparisons were made between both scaling approaches (Boothby and Sandiford, 1922; Durnin, 1959). However, within those articles a relationship with surface area, using the DuBois method (DuBois and DuBois,1916), was assumed for the non-linear option, rather than determining the regression shape from those datasets. Using those comparisons, a compelling argument was not made for the adoption of non-linear scaling for human datasets. Nonetheless, as discussed previously (Section 2.1.2.1), such linear models with non-origin intercepts are likely to introduce error into analyses and should be avoided for biological datasets. Yet, use of this approach has remained consistent within some areas of human metabolic research.

More recently, the appropriateness of both scaling methods (linear and non-linear) have been reexamined in the human literature (Rogers *et al.,* 1995; Heymsfield *et al.,* 2007; Markovic *et al.,* 2007). Though, due to sample and method limitations, a definitive conclusion on how basal metabolism scales against body mass has not yet been reached. As demonstrated in Figure 2.2, within a narrow mass range both regression methods can appear similar visually, which may result in the utilisation of an incorrect scaling model. Therefore, to assess the possibility of non-linearity within a dataset, the sample must be both large in number (>30: Jensen *et al.,* 2001) and broad in mass range. In addition, since basal metabolism is easily influenced by physiological and morphological variations (Fleisch, 1951; Mitchell, 1962; Holliday, 1971; Compher *et al.,* 2006), before a confirmed scaling model has been identified for humans, known covariates should be removed to prevent any masking of the true relationship. Consequently, participants must also be homogeneous except for changes in body mass.

However, in papers exploring this bivariate relationship, these concerns are often overlooked; many recruit heterogeneous samples to reach the wider mass ranges (Rogers *et al.,* 1995; Batterham and Jackson, 2003; Heymsfield *et al.,* 2007, 2009). Furthermore, within those papers found, basal metabolism was not the study aim and thus only resting metabolism was measured. Compared with basal metabolism, resting measures introduce further variables into the data that will increase metabolic rate, for example, non-post-absorptive states (Haugen *et al.,* 2003), recent exercise activity (Gillette *et al.,* 1994), the consumption of caffeinated beverages (Koot and Deurenberg, 1995), and the time of day of the measurement (Haugen *et al.,* 2003). Therefore, it has been difficult to accurately discern any specific scaling relationship within the human literature to date.

Accordingly, there were two aims within this experimental phase. The first was to determine whether it is more appropriate to scale human basal metabolism using a linear or non-linear approach. Throughout the scaling literature, two ubiquitous models have been used to describe metabolic data: first-order polynomial (linear) and simple power regressions (non-linear). It was therefore assumed that each model represented the most appropriate formula for its respective scaling method. As such,

with the exception of ratiometric scaling, unless a poor fit was demonstrated for both scaling options, no additional regression method was evaluated. The second aim within this phase, if a non-linear model was deemed more appropriate, was to assess whether or not the scaling exponent matched that reported for other homoeothermic species ($mass^{0.67}$). These aims would be assessed using a sample broad in mass range but otherwise physiologically and morphologically homogenous.

2.1.3 Postural changes and energy expenditure

So far the scaling of energy expenditure has mainly been discussed in relation to a basal state. However, the focus within the overall project goes well beyond that metabolic intensity, and so it also becomes necessary to understand how to scale metabolic rate across a range of non-basal states. By first understanding that relationship during a basal state, it was possible to establish a baseline for the relationship against which all other activity conditions could be compared, commencing with a change in posture. During non-basal states, the nature of the scaling relationship was assessed using oxygen consumption rather than metabolic rate. Accordingly, both units have been used to describe the scaling relationship and have been used in an intensity-specific way: metabolic rate for basal and oxygen consumption for non-basal intensities.

In animals, the stepwise increase between oxygen consumption and metabolic intensity corresponds with a steepening of the scaling regression between oxygen consumption and body mass (Taylor *et al.,* 1970, 1982; Kram and Taylor, 1990). That change in shape is caused by differences in mass-specific oxygen consumption capacity across the animal mass range. That is, while at rest, larger animals use less energy per kilogram of body mass (Kleiber, 1932; White and Seymour, 2003), but, they also have a larger capacity for an increase in energy expenditure when active, to accommodate for their greater requirement of energy expenditure at the same level of work (Weibel *et al.,* 2004). This results in a steeper scaling coefficient in active versus resting states when modelled (Taylor *et al.,* 1970, 1982; Kram and Taylor, 1990).

The current mechanisms believed responsible for this change in model coefficient

have been detailed within the allometric cascade theory (Darveau *et al.,* 2002; Hochachka *et al.,* 2003; Suarez, 2012). This theory links whole-animal metabolism with cellular metabolism, such that one or more of the many limiters along the metabolic pathway, such as pulmonary diffusion, cardiac output, and the function of sodium and calcium pumps, will affect the steepness of this regression relationship (Hochachka *et al.,* 2003). The proposed reason for this change in the model coefficient is the shift in the dominant metabolic pathway with an increase in activity level (Darveau *et al.,* 2002). For example, during a basal state the metabolic rate is primarily driven by the energy demand of the organs and the limiters to energy turnover are not stressed (Elia, 1992), whilst during maximal work, energy expenditure is driven by the working muscles but this rate can be limited at one or more points along the metabolic pathway. This reasoning seems to be the most plausible theory to explain the scaling of oxygen consumption and its relationship with metabolic intensity so far.

In humans, the effect of metabolic intensity on the nature of the scaling relationship still requires a more comprehensive investigation to understand both its scaling shape (linear or non-linear) and whether it differs across intensities (as detailed previously: Section 2.1.2.2). Since a simple change in posture can significantly increase oxygen consumption (Booyens and McCane, 1957; Taylor *et al.,* 2012), to begin this theme of investigation, this relationship was first explored between supine and standing states. Accordingly, this comprised the second part of this experimental phase, with the aim of determining whether or not a change in posture significantly increased metabolic intensity to modify the scaling shape.

To modify the shape of the scaling relationship, there would need to be a non-relative increase in oxygen consumption across the body-mass range. By moving from a supine to standing position, sympathetic nervous activity increases to promote venous return from lower-limb blood pooling (London *et al.,* 1983, Gaffney *et al.,* 1985; Pannier *et al.,* 1991) and activates the postural muscles to support the body (Danna-Dos-Santos *et al.,* 2014; Hellebrandt *et al.,* 1940). Consequently, oxygen consumption increases to accommodate these physiological changes within the body, with mean values ranging from 5-10% between supine to sitting (Benedict and

Benedict, 1924; Moreno and Lyons, 1961) and 10-25% between supine to standing states (Tepper and Hellebrandt, 1938; Booyens, 1957). Nevertheless, it is unknown whether those values change with body mass, and moreover, whether they would result in a significant change to the scaling relationship compared with that of a basal state. Accordingly, a secondary aim within this experimental phase was to determine whether or not a non-exercising state in humans would induce this shift in the scaling model. This was an important consideration to explore, for a change in the regression shape would mean that a unique means of analysing steady-state data may need to be applied to each new activity level tested when analysing energy expenditure.

2.1.4 Aims and hypotheses

In summary, the primary aim within this experimental phase was to identify whether it was more appropriate to scale human basal metabolism using a linear or non-linear approach. To investigate this possibility, participants spanning a wide mass range were tested during strict basal conditions. Though those participants varied considerably in size, they were similar in age, gender and adiposity, to minimise variations in metabolic rate beyond those generated as a consequence of a change in body mass (see Section 2.2).

The subsequent aim was to determine whether the scaling relationship observed during a basal state was modified by a change in posture, that being standing. If that increase in metabolic intensity resulted in a unique scaling relationship then separate scaling approaches would be required when predicting and normalising oxygen consumption data during different resting states in humans. To minimise the error between both regressions, a repeated-measures design was used and both intensities were tested during the same laboratory visit.

A consideration within this project was that, the scaling method adopted needed to be both statistically and biologically relevant for a metabolic dataset. Thus, the dataset was required to meet the assumptions of linear regression while either in a raw (linear: first-order polynomial) or log-transformed (non-linear: allometric) format (see Section 2.2.5.2 for details). Moreover, energy expenditure could not increase by a greater rate than body mass and must equal zero at zero mass.

To assess these aims, this experiment was designed to evaluate four hypotheses:

Hypothesis Two-One: It would be more appropriate to scale human basal metabolic rate against body mass using a non-linear (allometric) rather than linear approach.

Hypothesis Two-Two: Assuming a non-linear scaling approach best fits the basal dataset, the body-mass exponent observed would be statistically similar to that observed within mammalian studies ($mass^{0.67}$).

Hypothesis Two-Three: Non-linear regression would remain the more appropriate model to describe the scaling relationship between oxygen consumption and body mass during a standing (rest) state.

Hypothesis Two-Four: Assuming that oxygen consumption scaled nonlinearly against body mass during the standing condition, the body-mass exponent observed would be statistically similar to that applied to the basal dataset.

2.2 METHODS

2.2.1 Considerations for subject recruitment

When designing experiments that centre around the metabolic scaling of a single species, a wide body-mass range is required. This can be difficult to achieve. In previous human studies, this issue has been addressed by sampling children through to adults, of both genders (Boothby and Sandiford, 1922; Schofield, 1985; Rogers *et al.,* 1995). However, as the rate of energy transformation is not uniform within the body, varying across tissue types; from 9.6 $kJ.kg^{-1}$ in bone to 1841 $kJ.kg^{-1}$ in the kidneys (Table 2.1), any change in the tissue proportions of the body across participants will have a direct effect on whole-body and mass-specific basal metabolic rate. Therefore, the recruitment of a more homogeneous sample, with respect to age and maturational status, is necessary to minimise errors associated with body-mass scaling for whole-body metabolism.

2.2.1.1 Metabolic and compositional changes with age and gender

Since mass-specific basal metabolism reduces with age-related growth (Harris and Benedict, 1919; Mitchell, 1962), sample considerations were made to select an age range within which these variations were minimal. The primary cause for this reduction in mass-specific metabolic rate is the disproportionate growth rate of the tissues and organs (Holliday, 1971; Müller *et al.,* 2013), whereby the metabolically

Table 2.1: Variations in tissue-specific metabolic rates and the proportional differences of those tissues within ageing humans, for both a reference adult and neonate.

Tissue	Mass-specific metabolic rate ($kJ.kg^{-1}.day^{-1}$)	Adult (70 kg; 7530 $kJ.day^{-1}$)		Neonate (3.5 kg; 824 $kJ.day^{-1}$)	
		Percentage body mass (%)	Percentage of whole-body metabolic rate (%)	Percentage body mass (%)	Percentage of whole-body metabolic rate (%)
Liver	836.8	2.5	21.0	4.0	20.0
Kidney	1841.0	0.5	8.0	0.7	7.0
Brain	1004.2	2.2	20.0	10.0	44.0
Heart	1841.0	0.5	9.0	0.6	4.0
Skeletal muscle	54.4	40.0	22.0	22.0	5.0
Adipose tissue	18.8	21.4	4.0	12.0	<1.0
Bone	9.6	15.0	6.0	20.0	<1.0
Residual	variable	17.9	10.0	30.7	~ 18.0

Notes: The mass-specific metabolic rates and adult body proportions of the four highest contributing organs to basal metabolic rate (liver, kidney, brain and heart) were first identified (Elia, 1992). These were compiled with the mass-specific metabolic rates of the three tissue types that contributed the greatest percentage of body mass: bone (Heysfield *et al.,* 2002), skeletal muscle and adipose tissue (Elia, 1992). Neonate tissue masses were complied from Boyd (1962) and Holliday (1986), and used to calculate the tissue-specific percentages of whole-body metabolic rate.

more active tissues grow at slower rates than the less active tissues, such as the bones and muscles. These disproportionate growth rates result in dramatically different organ-specific contributions to whole-body metabolism between children and adults contributions for whole-body metabolic rate.(Table 2.1), particularly for the brain and skeletal muscle. Moreover, even after normalising for variations in body surface area, the basal metabolic rate of an adult is still 30% lower than that of a 1-y infant (Fleisch, 1951; Mitchell, 1962). Accordingly, for the purposes of this project, children (< 18 y) were excluded from the population sample.

In comparison, the body composition of adults shows fewer disproportionate changes with increments in body size (when controlling for adiposity). For example, across a healthy, adult-male mass range, the combined mass of the brain, liver, kidneys and heart (which account for 70-80% of whole-body basal metabolic rate: Holliday *et al.,* 1967) increase by only 2.5%[11]. Nevertheless, once maturation is reached, a 2% decrease in basal metabolic rate is still evident per decade, that becomes more apparent from 40 y in men and 50 y in women (Fleisch, 1951; Tzankoff and Norris, 1977). Therefore, to avoid possible age-related changes to metabolic rate, subjects over the age of 35 y were also excluded. This left a participant age range of 18-35 y.

Notwithstanding the impact of age, variations in basal metabolism still exist between genders. Women have a lower basal metabolic rate than men (Arciero *et al.,* 1993, Webb, 1981), even after controlling for menstrual-cycle fluctuations (Soloman *et al.,* 1982; Webb, 1986) and differences in lean body mass (Arciero *et al.,* 1985; Buchholz *et al.,* 2001). It is probable that the remaining differences in basal metabolism are, at least in part, a result of the sexual dimorphism evident between genders (Wells, 2007): men have a higher skeletal mass than women, particularly at the limbs, as well as a lower adiposity levels (Nindl *et al.,* 2002). As a result, normalising data against body mass does not effectively remove the gender differences in metabolic rate (Buchholz *et al.,* 2001), for it does not account for the variations in adiposity between

[11] Variations in adult-human organ sizes were calculated using magnetic resonance imaging (Personal communication: Müller, 2015). Organ size ranged from 4.4-6.9% body mass, with total difference of 2.5%, correlating negatively with body mass (r^2 = 0.35). Participants with a fat mass greater than 25% (Dual Energy X-ray Absorptiometry) were excluded from the calculations to replicate the population used for the current study.

both genders. Consequently, to negate this potential source of error, only men were recruited for this project.

2.2.1.2 Controlling for variations in body adiposity

At the same body mass, an increase in adiposity will result in lower mass-specific basal metabolic rates (Buchholz *et al.,* 2001; Heysmsfield *et al.,* 2002), yet a higher external work rate during ambulatory states (Goldman and Iampietro, 1962). Since both states would be investigated, it was essential that adiposity levels across participants remained within a narrow range. There are many methods to estimate body composition (Wagner and Heyward, 1999; Wells and Fewtrell, 2006), but for this experiment, it was necessary that the method chosen was both available for use within the current laboratory, and enabled an unbiased comparison between individuals of varying body sizes.

Skinfold callipers are an easily accessible and relatively inexpensive equipment used to measure subcutaneous adiposity. Previous approaches to estimate body fat percentage using these measurements (Durnin and Womersley, 1974; Jackson and Pollock, 1978) have been found to rely on invalid assumptions that introduce errors (Clarys *et al.,* 1987; Johnstone, 1982; Martin, 1984). However, absolute skinfold data can be used to provide an accurate comparative index (Martin *et al.,* 1985), although it becomes necessary to have a method to compare absolute skinfold measurements across individuals of varying body sizes. The method of choice was a height-adjusted sum of skinfolds (relative adiposity; see methods Section 2.2.4.4).

It was possible to compare those height-adjusted data against a previously-designed morphometric model of unisex anthropometric reference values[12], the anthropometric phantom, that was originally designed to compare variances in proportional growth (Ross and Wilson, 1974). This hypothetical individual was developed from population normative data (Garrett and Kennedy, 1971; Wilmore and Behnke, 1969, 1970). Utilising the principles of geometric similarity, each anthropometric measurement is

[12] A set of gender- and race-independent, normally distributed reference characteristics were generated for the adult phantom (Ross and Wilson, 1974). Those anthropometric values relevant to the current study include: stature, 170.18 cm; mass, 64.58 kg; lean body mass, 52.45 kg; fat mass, 12.13 kg; percentage fat, 18.78 kg.

assumed to be normally distributed with reference standard deviations provided; these are calculated from the average coefficient of variations within the compiled original datasets for each variable. To compare individual data, raw values are scaled to a common stature, from which a phantom *z*-score can then be assigned (Ross and Wilson, 1974). Application of this technique was utilised within the current project as a method of comparing anthropometric measures across participants. Moreover, the method provided a means to quantitatively assess and control participant homogeneity for measures of subcutaneous adiposity.

2.2.1.3 Determining the body-mass range and sample size

Prior to testing, it was necessary to determine both the body-mass range and the number of participants required to reduce the standard error of the mean of the derived regression coefficients. It was possible to determine these requirements by using data from the literature in combination with *a priori* statistical analysis.

When testing humans, it is impossible to meet the mass ranges previously analysed within comparative physiology. Multi-species studies now span a mass range of six magnitudes (Sieg *et al.,* 2009), and for single-species studies a 45-fold mass range still exists (Rubner, 1883 [dogs]). In contrast, the available mass range of adult humans is dramatically reduced, from 55 kg to 110 kg (5^{th} and 95^{th} percentiles: Australian Bureau of Statistics, 2012). This range is likely to be reduced further once adiposity is controlled for. Nevertheless, this narrower body-mass range, between human and animal studies, will not nullify the findings within this series of investigations. Indeed, since the focus within these experiments is the scaling of human metabolism, then masses far beyond that mass range may modify the observed outcome. While the selected mass could still be widened using a human population *i.e.* women and children, for the reasons addressed in Section 2.2.1.2, such populations were deemed likely to introduce covariants to the scaling relationship. So, it was considered necessary to sample from a single, controlled population first to ensure that a clear regression shape could be initially determined. Therefore, providing that the extent of this mass range could be obtained, the appropriate regression shape for adult males would still be discernable, despite the available mass range.

In addition to recruiting across a wide mass range, it was important that the sample was of sufficient size to satisfy the statistical requirements for both linear and non-linear regression analyses. After all, with a sample of two data points the shape of the regression would only ever appear linear. A similar outcome might also be observed if the distribution of participants are not even across the mass range tested but polarised at either end of the mass range. Therefore, the sample had to be both sufficient in number and evenly distributed across the mass range to obtain a clear regression shape.

For a linear regression, *a priori* testing generated a minimum sample-size requirement of 11 participants (G*Power v.3.1.9.2, 2014). However, a more reasonable sample size is considered to be ~50 participants (Harris, 1985; van Voorhis and Morgan, 2007) or the more conservative $N \geq 50 + 8v$, where, N is sample size and v the number of independent variables (Green, 1991). Thus, to conform to the linear regression sample requirements, the sample needed to exceed 50 participants.

A second *a priori* test was performed assuming a non-linear relationship (R-project v.3.2.1: R Development core team, 2016), to determine the sample size necessary to reduce the standard error of the mean mass exponent. The test was performed using a hypothetical mass-range between 55 kg and 110 kg, split into five body-mass groups to ensure an even mass distribution (extra small: 55-65 kg; small: 66-76 kg; medium: 77-87 kg; large: 88-98 kg; extra large: 99-110 kg). Testing against an arbitrary exponent of $mass^{0.67}$, adopted from the animal literature (White and Seymour, 2003), bootstrapping[13] was used to predict means and standard errors of the mean for group sample sizes of 5, 10, 15, 20, 25 and 30 (Figure 2.2). Compared with a sample size of 5 subjects per group, sample sizes of 10-15 participants halved the predicted standard error of the mean exponent (57% and 50%, respectively). Since additional subjects beyond these group sizes made minimal decreases to the standard error of the

[13] Bootstrapping (Efron, 1979; Fox and Weisberg, 2017) was used to predict means and standard errors of the means for regression coefficients within this project. For each coefficient, regressions were generated 1000, each with a slightly different sample. When applied to a known dataset, this was achieved by re-sampling from the available dataset. When applied to a hypothetical dataset, such as that used in the *a priori* test, random samples were generated based on fixed sample parameters to mimic a similar effect as re-sampling.

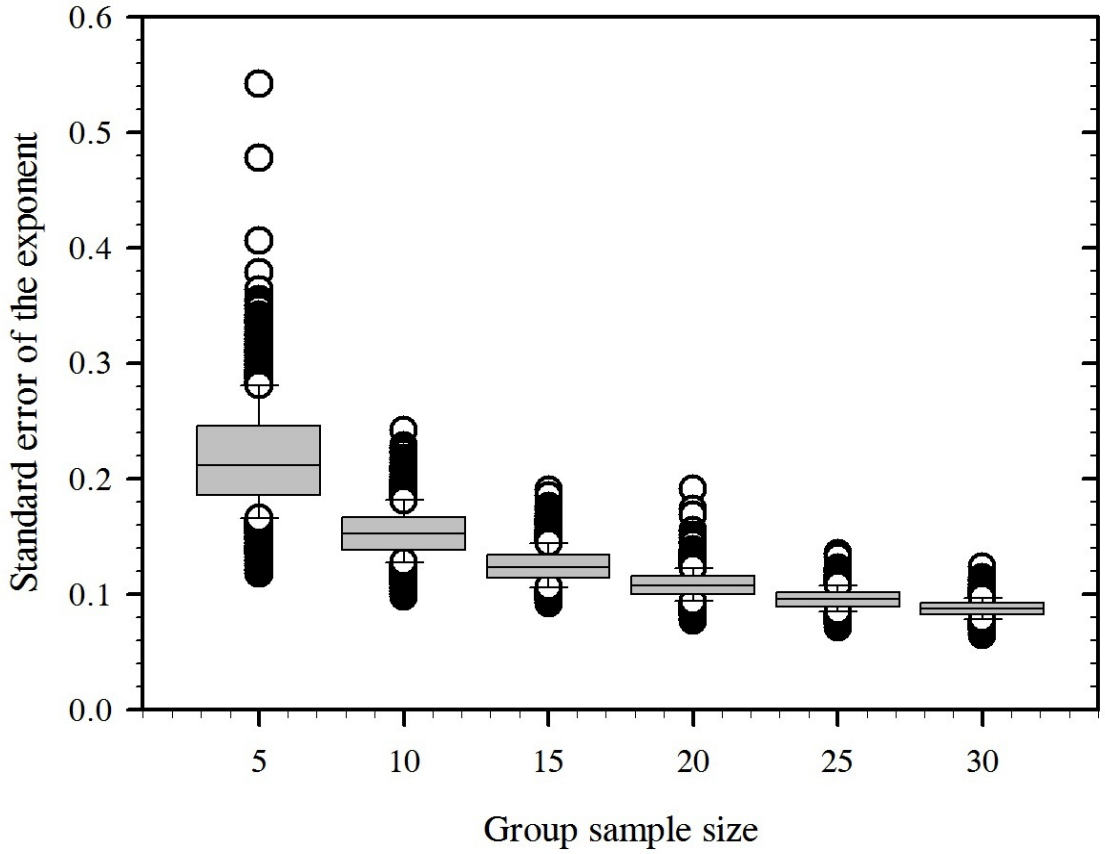

Figure 2.2: An *a priori* test to predict variations in the standard error of the mean mass exponent (non-linear regression) from changes in sample size. Assuming five body-mass groups throughout a hypothetical mass range (55-110 kg), group sample sizes of 5-30 were compared. Bootstrapping was used to predict the presented means and standard errors of the mean (1000 repetitions, using a new hypothetical sample each time).

mean, a sample size of 10-15 participants per group was recruited for the non-linear analysis. In an external human metabolic study, the estimated exponent stabilised with increases in sample size beyond ~30 participants (Jensen *et al.,* 2001). Thus, the target sample size for this study was deemed statistically appropriate. Moreover, in taking this grouped approach to the participant selection, it would also help ensure an even distribution of participants across the sampled mass range. Therefore, considering the requirements for both the linear and non-linear regression analyses, a target total sample size of 50-75 subjects was used for the project.

2.2.2 Subjects

A total of 72 healthy and physically-active men were recruited for this project (Table 2.2) from the local sporting and university population. Participants were evenly distributed across a two-fold mass range (56-117 kg; Figure 2.3). From that sample, 68 participants completed testing within this experimental phase (basal: $N=68$; standing: $N=67$). All subjects were screened to eliminate those with a history of cardiovascular, respiratory or musculo-skeletal pathologies contraindicative of participation in this experiment. Prior to starting the test, all participants were provided with an information package and completed a written, informed consent form. All experimental procedures were approved by the Human Research Ethics Committee (University of Wollongong; HE14/469).

2.2.3 Procedural overview

The shape of the scaling relationship was explored during two metabolic intensities: basal (supine) and standing (rest). The basal condition was used to establish a baseline for the scaling relationship in humans, while the standing condition was used to evaluate whether a change in posture could significantly modify that scaling relationship. Commencing at 0700 h, both trials were completed on the same day to reduce day-to-day variations in energy expenditure. The basal trial was completed first, consisting of a 60-min resting, supine stage in a minimal-stimulus, normothermic environment. Upon completion of that stage, a 10-min standing (stationary) stage was performed. For both trials, participants were dressed in laboratory-provided clothing (pre-fitted combat trousers, a shirt and thick socks: Figure 2.4) and fitted with an auditory canal thermistor (Figure 2.4C) and heart rate

Table 2.2: Subject physiological characteristics. Since a repeated-measures design was used within this project, data are presented for all subjects tested within Chapters 2-6: no differences were observed for any measure among Chapters ($P > 0.05$). Values displayed as means with standard deviations in parentheses, except for ranges.

Participant groups	Sample size (*N*)	Age (y)	Height (cm)	Body mass (kg)	Height-adjusted body mass (mm)	Sum of Skinfolds (mm)	Height-adjusted adiposity (mm)
All	72	23 (3)	182.0 (8.8)	81.6 (14.7)	66.2 (7.8)	61.7 (28.3)	56.7 (24.9)
Extra small	12	22 (3)	172.7 (5.2)	61.3 (2.2)	58.7 (5.6)	42.1 (10.5)	41.6 (10.8)
Small	17	22 (2)	175.8 (5.7)	71.7 (3.1)	65.4 (5.3)	54.4 (18.1)	50.6 (16.3)
Medium	19	23 (4)	184.0 (3.5)	81.4 (2.4)	64.8 (4.9)	55.4 (16.7)	51.4 (16.0)
Large	14	24 (3)	187.6 (6.2)	93.7 (2.6)	70.4 (7.7)	67.8 (20.4)	61.7 (19.3)
Extra large	10	24 (4)	193.1 (7.5)	106.2 (5.2)	74.1 (9.2)	105.7 (41.9)	91.5 (40.2)
Range	-	18-34	163.0-201.5	56.0-117.1	50.2-91.0	28.0-158.0	28.5-151.5

Notes: Skinfold measurements are reported as the sum of data from six sites (triceps, subscapular, abdominal, supraspinale, front thigh, and medial calf: Section 2.2.4.4). Height-adjusted morphological measures adjusted to the common stature of 170.18 cm (Ross and Wilson, 1974).

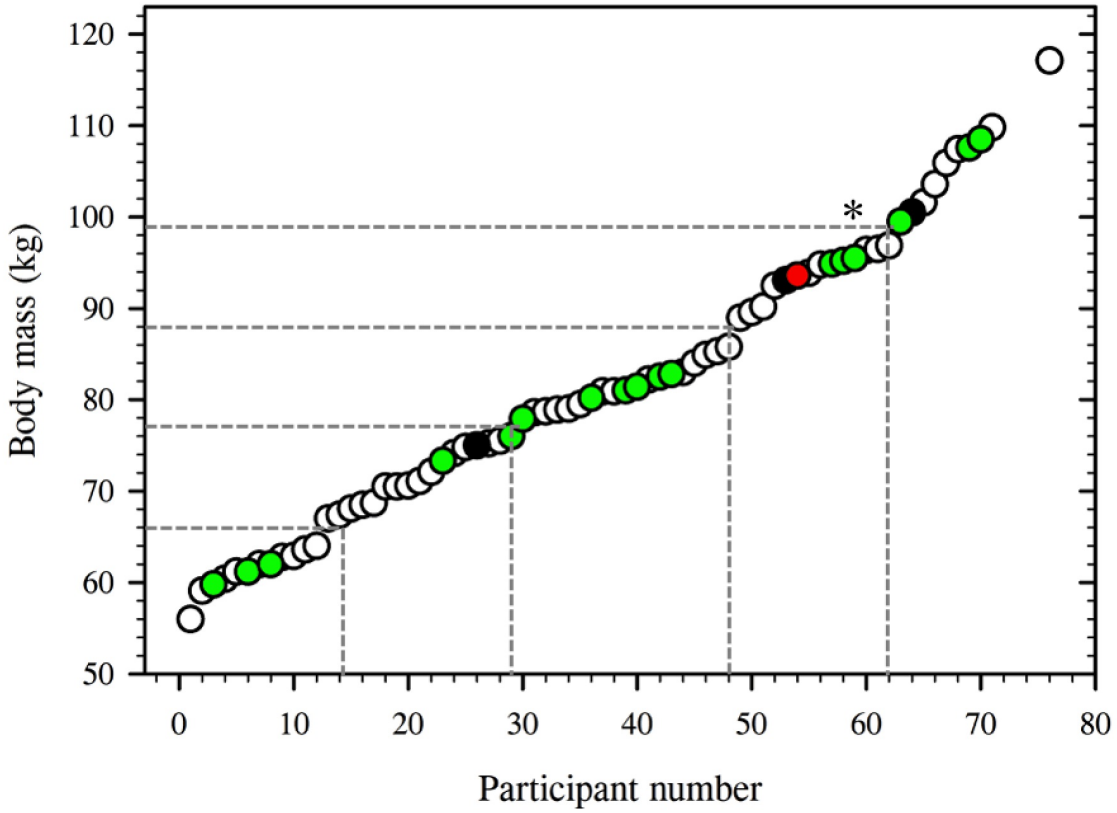

Figure 2.3: Scatter plot of the sample mass distribution, with participants arranged in ascending order of body mass. Data points are displayed for all 72 participants who completed testing throughout Chapters 2-6. Missing (N=3 [black symbols]) and partial datasets (N=1 [red symbols]) are identified using the coloured symbols. The green symbols (N=18) are used to indicate a subsection of the sample who completed a further two exploratory conditions (see Section 2.2.3.2) and the asterix (*) a partial dataset within that group. A break down of all sample sizes is displayed in Figure 2.8. The drop-lines signify the borders separating each of the five body-mass groups and their sample sizes.

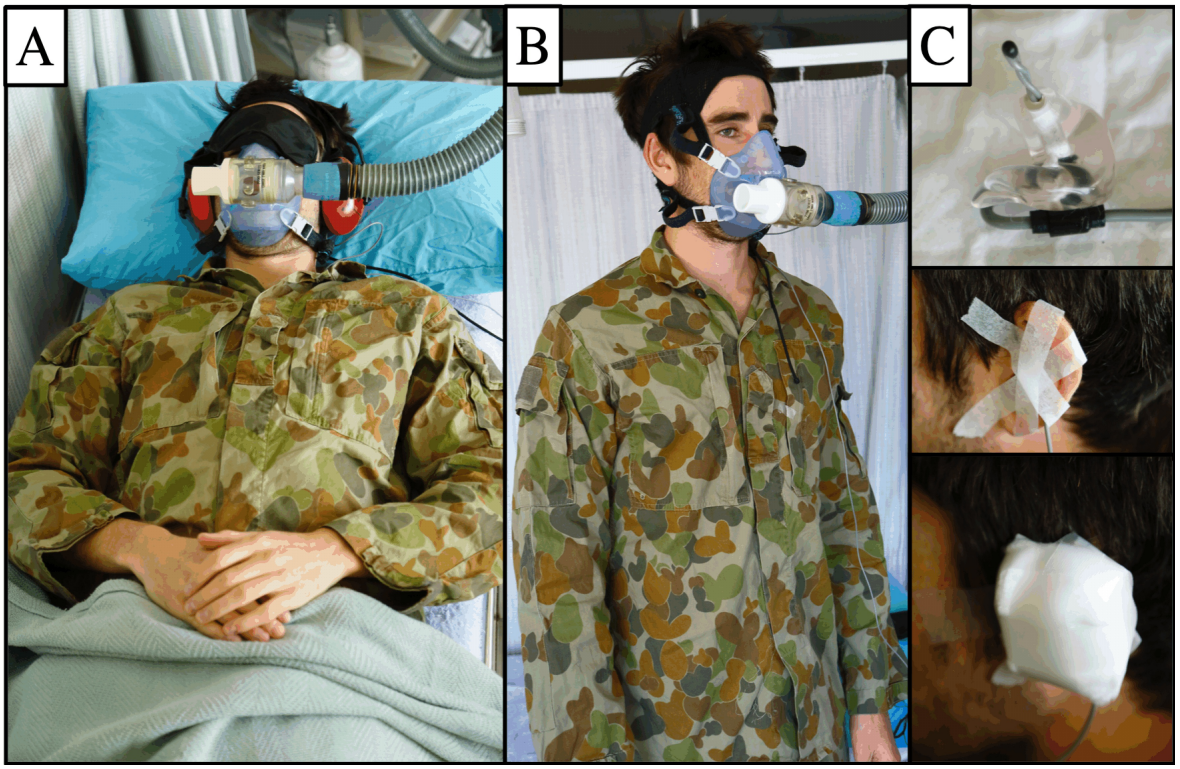

Figure 2.4: (Figure 2.4A) Basal oxygen consumption was measured in a motionless, low-stimulus, normothermic and supine condition. The respiratory tubing was supported using an adjustable crane arm to prevent postural neck stress. Following the basal stage, participants adopted a stationary standing posture next to the bed (Figure 2.4B), where data were further recorded. In the basal and standing stages participants wore an auditory canal thermistor, that was insulated from ambient temperatures using cotton-wool padding (Figure 2.4C).

monitor.

2.2.3.1 Measuring basal and standing oxygen consumption

To quantify basal oxygen consumption, from which basal metabolic rate can be approximated, all participants completed a 60-min supine resting stage in a fasted, but well-hydrated and well-rested state. On arrival at the laboratory, semi-nude and clothed body masses were first recorded. Participants then changed into laboratory provided clothing to standardise thermal gradients between participants, although that clothing was to be worn during all subsequent trials. Once changed, 150 mL water at body temperature (37°C) was consumed before an auditory-canal thermistor, heart-rate monitor and oral-nasal mask were fitted. Subjects were instructed to lie supine on a raised bed and to remain awake for the duration of the basal test (Figure 2.4A). When comfortable, a thin blanket was pulled over participants, to the level of the umbilicus, and external stimuli were minimised using an eye mask and ear protectors. To prevent any increase in oxygen consumption associated with a change in activity level, participants were instructed to lie as still as possible during data collection. However, subjects were instructed to change positions if they became uncomfortable, rather than remain in discomfort. Data immediately following such movements were excluded from the analysis. At the termination of the basal stage, the eye mask and ear protectors were removed for a five-minute seated rest, where participants consumed another 150 mL water (37°C). The 10-min standing stage then commenced with subjects standing stationary next to the gas-analysis system, where they were reconnected to the respiratory tubing (Figure 2.4B).

2.2.4 Experimental standardisation

Since basal metabolic rate can be easily influenced by a wide variety of stimuli (Benedict *et al.,* 1914; Compher, 2006), it was essential that subjects adhered to rigid pre-experimental standardisation procedures, to reduce data variability by removing, or at least minimising, the influence of unwanted independent variables. Participants were all instructed to arrive at the laboratory at 0700 h in a well-rested state, after adequate sleep (~8 h). The day prior to testing, subjects were instructed to refrain from strenuous exercise and to avoid all moderate-to-heavy physical activity within the previous 12 h (Gillette *et al.,* 1994; Williamson and Kirwan, 1997); such exercise

can prolong the return of metabolic rate back to basal levels. Participants fasted for 12 h prior to testing, after being advised to consume an evening meal high in carbohydrates and low in fat, to ensure there were no residual thermogenic effects of digestion on basal metabolism (Haugen *et al.,* 2003); an increase in oxygen consumption to sustain the energy requirements of digestion. The testing was conducted within an air-conditioned laboratory (~23°C; ~50% humidity). Clothing was fitted to participants by the researchers to minimise differences in thermal gradients, and a blanket was available if needed, to ensure that participants remained normothermic; to avoid the increases in metabolism associated with thermoregulatory control mechanisms (Stocks *et al.,* 2004; Taylor, 2014). The potential effects of external stimuli on cardiorespiratory responses where reduced through the use of an eye mask, low-level room lighting and ear protectors (McClave and Snider, 1992). The standing stage was performed stationary and without aid. If participants felt lightheaded, they were instructed to rock gently back and forth on their feet to reduce blood pooling in the lower limbs, if this occurred data collection was suspended until the participant was ready to continue the stage.

2.2.5 Experimental measurements

Oxygen consumption and heart rate were measured continuously during all trials. In addition, deep-body temperature was measured during the basal test to permit comparisons between human and mammalian scaling data. Semi-nude and clothed body masses were taken at the beginning of the trial. At the start of the testing series for each participant, anthropometrical measures (stretch stature and skinfold thicknesses) were recorded.

2.2.5.1 Oxygen consumption

Expired gas fractions and flows were sampled through an oronasal mask connected to a two-way mouthpiece, and analysed continuously using a static, gas-analysis system (TrueOne 2400, ParvoMedics Inc., Utah, U.S.A.). These data were used to derive oxygen consumption, carbon dioxide production, breathing frequency, tidal volume and minute ventilation as 15-s averages (Douglas-bag equivalents). Sampling from a mixing chamber, the analyser module (TrueOne 2400, ParvoMedics Inc., Utah, U.S.A.) used paramagnetic oxygen and infra-red carbon dioxide analysers (single

beam, single wave-length) to measure gas fractions to an accuracy of ±2.6% (±0.1% analyser accuracy: Crouter *et al.,* 2006; ±2.5% day-to-day calibration variation: manual calculation using the calibration logs). Analysers were calibrated at two points before each trial using *alpha* gas standards (16.00% oxygen, 4.00% carbon dioxide, balance nitrogen) and room air. Flow was calculated to an accuracy of ±3.8% (±2% analyser accuracy, TrueOne2400 manual; ±1.8% day-to-day calibration variation, manual calculation using the calibration logs) using a heated pneumotachograph (3813, Hans Rudolph Inc., Kansas, U.S.A.). At the start of each trial, flow was calibrated using a 3-L syringe, mimicking expired flows throughout the physiological range (50 to >300 L.min^{-1}).

Basal oxygen consumption data were used to approximate basal metabolic rate using Weir's (1949) abbreviated formula (Equation 2.1). Within this equation it is assumed that participants had a respiratory exchange ratio of 0.85 and were undertaking normal eating patterns prior to fasting (~12.5% total calories from protein: Weir, 1949). Using this formula, metabolic rate has been approximated during resting conditions within 0.5% error (Mansell and MacDonald, 1990).

Abbreviated Weir formula (1949)

$$\text{Daily energy expenditure} = ([3.941 \cdot \dot{V}O_2] + [1.106 \cdot \dot{V}CO_2]) \times (1.44 \cdot 4.184)$$

[kJ.day^{-1}] **Equation 2.1**

where:

Daily energy expenditure = basal metabolic rate [kJ.day^{-1}]

3.941 = energy expenditure per litre of oxygen [kcal.L^{-1}]

$\dot{V}O_2$ = volume of oxygen consumed [mL.min^{-1}]

1.106 = energy expenditure per litre of carbon dioxide [kcal.L^{-1}]

$\dot{V}CO_2$ = volume of carbon dioxide expired [mL.min^{-1}]

1.44 = conversion from minute to daily energy expenditure [min]

4.184 = conversion from kilocalories to kilojoules [conversion constant]

2.2.5.2 Deep-body temperature

Since the rate of metabolic enzymatic reactions are determined by the temperature at

which they occur (Guppy and Withers, 1999), it was possible that basal metabolism would also be influenced by deep-body temperature. For example, a 10°C increase in temperature doubles the reaction rate of enzyme reaction rates (Q_{10}). Accordingly, deep-body temperature was used to normalise basal metabolic rate to a common body temperature (36.2°C : White and Seymour, 2003). Deep-body temperature was measured from the auditory canal, to an accuracy of ±0.1°C (Edale instruments Ltd., Cambridge, U.K.). The thermistor was attached to a moulded plug that rested against the concha of the outer ear and protruded 1 cm into the external auditory canal. On the outer side of the thermistor, and across the outer ear, a large piece of cotton wool was taped to minimise the affect of the cooler environmental temperature (Figure 2.4C; Taylor *et al.,* 2014). Data were sampled at 15-s intervals using a portable data logger (Grant Instruments Ltd., 1206 Series Squirrel, U.K.). Thermistors were calibrated at the start of each testing block, across the physiological range (36°C to 40°C), in 1°C increments using a stirred water bath, against a certified reference thermometer (Dobros total immersion, Dobbie Instruments, Sydney, Australia). This calibration procedure has been used in recently published thermoregulatory work (Notley *et al.,* 2017).

Two analysis methods have arisen to explain the relationship between body temperature and metabolism. The first, normalises data to a common Q_{10} value (Chaui-Berlinck *et al.,* 2002; Guppy and Withers, 1999), and the second uses a single correction factor based on the universal temperature dependence of biological processes (Gillooly *et al.,* 2001). The argument for the latter is that, within a 0°C-40°C temperature range, the application of a constant Q_{10} value can introduce as much as a 15% error. However, this error is negligible when analysing within the narrow body-temperature ranges observed within animal metabolism research. In fact, utilising a constant Q_{10} value has been shown to be superior in explaining a higher amount of metabolic variance with body size when testing animal metabolism compared with using the universal temperature dependence method (White and Seymour, 2003). Therefore, correcting data to a common deep-body temperature, and thus a fixed Q_{10} value, will account for differences in circadian and seasonal fluctuations in basal metabolic rate. Accordingly, the following correction was adopted.

Deep-body temperature-adjusted basal metabolic rate

$$BMR_c = BMR \cdot 10^{[36.2 - T_b]\log(Q_{10})/10} \quad [kJ.day^{-1}] \qquad \textbf{Equation 2.2}$$

where:

BMR_c = temperature corrected basal metabolic rate [$kJ.day^{-1}$]

BMR = measured basal metabolic rate [$kJ.day^{-1}$]

10 = multiplicative constant [constant]

36.2 = mean multi-species mammalian deep-body temperature [°C]

T_b = measured deep-body temperature [°C]

Q_{10} = factorial increase in BMR associated with a temperature increase of 10°C (Q_{10} = 3) [non-dimensional unit]

10^{-1} = multiplicative constant = [constant]

Fixed values for both the Q_{10} rate and the corrected deep-body temperature (3 and 36.2°C respectively) are used in Equation 2.2. Both values were derived during analysis of the same dataset: 619 mammalian species, with deep-body temperature available for 507 species (White and Seymour, 2003). The mean body temperature of those 507 species available was 36.2°C. The Q_{10} value was then determined by utilising that mean deep-body temperature and comparing data using Q_{10} values between 2 and 4. A Q_{10} of 3.0 produced the highest correlation coefficient when the log of the temperature-adjusted basal metabolic rate was regressed against the log of body mass (White and Seymour, 2003).

That normalisation approach was used within the analysis for two purposes. Firstly, to confirm whether, using the same corrections, human basal metabolic rate falls on the same mass-to-basal metabolic rate curve defined for mammals ($mass^{0.67}$: White and Seymour, 2003). Secondly, to determine whether these corrective methods would help to minimise for the variations of basal metabolic rate within an adult-human mass range.

2.2.5.3 Cardiac frequency

Cardiac frequency was monitored using a chest-strap transmitter and an integrated adaptor in the gas-analysis system (15-s intervals; Plug in receiver, Polar Electro, Kempele, Finland). The heart-rate monitor detected events of ventricular

depolarisation, the electrical representation of the contraction of the left ventricle. In particular, the positive amplitude peak during the R wave was used to identify ventricular contractions, thus providing the ability to monitor the contraction frequency of the heart using a non-invasive method.

2.2.5.4 Anthropometric measures

Standing stretched-stature was measured using a stadiometer (Harpenden Stadiometer, Holtain Ltd., Crymych, UK) during the participant's first visit at the laboratory. Participants stood with their feet and heels together and the calcaneus, gluteal muscles, scapulae and occipital bone in contact with the vertical section of the stadiometer. The head angle was adjusted to ensure a horizontal (Frankfort) plane: an imaginary line drawn between the inferior margin of the orbit and the superior margin of the external auditory meatus. Subjects were instructed to stand tall, the headboard was then brought down until it was in contact with the vertex (highest point of the head). The researcher then instructed the participant to take a deep inspiration, whereupon the researcher applied a gentle vertical lift to the head, through the mastoid process. This resulted in a height that was largely independent of time-related inter-vertebral compression (Palmer, 1930; Redfield and Meredith, 1938).

Semi-nude (underwear) and clothed (wearing full testing garments but no shoes) masses were taken at the start of all testing visits using digital scales (MS3200, Medical Scale, Charder, Taichung, Taiwan). The basal, post-void mass for each participant was measured semi-nude and in a fasted state, to provide the metabolically dependent body mass. The scales were calibrated using known masses across the physiological range (50 kg, 70 kg, 90 kg and 110 kg) at the start of each testing block.

Height-adjusted adiposity and body mass

Skinfold thicknesses were measured at six sites using callipers (Eiken skinfold calliper, Meikosha, Tokyo, Japan: triceps, subscapular, supraspinale, abdominal, anterior thigh, medial calf: Figure 2.5A; Marfell-Jones *et al.*, 2006). The callipers were calibrated once a month by ensuring the tension in the calipers remained at 10 $g.mm^{-2}$; this tension was tested during both unloaded and loaded (200 g on the moving

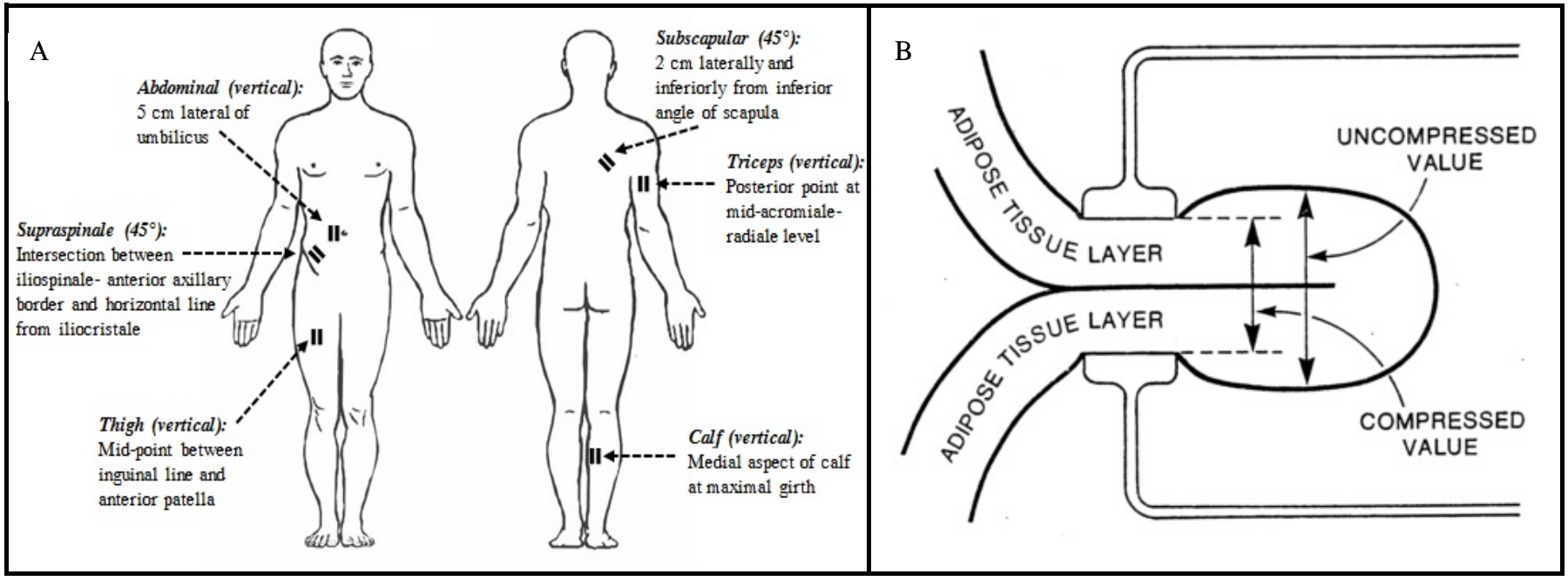

Figure 2.5: Schematic representation of skinfold measurement locations, with both the anatomical landmarks and angles used for each measurement (Figure 2.5A; Marfell-Jones *et al.,* 2006). Schematic representation of skinfold compressibility with the application of a calliper (Figure 2.5B; Martin, 1984).

arm) conditions. Each measurement was taken from a double-fold of skin and the underlying subcutaneous adipose tissue (Figure 2.5B). Two measurements were taken at each site, if a difference of greater than 5 mm occurred, the measurement was repeated and the mode value accepted for that site. The sum of all six site measurements was then recorded for each individual, and was used to derive the relative adiposity of each participant.

As mentioned in Section 2.2.1.2, subcutaneous adiposity was matched within this experimental series to minimise the metabolic impact of variations in tissue proportions. Rather than relying on predictive equations to estimate body adiposity, which rely on several invalid assumptions that can introduce estimation errors (Johnston, 1982; Martin *et al.,* 1985; Clarys *et al.,* 1987), adiposity was reported as the simple sum of six skinfolds. However, reporting the raw sum does not necessarily permit accurate comparisons of adiposity among participants of different body sizes, due to an increase in skin thickness with increases in body size (Martin *et al.,* 1984; Clarys *et al.,* 1987). Therefore, it was also necessary to remove this body-size effect among those data.

To remove that relationship between body size and skinfold thickness, sum of skinfold data were adjusted to the common stature of the hypothetical phantom (170.18 cm: Ross and Wilson, 1974). Equation 2.3 was used to generate these height-adjusted data, where *"l"* represented a participant's six-site sum of skinfold measure (Ross and Wilson, 1974; Ross and Ward, 1985). These height-adjusted data could then be compared against the age- and gender-specific normative data from the O-scale system to generate a proportional adiposity rating for each individual (Ross and Ward, 1985). Furthermore, this process enabled those data to be categorised using a standard nine (stanine) distribution (Figure 2.6), where each division was 0.5 standard deviations apart across a normal distribution. Thus, this method permitted the categorisation of an individual's adiposity measurement against normative data for adults of the same age.

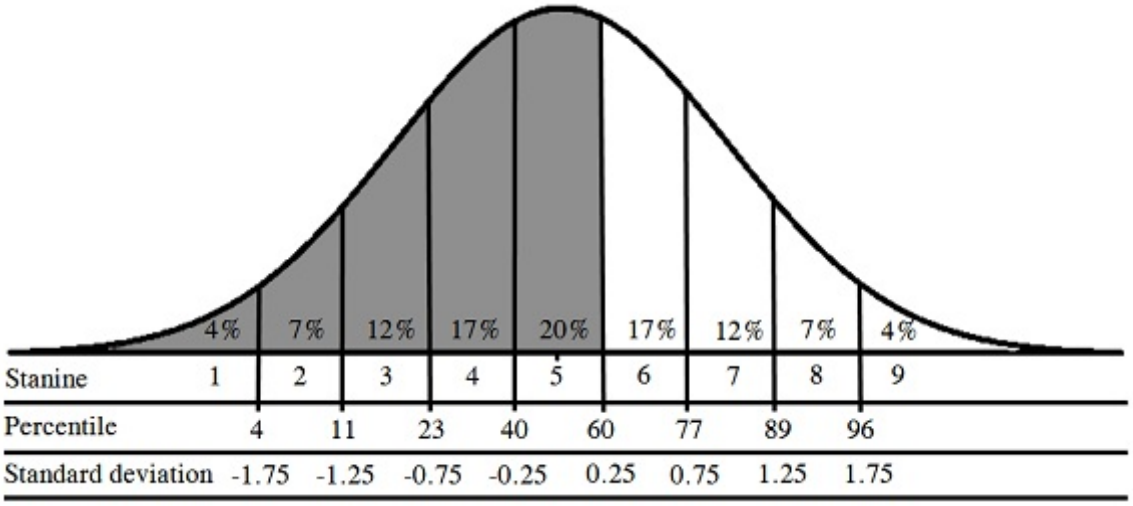

Figure 2.6: Normal distribution graph representing participant selection based on their height-adjusted sum of six skinfold measurements derived from age-specific population normative data. The normative data were split evenly into standard nine (stanine) categories, each representing a width of 0.5 standard deviations (Ward, 1988). To reduce inter-subject variations in adiposity, participants were recruited who were below the 60% percentile, as represented by the shaded area under the graph.

Phantom stratagem (Ross and Ward, 1974)

$z = l \cdot (170.18/h)^{d}$ [morphological units] **Equation 2.3**

where:

z = height-adjusted measure of l [morphological units]

l = size of any measurable unit [anthropometric unit]

170.18 = phantom height constant [cm]

h = standing height [cm]

d = dimensional exponent: d=1 for all lengths, girths and skinfolds, d=2 for all areas, and d=3 for all masses [dimensional exponent]

Using this comparative index for subcutaneous adiposity, it was possible to set an exclusion criterion to ensure participants had a similar height-adjusted adiposity measures. For this series of experiments, participants were selected who had average-to-low adiposity; a seven on the stanine rating, or less than the 60% percentile (Figure 2.6 [shaded area]). This threshold resulted in a height-adjusted sum of skinfold cutoff of 88 mm (Ross and Ward, 1985; Landers *et al.,* 2013). Nevertheless, it was probable that proportionality differences would still exist after controlling for adiposity. For example, two individuals may have a similar adiposity and body mass, but may vary in stature, muscularity or both. Accordingly, Equation 2.5 was also used to identify instances within the sample where a participant's height-to-mass proportionality varied greatly from the rest of the sample. In this instance, "*l*" represented a participant's unadjusted semi-nude body mass in kilograms. These data could once again be expressed using a stanine categorical system to compare those height-adjusted masses with normative data (Ross and Ward, 1985). While there was no exclusion criterion set for this measure within this series of experiments, the derived values could be used for covariance analyses if participants varied greatly in height-to-mass proportionality.

2.2.6 Design and analysis

2.2.6.1 Experimental design

This experimental stage was based on a five by four factorial design (Figure 2.7), with five levels of the first factor (body size: extra-small, small, medium, large, extra-large) and four levels of the second factor (metabolic intensity: basal [supine],

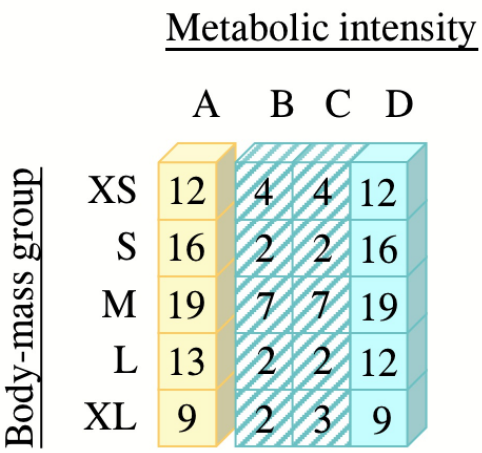

Figure 2.7: A schematic of the current experimental phase design, including the pilot study, as a five by four factorial design. The first factorial, body-size consisted of five levels: extra-small (XS: 55-65 kg); small (S: 66-76 kg); medium (M: 77-87 kg); large (L: 88-98 kg); and extra-large (XL: 99-110 kg). The second factorial, activity level, had four levels: basal (Column A: supine, rest); 100% mass-supported standing (Column B), 50% mass-supported standing (Column C); normal standing (Column D: unaided). The sample size for each body size and activity intensity used is identified within the respective coloured box. The two mass-supported standing conditions (hashed boxed) were exploratory tests only (see Section 2.3.3.1).

100% mass-supported standing, 50% mass-supported standing and standing [unaided; resting]). The two mass-supported stages were part of an exploratory study (see Section 2.3.3.1). Data are presented as means with standard deviations (SD) used to describe data distributions and standard errors of the mean (±) used to provide information regarding the precision of the mean.

2.2.6.2 Data analysis

Determining the sample homogeneity

Before performing any scaling analyses, the homogeneity of the sample was evaluated. Raw and height-adjusted morphological data (sum of skinfolds and body masses) were compared among the five body-mass groups[14] using one-way analysis of variance. If any between-group differences remained among those height-adjusted data, analysis of covariance was used to determine whether or not it was necessary to include that variable as a covariate when assessing the scaling regression. That outcome would be confirmed by the presence of a significant interaction effect.

Determining the shape of the scaling models

Since both linear (first-order polynomial: Equation 2.4) and non-linear (allometric: Equation 2.5) treatments of metabolic rate appear in the literature, data collected during these trials were first evaluated to determine which analysis method was more appropriate. As established within Section 2.1.2, for either scaling model (linear or non-linear) to be deemed suitable for further analyses, the model had to satisfy both the statistical and biological assumptions (Sholl, 1948). Thus, the model had to satisfy the four assumptions of linear regression (Poole and O'Farrell, 1971; Weisberg, 2014): linearity, an equal variance of error among residuals (homeoscedasticity), normality of variables and no autocorrelation between variables (an underlying correlation between both variables, violating the assumption of independence). Furthermore, the model also required an origin intercept (biological assumption; Section 2.1.2.1). Using these model constraints, it was possible to establish a schematic decision-making flow chart to systematically assess the appropriateness of

[14] To permit size comparisons within the sample, the mass range was divided into five body-mass groups: extra small (≤65 kg), small (66-76 kg), medium (77-87 kg), large (88-98 kg) and extra large (≥99 kg).

each model, for any metabolic intensity (Figure 2.8).

Linear scaling model

$$y = a \cdot x + c + e$$ **Equation 2.4**

where:

y = dependent physiological variable [physiological units]

a = multiplicative constant [physiological units]

x = independent morphological variable [morphological units]

c = ordinate intercept [morphological units]

e = multiplicative error [physiological units]

Non-linear scaling model

$$y = a \cdot x^{b} + e$$ **Equation 2.5**

where:

y = dependent physiological variable [physiological units]

a = multiplicative constant [physiological units]

x = independent morphological variable [morphological units]

b = scaling exponent (slope) [morphological units]

e = multiplicative error [physiological units]

For each scaling model, linearity was visually assessed using a scatter plot of the relationship between metabolic rate, or oxygen consumption during non-basal states, and body mass. Residual plots were used to evaluate the error variance among those model residuals, whereby a uniform distribution was deemed suitable (Casson and Farmer, 2014; Weisberg, 2014). The distribution of data within each variable was assessed using histogram plots, skewness and kurtosis z-scores and the Shapiro-Wilk test. With sample sizes between 50-300, a z-score threshold of $\leq \pm 3.29$ corresponds to a normal distribution at the 5% probability level (Kim, 2013). The Shapiro-Wilk test (Shapiro and Wilk, 1965; Ahad *et al.,* 2011), statistically compares a chosen dataset against a generated, normally-distributed dataset with the same mean and standard deviation. A perfect normal distribution is identified by a test statistic (W) of 1, and a significant test result indicates a non-normal data distribution. This test was also performed on the regression residuals for each scaling model to confirm a normal

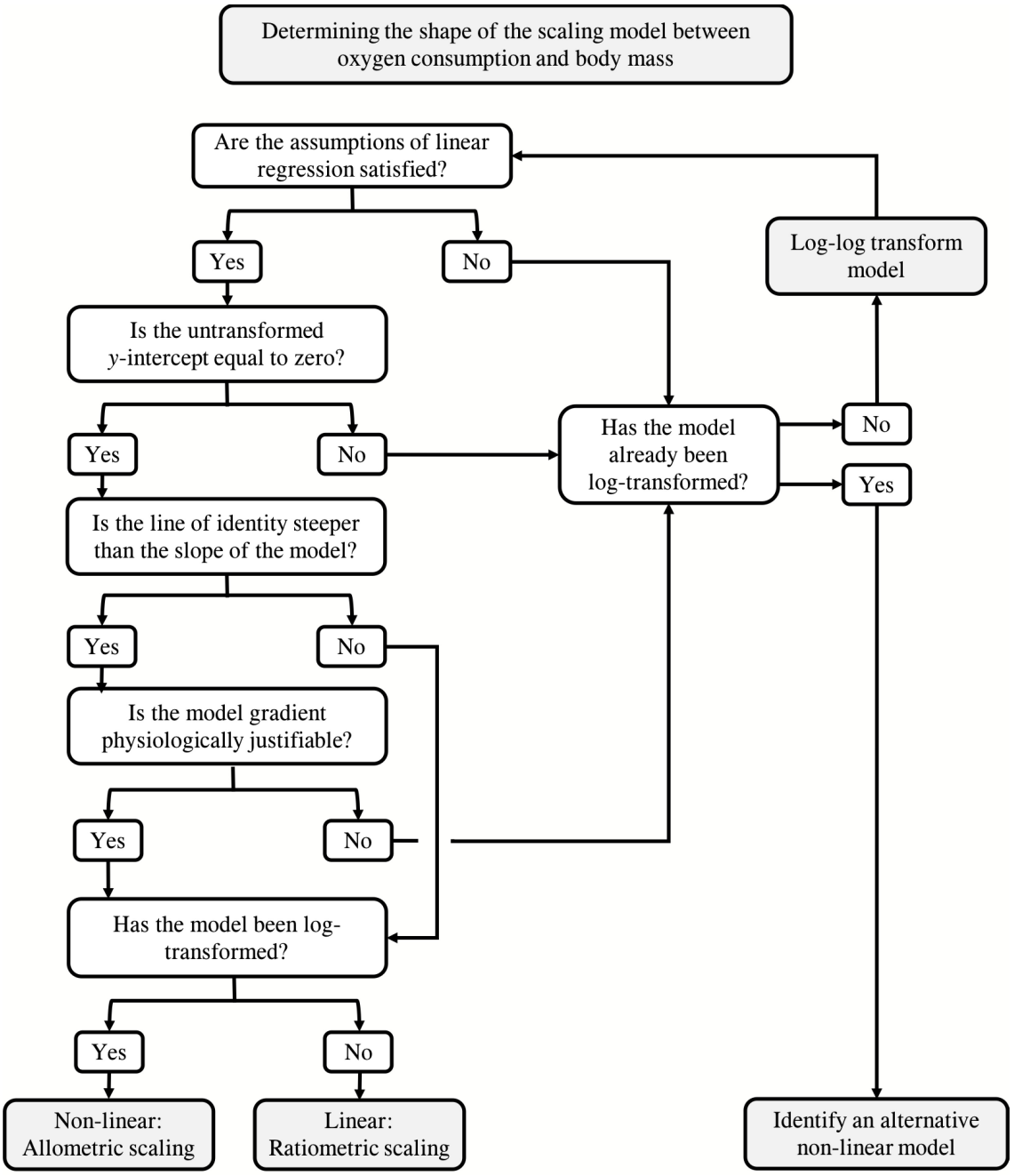

Figure 2.8: A decision-making flow chart designed to identify the appropriate scaling model for the relationship between oxygen consumption and body mass.

distribution before comparing between models using analysis of covariance. The presence of autocorrelation between variables was assessed using the Durbin-Watson test (Durbin and Watson, 1950, 1951). Within the test, the null hypothesis evaluated is that the residuals are not serially correlated, that is, that there is no first-order correlation. A perfect absence of autocorrelation between variables was expressed by a Durbin-Watson test statistic of 2. Prior to performing those analyses on the non-linear model, data were log transformed, using a Log_{10} base, to provide a linear function (Equation 2.6; Figure 2.9). In this form, the non-linear model could be assessed using robust statistical comparisons that assume linearity. However, due to the nature of regression data, some error is inherent during that transformation process. As a result, a regression applied to a log-transformed dataset will not be identical to a non-linear regression applied to those data when untransformed (Jansson, 1985; Newman, 1993; Xiao *et al.,* 2011). Accordingly, to apply a log-transformed regression to an untransformed dataset will introduce further errors, and thus the appropriate value must be used when describing those data depending upon the units discussed (Sholl, 1948; McWilliams *et al.,* 1964; Xiao *et al.,* 2011). For this reason, both non-linear and log-transformed regression coefficients have been reported. It is recommended that the non-linear regression coefficients be used to predict and normalise untransformed (raw) metabolic data.

Log_{10}-transformed non-linear scaling model

$$Log_{10}(y) = b \cdot Log_{10}(x) + Log_{10}(a) + e \qquad \textbf{Equation 2.6}$$

where:

y = dependent physiological variable [physiological units]

b = scaling exponent (slope) [morphological units]

x = independent morphological variable [morphological units]

a = allometric multiplicative constant; logged ordinate intercept [morphological units]

e = multiplicative error [physiological units]

The biological assumption of an origin intercept was assessed while both datasets were untransformed, as data in this format should represent the population it is describing. For the linear models, a t-test was used to assess the null hypothesis that

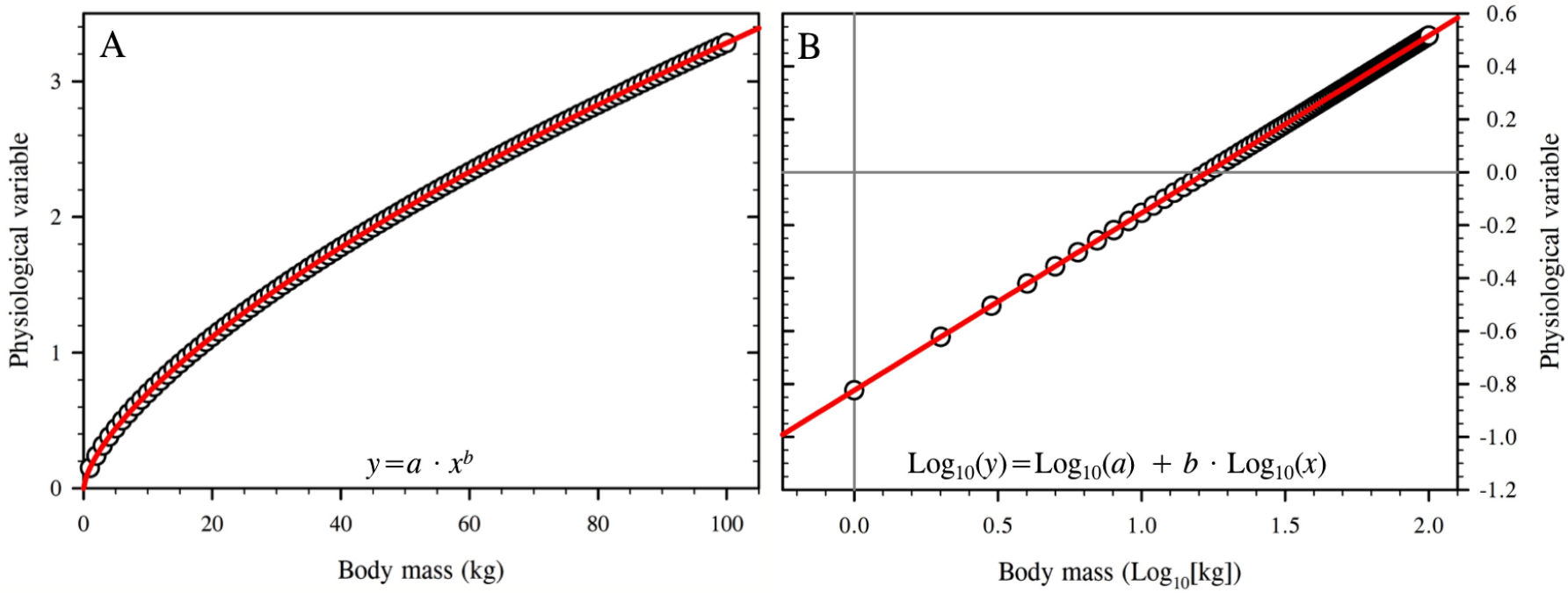

Figure 2.9: Scatter diagram of a non-linear, allometric model (Figure 2.9A) with hypothetical body masses ranging from 1 to 100 kg, and hypothetical physiological data generated using the equation: $y = 0.15 \cdot x^{0.67}$. Figure 2.9B displays those same data when $\log_{10}$ transformed. In both regression equations, the "*b*" value primarily dictates the shape of the regression slope. It is a change in this value that dictates whether or not unique scaling regressions are required to describe the relationships between different datasets. Note how, when log transformed, some data become negative values, that is because $\mathrm{Log}_{10}(1)$ equals zero. Therefore, any untransformed value less than one becomes negative when log transformed.

the intercept was equal to zero at a 5% probability level (Weisberg *et al.,* 2014). In contrast, this assumption did not require testing for the non-linear models, as an origin intercept is inherent within the constraints of the model equation.

Bootstrapping was used to predict the most-likely regression coefficients for all regressions evaluated (Efron, 1979; Fox and Weisberg, 2017). Each regression was generated 1000 times using statistical software (R-project v.3.2.1: R Development core team, 2016). A re-sampling method was used from the original dataset, so that a slightly different sub-sample for each new equation formed, each of which was drawn from the complete pool of participants. Using this method, is was possible to generate means and standard errors of the mean for each regression coefficient. Those mean values were then used for all regression analyses and have been reported within the text.

Comparing differences between scaling models

Analyses of covariance were used to assess both between- and within-intensity differences between regression slopes. These tests was performed to evaluate both the effect of temperature normalisation and an increase in metabolic intensity (change in posture) on the shape of the scaling regressions. A difference between regression slopes was identified by a significant interaction effect. Such a response would indicate the need to describe datasets using unique regression coefficients: multiplicative constant (linear models) and mass exponent (non-linear models). Therefore, identifying differences in these values was a primary focus within this project.

An objective within this experimental phase was to determine whether the human scaling relationship between basal metabolic rate and body mass varied with that used in comparative physiology ($mass^{0.67}$: White and Seymour, 2003). This objective was only assessed if non-linear regression was the more suitable scaling method for human metabolic data. Since $mass^{0.67}$ is not uniformly confirmed for animal data, rather those regressions are only confirmed to be not dissimilar, the human mass exponent was tested directly against the value 0.67 instead of using analysis of covariance with an animal dataset. An adaptation of the regression-intercept, null-hypothesis t-test was

used to perform this comparison on the $\log_{10}$-transformed data (Equation 2.7).

Null-hypothesis t-test

$$T_1 = (\hat{\beta}_1 - 0.67) / SEM(\hat{\beta}_1) \qquad \textbf{Equation 2.7}$$

where:

T_1 = test statistic [non-dimensional units]

$\hat{\beta}_1$ = mass exponent (slope) [morphological units]

0.67 = mammalian mass exponent [morphological units]

$SEM(\hat{\beta}_1)$ = standard error of the mean for the mass exponent [morphological units]

Evaluating the model-specific normalised metabolic data

The ability to normalise metabolic data for variations in body mass, without systematic errors, was an essential requirement for the chosen scaling model because a valid model permits others to predict mass-specific values for individuals in whom those data are not available. An inability to generate mass-independent metabolic data from the regression equation would demonstrate an inaccurate model fit. To test this requirement, metabolic data were normalised using four separate approaches: ratiometric (y/x; to demonstrate the unsuitability of this method for metabolic data), two intercept-adjusted ratios ($[y-c]/x$ and $y/[x+c/a]$: linear model) and an allometric ratio (y/x^b: non-linear model). Two linear, intercept-adjusted methods were tested as the latter is supposed to reduce normalisation errors by accounting for the residual variations in metabolic rate (y: Albrecht *et al.,* 1993). The effectiveness of each approach was assessed by performing a Pearson's correlation coefficient test (Pearson, 1900, 1920) on those normalised residuals, ordered by participant body

mass. A *rho*[15] value approaching zero represented a successful attempt.

Comparing mean physiological variables

Two-way factorial analysis of variance was used to compare mean oxygen consumption and cardiac frequency data among body-mass groups and between metabolic intensities. Tukey's honestly significant difference (*HSD*) *post hoc* test was used to isolate significant differences. These tests permitted the comparison of absolute data across the body-mass range and between metabolic intensities.

Dealing with outliers

Potential data outliers were identified using four assessments: raw and $\log_{10}$-transformed scatter plots, box plots, Bonferroni test (Cook and Weisberg, 1982; Williams, 1987; Fox, 1997) and Cook's distance (Cook, 1977). A visual assessment of the scatter plots was firstly used to identify any obvious outliers, such as may be associated with experimental error (*e.g.* a leaking mask). The box plots were used to identify extreme data points (Chambers *et al.,* 1983): determined as any data point 1.5 times the inter-quartile range[16] beyond the upper and lower quartiles. However, potential outliers throughout the central distribution of data points can no be identified by this test. The Bonferroni test assessed each observation, as studentised residuals assuming a t-distribution, and outputs the largest absolute studentised residuals (Cook and Weisberg, 1982; Weisberg, 2014). The Cook's distance test identified individual observations with a large influence on the regression shape, that may have a significant impact on the regression model[17] (Cook, 1977; Fox, 1991; Hair *et al.,* 1998). A threshold for this test was identified as $4/n\text{-}k\text{-}2$, where n was the number of observations and k was the number of explanatory variables. However, any values substantially higher than the rest were also evaluated (Fox, 1991). Data points flagged in two or more tests were assessed by researchers and only removed if their omission significantly affected the shape of the regression or there was evidence of some

[15] *Rho*, or the correlation coefficient, is the numerical measure for the strength and direction of any linear relationship between two variables ($-1 \leq rho \leq 1$).

[16] Inter-quartile range is the difference between the 1st and 3rd quartiles, representing the range where 50% of the data lies.

[17] Data points with a large impact are those that had large residuals, an increased distance from the predicted values, or those with few or no nearby observations.

experimental error.

2.3 RESULTS

2.3.1 Pre-experimental standardisation

The first objective of this experimental phase was to examine the shape of the scaling relationship between body mass and basal metabolic rate in men, and to determine whether that relationship was linear or non-linear. The second aim was to evaluate whether or not a change in posture (increase in metabolic intensity) modified that scaling relationship. To successfully conduct these analyses, it was essential to first ensure that participants from each of the five body-mass groups were morphologically similar (see Section 2.2.1), and that those data were truly basal. These procedures would minimise the influence of those variables on the scaling relationship. The veracity of those assumptions was tested before evaluating the scaling relationship.

2.3.1.1 Evaluating the sample morphometry

A total of 72 participants were tested throughout Chapters 2-6. Accordingly, a sufficient sample size was obtained to confidently generate both linear and non-linear regression models. Of that sample, 68 participants were tested within this exploratory phase. Since a repeated-measures design was used throughout this project, for the morphometric analyses presented in this section data have been displayed for the full 72 participants. An exception to this occurred for the skinfold datasets, where data for three participants could not be collected, leaving a total of 69 participants for those measures. No significant differences between the full and Chapter-specific samples were realised for any of the measures presented in this subsection ($P > 0.05$).

To permit scaling analysis, the sample was recruited across a wide mass-range (Figure 2.3). That range exceeded the 5th and 95th percentiles of the specified age- and gender-specific population normative data (Section 2.2.1.2; Australian Bureau of Statistics, 2012). Body mass differed significantly among all five body-mass groups (Figure 2.10A; Table 2.2; $P < 0.05$), representing a substantial increase in body mass across the sample. Despite those planned differences in body mass, participants were still considered proportionally similar for height-to-mass proportionality: height-adjusted body mass (Figure 2.10B; $P > 0.05$). That is, only two participants had

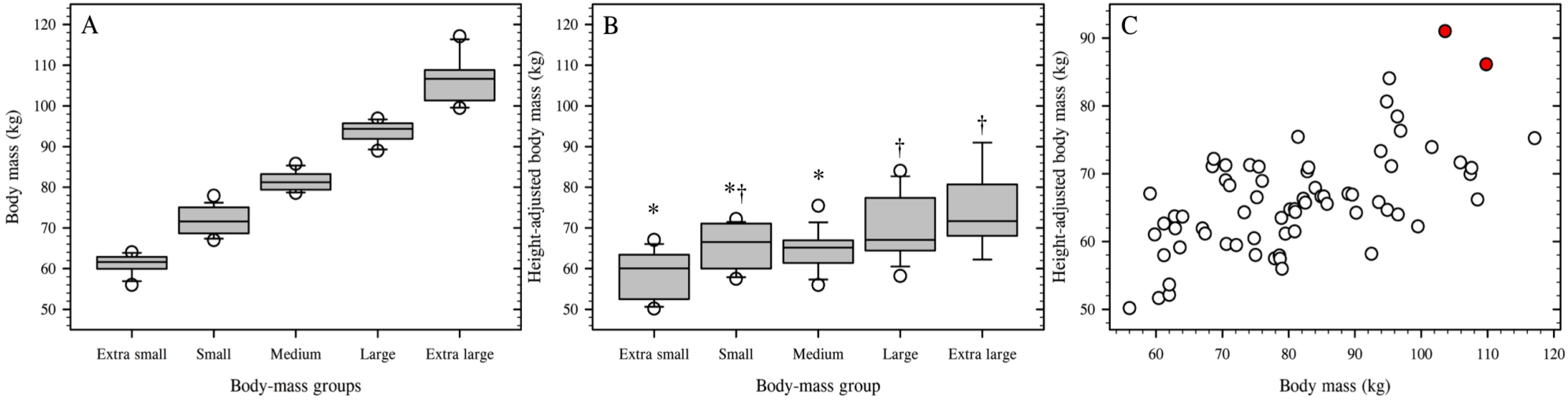

Figure 2.10: Box plots of the between-group differences in body mass for raw (Figure 2.10A) and height-adjusted (Figure 2.10B) measures. Significant differences were identified among all body-mass groups when data were raw, these are not identified on Figure 2.10A ($P<0.05$). In Figure 2.10B, the symbols indicate significant differences from the Extra-large group (*) and the Extra-small group (†; $P<0.05$). Figure 2.10C displays the individual differences in height-adjusted body mass for the same sample. The red data points indicate the identified potential outliers. As a repeated-measures design was utilised throughout this project, morphological data are presented for all 72 participants (Extra small: $N=12$; Small: $N=17$; Medium: $N=19$; Large: $N=14$; Extra large: $N=10$).

extreme values for that measure, compared with the rest of the cohort (Figure 10C; $P<0.05$). As analysis of covariance revealed no covariant effect of that measure on the scaling relationships ($P>0.05$), data from those two participants could be kept within the dataset without adding an additional variable to the scaling relationship.

Mass-dependent differences in sum of skinfold data (Figure 2.11A; $P<0.05$) were reduced by adjusting those data for individual variations in standing height (Figure 2.11B; $P<0.05$). All but six participants' height-adjusted sum of skinfold data were within the pre-defined inclusion criterion (<88 mm; Figure 2.11C), three of whom were identified as potential outliers. Analysis of covariance was performed on the scaling relationships to confirm whether or not those variations influenced the regression shape. No covariant relationship was found for those data, for any scaling relationship ($P>0.05$). Accordingly, it was not necessary to include those height-adjusted data as a covariant within the scaling models, and data points from all participants were kept within the sample.

In summary, adjusting morphometric data for individual variations in standing height successfully minimised the mass-dependent relationship among those data. While some differences did remain, including those variables as covariants in the scaling relationships did not significantly modify those regression slopes. Consequently, all data points could be kept within the basal and standing datasets without influencing the scaling relationships. Moreover, it could be assumed that any differences in body mass among participants represented a proportional change in body size and subcutaneous adiposity. Therefore, the sample was considered a good representation of body size within the specific population for scaling and regression purposes.

2.3.1.2 Validating the basal data

Before performing any scaling analyses, the basal dataset were first evaluated to determine whether or not it satisfied the pre-determined assumptions: steady state, respiratory exchange ratio ~ 0.85 and realistic values. The sampling time frame was selected to ensure a steady state. Data were removed from the first 15 min of the test, to permit participants to reach a resting state after travel to the laboratory and the preparation process. In previous work, data collected while using this procedure are

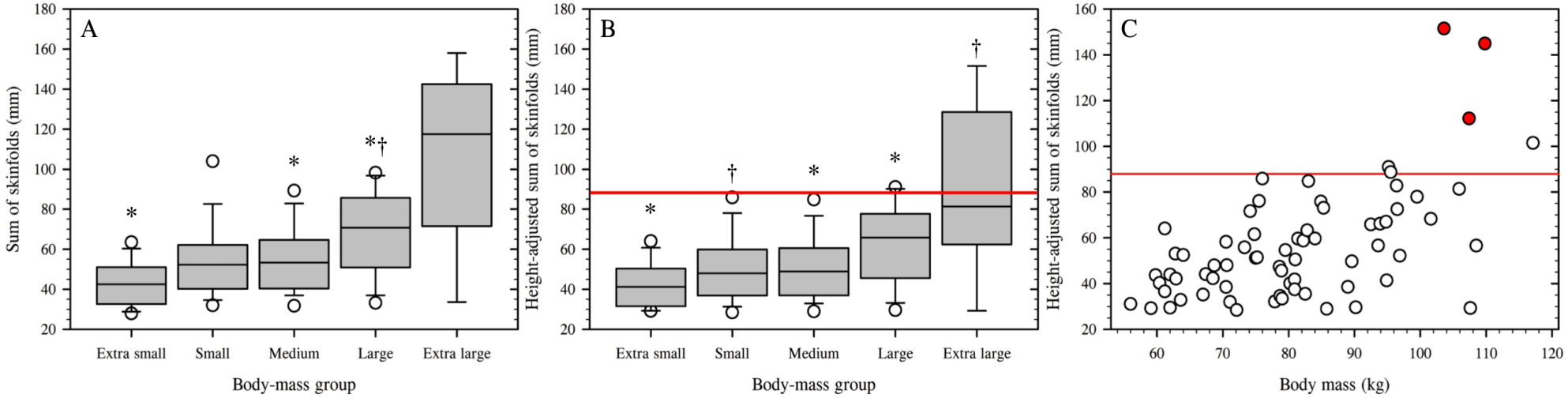

Figure 2.11: Box plots of the between-group differences in body mass for raw (Figure 2.11A) and height-adjusted (Figure 2.11B) measures. The symbols indicate significant differences from the Extra-large group (*) and the Extra-small group (†; $P < 0.05$). Figure 2.11C displays the individual differences in height-adjusted body mass for those participants. The red data points indicate the identified potential outliers. The red line in Figures 2.11B and 2.11C indicates the pre-identified adiposity threshold (< 88 mm). As a repeated-measures design was utilised throughout this project, morphological data are presented for 69 out of 72 participants, adiposity measurements could not be taken on 3 participants (Extra small: $N = 12$; Small: $N = 16$; Medium: $N = 19$; Large: $N = 13$; Extra large: $N = 9$).

similar to those estimated after participants have slept at the laboratory overnight (Fredrix *et al.,* 1990; Turley *et al.,* 1993). Data were also removed from the last 5 min of the test and at any time point when participants moved. In this way, there remained approximately a 40-min period where only resting data were sampled. Within that 40-min period, a steady state was observed with a low mean intra-individual coefficient of variance recorded for both oxygen consumption (12% [±0.01]) and cardiac frequency (6% [±0.01]). For tests longer than 30 min, accurate metabolic estimations can be calculated providing the oxygen consumption coefficient of variance is less than 20% (Frankenfield *et al.,* 1994; McClave *et al.,* 2003). Moreover, a mean respiratory exchange ratio of 0.87 (±0.01) was observed, indicating a normal breathing pattern and mixed-substrate oxidation, as anticipated during a post-absorptive state. Thus, data were assumed to be sampled during a resting, steady state and satisfied the conditions required to approximate basal metabolic rate using the Weir (1949) formula: basal conditions and a respiratory exchange ratio of ~0.85.

The mean estimated basal metabolic rate for the sample was 8065.3 $kJ.day^{-1}$ (±117.8) with a mean body mass of 81.6 kg (SD 14.7). Those data were greater than those reported by Schofield (1985) for men aged 18-30 y (6870 $kJ.day^{-1}$ [±15.7]; 63.0 kg [SD 8.7]), whose mean sample were much lighter. However, those present metabolic data were less than those reported in a more modern study where obese participants were tested (9409 $kJ.day^{-1}$ [±15.7]; 123.9 kg [SD 22.6]; Lazzer *et al.,* 2010). Among those three datasets, mean absolute oxygen consumption increased with mean body mass, as would be expected, with those data from this experimental phase situated between those reported in the two published studies. Together with the above measurement assumption, those basal data were considered to be realistic and suitable for scaling analyses.

2.3.2 Scaling whole-body basal metabolic rate with body mass

The primary focus within this experimental phase was to determine whether or not the scaling relationship between basal metabolic rate and body mass was linear or non-linear. To determine the shape of that relationship, both linear and non-linear models were applied to the dataset and their fit was assessed using the steps outlined in the

decision making flow chart (Figure 2.8). First, the assumptions of linear regression[18] were evaluated for each regression: linear and $\log_{10}$-transformed non-linear.

To evaluate the assumption of normality, the data-point distribution of the basal metabolic rate and body mass variables was assessed, using both the untransformed (linear regression) and $\log_{10}$-transformed (non-linear regression) data formats. Histograms for both variables displayed approximate normal distributions (Figure 2.12). Those observations were also confirmed statistically, where skewness and kurtosis *z*-scores were all less than ± 3.26, demonstrating conformity to a normal distribution at the 5% probability level (Kim, 2013; Table 2.3; $P > 0.05$). Moreover, no difference from a normal distribution was observed using the Shapiro-Wilk test (Table 2.3; $P > 0.05$). Therefore, both variables conformed to the assumption of normality and could be used in either format when evaluating the scaling relationships (Poole and O'Farrell, 1971; Weisberg, 2014). Thus, the assumption of normality was satisfied for data while in both linear and non-linear formats.

Scatter and residual plots were used to visually assess linearity and homeoscedasticity, respectively. Those assumptions were confirmed for the linear and non-linear datasets (Figure 2.13), indicating that both scaling models adequately described the shape of the scaling relationship within the mass range tested. Among those model residuals, no first-order correlation (autocorrelation) was observed (Durbin-Watson test: Table 2.3; $P > 0.05$). This meant that despite both variables being inherently related, as is unavoidable in biological datasets, that underlying relationship did not invalidate the regression assumption that variables are independent. Consequently, both scaling models (linear and non-linear) satisfied the assumptions of linear regression and thus were considered suitable, statistically, to describe the scaling relationship between basal metabolic rate and body mass (Figure 2.8).

Nevertheless, that outcome demonstrates the importance of also assessing the biological model assumptions when scaling biological datasets. For if the assessment process had finished with the statistical assumptions, either model would be

[18] The assumptions of linearity: normal distribution, linearity, homeoscedasticity and no autocorrelation among variables.

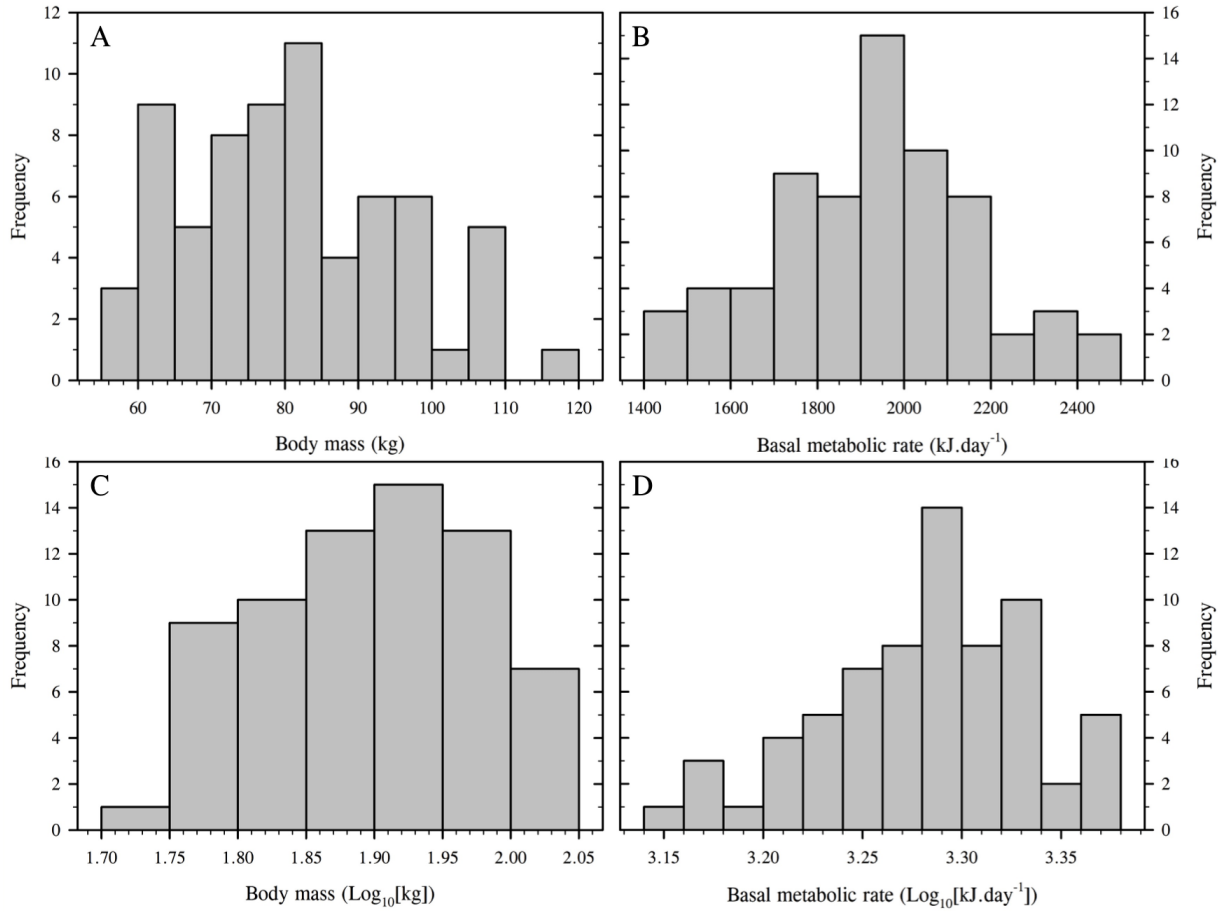

Figure 2.12: Plotted histograms of the sample frequency distributions for body mass (N=72; Figures 2.12A and 2.12C) and basal metabolic rate (N=68; Figures 2.12B and 2.12D). Data are presented in both untransformed (top) and $\log_{10}$-transformed (bottom) formats to correspond with the linear and non-linear scaling models, respectively.

Table 2.3: Test statistics for the basal scaling models to assess normality and autocorrelation among the regression variables and model residuals. Data were presented in raw and $\log_{10}$-transformed formats (N=68). No significant values were identified at the 5% probability level.

	Regression variables				Regression model residuals	
	Basal metabolic rate		Body mass			
	Raw ($kJ.day^{-1}$)	Log-transformed ($Log_{10}[kJ.day^{-1}]$)	Raw (kg)	Log-transformed (Log_{10}[kg])	Linear	Log_{10} transformed
Skewness statistic	0.25	-0.14	0.35	0.04	-0.19	-0.31
Z-score	-0.88	-0.48	1.20	0.14	-0.64	-1.06
Kurtosis statistic	0.24	-0.05	-0.74	-0.92	-0.87	-0.83
Z-score	0.42	-0.10	-1.30	-1.60	-1.52	-1.44
Shapiro-Wilk statistic	0.99	0.98	0.97	0.98	0.98	0.97
Durbin-Watson statistic	-	-	-	-	1.63	1.68

Notes: Basal metabolic data were derived using the Weir formula (1949) from observed basal oxygen data ($L.min^{-1}$). A perfect normal distribution would be identified by a Shapiro-Wilk test statistic of 1 (Shapiro and Wilk, 1965). A perfect absence of autocorrelation between variables was expressed by a Durbin-Watson test statistic of 2 (1950; 1951).

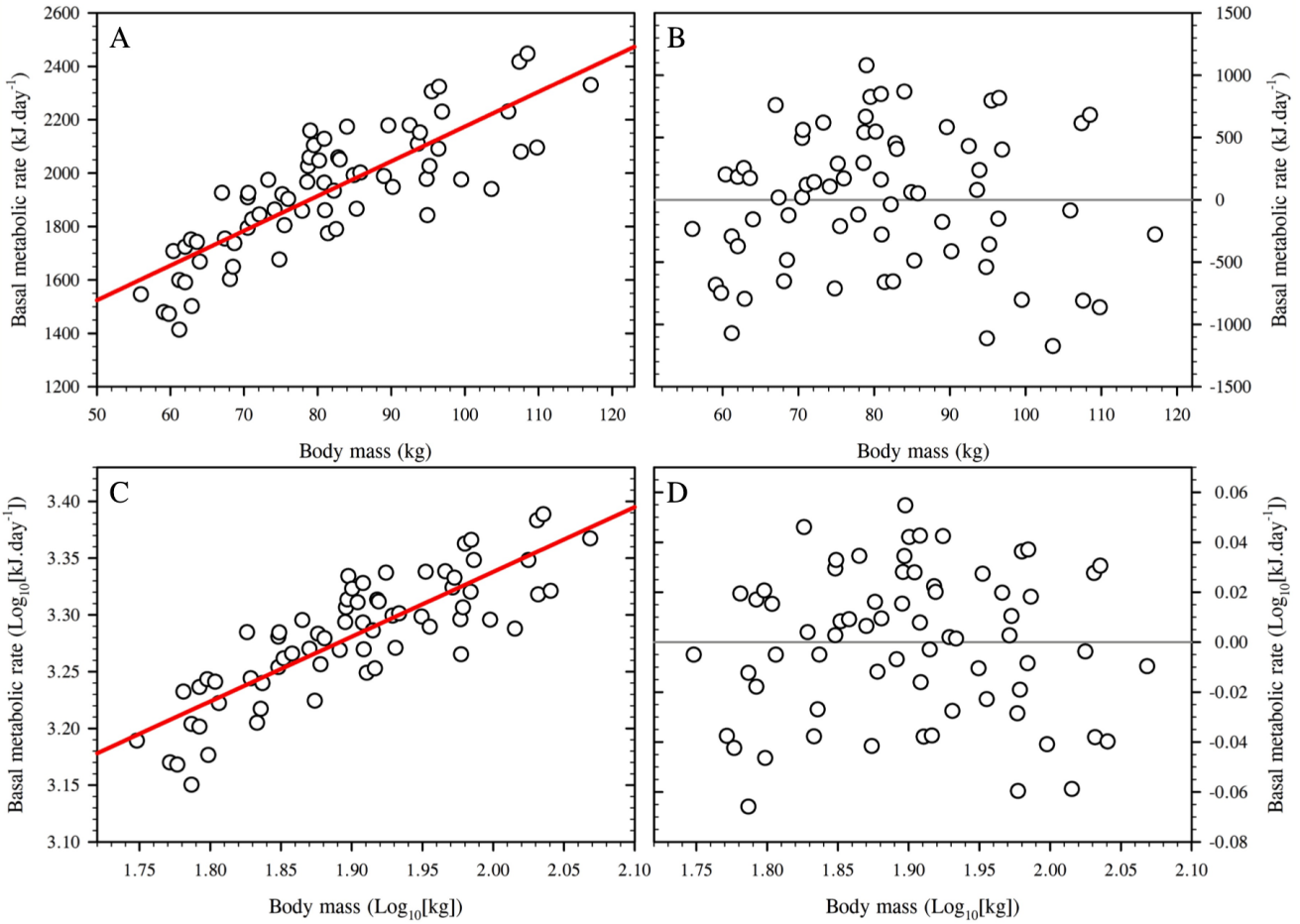

Figure 2.13: Scatter (Figures 2.13A and 2.13C) and residual plots (Figures 2.13B and 2.13D) used to assess model linearity and homeoscedasticity for the scaling relationship between basal metabolic rate and body mass, respectively (N=68). For the non-linear model, the dataset was first $\log_{10}$ transformed to assess whether, while in that linear format, those data satisfied the two assumptions.

considered suitable and a linear model would be selected due to the superior fitting capabilities and analyses available. However, the biological assumption of an origin intercept was not met when those data were described using the linear regression (Figure 2.14 [solid line]). Instead, a significant positive ordinate-intercept was observed (3659.07 $L.min^{-1}$; $P<0.05$). As a result, the non-linear regression was the only model to satisfy both the statistical and biological assumptions, leading to the acceptance of Hypothesis Two-One.

2.3.2.1 Normalising the basal metabolic dataset

To compare metabolic data among individuals of different body sizes it is important to remove the effect of body mass on those data. This can be sufficiently achieved if the shape of the scaling relationship between both variables is understood. When mass-independent data are successfully normalised, they display a near-zero correlation with body mass. The ability to generate mass-independent data from the basal metabolic dataset was assessed using four normalisation approaches: ratiometric, two intercept-adjusted ratio methods and allometric ratio. The efficacy of each method was tested using Pearson's correlation coefficient.

As anticipated, ratiometric normalisation was not an appropriate method to remove the mass relationship among those data. Using that normalisation method overcorrected the original mass relationship among those data, resulting in a systemic error remaining among those data (Figure 2.15A; $P<0.05$). This outcome is not a new observation (Tanner, 1949; Packard and Boardman, 1988; Katch, 1973), but was performed to demonstrate the unsuitability of ratiometric normalisation for metabolic datasets with a non-origin intercept. As a result, this method should be avoided when normalising metabolic data.

To normalise the dataset using the linear regression two methods known as intercept-adjusted ratios were tested. Typically, the linear regression equation would be rearranged so that the normalised residuals are generated with the following formula: $y_{adj} = y\text{-}c/x$, where y_{adj} is the normalised residual, y the measured value of metabolic rate, c the regression intercept and x body mass. However, this method can sometimes produce spurious correlations among those normalised residuals, which

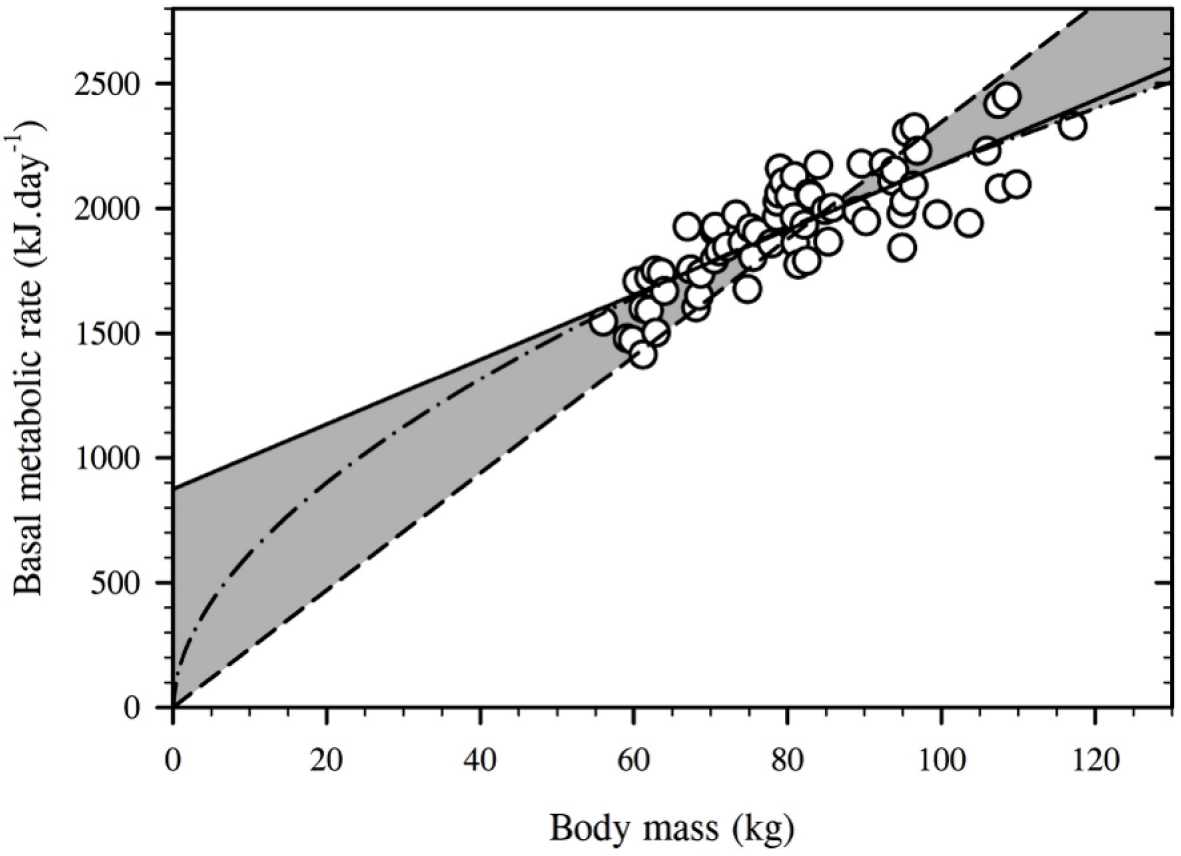

Figure 2.14: A scatter plot of the scaling relationship between basal metabolic rate and body mass for 68 men. Three regression models were applied to the plotted data: linear (first-order polynomial), ratiometric (first-order polynomial with a forced-zero intercept) and non-linear (allometric). The shaded area represents the predictive error among the three scaling models.

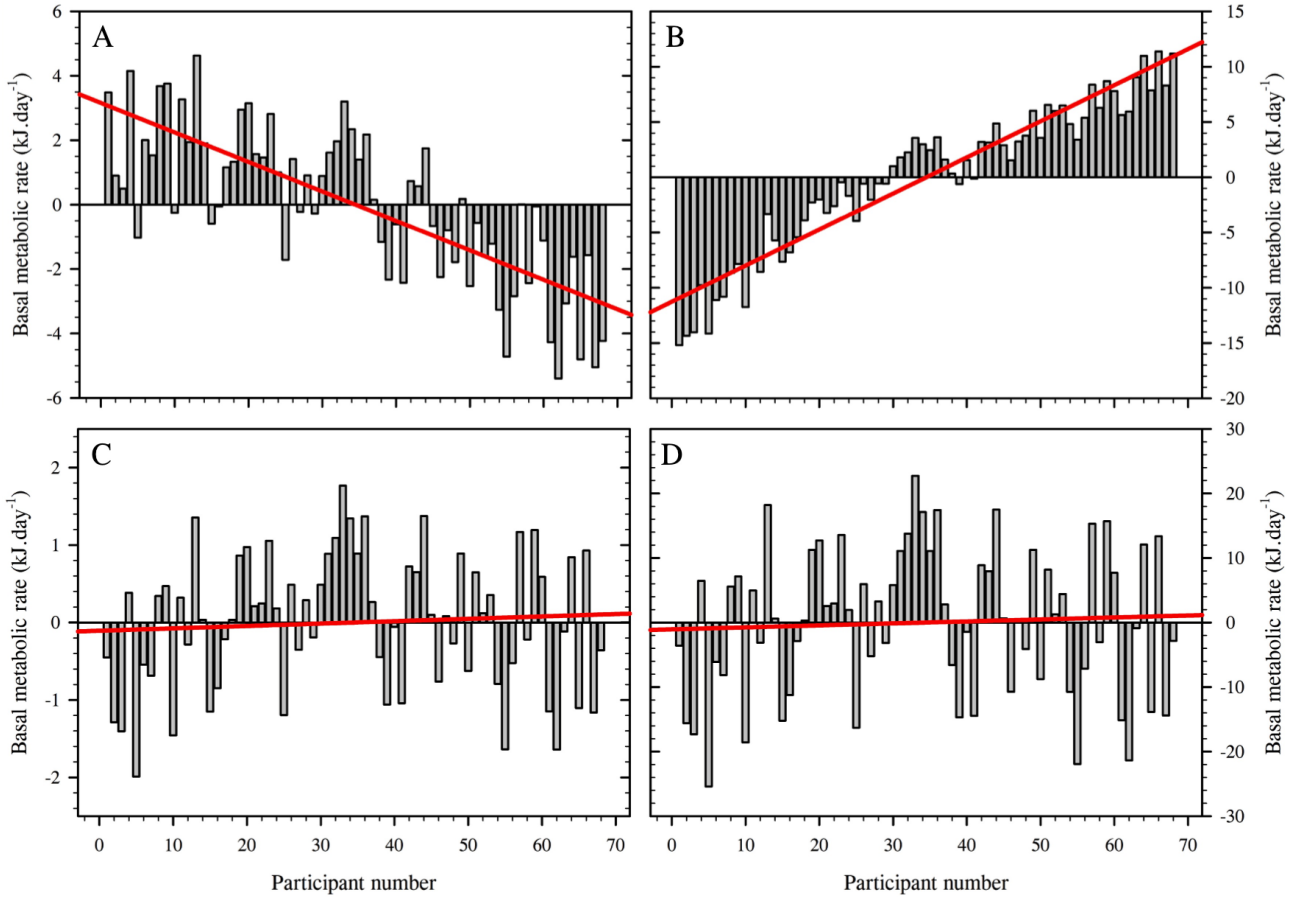

Figure 2.15: Bar graphs displaying the remaining correlation between body mass and metabolic rate for each normalisation method: ratiometric (Figure 2.15A; r=-0.75; P<0.05), intercept adjusted (Figure 2.15B; r=0.95; P<0.05), intercept and variance adjusted (Figure 2.15C; r=0.07; P>0.05) and allometric (Figure 2.15D; r=0.05; P>0.05). Basal metabolic rate data are presented for 68 men, ordered from lightest to heaviest across the abscissa.

can be avoided if the residual variation in the dependent variable is also considered (Albrecht *et al.,* 1993). That observation was supported when normalising the present dataset with both approaches (Figures 2.15B and 2.15C): a systematic bias still present among the dataset normalised using the first approach (Figures 2.15B; $P<0.05$). Accordingly, to normalise a dataset that does satisfy the assumptions for a linear model, the latter normalisation approach should be adopted to confidently remove the mass relationship from those data.

The allometric approach (y/x^b) was used to evaluate the normalisation process for the non-linear model on the untransformed dataset. This normalisation approach demonstrated the lowest remaining correlation among the metabolic residuals (Figure 2.15D; $P>0.05$). Accordingly, it was concluded that this was a suitable normalisation approach for the non-linear dataset. Moreover, the normalisation approach was relatively simple to perform reducing the chance of error during calculations, y/x^b, where y is the measured metabolic rate, x is body mass and b is the mass exponent.

2.3.2.2 Adjusting basal metabolic rate to deep-body temperature

Analysis of variance was used to assess the effect of deep-body temperature on the mass exponent. Metabolic data were adjusted from a mean temperature of 36.3°C ($\pm$0.03) to the pre-defined common temperature of 36.2°C using Equation 2.2, to account for potential differences in metabolic enzyme reaction rates (see Section 2.2.4.2). If the mass exponent was modified, then deep-body temperature would need to be included in the scaling regression when predicting and normalising human metabolic data.

Before comparing the two scaling models, it was first necessary to confirm that the scaling relationship remained non-linear after the temperature adjustment and if so, that the model residuals for both scaling regressions had a normal distribution when $\log_{10}$ transformed, an assumption of analysis of covariance. The temperature measurement for one individual failed during the basal trial, therefore these analyses were performed using a sample of 67, rather than 68 (full basal dataset).

The $\log_{10}$-transformed basal dataset satisfied the assumption of normality. The distribution of those data had approximate normality when plotted to a histogram distribution (Figure 2.16A), and was statistically similar to a normal distribution at the 5% probability level when assess using skewness and kurtosis *z*-scores and the Shapiro-Wilk test (Table 2.4; $P > 0.05$). Moreover, an equal variance of error (Figure 2.16B) and no presence of autocorrelation (Table 2.4; $P > 0.05$) were observed. Consequently, all the assumptions of linear regression were satisfied, thus the scaling relationship for the temperature-adjusted basal metabolic rate could be confidently described using non-linear regression.

Since both $\log_{10}$-transformed, non-linear regressions demonstrated a normal distribution of regression residuals (unadjusted: Table 2.3; temperature-adjusted: Table 2.4; $P > 0.05$), it was possible to compare both models using analysis of covariance. Adjusting the metabolic data to a common deep-body temperature did not significantly modify the body-mass exponent (unadjusted: 0.55; temperature-adjusted: 0.57; Figure 2.17; $P > 0.05$), despite a significantly lower mean basal metabolic rate in the temperature-adjusted dataset (unadjusted: 8112.2 $kJ.day^{-1}$ [$\pm$117.8]; temperature adjusted: 7943.6 $kJ.day^{-1}$ [$\pm$118.0]; $P < 0.05$). Thus, the scaling regression was not modified by variations in deep-body temperature. Accordingly, it was concluded that when assessing data in healthy humans, only basal metabolic rate and body mass were required to generate the scaling regression.

2.3.2.3 Comparing the human and animal body-mass exponents

Since deep-body temperature did not modify the basal scaling relationship in humans, it was possible to directly compare the human mass exponent with that used for animals in comparative physiology: $mass^{0.67}$ (White and Seymour, 2003, 2004). A t-test was used to compare both body-mass exponents, this was performed using the $\log_{10}$-transformed human model ($mass^{0.57}$), although $mass^{0.67}$ is applied to both raw and log-transformed animal datasets. The human body-mass exponent was statistically smaller than that applied to the animal dataset ($P < 0.05$). The difference between both exponent values can be observed in Figure 2.17, where the red line signifies the comparative-physiology exponent.

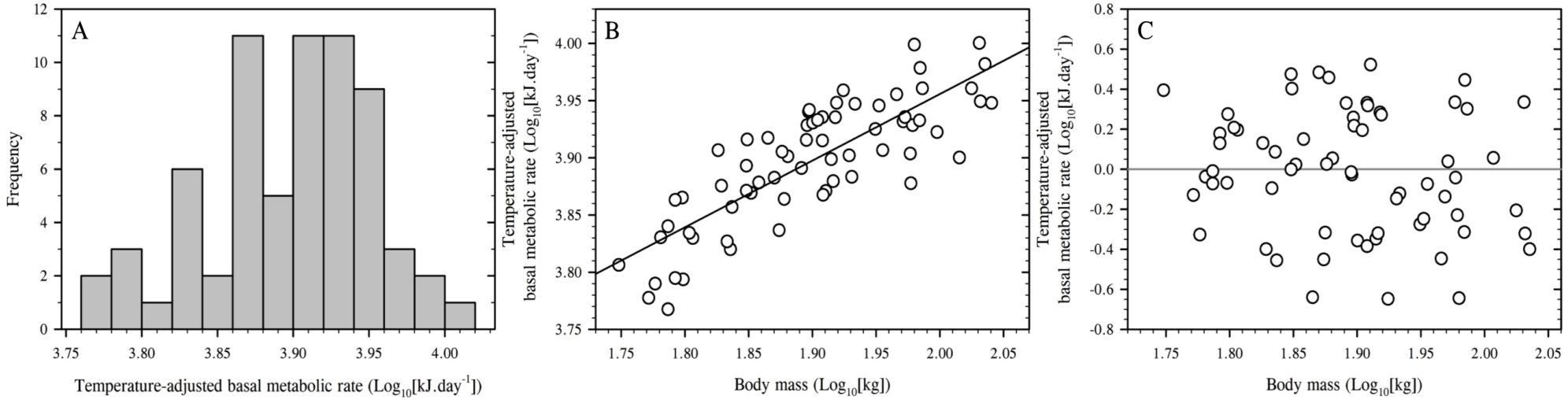

Figure 2.16: Histogram plot displaying the frequency distribution of the temperature-adjusted basal metabolic rate data (Figure 2.16A). Scatter (Figure 2.16B) and residual (Figure 2.16C) plots used to assess the assumptions of linearity and homeoscedasticity respectively for those basal data when plotted against body mass. All basal data (N=67) were estimated from oxygen consumption ($L.min^{-1}$) using the abbreviated Weir formula (1949), then adjusted to the common deep-body temperature of 36.2°C using Equation 2.2.

Table 2.4: Test statistics used to evaluate normality and autocorrelation among the temperature-adjusted metabolic data and residuals for the corresponding linear and non-linear scaling regressions ($N=67$). Data for the non-linear regression were $\log_{10}$ transformed before analysis. Significant values are identified using the symbol (*; $P<0.05$).

	Temperature-adjusted basal metabolic rate		Regression model residuals	
	Raw ($kJ.day^{-1}$)	Log-transformed ($Log_{10}[kJ.day^{-1}]$)	Linear	Non-linear ($\log_{10}$ transformed)
Skewness statistic	-0.17	-0.43	-0.07	-0.19
Z-score	-0.58	-1.48	-0.12	-0.66
Kurtosis statistic	-0.55	-0.43	-0.89	-0.93
Z-score	-0.94	-0.74	-1.54	-1.62
Shapiro-Wilk statistic	0.98	0.97	0.98	0.97
Durbin-Watson statistic	-	-	1.52*	1.59

Notes: Basal metabolic data were derived using the Weir formula (1949) from observed basal oxygen data ($L.min^{-1}$). Deep-body temperature was measured using an auditory-canal thermistor and used to adjust all basal metabolic data to 36.2°C using Equation 2.4 (see Section 2.2.4.2).

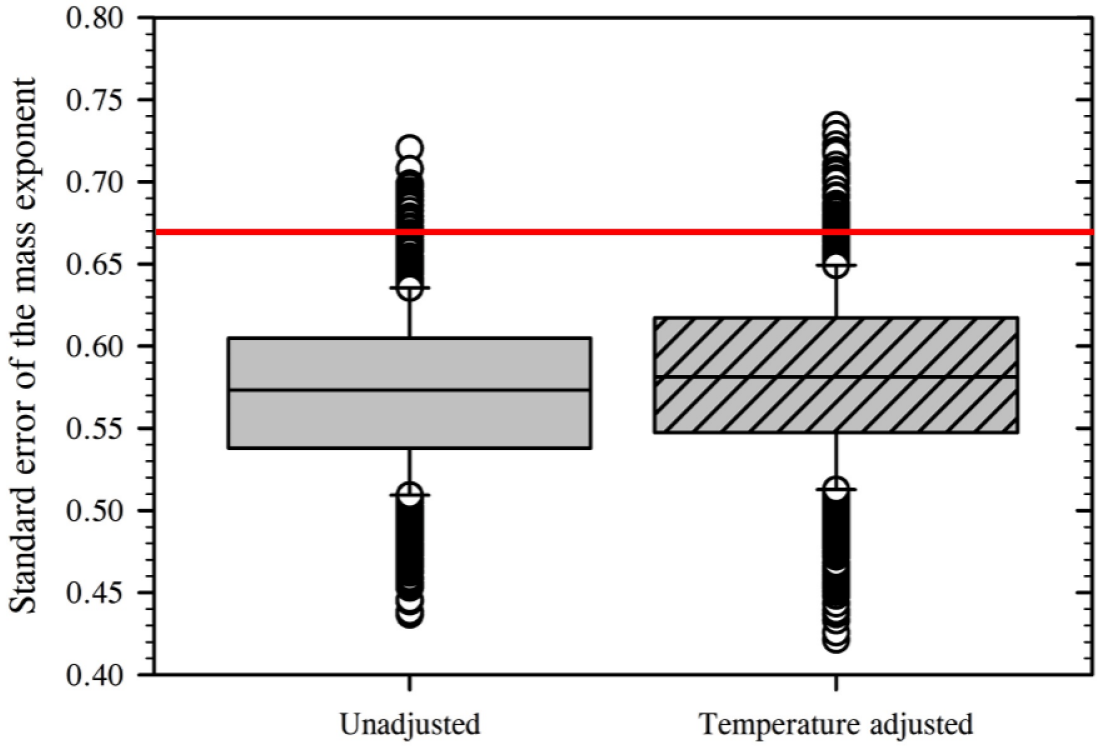

Figure 2.17: Box plot displaying the means and standard errors of the means for the untransformed (solid fill) and temperature-adjusted (36.2°C; hashed fill) mass exponents for the scaling relationship between basal metabolic rate ($kJ.day^{-1}$) and body mass (kg) in humans. Data ($N=67$) were generated using bootstrapping (1000 repetitions, re-sampling method) and are presented for the log_{10}-transformed regressions, as this format was used for the statistical comparisons. The red line signifies the animal exponent used in comparative physiology ($mass^{0.67}$: White *et al,*. 2003; White and Kearney, 2014). No significant interaction was realised between the two scaling regressions (mass exponents; $P>0.05$).

2.3.3 The effect of posture change when scaling oxygen consumption

A secondary aim of this research was to determine whether or not an increase in metabolic intensity resulted in a change to the scaling model. Within this experimental phase, this aim was explored during non-exercise states, with the intention of identifying the minimum increase in metabolic intensity required to modify the scaling regression (mass exponent). This research aim was explored with a change in posture from supine (basal) to standing, and during two exploratory states: 50% and 100% mass-supported standing.

2.3.3.1 Exploratory investigation: scaling mass-supported standing

In animals ($mass^{0.67}$: White and Seymour, 2003 [basal]; $mass^{0.81}$: Taylor *et al.,* 1981 [peak exercise]), and some allometric human studies (Rogers *et al.,* 1995; Markovic *et al.,* 2007), the scaling exponent has been modified by an increase in metabolic intensity (exercise). However, to the author's knowledge, the minimum increase in energy expenditure required to change the mass exponent has not been explored. Therefore, an exploratory investigation was undertaken to assess the feasibility of evaluating this research theme during resting states in humans. Nonethelesss, due to method constraints, those data could not be used for comparisons within the main study (see below).

As scaling during bipedal locomotion comprised a wider project theme (Chapters 3-6), during this exploratory investigation, all non-basal resting conditions were tested during a standing posture: 50% and 100% mass-supported standing. The stages were designed to isolate a passive change in posture (basal to 100% mass-supported standing) followed by the action of supporting ones body mass (100% mass-supported standing to 50% mass-supported standing to standing [unaided]), with the aim of determining the effect of each metabolic increment on the scaling model.

To investigate this aim, a subset of participants (N=17; 22 y [SD 4]; 81.9 kg [SD 14.5], range= 62.0-108.7 kg; 182.7 cm [SD 9.7], range=168.2-201.5 cm; height-adjusted sum of skinfolds: 54.0 mm [SD 19.8], range=29.3-91.0 mm) were selected to complete the two further test conditions on a subsequent laboratory visit (Figure 2.3 [green symbols]). The investigation initially started with 18 participants, but one

was unable to complete the 100% mass-supported stage (identified by the asterix [*] in Figure 2.3), so his data were removed from the sample.

Wearing the same clothing and equipment used during the main study (Figure 2.4), participants completed two, 10-min standing (stationary) stages, with 5-min seated rest between conditions. The 50% mass-supported stage was performed first. To support their body mass, subjects were suspended using a whole-body harness, fitted with neoprene foam to reduce any pressure points. The harness was attached to an overhead beam, used to support the participant's mass at five points to encourage a normal standing position: the top of both shoulders, the two most lateral points of the hips, and an attachment point at the centre of the back between the shoulders. The level of support was controlled manually, with the necessary rope tension determined using a set of digital scales (MS3200, Medical Scale, Charder, Taichung, Taiwan).

The shape of each scaling relationship was assessed using the same decision-making process used in the main study (Figure 2.8). Accordingly, for either the linear or non-linear model to be deemed suitable, it had to satisfy both the assumptions of linear regression and have an ordinate intercept. Once the shape of each model (linear or non-linear) was determined, the effect of metabolic intensity could be compared using analysis of covariance. Mean oxygen consumption and cardiac frequency data were compared between groups using repeated-measures analyses of variance.

Unfortunately, those measured data were too scattered to accurately determine the model shapes (Figure 2.18). Weak linear relationships were observed for both exploratory conditions when in untransformed and $\log_{10}$-transformed units (Table 2.5). Both linear and non-linear regression models displayed an equal variance of residual error (Figure 2.19). Surprisingly, an origin intercept was realised for both linear models ($P > 0.05$), indicating the potential to use either linear or non-linear regression for these conditions. Non-linear was selected so that those data could be compared with the basal and standing conditions.

However, the corresponding physiological responses for the two mass-supported states were not realistic. While it was considered that the low sample size would have

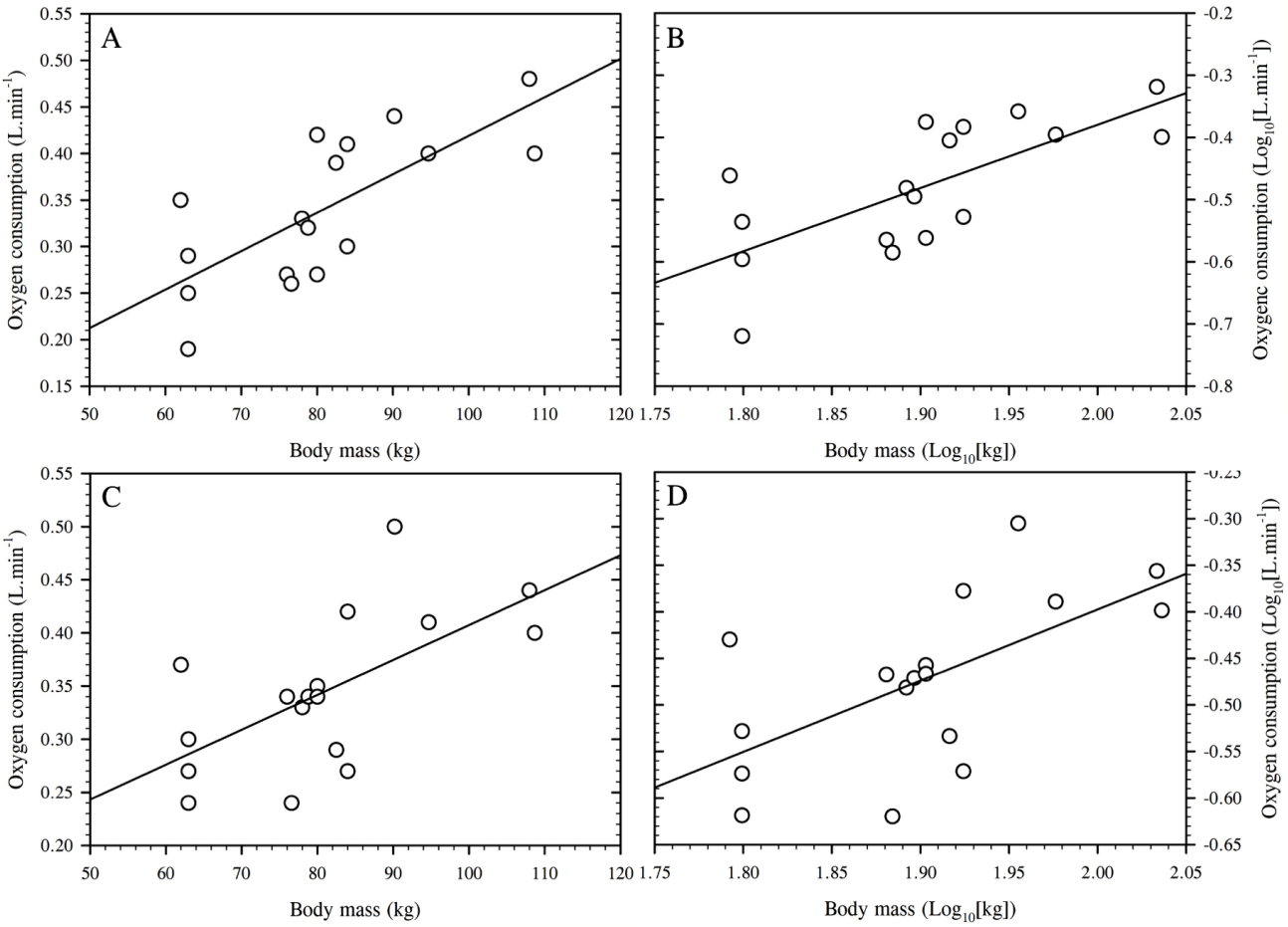

Figure 2.18: Scatter plots used to assess the assumption of linearity for the scaling relationship between mass-supported oxygen consumption (standing) and body mass within the exploratory dataset (N=17). Figure 2.18A displays the 50% mass-supported stage in the linear format (r^2=0.53), and Figure 2.18B, the same model when $\log_{10}$ transformed (r^2=0.32). The linear model for the 100% mass-supported standing stage is displayed in Figure 2.18C (r^2=0.40), and the corresponding $\log_{10}$-transformed model in Figure 2.18D (r^2=0.39).

Table 2.5: Test statistics used to evaluate normality and autocorrelation in oxygen consumption oxygen consumption during the mass-supported standing trials and corresponding regression residuals ($N=17$). Data for the non-linear regression were $\log_{10}$ transformed before analysis. No significant values were identified ($P>0.05$).

	Oxygen consumption				Regression model residuals			
	100% supported		50% supported		100% supported		50% supported	
	Raw ($L.min^{-1}$)	Log-transformed ($Log_{10}[L.min^{-1}]$)	Raw ($L.min^{-1}$)	Log-transformed ($Log_{10}[L.min^{-1}]$)	Linear	Non-linear	Linear	Non-linear
Skewness statistic	0.34	<-0.01	-0.19	-0.40	0.39	-0.02	0.34	<-0.01
Z-score	0.62	<-0.01	-0.24	-0.76	0.70	-0.04	0.26	<-0.01
Kurtosis statistic	-0.83	-1.07	-1.19	-0.78	-0.35	-0.61	-1.49	-1.14
Z-score	-0.78	-1.00	-1.12	-0.74	-0.32	-0.58	-1.40	-1.08
Shapiro-Wilk statistic	0.96	0.97	0.97	0.96	0.95	0.95	0.93	0.98
Durbin-Watson statistic	-	-	-	-	1.65	1.81	2.17	2.09

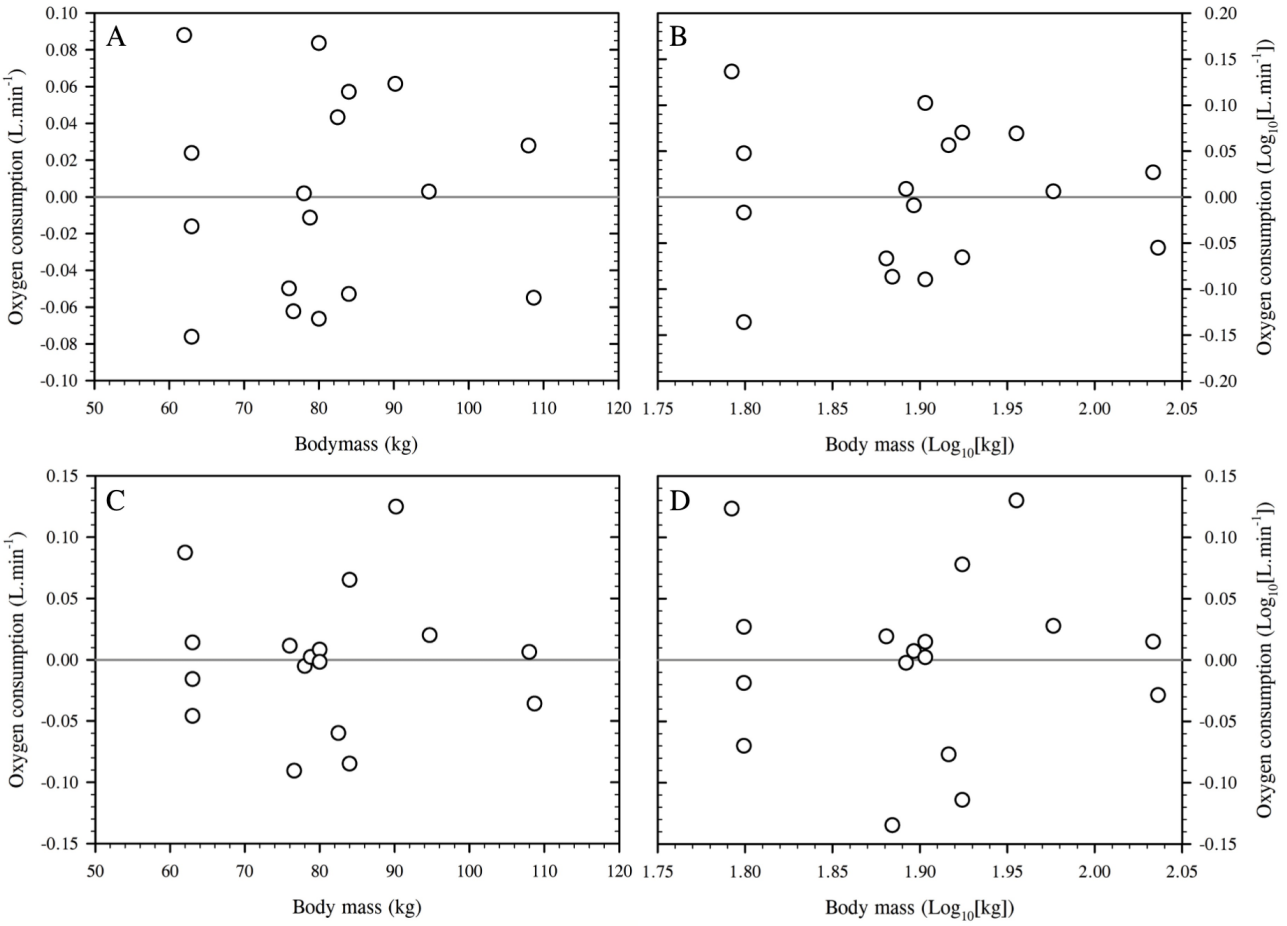

Figure 2.19: Residual plots used to assess the assumption of heteroscedasticity for the scaling relationship between mass-supported oxygen consumption (standing) and body mass within the exploratory dataset (N=17). Figure 2.19A displays the residuals for the 50% mass-supported stage in the linear format, and Figure 2.19B, the same regression residuals when $\log_{10}$ transformed. The linear regression residuals for the 100% mass-supported standing stage is displayed in Figure 2.19C, and the corresponding $\log_{10}$-transformed regression residuals in Figure 2.19D.

induced some error upon the regression coefficients, the observed mass exponents were atypical than expected. Both mass exponents were greater than that applied to the unaided-standing dataset ($mass^{0.68}$: Section 2.5.3.2): $mass^{1.06}$ for 50% supported standing and $mass^{0.79}$ for 100% mass-supported standing (Figure 2.20A). The former value is also greater than $mass^{1}$, which for metabolic scaling is physiologically impossible.

It is suspected that these inflated oxygen-consumption exponents were a response to some methodological constraints, for an inverse trend was present between cardiac frequency and metabolic intensity, when calculated using matched participant samples (basal: 58 $b.min^{-1}$ [±9]; 100% mass-supported standing: 96 $b.min^{-1}$ [±14]; 50% mass-supported standing: 90 $b.min^{-1}$ [±14]; unaided standing: 86 $b.min^{-1}$ [±12]; Figure 2.20B; $P<0.05$). Despite the best efforts of investigators to remove the likelihood of these factors (loosened chest straps and the fitting of neoprene padding about the harness), that relationship between cardiac frequency and the percentage of body mass supported may be reflective of an increase in pain response to the suspension and a potential restriction upon the chest wall, and consequently respiratory mechanics. That is, as body mass increased a greater total mass would have been supported, increasing these responses and potentially artificially elevating oxygen consumption among the heavier participants. Consequently, the mass-supported conditions were unlikely to be reflective of a weightless, standing resting condition and were therefore removed from the main scaling comparisons.

2.3.3.2 Scaling oxygen consumption during unaided standing

A change in posture from supine to standing significantly increased oxygen consumption from 0.27 $L.min^{-1}$ (± <0.01) while supine to 0.33 $L.min^{-1}$ (±0.01) during standing ($P<0.05$), and a similar response was observed for the cardiac frequency data (supine: 59 $b.min^{-1}$ [±8]; standing: 80 $b.min^{-1}$ [±14]; $P<0.05$). Thus, the standing condition was considered a separate metabolic intensity from the basal state.

The shape of the standing scaling model was determined using the decision-making flow chart (Figure 2.8), before comparing the basal (supine) and standing models with

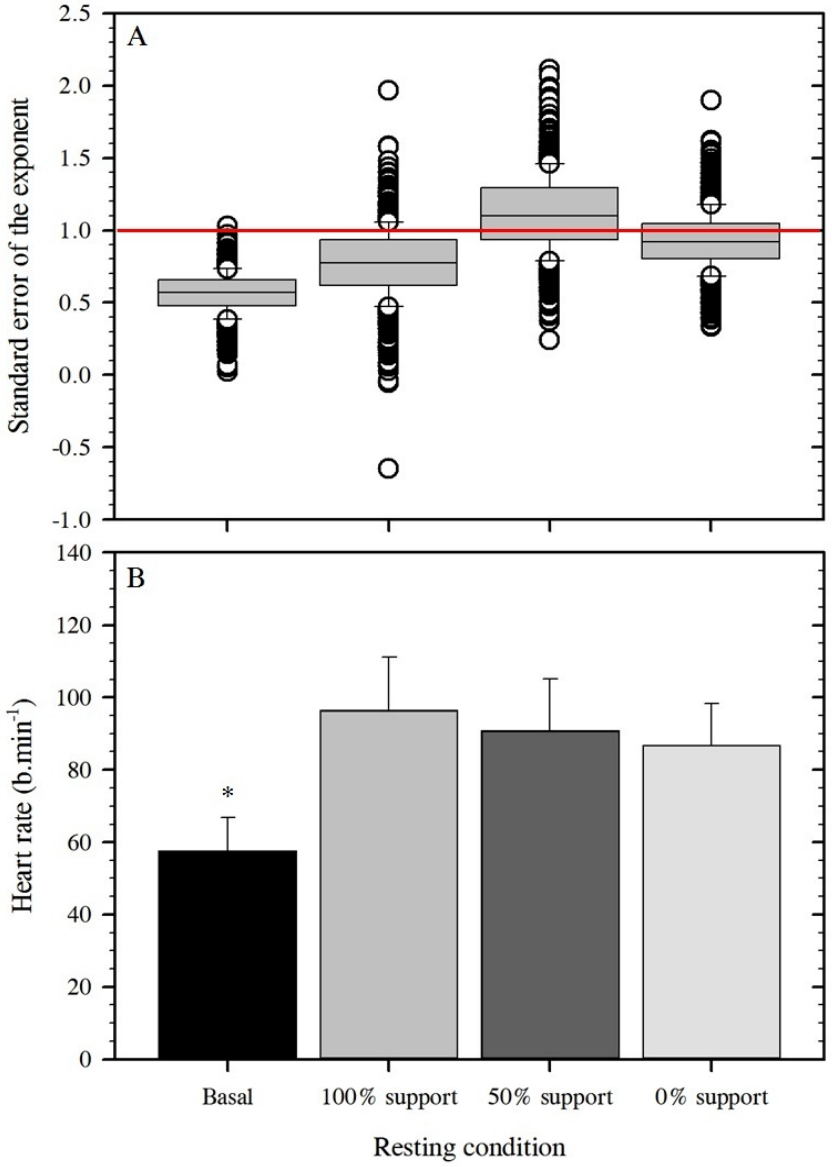

Figure 2.20: (Figure 2.20A) Box plot of the mass exponents and corresponding standard error of the mean (generated using bootstrapping) for the four metabolic intensities tested within this Chapter, for comparison against the two exploratory mass-supported standing stages. All standard errors of the mean were generated from models using a matched dataset ($N=17$). The red line identifies the value at which the predicted exponents became non-physiological (>1). No significant differences between exponents were realised ($P>0.05$). (Figure 2.20B) Bar chart of the relationship between mean cardiac frequency and metabolic intensity. Cardiac frequency during the basal condition was significantly lower than all other conditions (*; $P<0.05$).

one another. The assumption of normality was satisfied using all three normality assessments, for both raw and $\log_{10}$-transformed data formats: histogram plots (Figure 2.21), skewness and kurtosis z-scores and the Shapiro-Wilk test (Table 2.6; $P > 0.05$). Linearity and homeoscedasticity were also confirmed using a visual assessment of the scatter and residual (Figure 2.22) plots. Finally, the no first-order correlation was realised between those regression variables (Durbin-Watson test: Table 2.6; $P > 0.05$). Accordingly, both the linear and $\log_{10}$-transformed non-linear models satisfied the assumptions of linearity, and thus were considered statistically suitable for scaling purposes.

Nevertheless, a significant positive intercept was observed when the linear regression was extrapolated to the ordinate (0.12 $L.min^{-1}$; $P < 0.05$), violating the biological assumption of an origin intercept. That is, it is impossible to have any metabolic rate at zero mass. Therefore, the model could not be accurately used to describe standing oxygen consumption data outside of the tested mass range. It was therefore concluded that the linear regression was not suitable to describe the scaling relationship during a standing state and the non-linear model was selected for that purpose. Leading to the acceptance of Hypothesis Two-Three.

Since both supine (basal) and standing states scaled using a non-linear model, it was possible to evaluate the effect metabolic intensity on the scaling relationship using analysis of covariance, thus comparing the two mass exponents. The mass exponent numerically increased with the postural change from supine and standing, but, this increase was not significant (Figure 2.23; $P > 0.05$). Accordingly, both scaling models could be described using the same body-mass exponent (leading to the acceptance of Hypothesis Two-Four). For reference, a list of all regression models analysed within this Chapter is presented in Table 2.7.

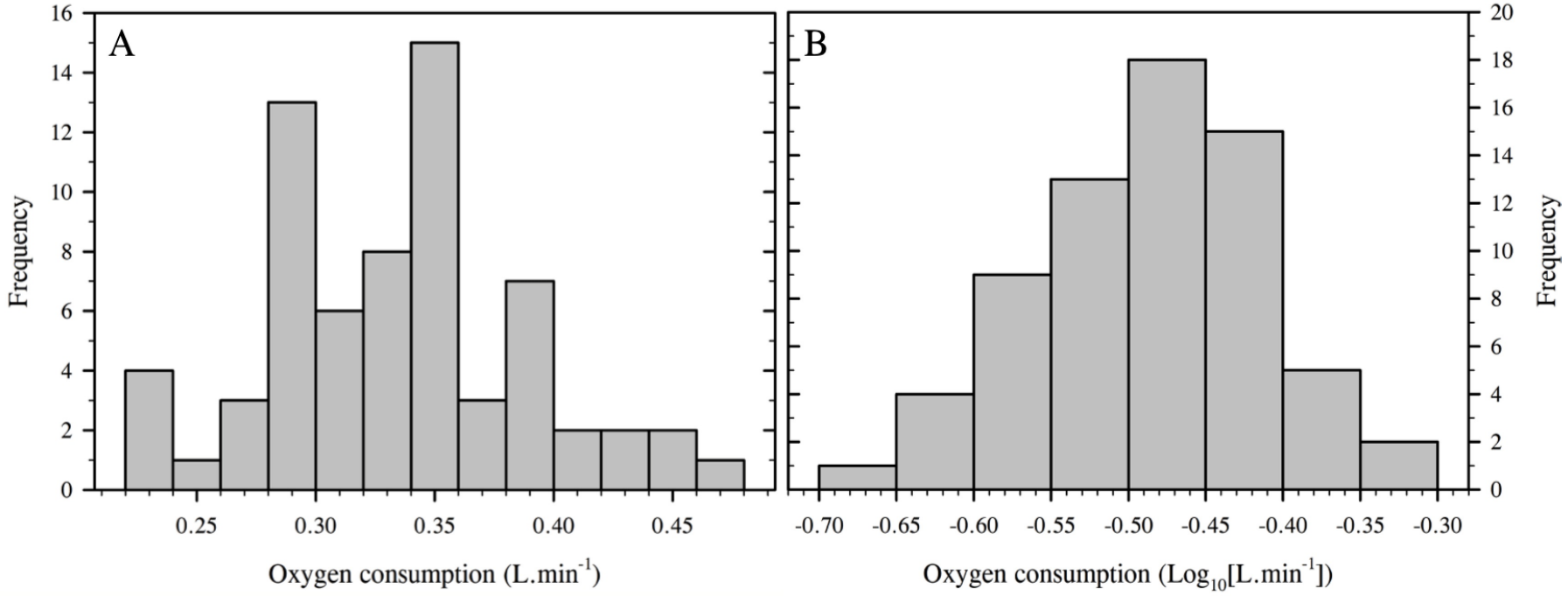

Figure 2.21: Histogram plots of oxygen consumption during standing for 67 men. Data are displayed in untransformed (Figure 2.19A) and $\log_{10}$-transformed (Figure 2.19B) units. These plots were used as part of the assessment of normality within the dataset.

Table 2.6: Test statistics used to evaluate normality and autocorrelation among the standing oxygen consumption data and the regression residuals ($N=67$). Data for the non-linear regression were $\log_{10}$ transformed before analysis. No significant values were identified ($P>0.05$).

	Standing oxygen consumption		Regression residuals	
	Raw ($L.min^{-1}$)	Log transformed ($Log_{10}[L.min^{-1}]$)	Linear	Non-linear (log_{10} transformed)
Skewness statistic	0.25	-0.18	0.42	0.10
Z-score	0.84	-0.62	1.44	0.18
Kurtosis statistic	-0.24	-0.27	-0.57	-0.78
Z-score	-0.42	-0.46	-1.00	-1.34
Shapiro-Wilk statistic	0.98	0.98	0.97	0.99
Durbin-Watson statistic	-	-	1.86	1.80

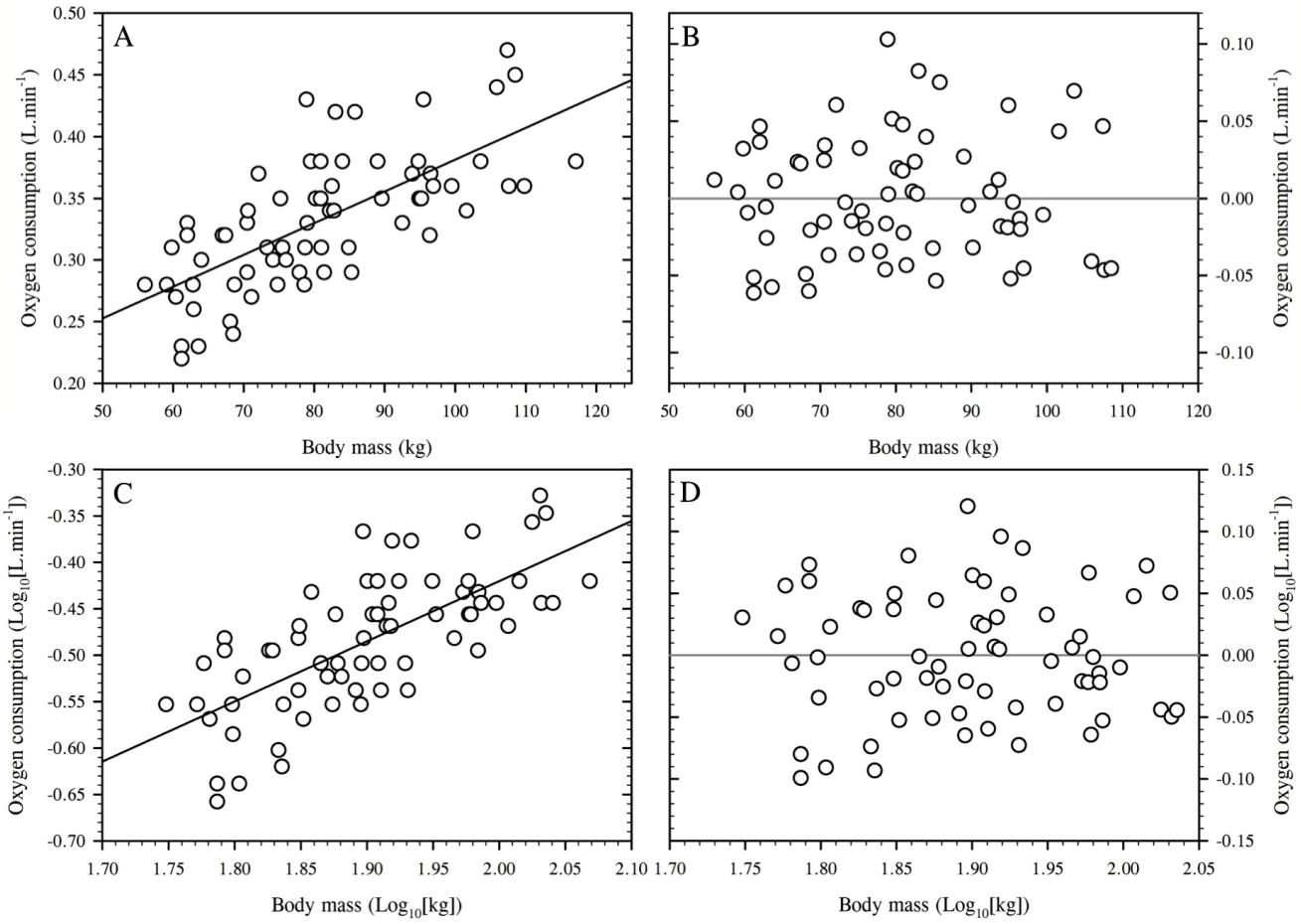

Figure 2.22: Scatter (left) and residual (right) plots used to assess the assumptions of linearity and homeogeneity, respectively, for the linear (Figures 2.20A and 2.20C) and log_{10}-transformed non-linear (Figures 2.20B and 2.20C) scaling regressions applied to the standing dataset. Data are displayed for 67 men.

2.4 DISCUSSION

2.4.1 Scaling basal metabolic rate in humans

The mass-dependent nature of human metabolism has been recorded since the late 18th century (Lavoisier and DeLaplace, 1780). For human data, attempts to describe that scaling relationship have led to the emergence of both linear (first-order polynomial: Harris and Benedict, 1919; Schofield, 1985; Cole and Henry, 2005) and non-linear models (allometric: Boothby and Sanders, 1922; Durnin, 1981; Rogers *et al.,* 1995). Both of those scaling models are used within the literature, despite the presence of systematic errors between predictive values as the mass range widens (Figure 2.1). This outcome can lead to spurious metabolic predictions if the less suitable method is adopted. To date, no consensus has been reached regarding which method is more suitable, most likely due to the sample and analysis methods adopted (see Section 2.2.1). Accordingly, the primary aim within this research phase was to establish which scaling method (linear or non-linear) was more appropriate to describe a human basal metabolic dataset. With the secondary aim being to determine whether a change in posture was a sufficient increase in metabolic rate to modify the scaling model.

To the author's knowledge, this is the first study where the scaling relationship between basal metabolic rate and body mass has been comprehensively evaluated in humans. While the theme had been investigated previously, few authors had directly compared linear and non-linear models using the same dataset (exceptions: Harris and Benedict, 1918, 1919 [indirectly]; Boothby and Sanders, 1922; Durnin, 1981). Among those studies, two main limitations prevented the attainment of a conclusive scaling outcome. The first limitation was that morphometric differences were only controlled in one sample (height to mass ratio: Harris and Benedict, 1918, 1919). Without performing this step, morphological and physiological differences can modify the scaling relationship, meaning that the derived regression will not be applicable to a wider population (Section 2.2.1). The second limitation was the assumption of a universal mass exponent, be it $mass^{0.67}$ or a derived surface area (DuBois and DuBois, 1916) for the non-linear regression (Harris and Benedict, 1918, 1919; Boothby and Sanders, 1922). Consequently, only one author made between-model comparisons using an appropriate non-linear model for their sample population (Durnin, 1981).

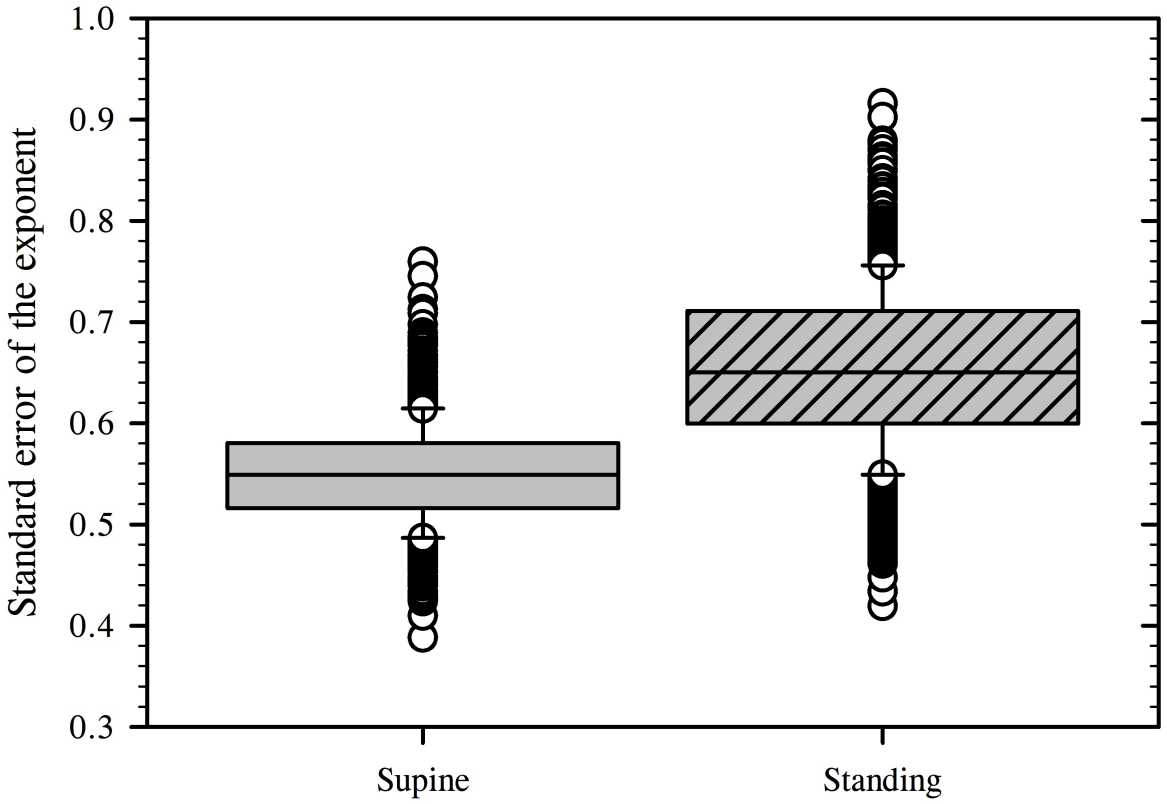

Figure 2.23: Means and standard errors of the mean for mass exponents for the scaling relationship between basal metabolic rate ($kJ.day^{-1}$) and body mass (kg) in humans (unadjusted [solid fill]; temperature adjusted [hashed fill]). Data ($N=67$) were generated using bootstrapping (1000 repetitions, re-sampling method) and are presented for the log_{10}-transformed regressions, as this format was used for the statistical comparisons. No significant interaction was realised between the two scaling regressions (mass exponents; $P>0.05$).

Table 2.7: Regression equations are presented for all metabolic intensities evaluated within this experimental Chapter. Equations are presented in linear (first-order polynomial), allometric and $\log_{10}$-transformed formats. All regressions were bootstrapped to predict the most-likely regression coefficients for each scaling model.

	Linear		**Non-linear ($\log_{10}$ transformed)**		**Non-linear (allometric)**
Basal metabolic rate (kJ.day^{-1})	**Equation**	r^2	**Equation**	r^2	**Equation**
Unadjusted (N=68)	$y = \mathbf{54.48} \cdot x + 3569.07$	0.68	$\text{Log}_{10}(y) = \mathbf{0.57} \cdot \text{Log}_{10}(x) + 2.82$	0.70	$y = 739.03 \cdot x^{\mathbf{0.55}}$
Temperature adjusted (N=67)	$y = \mathbf{54.77} \cdot x + 3542.37$	0.64	$\text{Log}_{10}(y) = \mathbf{0.58} \cdot \text{Log}_{10}(x) + 2.79$	0.67	$y = 668.88 \cdot x^{\mathbf{0.57}}$
Oxygen consumption (L.min^{-1})	**Equation**	r^2	**Equation**	r^2	**Equation**
Basal (supine) (N=68)	$y = \mathbf{0.002} \cdot x + 0.13$	0.65	$\text{Log}_{10}(y) = \mathbf{0.55} \cdot \text{Log}_{10}(x) - 1.61$	0.67	$y = 0.03 \cdot x^{\mathbf{0.54}}$
Standing (N=67)	$y = \mathbf{0.003} \cdot x + 0.12$	0.49	$\text{Log}_{10}(y) = \mathbf{0.65} \cdot \text{Log}_{10}(x) - 1.72$	0.50	$y = 0.02 \cdot x^{\mathbf{0.68}}$

Accordingly, within this investigation, the shape of the basal scaling relationship was explored by applying both linear and non-linear models to the dataset, with the only model constraints being that the linear model was a first-order polynomial regression (Equation 2.4) and the non-linear model was a simple allometric regression (Equation 2.5). The suitability of each model was determined using a systematic, statistical assessment process (Figure 2.8), which is believed to provide a clear and reproducible evaluation method.

The sample used to determine those regression models satisfied all pre-determined requirements, exceeding the anticipated mass range for adult males, encompassing masses between 56 kg and 117 kg. Participants were evenly distributed across that mass range, with a sample size ($N=68$) sufficient to obtain a stabilised mass exponent and reduce the standard error of the exponent for the non-linear regression, which, of the two regression models, had greater sample requirements. Moreover, participants were controlled for variations in age, gender and subcutaneous adiposity, ensuring that any differences in metabolic rate were a direct response to changes in body mass.

The assumptions of linear regression were evaluated for both models to determine their fit of the dataset. Both linear and non-linear ($\log_{10}$ transformed) regressions satisfied the four assumptions of linear regression: normality of variables, linearity, homeoscedasticity and no autocorrelation (Figure 2.12; Figure 2.13; Table 2.3; $P>0.05$). Therefore, within the sample mass range, both models could be used to analyse those data. The fact that both models statistically fit the dataset could be a potential reason why both linear and non-linear regressions have been used to describe data during the same metabolic intensity. Indeed, if both linear and non-linear models appear to fit the same dataset, customarily, the linear approach is adopted, as its corresponding analyses are considered more robust.

Nevertheless, when those regressions were extrapolated beyond the mass range of the current sample, the linear regression displayed a significant non-zero ordinate intercept (3650.28 $kJ.day^{-1}$; Figure 2.14; $P<0.05$). While it may be argued that a non-zero intercept is irrelevant if only comparing data within the tested mass range, this limits the applicability of the model beyond the tested mass range. Indeed, if that

linear model were applied to a neonate of 3.5 kg (as per Table 2.1), a metabolic rate of ~3849.01 kJ.day^{-1} is predicted, yet it should be less than a quarter of that value: ~824 kJ.day^{-1} (Boyd, 1962; Holliday, 1986). This poor fit has been recognised in some linear scaling work, leading to multiple age- and mass-dependent scaling models (Harris and Benedict, 1919; Schofield, 1985; Cole and Henry, 2005). While the impact of age on metabolism has already been acknowledged (Section 2.2.1.1), potentially justifying separate scaling models, it is argued that each age-dependent model should at least closely predict data points near to the mass range tested, unlike the stark changes in regressions currently observed. Consequently, the linear model was not considered suitable to describe the basal metabolic dataset in humans, for it did not satisfy the biological model assumption (Sholl, 1948).

It has been proposed that these mass and age differences can be described, at least in part in humans, using non-linear, allometric regression (Durnin, 1981). Indeed, predicting basal metabolic rate using the non-linear model derived within this Chapter resulted in a neonatal value of 1450.55 kJ.day^{-1}, still elevated, but much closer than that predicted using the linear regression. Moreover, the origin intercept is inherent within the non-linear model constraints, satisfying the biological model assumption. The importance of a realistic model is incontestable for purposes where that regression may be used to evaluate data points at the extreme of, or beyond its tested mass range: for it is at these masses where discrepancies are most likely to occur. To demonstrate the applicability of a non-linear model for humans beyond the present mass range tested, data have been pooled from this Chapter and the Schofield dataset (1985) in Figure 2.24. For reference, the linear model from this Chapter has also been applied to the figure. As evidenced, non-linear regression is applicable throughout the human mass range, with a similar exponent to the adult-specific value derived within this Chapter (combined dataset: mass$^{0.52}$; present study: mass$^{0.54}$). Accordingly, non-linear regression was the only scaling method that satisfied all the pre-requisite model assumptions, and therefore was deemed the more suitable scaling model to describe the relationship between basal metabolic rate and body mass in humans (Hypothesis Two-One accepted). Moreover, this scaling approach permits the further study and comparison of similar models within those broader mass ranges *i.e.* women and children, and the possibility of generating a simple human-specific scaling

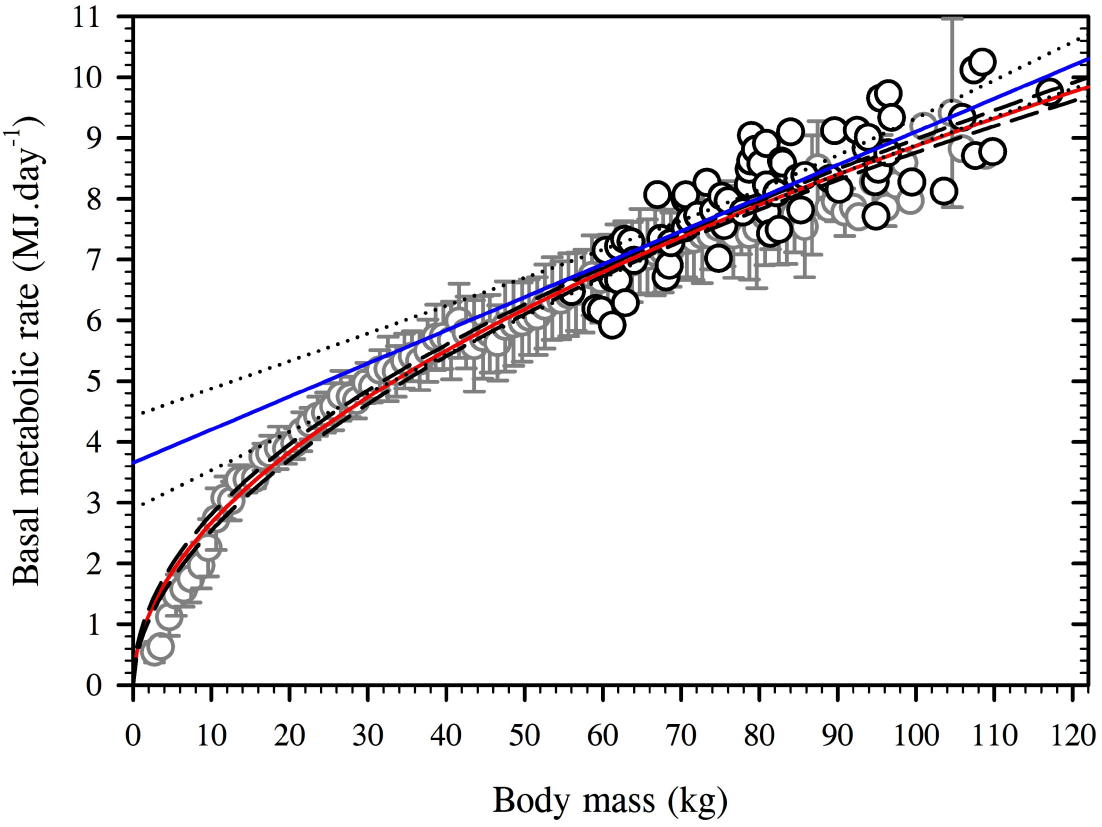

Figure 2.24: The basal scaling relationship for a combined dataset of 4181 healthy males (present dataset: $N=68$ [black symbols]; Schofield [1985] dataset: $N=4113$ [grey symbols]). Data from the Schofield dataset are presented as 1-kg averages with standard deviations. The combined datasets can be described using a single allometric model, $y=0.804 \cdot x^{0.521}$, indicated by the red line, with the 95% confidence intervals (dashed lines). The blue line represents the adult-specific linear model derived within this Chapter, with its 95% confidence intervals identified by the dotted lines.

model for metabolic data.

2.4.2 Evaluating non-linear scaling for human basal metabolism

Having established that non-linear, allometric regression was the more appropriate scaling model to describe the human dataset, two subsequent aims were investigated. The first of these aims was to determine whether or not adjusting those data to a common deep-body temperature would modify the mass exponent. Secondly, it was necessary to identify whether or not the human mass exponent was significantly different from the mammalian scaling value of $mass^{0.67}$.

2.4.2.1 The effect of adjusting data to a common deep-body temperature

Since the rate of enzymatic reactions is influenced by the surrounding temperature (Běhrádek, 1930; Guppy and Withers, 1999), a strong relationship is observed between deep-body temperature and metabolic rate. For example, during states of fever in humans, metabolic rate increases by up to 13% for every 1°C increase in deep-body temperature (Gore *et al.,* 2003). Moreover, accounting for this relationship in animals has improved the accuracy of the inter-species scaling regression, to the extent that reptilian (cold blooded) and avian (higher resting body temperatures) species can be scaled with mammalian data using the same exponent: $mass^{0.67}$ (White and Seymour, 2003). Therefore, it was considered likely that some of the inter-individual variations in basal metabolic rate may be explained by differences in deep-body temperature. Accordingly, this process had the potential to increase the accuracy of the human scaling model, and also to permit accurate comparisons between human and animal data.

Adjusting data to a common deep-body temperature significantly reduced mean basal metabolic rate (unadjusted basal metabolic rate: 8112.2 $kJ.day^{-1}$ [$\pm$125.2]; temperature-adjusted basal metabolic rate: 7982.3 $kJ.day^{-1}$ [$\pm$122.5]; $P < 0.05$). Nevertheless, the basal mass exponent was not significantly modified after adjusting for deep-body temperature (unadjusted: $mass^{0.55}$ [allometric]; adjusted: $mass^{0.57}$ [allometric]; Figure 2.17; $P > 0.05$). There are two likely reasons for this outcome: the temperature range of the sample and no presence of correlation between that measure and either scaling variable. Firstly, the adjusted temperature of 36.2°C was

similar to the mean resting temperature of the sample (36.32°C [±0.03]; range: 35.70-36.80°C). Indeed, resting deep-body temperature measurements tend to vary by only 1-2°C within a healthy population, with exception for axilla and sublingual measurements (Darowski, 1991; Sund Levander *et al.,* 2002; Taylor *et al.,* 2014). Accordingly, while the Q_{10} adjustments[19] made to those basal data significantly decreased mean metabolic rate, the initial participant deep-body temperature range was not sufficient to produce any meaningful change to the distribution of those data when plotted, and thus modify the mass exponent. Secondly, no first-order correlation was observed between body temperature and either body mass (Figure 2.25A) or metabolic rate (Figure 2.25B). Therefore, deep-body temperature was unlikely to have a covariant effect on the scaling relationship between basal metabolic rate and body mass.

Consequently, it was concluded that it was not necessary to adjust metabolic data for variations in deep-body temperature when scaling human basal metabolic rate against body mass. This result contrasted the relationship observed in comparative physiology, most likely because the mass range across animals, even within mammals, is much broader (*i.e.* 30.5°C *Histiotus velatus* [bat] to 40.7°C *Sciurus niger* [squirrel]: extracted from Sieg *et al.,* 2009). Nevertheless, this step should still be considered in instances were deep-body temperature might be more variable, such as when testing in non-normothermic environments or non-healthy populations.

2.4.2.2 Comparing the human mass exponent against mass$^{0.67}$

Mass$^{0.67}$ has been used, often indiscriminately (Dodds *et al.,* 2001; Savage *et al.,* 2004; White *et al.,* 2007), to describe the scaling relationship between basal metabolic rate and body mass across five orders of magnitude in animals (White and Seymour, 2003). To determine whether or not humans could be described using that same mass exponent, mass$^{0.67}$ was compared against the human basal mass exponent derived in this experiment. Since the human mass exponent was compared against a set value (0.67), rather than another regression model and its associated error, this

[19] A Q_{10} classification defines the relationship between an enzyme's rate of reaction and its temperature. For example, a $Q10$ of 2 means the reaction rate will double with every 10°C elevation in temperature.

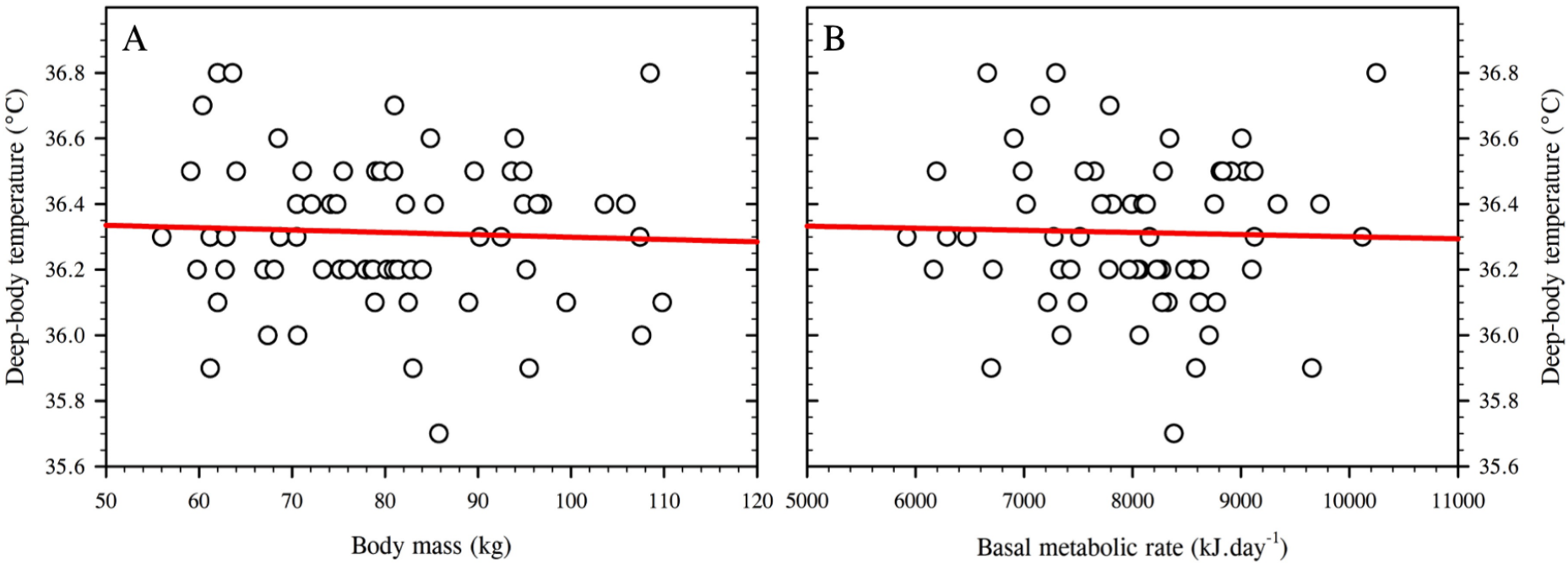

Figure 2.25: Scatter plots displaying the relationship between deep-body temperature and body mass (Figure 2.24A; $r=0.05$; $P>0.05$) and basal metabolic rate (Figure 2.24B; $r=0.03$; $P>0.05$). Data are presented for 67 men. The red line displays the correlation between both variables analysed using Pearson's correlation coefficient. Deep-body temperature was measured using an insulated auditory-canal thermistor (Figure 2.4C). Basal metabolic rate was approximated from oxygen consumption ($L.min^{-1}$) using the abbreviated Weir formula (1949: Equation 2.1).

analysis was performed using a t-test, with the null hypothesis that the human mass exponent was equal to 0.67. Since $mass^{0.67}$ is applied to log-transformed animal data, the analysis was conducted on the log_{10}-transformed human dataset ($mass^{0.57}$: Table 2.7).

The log_{10}-transformed human body-mass exponent ($mass^{0.57 \pm 0.05}$; 95% confidence interval range: $mass^{0.472\text{-}0.668}$) was statistically smaller than the animal value of $mass^{0.67}$ ($P < 0.05$). As a result, scaling human basal metabolic data using the latter value will introduce errors into the calculations. Thus, Hypothesis Two-Two was rejected. This lack of fit between $mass^{0.67}$ and human basal metabolic rate may explain why some early researchers advocated against the use of non-linear scaling for humans and their disdain for the surface-area law (Harris and Benedict, 1918, 1919).

The fact that the human basal metabolism could not be described using the exponent $mass^{0.67}$ was not a scaling anomaly. There is growing evidence within comparative physiology to support the use of phylogenic-specific basal mass exponents (*e.g.* mammals < 350 g: $mass^{0.69}$; mammals > 350 g: $mass^{0.76}$; White *et al.,* 2009), indicating that the scaling exponent may vary depending upon variables such as the mass range (White *et al.,* 2009) and an animal's method of thermoregulation (endothermic: $mass^{0.67}$; ectothermic: $mass^{0.84}$; White *et al.,* 2007). A particular reason for this outcome could also be the type of observations used, for example individual versus mean species data points; this effect can even be observed in Figure 2.26. In that figure, primates data points with corresponding deep-body temperatures have been extracted from the Sieg (2009) database and plotted alongside the human data from this investigation. When both sets of data were collectively scaled against body mass data the mass exponent is elevated compared with the human-specific value. Therefore, it appears that the size of the exponent is a function of the number of species and the mass range scaled, potentially congregating at the universal basal value of $mass^{0.67}$ once phylogenic variances such as deep-body temperature have been normalised (White and Seymour, 2003, 2004). However, by adopting this generalised mass exponent, species-specific variations in basal metabolic rate may be ignored. Consequently, it was concluded that the exponent $mass^{0.55}$ (untransformed, allometric; Table 2.7) should be used during all human-specific basal metabolism analyses.

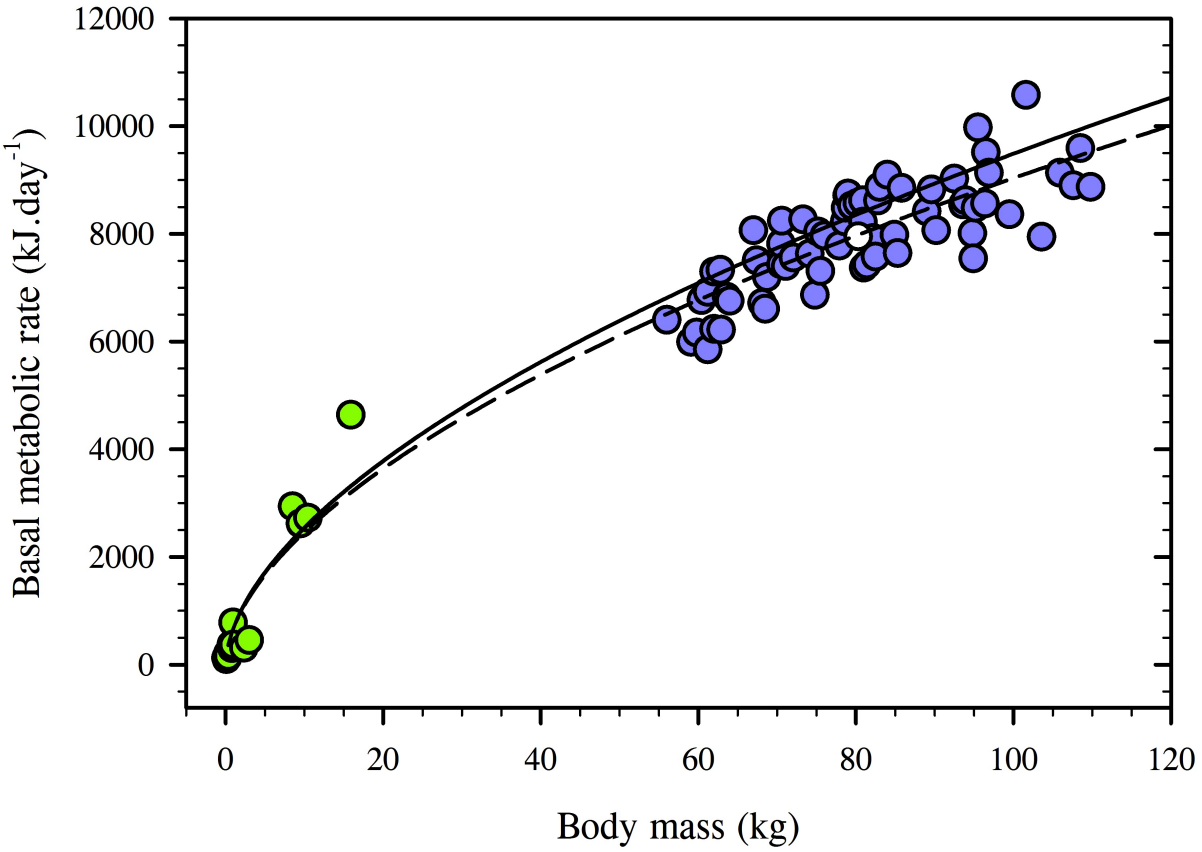

Figure 2.26: Scatter plot of the scaling relationship between basal metabolic rate and body mass in humans [purple] and primates [green]. The mean human basal metabolic rate is represented using the white data point. Two allometric regressions have been applied to the Figure; the human-only scaling regression ($mass^{0.55}$: dashed line) and the combined human and primate scaling regression ($mass^{0.60}$: solid line).

2.4.3 The effect of postural change on the scaling relationship

The next aim within this research phase was to determine whether or not a change in posture, from supine (basal) to standing (resting), would result in a different scaling regression from that observed during the basal condition. This was a novel aspect of this research, and permitted an assessment of the effect of a slight increase in the metabolic intensity on the scaling relationship. To evaluate this aim, the shape (linear or non-linear) of the scaling relationship was first determined using the process outlined in Figure 2.8. Since energy expenditure during non-basal states are typically described using oxygen consumption, for the remainder of this project, the scaling relationship was discussed in relation to that measure, rather than metabolic rate. This enabled the scaling of data with the least number of unit transformations.

Since a log transformation generates a linear model from an allometric (power) equation, it was possible to use the assumptions of linear regression to evaluate the model fit for both the linear and non-linear models. Both regressions satisfied these assumptions, indicating that statistically both models could be used to describe the standing dataset. However, a significant non-zero ordinate intercept was observed in the linear model (0.12 $L.min^{-1}$; $P<0.05$), violating the biological assumption, and resulting in spuriously high predictions of oxygen consumption at light mass ranges. Consequently, the linear regression was also not considered suitable for the standing dataset, with the non-linear model being the more suitable scaling method during both resting states (Hypothesis Two-Three accepted). Moreover, this meant that is was possible to statistically compare the regression slope (mass exponent) with that applied to the basal dataset.

The standing state represented a significant (21%) increase in metabolic intensity from the supine (basal) condition (basal: 0.27 $L.min^{-1} \pm < 0.01$; standing: 0.33 $L.min^{-1}$ ± 0.01; $P<0.05$). It was therefore possible that the scaling exponent observed for this metabolic intensity would increase compared with the basal condition, as has been observed by others (animals: Taylor *et al.,* 1981; humans: Rogers *et al.,* 1995; Markovic *et al.,* 2007). However, the body-mass exponent was statistically similar to the value applied to the basal oxygen consumption relationship (supine [basal]: $mass^{0.54}$ [untransformed, allometric]; standing: $mass^{0.68}$ [untransformed, allometric];

$P > 0.05$). As a result, Hypothesis Two-Four was accepted. During standing, although there is an increase in oxygen consumption, the work performed is relatively passive: the body is supported mainly by its skeletal structure and muscle activation occurs mainly for postural support (Danna-Dos-Santos *et al.,* 2014; Hellebrandt *et al.,* 1940). Therefore, the demand for oxygen at the muscle sites remains relatively low and is thus unlikely to contribute to the overall shape of the scaling relationship.

Consequently, a single mass exponent can be used to describe and normalise the relationship between oxygen consumption and body mass during both basal and standing states in humans. It is anticipated that this mass exponent can also be applied to other resting states between those two metabolic intensities (*e.g.* sitting), since the metabolic strain will be less than that of standing. To describe these resting intensities, the mass exponent derived for basal oxygen consumption during the untransformed state was selected: $mass^{0.54}$. This is because the basal oxygen consumption mass exponent represented the scaling relationship least influenced by external variables and that underwent the least number of data transformations.

2.5 CONCLUSION

The scaling relationship between basal metabolic rate and body mass in humans has been explored for the last century. However, this is the first investigation where the shape of the scaling relationship (linear or non-linear) has been directly explored using an appropriate sample (large in number and controlled for morphological and physiological differences, other than a change in body mass) and a systematic, statistical approach to determine the scaling shape. In this way, the analyses were defensible, repeatable and applicable to a wider population. This relationship was important to establish because, even though adult man spans a relatively narrow mass range, compared with that observed within and across other species, understanding this relationship gives the ability to predict and remove the effect of body mass on metabolic data.

Non-linear, allometric regression was found to be the more suitable scaling method to describe the relationship between basal metabolic rate and body mass in adult humans. Thus, significant changes to the mass exponent can be used to identify variables that

modify the scaling relationship. For humans, the observed value for basal metabolic rate was $mass^{0.54}$. This value was significantly smaller than that applied to animal datasets ($mass^{0.67}$), and was not modified by adjusting data for variations in body temperature. Therefore, $mass^{0.54}$, rather than $mass^{0.67}$, should be used to describe human-specific metabolic data, unless it is combined or compared with data from other animal species.

A secondary aim was to identify whether or not an increase in metabolic intensity would result in a change to the shape of the basal scaling relationship. Despite those states representing significantly different metabolic intensities, non-linear regression remained the more appropriate scaling method for the standing state and that mass exponent was not statistically different from the basal value. Accordingly, a single mass exponent could be used to describe the scaling relationship between oxygen consumption and body mass in adult humans throughout the range of resting intensities, between supine (basal) and standing conditions. For this purpose, the basal exponent of $mass^{0.54}$ (basal oxygen consumption) was selected, for it represented the scaling relationship influenced by the least number of additional variables.

2.6 REFERENCES

Ahad, N.A., Yin, T.S., Othman, A.R., and Yaacob, C.R. (2011). Sensitivity of normality tests to non-normal data. *Sains Malaysiana*. 40(6):637-641.

Albrecht, G.H., Gelvin, B.R., and Hartman, S.E. (1993). Ratios as a size adjustment in morphometrics. *American Journal of Physical Anthropology*. 91(4):441-468.

Allen, J.A. (1877). The influence of physical conditions in the genesis of species. *Radical Review*. 1:108-140.

Archiza, B., Welch, J.F., and Sheel, A.W. (2017). Classical experiments in whole-body metabolism: closed-circuit respirometry. *European Journal of Applied Physiology*. 117(10):1929-1937.

Arciero, P.J., Goran, M.I., and Poehlman, E.T. (1993). Resting metabolic rate is lower in women than in men. *Journal of Applied Physiology*. 75(6):2514-2530.

Atchley, W.R., and Anderson, D. (1978). Ratios and the statistical analysis of biological data. *Systematic Zoology*. 27(1):71-78.

Atwater, W.O., and Benedict, F.G. (1905). *A respiration calorimeter*. Carnegie Institution of Washington, Washington DC.

Atwater, W.O., and Rosa, E.B. (1899). A new respiration calorimeter and experiments on the conservation of energy in the human body, II. *Physical Review (Series I)*. 9(4):214.

Australian Bureau of Statistics. (2012). *4338.0 - Profiles of Health, Australia: Physical Measurements*. Australian Bureau of Statistics, Canberra.

Baker, M.A., Stocking, R.A., and Meehan, J.P. (1972). Thermal relationship between tympanic membrane and hypothalamus in conscious cat and monkey. *Journal of Applied Physiology*. 32(6):739-742.

Běhrádek, J. (1930). Temperature coe fficients in biology. *Biological Reviews*. 5(1):30-58.

Benedict, F.G. (1938). *Vital energetics. A study in comparative basal metabolism.* Carnegie Institution, Washington.

Benedict, F.G., and Benedict, C.G. (1924). Body posture and minor muscular movements as affecting heat production. *Proceedings of the National Academy of Sciences*. 10(12):498-500.

Benedict, F.G., and Carpenter, T.M. (1910). *The metabolism and energy transformations of healthy man during rest*. Carnegie Institution of Washington, Washington DC.

Benedict, F.G., Emmes, L.E., Roth, P., and Smith, H.M. (1914). The basal, gaseous metabolism of normal men and women. *Journal of Biological Chemistry*. 18(2):139-155.

Bergmann, C. (1848). *Über die Verhältnisse der Wärmeökonomie der Thiere zu ihrer Grösse*. Vandenhoeck und Ruprecht, Göttingen.

Boothby, W.M., and Sandiford, I. (1922). Summary of the basal metabolism data on 8,614 subjects with especial reference to the normal standards for the estimation of the basal metabolic rate. *Journal of Biological Chemistry*. 54(4):783-803.

Booyens, J., and McCance, R.A. (1957). Individual variations in expenditure of energy. *The Lancet*. 269:225-229.

Boulant, J.A. (1981). Hypothalamic mechanisms in thermoregulation. *Federation Proceedings*. 40:2843-2850.

Boyd, E. (1962). Organ weights from birth to maturity: Man, North American. In: Altman, P.L., and Dittmer, D.S. (Ed.). *Growth, Including Reproduction and Morphological Development*. Biological Handbooks, Federation of American Societies for Experimental Biology, Washington. Pp.346-348.

Buchholz, A.C., Rafii, M., and Pencharz, P.B. (2001). Is resting metabolic rate different between men and women? *British Journal of Nutrition*. 86(6):641-646.

Carnot, S. (1824). *Reflections on the motive power of fire, and on machines fitted to develop that power*. Bachelier, Paris.

Carathéodory, C. (1909). Untersuchungen über die Grundlagen der Thermodynamik. *Mathematische Annalen*. 67(3):355-386.

Casson, R.J., and Farmer, L.D. (2014). Understanding and checking the assumptions of linear regression: a primer for medical researchers. *Clinical and Experimental Ophthalmology*. 42(6):590-596.

Chambers, J.M., Cleveland, W.S., Kleiner, B., and Tukey, P.A. (1983). *Graphical methods for data analysis*. Duxbry Press, Massachusetts.

Chaui-Berlinck, J.G., Monteiro, L.H.A., Navas, C.A., and Bicudo, J.E.P. (2002). Temperature effects on energy metabolism: a dynamic system analysis. *Proceedings of the Royal Society of London B: Biological Sciences*. 269(1486):15-19.

Clarys, J.P., Martin, A.D., Drinkwater, D.T., and Marfell-Jones, M.J. (1987). The skinfold: Myth and reality. *Journal of Sports Sciences*. 5(1):3-33.

Clausius, R. (1850). Über die bewegende Kraft der Wärme und die Gesetze, welche sich daraus für die Wärmelehre selbst ableiten lassen. *Annalen der Physik*. 155(3):368-397.

Cole, T.J., and Henry, C.J.K. (2005). The Oxford Brookes basal metabolic rate database–a reanalysis. *Public Health Nutrition*. 8(7A):1202-1212.

Compher, C., Frankenfield, D., Keim, N., and Roth-Yousey, L. (2006). Best practice methods to apply to measurement of resting metabolic rate in adults: a systematic review. *Journal of the American Dietetic Association*. 106(6):881-903.

Cook, R.D. (1977). Detection of influential observation in linear regression. *Technometrics*. 19(1):15-18.

Cook, R.D., and Weisberg, S. (1982). *Residuals and influence in regression*. Chapman and Hall, New York.

Crouter, S.E., Antczak, A., Hudak, J.R., DellaValle, D.M., and Haas, J.D. (2006). Accuracy and reliability of the ParvoMedics TrueOne 2400 and MedGraphics VO2000 metabolic systems. *European Journal of Applied Physiology*. 98(2):139-151.

Danna-Dos-Santos, A., Boonstra, T.W., Degani, A.M., Cardoso, V.S., Magalhaes, A.T., Mochizuki, L., and Leonard, C.T. (2014). Multi-muscle control during bipedal stance: an EMG–EMG analysis approach. *Experimental Brain Research*. 232(1):75-87.

Darowski, A., Weinberg, J.R., and Guz, A. (1991). Normal rectal, auditory canal, sublingual and axillary temperatures in elderly afebrile patients in a warm environment. *Age and Ageing*. 20(2):113-119.

Darveau, C.A., Suarez, R.K., Andrews, R.D., and Hochachka, P.W. (2002). Allometric cascade as a unifying principle of body mass effects on metabolism. *Nature*. 417(6885):166-170.

Dodds, P.S., Rothman, D.H., and Weitz, J.S. (2001). Re-examination of the "3/4-law" of metabolism. *Journal of Theoretical Biology*. 209:9-27.

DuBois, D., and DuBois, E.F. (1916). Clinical calorimetry: tenth paper a formula to estimate the approximate surface area if height and weight be known. *Archives of Internal Medicine*. 17(6_2):863-871.

Durbin, J., and Watson, G.S. (1950). Testing for serial correlation in least squares regression: I. *Biometrika*. 37(3/4):409-428.

Durbin, J., and Watson, G.S. (1951). Testing for serial correlation in least squares regression. II. *Biometrika*. 38(1/2):159-177.

Durnin, J.V.G.A. (1959). The use of surface area and of body-weight as standards of reference in studies on human energy expenditure. *British Journal of Nutrition*. 13(1):68-71.

Durnin, J.V.G.A. (1981). Basal metabolic rate in man. *Report of a Joint FAO/WHO/UNU Expert Consultation on Energy and Protein Requirements*.

Durnin, J.V.G.A., and Womersley, J.(1974). Body fat assessed from total body density and its estimation from skinfold thickness: measurements on 481 men and women aged from 16 to 72 years. *British Journal of Nutrition*. 32(1):77-97.

Edholm, O.G., and Weiner, J.S. (1981). Thermal physiology. In: Edholm,O.G., and Weiner, J.S. (Ed.). *Principles and practice of human physiology*. Academic Press, New York. Pp.111-190.

Efron, B. (1979). Computers and the theory of statistics: thinking the unthinkable. *SIAM review*. 21(4):460-480.

Einstein, A. (1905). Does the inertia of a body depend upon its energy-content. *Annalen der Physik*. 18(13):639-41.

Elia, M. (1992). Organ and tissue contribution to metabolic rate. In: Kinney, J.H., and Tucker, H.N. (Ed.). *Energy metabolism: tissue determinants and cellular corollaries*. Raven Press, New York. Pp.61-80.

Fick, A. (1870). The measurement of cardiac ventricular output. *Physikalisch-Medizinische Gesellschaft*. 16:182-183.

Flancbaum, L., Choban, P.S., Sambucco, S., Verducci, J., and Burge, J.C. (1999). Comparison of indirect calorimetry, the Fick method, and prediction equations in estimating the energy requirements of critically ill patients. *The American Journal of Clinical Nutrition*. 69(3):461-466.

Fleisch, A. (1951). Le métabolisme basal standard et sa détermination au moyen du "Metabocalculator". *Helvetica Medica Acta*. 18:23-44.

Fortney, S.M., and Vroman, N.B. (1985). Exercise, performance and temperature control: temperature regulation during exercise and implications for sports performance and training. *Sports Medicine*. 2(1):8-20.

Fox, J. (1991). *Regression diagnostics: An introduction*. Volume 79. Sage, London.

Fox, J. (1997). *Applied regression analysis, linear models, and related methods*. Sage, London.

Fox, J., and Weisberg, S. (2017). *An R Companion to Applied Regression*. Sage, London.

Frankenfield, D.C., Oniert, L.A., Badellino, M.M., Wiles III, C.E., Bagley, S.M., Goodarzi, S., and Siegel, J.H. (1994). Correlation between measured energy expenditure and clinically obtained variables in trauma and sepsis patients. *Journal of Parenteral and Enteral Nutrition*. 18(5):398-403.

Fredrix, E.W., Soeters, P.B., Deerenberg, I.M., Kester, A.D., Von Meyenfeldt, M. F., and Saris, W.H. (1990). Resting and sleeping energy expenditure in the elderly. *European Journal of Clinical Nutrition*. 44(10):741-747.

Gaffney, F.A., Nixon, J.V., Karlsson, E.S., Campbell, W., Dowdey, A.B.C., and Blomqvist, C.G. (1985). Cardiovascular deconditioning produced by 20 hours of bedrest with head-down tilt (-5) in middle-aged healthy men. *The American Journal of Cardiology*. 56(10):634-638.

Garrett, J.W., and Kennedy, K.W. (1971). *A collection of anthropometry*. Volume 1-2. National Technical Informational Service, Springfield, Virginia.

Garrow, J.S. (1985). The contribution of protein synthesis to thermogenesis in man. *International Journal of Obesity*. 9:97-101.

Geppert, J., and Zuntz, N. (1888). Ueber die regulation der athmung. *Pflügers Archiv European Journal of Physiology*. 42(1):189-245.

Gillette, C.A., Bullough, R.C., and Melby, C.L. (1994). Postexercise energy expenditure in response to acute aerobic or resistive exercise. *International Journal of Sport Nutrition*. 4(4):347-360.

Gillooly, J.F., Brown, J.H., West, G.B., Savage, V.M., and Charnov, E.L. (2001). Effects of size and temperature on metabolic rate. *Science*. 293(5538):2248-2251.

Goldman, R.F., and Iampietro, P.F. (1962). Energy cost of load carriage. *Journal of Applied Physiology*. 17(4):675-676.

Gore, D.C., Chinkes, D., Sanford, A., Hart, D.W., Wolf, S.E., and Herndon, D.N. (2003). Influence of fever on the hypermetabolic response in burn-injured children. *Archives of Surgery*. 138(2):169-174.

Green, S.B. (1991). How many subjects does it take to do a regression analysis. *Multivariate Behavioral Research.* 26(3):499-510.

Guppy, M., and Withers, P. (1999). Metabolic depression in animals: physiological perspectives and biochemical generalizations. *Biological Reviews of the Cambridge Philosophical Society*. 74(1):1-40.

Hair, J.F., Anderson, R.E., Tatham, R.L., and Black, W.C. (1998). *Multivariate data analysis*. Prentice-Hall International, Upper Saddle River, NJ.

Haldane, J. (1892). A new form of apparatus for measuring the respiratory exchange of animals. *The Journal of Physiology*. 13(5):419-430.

Harris, J.A., and Benedict, F.G. (1918). A biometric study of human basal metabolism. *Proceedings of the National Academy of Sciences*. 4(12):370-373.

Harris, J.A., and Benedict, F.G. (1919). *A biometry study of basal metabolism*. Carnegie Institution of Washington, Washington DC.

Harris, R.J. (1985). *A primer of multivariate statistics*. Academic Press, New York.

Haugen, H.A., Melanson, E.L., Tran, Z.V., Kearney, J.T., and Hill, J.O. (2003). Variability of measured resting metabolic rate. *The American Journal of Clinical Nutrition*. 78(6):1141-1144.

Hellebrandt, F.A., Brogdon, E., and Tepper, R.H. (1940). Posture and its cost. *American Journal of Physiology - Legacy Content*. 129:773-781.

Heusner, A.A. (1982). Energy metabolism and body size I. Is the 0.75 mass exponent of Kleiber's equation a statistical artifact? *Respiration Physiology*. 48:1-12.

Heymsfield, S.B. (2009). Development of imaging methods to assess adiposity and metabolism. *International Journal of Obesity*. 32(S7): S76.

Heysmfield, S.B., Gallagher, D., Kotler, D.P., Wang, Z., Allison, D.B., and Heshka, S. (2002). Body-size dependence of resting energy expenditure can be attributed to nonenergetic homogeneity of fat-free mass. *American Journal of Physiology. Endocrinology and Metabolism*. 282:E132.

Heymsfield, S.B., Gallagher, D., Mayer, L., Beetsch, J., and Pietrobelli, A. (2007). Scaling of human body composition to stature: new insights into body mass index. *The American Journal of Clinical Nutrition*. 86(1):82-91.

Himms-Hagen, J. (1976). Cellular thermogenesis. *Annual Review of Physiology*. 38(1):315-351.

Hochachka, P.W., Darveau, C.A., Andrews, R.D., and Suarez, R.K. (2003). Allometric cascade: a model for resolving body mass effects on metabolism. *Comparative Biochemistry and Physiology Part A: Molecular and Integrative Physiology*. 134(4):675-691.

Holliday, M.A. (1971). Metabolic rate and organ size during growth from infancy to maturity and during late gestation and early infancy. *Pediatrics*. 47(1):169-179.

Holliday, M.A. (1986). Body composition and energy needs during growth. In: Falkner, F. (Ed.). *Postnatal Growth Neurobiology*. Springer, New York. Pp.101-117.

Holliday, M.A., Potter, D., Jarrah, A., and Bearg, S. (1967). The relation of metabolic rate to body weight and organ size. *Pediatric Research*. 1(3):185.

Jackson, A.S., and Pollock, M.L. (1978). Generalized equations for predicting body density of men. *British Journal of Nutrition*. 40(3):497-504.

Jansson, M. (1985). A comparison of detransformed logarithmic regressions and power function regressions. *Geografiska Annaler: Series A, Physical Geography*. 67(1-2):61-70.

Jensen, K., Johansen, L., and Secher, N.H. (2001). Influence of body mass on maximal oxygen uptake: effect of sample size. *Ergonomics*. 84(3):201-205.

Jéquier, E. (1986). Human whole body direct calorimetry. *IEEE Engineering in Medicine and Biology Magazine*. 5(2):12-14.

Johnston, F.E. (1982). Relationships between body composition and anthropometry. *Human Biology*. 54:221-245.

Johnstone, A.M., Murison, S.D., Duncan, J.S., Rance, K.A., and Speakman, J.R. (2005). Factors influencing variation in basal metabolic rate include fat-free mass, fat mass, age, and circulating thyroxine but not sex, circulating leptin, or triiodothyronine. *The American Journal of Clinical Nutrition*. 82(5):941-948.

Kaiyala, K.J., and Ramsay, D.S. (2011). Direct animal calorimetry, the underused gold standard for quantifying the fire of life. *Comparative Biochemistry and Physiology Part A: Molecular & Integrative Physiology*. 158(3):252-264.

Karp, N.A., Segonds-Pichon, A., Gerdin, A.K.B., Ramírez-Solis, R., and White, J.K. (2012). The fallacy of ratio correction to address confounding factors. *Laboratory Animals*. 46(3):245-252.

Katch, V.L. (1973). Use of the oxygen/body weight ratio in correlational analyses: spurious correlations and statistical considerations. *Medicine and Science in Sports*. 5(4):253-257.

Kerslake, D.M. (1972). *The stress of hot environments*. Volume 29. Cambridge University Press, London.

Kenny, G.P., and Jay, O. (2013). Thermometry, calorimetry, and mean body temperature during heat stress. *Comprehensive Physiology*. 3:1689-1719.

Kenny, G.P., Notley, S.R., and Gagnon, D. (2017). Direct calorimetry: a brief historical review of its use in the study of human metabolism and thermoregulation. *European Journal of Applied Physiology*. 117(9):1765-1785.

Kenny, G.P., Webb, P., Ducharme, M.B., Reardon, F.D., and Jay, O. (2008). Calorimetric measurement of postexercise net heat loss and residual body heat storage. *Medicine and Science in Sports and Exercise*. 40(9):1629-1636.

Kim, H.Y. (2013). Statistical notes for clinical researchers: assessing normal distribution (2) using skewness and kurtosis. *Restorative Dentistry and Endodontics*. 38(1):52-54.

Kleiber, M. (1932). Body size and metabolism. *Journal of Agricultural Science*. 6:315-353.

Koot, P., and Deurenberg, P. (1995). Comparison of changes in energy expenditure and body temperatures after caffeine consumption. *Annals of Nutrition and Metabolism*. 39(3):135-142.

Kram, R., and Taylor, C.R. (1990). Energetics of running: a new perspective. *Nature*. 346(6281):265-267.

Krustrup, P., González-Alonso, J., Quistorff, B., and Bangsbo, J. (2001). Muscle heat production and anaerobic energy turnover during repeated intense dynamic exercise in humans. *The Journal of Physiology*. 536(3):947-956.

Landers, G.J., Ong, K.B., Ackland, T.R., Blanksby, B.A., Main, L.C., and Smith, D. (2013). Kinanthropometric differences between 1997 World championship junior elite and 2011 national junior elite triathletes. *Journal of Science and Medicine in Sport*. 16(5):444-449.

Lavoisier, A.L., and Laplace, S. (1780). Mémoire sur la chaleur. *Mémoires de l'Academie des Sciences*. Pp.355-405.

Lazzer, S., Bedogni, G., Lafortuna, C.L., Marazzi, N., Busti, C., Galli, R., De Col, A., Agosti, F., and Sartorio, A. (2010). Relationship between basal metabolic rate, gender, age, and body composition in 8,780 white obese subjects. *Obesity*. 18(1):71-78.

Levine, J.A. (2005). Measurement of energy expenditure. *Public Health Nutrition*. 8(7A):1123-1132.

Levinson, M.R., Groeger, J.S., Miodownik, S., Ray, C., and Brennan, M.F. (1987). Indirect calorimetry in the mechanically ventilated patient. *Critical Care Medicine*. 15(2):144-147.

Liggett, S.B., John, R.E.S., and Lefrak, S.S. (1987). Determination of resting energy expenditure utilizing the thermodilution pulmonary artery catheter. *Chest*. 91(4):562-566.

Lind, A.R. (1963). A physiological criterion for setting thermal environmental limits for everyday work. *Journal of Applied Physiology*. 18(1):51-56.

Livesey, G., and Elia, M. (1988). Estimation of energy expenditure, net carbohydrate utilization, and net fat oxidation and synthesis by indirect calorimetry: evaluation of errors with special reference to the detailed composition of fuels. *The American Journal of Clinical Nutrition*. 47(4):608-628.

London, G.M., Levenson, J.A., Safar, M.E., Simon, A.C.H., Guerin, A.P., and Payen, D. (1983). Hemodynamic effects of head-down tilt in normal subjects and sustained hypertensive patients. *The American Journal of Physiology*. 245(2):H194-H202.

Lusk, G. (1928). *The Elements of the Science of Nutrition*. W.B. Saunders Company, London.

Magnus-Levy, A. (1893). Ueber die Grösse des respiratorischen Gaswechsels unter dem Einfluss der Nahrungsaufnahme. *Archiv für die gesamte Physiologie des Menschen und der Tiere*. 55(1-2):1-126.

Mansell, P.I., and Macdonald, I.A. (1990). Reappraisal of the Weir equation for calculation of metabolic rate. *American Journal of Physiology-Regulatory, Integrative and Comparative Physiology*. 258(6):R1347-R1354.

Marfell-Jones, M., Olds, T., Stewart, A., and Carter, L. (2006). International standards for anthropometric assessment. *International Society for the Advancement of Kinanthropometry*. Potchefstroom, South Africa.

Markovic, G., Vucetic, V., and Nevill, A.M. (2007). Scaling behaviour of in athletes and untrained individuals. *Annals of Human Biology*. 34(3):315-328.

Martin, A.D. (1984). *An anatomical basis for assessing human body composition: evidence from 25 dissections*. Unpublished doctoral thesis, Simon Fraser University, Canada.

Martin, A.D., Drinkwater, D.T., and Clarys, J.P. (1984). Human body surface area: validation of formulae based on a cadaver study. *Human Biology*. 56:475-488.

Martin, A.D., Ross, W.D., Drinkwater, D.T., and Clarys, J.P. (1985). Prediction of body fat by skinfold caliper: assumptions and cadaver evidence. *International Journal of Obesity*. 9:31-39.

Mayer, J.R. (1845). *Die organische Bewegung in ihrem Zusammenhange mit dem Stoffwechsel*. C. Drechsler, Heilbronn.

McClave, S.A., Lowen, C.C., Kleber, M.J., McConnell, J.W., Jung, L.Y., and Goldsmith, L.J. (2003). Clinical use of the respiratory quotient obtained from indirect calorimetry. *Journal of Parenteral and Enteral Nutrition*. 27(1):21-26.

McClave, S.A., and Snider, H.L. (1992). Use of indirect calorimetry in clinical nutrition. *Nutrition in Clinical Practice*. 7(5):207-221.

McNab, B.K. (1997). On the utility of uniformity in the definition of basal rate of metabolism. *Physiological Zoology*. 70(6):718-720.

McWilliams, P.C., Furchner, J.E., and Richmond, C.R. (1964). Application of Regression Analysts to the Power Function. *Health Physics*. 10(11):817-822.

Mitchell, H.H. (1962). *Comparative nutrition of man and domestic animals*. Volume 1. Academic Press, New York. Pp.3-90.

Moreno, F., and Lyons, H.A. (1961). Effect of body posture on lung volumes. *Journal of Applied Physiology*. 16(1):27-29.

Müller, M.J., Langemann, D., Gehrke, I., Later, W., Heller, M., Glüer, C.C., Heymsfield, S.B., and Bosy-Westphal, A. (2011). Effect of constitution on mass of individual organs and their association with metabolic rate in humans-a detailed view on allometric scaling. *PLoS One*. 6:e22732. Pp.1-9.

Müller, M.J., Wang, Z., Heymsfield, S.B., Schautz, B., and Bosy-Westphal, A. (2013). Advances in the understanding of specific metabolic rates of major organs and tissues in humans. *Current Opinion in Clinical Nutrition and Metabolic Care*. 16(5):501-508.

Neilsen, M. (1938). Die Regulation der Kopertemperatur bei Muskelerbeit. *Skandinavisches Archiv fur Physiologie*. 79:193-230.

Newman, M.C. (1993). Regression analysis of log transformed data: Statistical bias and its correction. *Environmental Toxicology and Chemistry*. 12(6):1129-1133.

Nindl, B.C., Schoville, C.R., Sheehan, K.M., Leone, C.D., and Mello, R.P. (2002). Gender differences in regional body composition and somatotrophic influences of IGF-1 and leptin. *Journal of Applied Physiology*. 92(4):1611-1618.

Notley, S.R., Park, J., Tagami, K., Ohnishi, N., and Taylor, N.A.S. (2017). Variations in body morphology explain sex differences in thermoeffector function during compensable heat stress. *Experimental Physiology*. 102(5):545-562.

Packard, G.C., and Boardman, T.J. (1988). The misuse of ratios, indices, and percentages in ecophysiological research. *Physiological Zoology*. 61(1):1-9.

Packard, G.C., and Boardman, T.J. (1999). The use of percentages and size-specific indices to normalize physiological data for variation in body size: wasted time, wasted effort? *Comparative Biochemistry and Physiology Part A: Molecular and Integrative Physiology*. 122(1):37-44.

Palmer, C.E. (1930). Diurnal variations of height and weight in the human body during growth. *The Anatomical Record*. 45:234-235.

Pannier, B.M., Lacolley, P.J., Gharib, C., London, G.M., Cuche, J.L., Duchier, J. L., Levy, B.I., and Safar, M.E. (1991). Twenty-four hours of bed rest with head-down tilt: venous and arteriolar changes in limbs. *American Journal of Physiology - Heart and Circulatory Physiology*. 260:H1043-H1050.

Pearson, K. (1900). Mathematical contributions to the theory of evolution. VIII. On the correlation of characters not quantitatively measurable. *Proceedings of the Royal Society of London*. 66(424-433):241-244.

Pearson, K. (1920). Notes on the history of correlation. *Biometrika*. 13(1):25-45.

Piironen, P. (1970). Sinusoidal signals in the analysis of heat transfer in the body. In: Hardy, J.D., Gagge, A.P., and Stolwijk, J.A.J. (Ed.). *Physiological and Behavioral Temperature Regulation*. Charles C Thomas, Springfield, Ill. Pp.358-366.

Planck, M. (1927). *Treatise on Thermodynamics*. Longmans, Green, London.

Poole, M.A., and O'Farrell, P.N. (1971). The assumptions of the linear regression model. *Transactions of the Institute of British Geographers*. 52:145-158.

Quenouille, M.H., Boyne, A.W., Fisher, W.B., and Leitch, I. (1951). *Statistical Studies of Recorded Energy Expenditure of Man. Part I. Basal Metabolism Related to Sex, Stature, Age, Climate and Race*. Commonwealth Bureau of Animal Nutrition Technical Communication No.17. Commonwealth Agricultural Bureau, Aberdeen.

Redfield, J.E., and Meredith, H.V. (1938). Changes in the stature and sitting height of preschool children in relation to rest in the recumbent position and activity following rest. *Child Development*. 9(3):293-302.

Richet, C. (1889). *La Chaleur Animale*. Felix Alcan, Bibliotheque Scientifique Internationale, Paris.

Rogers, D.M., Olson, B.L., and Wilmore, J.H. (1995). Scaling for the $\dot{V}O_2$-to-body size relationship among children and adults. *Journal of Applied Physiology*. 79(3):958-967.

Ross, W.D., and Ward, R. (1985). *The O-scale system*. Rosscraft, Surrey, BC.

Ross, W.D., and Wilson, N.C. (1974). A stratagem for proportional growth assessment. *Acta Paediatrica Belgica*. 28:169-182.

RStudio Team. (2016). RStudio: Integrated Development for R. RStudio, Inc. Boston, MA. URL:http://www.rstudio.com/.

Rubner, M. (1883). Über den einfluss der körpergrösse auf stoffund kraftwechsel. *Zeitschrift für Biologie*. 19:535-562.

Sarrus, F., and Rameaux, J.F. (1839). Mathématique appliquée à la physiologie. *Bulletin de l'Academie Royale de Medicine de Paris*. 3:1094-1100.

Savage, V.M., Gillooly, J.F., Woodruff, W.H., West, G.B., Allen, A.P., Enquist, B.J., and Brown, J.H. (2004). The predominance of quarter power scaling in biology. *Functional Ecology*. 18(2):257-282.

Schmidt-Nielsen, K. (1984). *Scaling: why is animal size so important?* Cambridge University Press, New York.

Schoffelen, P.F.M., and Plasqui, G. (2018). Classical experiments in whole-body metabolism: open-circuit respirometry—diluted flow chamber, hood, or facemask systems. *European Journal of Applied Physiology*. 118(1):33-49.

Schofield, W.N. (1985). Predicting basal metabolic rate, new standards and review of previous work. *Human Nutrition: Clinical Nutrition*. 39:5-41.

Shapiro, S.S., and Wilk, M.B. (1965). An analysis of variance test for normality (complete samples). *Biometrika*. 52(3/4), 591-611.

Shephard, R.J. (2017). Open-circuit respirometry: a brief historical review of the use of Douglas bags and chemical analyzers. *European Journal of Applied Physiology*. 117:381-387.

Sholl, D. (1948). The quantitative investigation of the vertebrate brain and the applicability of allometric formulae to its study. *Proceedings of the Royal Society of London B*. 135(879):243-258.

Sieg, A.E., O'Connor, M.P., McNair, J.N., Grant, B.W., Agosta, S.J., and Dunham, A.E. (2009). Mammalian metabolic allometry: do intraspecific variation, phylogeny, and regression models matter? *The American Naturalist*. 174(5):720-733.

Solomon, S.J., Kurzer, M.S., and Calloway, D.H. (1982). Menstrual cycle and basal metabolic rate in women. *American Journal of Clinical Nutrition*. 36(4):611-616.

Stock, M.C., Davis, D.W., Manning, J.W., and Ryan, M.L. (1992). Lung mechanics and oxygen consumption during spontaneous ventilation and severe heart failure. *Chest*. 10(1):279-283.

Stocks, J.M., Taylor, N.A.S., Tipton, M.J., and Greenleaf, J.E. (2004). Human physiological responses to cold exposure. *Aviation, Space, and Environmental Medicine*. 75(5):444-457.

Suarez, R.K. (2012). Energy and metabolism. *Comprehensive Physiology*. 2:2527-2540.

Sund Levander, M., Forsberg, C., and Wahren, L.K. (2002). Normal oral, rectal, tympanic and axillary body temperature in adult men and women: a systematic literature review. *Scandinavian Journal of Caring Sciences*. 16(2):122-128.

Takala, J., Keinänen, O., Väisänen, P., and Kari, A. (1989). Measurement of gas exchange in intensive care: laboratory and clinical validation of a new device. *Critical Care Medicine*. 17(10):1041-1047.

Tanner, J.M. (1949). Fallacy of per-weight and per-surface area standards, and their relation to spurious correlation. *Journal of Applied Physiology*. 2(1):1-15.

Taylor, C.R., Heglund, N.C., and Maloiy, G.M.O. (1982). Energetics and mechanics of terrestrial locomotion. I. Metabolic energy consumption as a function of speed and body size in birds and mammals. *Journal of Experimental Biology*. 97(1):1-21.

Taylor, C.R., Maloiy, G.M.O., Weibel, E.R., Langman, V.A., Kamau, J.M., Seeherman, H.J., and Heglund, N.C. (1981). Design of the mammalian respiratory system. III. Scaling maximum aerobic capacity to body mass: wild and domestic mammals. *Respiration physiology*. 44(1):25-37.

Taylor, C.R., Schmidt-Nielsen, K., and Raab, J.L. (1970). Scaling of energetic cost of running to body size in mammals. *American Journal of Physiology - Legacy Content*. 219(4):1104-1107.

Taylor, N.A.S. (2014). Human heat adaptation. *Comprehensive Physiology*. 4:325-365.

Taylor, N.A.S., Lewis, M.C., Notley, S.R., and Peoples, G.E. (2012). A fractionation of the physiological burden of the personal protective equipment worn by firefighters. *European Journal of Applied Physiology*. 112(8):2913-2921.

Taylor, N.A.S., and Machado-Moreira, C.A. (2013). Regional variations in transepidermal water loss, eccrine sweat gland density, sweat secretion rates and electrolyte composition in resting and exercising humans. *Extreme Physiology and Medicine*. 2(1):1-29.

Tepper, R.H., and Hellebrandt, F.A. (1938). The influence of the upright posture on the metabolic rate: With a note on standards. *American Journal of Physiology-Legacy Content*. 122(3):563-568.

Thomson, W. (1853). XVII. On the restoration of mechanical energy from an unequally heated space. *The London, Edinburgh, and Dublin Philosophical Magazine and Journal of Science*. 5(30):102-105.

Turell, D.J., and Alexander, J.K. (1964). Experimental evaluation of Weir's formula for estimating metabolic rate in man. *Journal of applied physiology*. 19(5):946-948.

Turley, K.R., McBride, P.J., and Wilmore, J.H. (1993). Resting metabolic rate measured after subjects spent the night at home vs at a clinic. *The American Journal of Clinical Nutrition*. 58(2):141-144.

Tzankoff, S.P., and Norris, A.H. (1977). Effect of muscle mass decrease on age-related BMR changes. *Journal of Applied Physiology: Respiratory, Environmental and Exercise Physiology*. 43(6):1001-1006.

Voit, E. (1901). Über die Grösse des Energiebedarfs der Tiere in Hungerzustande. *Zeitschrift für Biologie*. 41:113-154.

Von Hoesslin, H. (1888). Über die Ursache der scheinbaren Abhängigkeit des Umsatzes von der Grösse der Körperobernäche. *Archiv für Anatomie, Physiologie und Wissenschaftliche Medicin*. 11(1888):323-379.

Van Voorhis, C.W., and Morgan, B.L. (2007). Understanding power and rules of thumb for determining sample sizes. *Tutorials in Quantitative Methods for Psychology*. 3(2):43-50.

Wagner, D.R., and Heyward, V.H. (1999). Techniques of body composition assessment: a review of laboratory and field methods. *Research Quarterly for Exercise and Sport*. 70(2):135-149.

Ward, R. (1988). *The O-scale system for human physique assessment*. Unpublished doctoral dissertation, Simon Fraser University, Canada.

Webb, P. (1981). Energy expenditure and fat-free mass in men and women. *American Journal of Clinical Nutrition*. 34(9):1816-1826.

Webb, P. (1985). *Human Calorimeters: Endocrinology and Metabolism Series*. Volume 7. Praeger Publishers, New York.

Webb, P. (1986). 24-hour energy expenditure and the menstrual cycle. *American Journal of Clinical Nutrition*. 44(5):614-619.

Weibel, E.R., Bacigalupe, L.D., Schmitt, B., and Hoppeler, H. (2004). Allometric scaling of maximal metabolic rate in mammals: muscle aerobic capacity as determinant factor. *Respiratory Physiology and Neurobiology*. 140(2):115-132.

Weir, J.D.V. (1949). New methods for calculating metabolic rate with special reference to protein metabolism. *The Journal of Physiology*. 109(1-2):1-9.

Weisberg, S. (2014). *Applied Linear Regression*. Wiley, Minnesota.

Wells, J.C.K. (2007). Sexual dimorphism of body composition. *Best Practice and Research. Clinical Endocrinology and Metabolism*. 21(3):415-430.

Wells, J.C.K. and Fewtrell, M.S. (2006). Measureing body composition. *Archives of Disease in Childhood*. 91(7):612-617.

West, G.B., Brown, J.H., and Enquist, B.J. (1997). A general model for the origin of allometric scaling laws in biology. *Science*. 276(5309):122-126.

Westenskow, D.R., Schipke, C.A., Raymond, J.L., Saffle, J.R., Becker, J.M., Young, E.W., and Cutler, C.A. (1988). Calculation of metabolic expenditure and substrate utilization from gas exchange measurements. *Journal of Parenteral and Enteral Nutrition*. 12(1):20-24.

Whipp, B.J., and Wassermann, K. (1969). Efficiency of muscular work. *Journal of Applied Physiology*. 26(5):644-648.

White, C.R., Blackburn, T.M., and Seymour, R.S. (2009). Phylogenetically informed analysis of the allometry of mammalian basal metabolic rate supports neither geometric nor quarter power scaling. *Evolution: International Journal of Organic Evolution*. 63(10):2658-2667.

White, C.R., Cassey, P., and Blackburn, T.M. (2007). Allometric exponents do not support a universal metabolic allometry. *Ecology*. 88(2):315-323.

White, C.R., and Kearney, M.R. (2014). Metabolic scaling in animals: Methods, empirical results, and theoretical explanations. *Comprehensive Physiology*. 4:321-256.

White, C.R., and Seymour, R.S. (2003). Mammalian basal metabolic rate is proportional to body mass$^{2/3}$. *Proceedings of the National Academy of Sciences*. 100:4046-4049.

White, C.R., and Seymour, R.S. (2004). Does basal metabolic rate contain a useful signal? Mammalian BMR allometry and correlations with a selection of physiological, ecological, and life-history variables. *Physiological and Biochemical Zoology*. 77(6):929-941.

Williams, D.A. (1987). Generalized linear model diagnostics using the deviance and single case deletions. *Applied Statistics*. 36(2):181-191.

Williams, R.R., and Fuenning, C.R. (1991). Circulatory indirect calorimetry in the critically ill. *Journal of Parenteral and Enteral Nutrition*. 15(5):509-512.

Williamson, D.L., and Kirwan, J.P. (1997). A single bout of concentric resistance exercise increases basal metabolic rate 48 hours after exercise in healthy 59–77-year-old men. *The Journals of Gerontology Series A: Biological Sciences and Medical Sciences*. 52(6):M352-M355.

Wilmore, J.H., and Behnke, A.R. (1969). An anthropometric estimation of body density and lean body weight in young men. *Journal of Applied Physiology*. 27(1):25-31.

Wilmore, J.H., and Behnke, A.R. (1970). An anthropometric estimation of body density and lean body weight in young women. *American Journal of Clinical Nutrition*. 23(3):267-274.

Xiao, X., White, E.P., Hooten, M.B., and Durham, S.L. (2011). On the use of log transformation vs. nonlinear regression for analyzing biological power laws. *Ecology*. 92(10):1887-1894.

Zuntz, N. (1901). Ueber die Bedeutung der verschiedenen Nährstoffe als Erzeuger der Muskelkraft. *Pflügers Archiv European Journal of Physiology*. 83:557-571.

3: SCALING AMBULATORY OXYGEN CONSUMPTION DATA DURING STEADY-STATE AND MAXIMAL EXERCISE

3.1 INTRODUCTION

During resting states (basal and standing), it has been established that the scaling relationship between oxygen consumption and body mass is best described using a non-linear, allometric regression ($y=ax^b$: see Chapter 2). Investigations into that relationship have also been expanded to non-resting states in both animals (Taylor *et al.,* 1970, 1981) and humans (Bergh *et al.*, 1991; Rogers *et al.,* 1995; Batterham and Jackson, 2003; Markovic *et al.,* 2007). Within those human studies, an increase in metabolic rate was explored (Table 3.1), collectively demonstrating a relationship between metabolic intensity and the steepness of the regression slope. There are, however, inconsistencies among the exponents reported for each state, most likely due to the use of heterogenous samples, which introduce covariant variables that may influence the scaling relationship, in some studies, the length of testing steady-state stages (3 min: Bergh *et al.,* 1991; Batterham and Jackson, 2003), which may have been insufficient to permit attainment of a steady state. For that reason, the precise scaling relationship between oxygen uptake and body mass during non-resting states remains unconfirmed, which may lead to potentially erroneous normalisation and prediction practices. Accordingly, the primary focus within this experimental phase was to determine how that relationship scaled during submaximal (walking) and maximal (running) intensities. By testing the same participants as used in Chapter 2, and by combining those data with data obtained during exercise of submaximal and maximal intensities, it becomes possible to assess that scaling relationship throughout the entire physiological range.

During a basal state, the shape of the scaling relationship between oxygen consumption and body mass ($mass^{0.54}$) is, at least in part, a consequence of a proportional decrease in the organ mass of the most metabolically active tissues, relative to the total body mass, as body size increases (Holliday *et al.,* 1967; Holliday, 1986; Gallagher *et al.,* 1998; Wang *et al.,* 2010; Müller *et al.,* 2011). At rest, organ metabolism determines ~80% of whole-body energy turnover (Elia, 1992). However, as activity intensity and, consequently, energy expenditure

Table 3.1: Studies investigating the scaling of peak and submaximal oxygen consumption against body mass in adult humans (>18 y), using non-linear allometric approaches ($y=ax^b$). Exponents are identified for rest (non-basal), submaximal and peak exercise conditions and are identified using the following abbreviations: M= male; F= female; C= Combined male and female exponent.

	Exponent							
Source	Rest (non-basal)	Submaximal ($km.h^{-1}$)	Maximal	Sample size (*N*)	Adiposity controlled	Heterogeneous	Small samples	Other sample comments
Bergh *et al.* (1991)	-	variable: 0.76	0.71	C=134	N	Y	Y	5x sporting categories used: Exponents provided are from sample mean Age used as covariant 4-min stages
Nevill *et al.* (1992)	-	-	C=0.67 M=0.63 F=0.72	C=308 max: M=112 F=92	N	Y	N	Mass ranges not stated (~48-100 kg)
Nevill and Holder (1994)	-	-	M=0.68 F=0.57	C=1732 M=852 F=880	N	Y	N	Mass and age ranges not stated

Source	Exponent: Rest (non-basal)	Exponent: Submaximal ($km.h^{-1}$)	Exponent: Maximal	Sample size (*N*)	Adiposity controlled	Heterogeneous	Small samples	Other sample comments
Rogers *et al.* (1995)	C = 0.83 M = 0.45 F = 0.38	4.8: C = 0.90 M = 0.61 F = 0.55 8: C = 0.96 M = 0.75 F = 0.73	C = 1.02 M = 0.98 F = 0.80	C = 60 M = 15 F = 15	N	Y	Y	Adults (*N* = 30) and children (*N* = 30) *N* = 16 used for resting condition Combined value in table is for adults only
Welsman *et al.* (1996)	-	-	C = 0.80	C = 146 Adults: M = 8 F = 16	N	Y	Y	Majority of subjects were not adults *N* = 122
Heil (1997)	-	-	C = 0.76	C = 440 M = 211 F = 231	N	Y	N	20-79 y 35-132 kg (all) males = 55-132 kg
Batterham *et al.* (1999)	-	-	M = 0.65	M = 1314	N	Y	N	17-66 y 54.7-134.5 kg Advised use of fat free mass

	Exponent							
Source	Rest (non-basal)	Submaximal ($km.h^{-1}$)	Maximal	Sample size (*N*)	Adiposity controlled	Heterogeneous	Small samples	Other sample comments
Jensen *et al.* (2001)	-	-	C = 0.73	C = 967 M = 655 F = 312	N	Y	Y	15-56 y 40-115 kg Elite athletes 25x sports
Batterham and Jackson (2003)	-	2.74 (10%): 0.83	M = 0.94	M = 1629	N	Y	N	55.4-109.4 kg 20-68 y
Nevill *et al.* (2003)	-	-	C = 0.94	C = 174 M = 98 F = 76	N	Y	N	Endurance athletes: 7x sports Mass and age ranges not provided
Markovic *et al.* (2007)	0.69	5: 0.76 7.5: 0.76 ventilatory threshold: 0.84	Control = 0.89; athlete = 0.67	C = 313	N	Y	Y	*N* = 270 athletes (10 sports), *N* = 43 untrained; All men over 18 y; Mass range: athletes = 56-119 kg, untrained = 57-97 kg, Not stated whether adiposity was controlled

	Exponent							
Source	Rest (non-basal)	Submaximal ($km.h^{-1}$)	Maximal	Sample size (*N*)	Adiposity controlled	Heterogeneous	Small samples	Other sample comments
Lolli *et al.* (2017)	-	-	C: 0.71	C = 6514	N	Y	???	Meta-analysis of heterogeneous samples Wide mass, age and adiposity range included Only means provided

Notes: The four studies where multiple exponents are cited used a repeated-measures design. Results presented from the Markovic and colleagues (2007) are only displayed for their control group, whereby the population more closely resembled that tested within this project.

increases, the proportional contribution to whole-body energy expenditure that those organs provide decreases, while that from skeletal muscle increases. As a result, when activity increases above basal levels, a shift in the predominant tissue type and tissue mass determining overall oxygen consumption is likely to increase the scaling exponent. However, to the author's knowledge, the increase in metabolic rate necessary to significantly modify the mass exponent from the basal value has yet to be sufficiently explored.

During maximal exercise, the skeletal muscles contribute to approximately 90% of whole-body oxygen consumption (Hochachka, 1994; Hochachka and Somero, 2002). That change is coupled with a shift in the predominant energy pathway, modifying the limiting rate of oxygen consumption (Fell, 1997; Hochachka *et al.,* 2003). Together, those changes are expected to increase the steepness of the scaling relationship. For instance, if the maximum capacity of all of the processes in the path oxygen takes from the lungs to the mitochondria are taken into consideration, as well as how each may limit the rate of whole-body maximal oxygen consumption, a theoretical maximum exponent of mass$^{0.92}$ has been proposed (Darveau *et al.,* 2002). As a result, it is likely that a unique scaling exponent would be required for different activity levels throughout the physiological range. For this reason, a range of intensities were explored within this project.

3.1.1 Scaling steady-state oxygen consumption

To the author's best knowledge, the minimum increase in metabolic intensity required to modify the shape of the scaling regression from that of a basal state is unknown. In Chapter 2, changing from a supine (basal) to standing posture did not result in a significant modification to that scaling relationship. Within this experimental phase, the next increment in metabolic intensity tested was that of steady-state walking, wherein the increase in oxygen consumption was both velocity and body-size dependent, and would be reflective of the energy required to both support and move the body (Taylor *et al.,* 1970, 1974, 1982; Cavagna and Kaneko, 1977; Abe *et al.,* 2008).

Unlike the previous states tested, steady-state walking can be performed at either a

relative intensity (a percentage of a person's peak aerobic power) or a fixed velocity, both of which may have different impacts on the shape of the scaling relationship. During any relative state, the mass exponent is expected to increase proportionally with an increase in metabolic intensity (allometric cascade: Darveau *et al.,* 2002). However, during walking at a fixed velocity, unique body-size interactions may affect the shape of the scaling regression in two separate ways. For example, smaller individuals must walk at a higher relative intensity to maintain the same absolute velocity as larger subjects (Taylor *et al.,* 1982): steepening the shape of the slope only at the lighter end, and thus potentially reducing the mass exponent. Nevertheless, as those smaller individuals have a lighter mass to carry, their absolute oxygen consumption may still be considerably lower than individuals at the heavier end of the mass range. Therefore, the body-mass differences in relative intensity may not have as much of an impact on the scaling relationship as might be expected. As those body-size differences have the greatest potential to be expressed during fixed-velocity, steady-state walking, it was the method of choice for the steady-state testing within this experimental phase.

While much research has been performed exploring the energy expenditure of ambulation, in relation to body size, most attention has been focussed on the cost of movement (nett oxygen consumption) per step, unit of distance, and as a function of body size (Rubenson *et al.,* 2007; Weyand *et al.,* 2010; Ludlow and Weyand, 2017). Limited research has been published examining the scaling relationship between whole-body oxygen consumption and body mass during walking states (Rogers *et al.,* 1995; Batterham and Jackson, 2003; Markovic *et al.,* 2007; Table 3.1). Among those papers it appears that, within the same sample, the mass exponent increased with metabolic intensity, as hypothesised within the allometric cascade theory. However, across samples, discrepancies exist in the observed exponents for any given intensity. As discussed, those mass-exponent inconsistencies are most likely due to sample and method limitations. Together, those factors lead to uncertainty regarding the best non-linear approach to adopt during the analysis of submaximal, steady-state data. Therefore, this experimental phase was designed to minimise those limitations with the aim of identifying the most appropriate mass exponent to describe the scaling relationship between whole-body oxygen consumption and body mass during fixed-

velocity walking.

3.1.2 Scaling peak oxygen consumption

The scaling of peak oxygen consumption is not a novel concept, and is often used as a means of comparing data among individuals of varying body sizes (Åstrand and Rodahl, 1986), and with the general aim of enabling mass-independent comparisons among people of varying size. Despite the popularity of this physiological assessment, the most appropriate regression equation to describe those data remains unclear, with multiple alternative methods to the almost ubiquitous ratiometric approach ($y=ax$) being suggested (Bergh *et al.,* 1991 [non-linear, whole-body mass]; Nevill *et al.,* 2004 [non-linear, muscle girths]; Lolli *et al.,* 2017 [non-linear, fat-free body mass]). A growing body of research has supported the use of whole-body mass as the independent variable for a non-linear, power regression to describe those data ($y=ax^b$: Table 3.1). However, instead of those studies producing a unifying peak mass exponent, a wide range of exponents has been observed ($mass^{0.14\text{-}2.58}$: Jensen *et al.,* 2001), leaving uncertainty regarding which exponent one should adopt for normalising peak data. It is possible that peak oxygen consumption scales by the same mass exponent as observed during basal states ($mass^{0.67}$: Åstrand and Rodahl, 1986; Nevill *et al.,* 1992; Markovic *et al.,* 2007). Though, it seems more likely that a larger mass exponent would more accurately describe those data, with some researchers proposing significantly higher mass exponents ($mass^{0.81}$: Taylor *et al.*, 1981 [animals]; $mass^{0.92}$: Darveau *et al.,* 2002 [theoretical]; $mass^{0.94}$: Batterham and Jackson, 2003 [humans]). Thus, peak exercise oxygen uptake is likely to scale by a non-linear function of body mass. However, the precise mass exponent still eludes researchers and, as a result, it is unknown whether it differs from values observed during resting and submaximal states.

As with other scaling analyses, the characteristics of the sample tested can have a noticeable impact on the shape of the scaling regression observed. Multiple large-sample studies have been conducted where the scaling of peak oxygen consumption has been explored, which, while satisfying sample-size concerns (see Section 2.2.1.3), is often approached by using a heterogeneous sample ($N=1732$: Nevill and Holder, 1994; $N=1314$: Batterham *et al.,* 1999; $N=967$: Jensen *et al.,* 2001). The

use of such samples introduces uncontrolled physiological and morphological covariates into the regression equation; noise. For example, in samples where subcutaneous adiposity was not controlled, even though it does not directly contribute to an individual's peak oxygen consumption (Goran *et al.,* 2000), the regression will be skewed when oxygen uptake values are plotted against body mass (Lolli *et al.,* 2017). This is because the heavier individuals have a greater proportion of body mass that is not contributing to the exercise-specific metabolic rate. It can, therefore, be supposed that the observed exponents are unlikely to be representative of the true mass relationship with peak oxygen consumption.

Often the limitation associated with using a heterogeneous sample can be addressed by performing multiple-linear regression analyses, producing both a combined (whole-body mass alone) and individual-variable mass exponents. However, that approach can introduce two other potential pathologies when scaling. Firstly, splitting a sample into separate groups for individual analyses has often reduced the sample size significantly (Jensen *et al.,* 2001; Markovic *et al.,* 2007), decreasing the accuracy of any mass exponents observed. Secondly, to generate a combined mass exponent, the exponents for each covariate must be statistically similar (Vanderburgh, 1998). Unfortunately, an evaluation of those assumptions is often not addressed. Therefore, within this experimental phase, the scaling relationship was assessed using an appropriately large and homogeneous sample.

3.1.3 Aims and hypotheses

At present, it remains unclear whether metabolic intensity modifies the scaling relationship between oxygen consumption and body mass. Accordingly, the primary objective of this experimental phase was to identify whether that covariant relationship was present among human metabolic data. That objective was investigated by extending this research from resting (basal and standing: Chapter 2) to two exercising intensities: steady-state walking (submaximal, absolute) and running (peak exercise, relative). By testing the same participants used within Chapter 2, the resulting data could also be compared with the supine (basal) and standing conditions, thereby permitting exploration of the effect of body mass, a postural change and movement upon the scaling relationship throughout the physiological range.

In addition, a preliminary exploratory study was conducted to analyse whether supporting the body mass and moving the body independently affected the scaling relationship between oxygen consumption and body mass at lower exercise intensities. That aim was explored using a sub-sample of participants, who were tested during a 50% mass-supported walk, where data were compared with the standing and unaided walking trials.

To assess those aims, this experimental phase was designed to investigate four hypotheses:

Hypothesis Three-One: The relationship between oxygen consumption and body mass during ambulatory states (steady-state walking and peak exercise) would be more closely be scaled using non-linear (allometric) regressions with an exponent less than one.

Hypothesis Three-Two: The exponents observed during steady-state walking and maximal (running) conditions would be significantly greater than those observed during resting states (Chapter 2).

Hypothesis Three-Three: Peak oxygen consumption would scale by a significantly greater mass exponent than observed during submaximal (walking) and resting (basal and standing) conditions.

Hypothesis Three-Four: Walking (unsupported, carrying own mass) will significantly increase the steepness of the scaling relationship (mass-exponent) compared with a standing state, and by a greater amount than observed during mass-supported walking.

3.2 METHODS

3.2.1 Subjects

Using a repeated-measures design, 68 healthy and physically-active men were tested within this experimental phase, most of whom also completed the resting stages explored in Chapter 2 (N=68). All 68 subjects completed the walking stage, but only 63 performed the peak-exercise trial. Physiological and morphological variables were matched among the participants (see Section 2.2.1; Table 2.2), except for body mass, for which a wide range was sought (56.0-117.1 kg).

Of those participants, 15 were selected for further testing within an exploratory investigation, which was an extension of the supported-standing study described in Chapter 2 (Section 2.2.3.2). Those subjects were selected, where possible, to represent a balanced distribution of the main cohort across the entire mass range, for which no morphological or physiological differences were found (Table 2.2; $P > 0.05$). A distribution of the participants tested within this experimental phase, and the trials completed by each subject, is displayed in Figure 3.1.

All participants were recruited from local sports teams and the local university population. Subjects were screened to eliminate those with a history of cardiovascular, respiratory or musculo-skeletal dis-functions contraindicative of participation in this experiment. Prior to commencing testing, subjects were supplied with an information package and provided written, informed consent. The procedures performed within this experimental phase were approved by the Human Research Ethics Committee (University of Wollongong; HE14/469).

3.2.2 Procedural overview

The scaling relationship between oxygen consumption and body mass was measured during two exercise intensities; steady state (walking) and peak (running). Those tests were completed as part of a wider experiment, whereby participants completed a total of three walking trials (5%, 0%, -5% gradients: see Chapter 4), performed in a balanced order, with only level walking performed here. At the end of each walking trial, subjects completed an incremental ramp test to volitional exhaustion (peak running), and because three steady-state trials were performed, all subjects completed three maximal trials. The first two peak sessions were familiarisation trials, whereas, in the third session, peak oxygen consumption (peak aerobic power) was measured, thereby ensuring that those data were minimally influenced by familiarity, and approximated maximal aerobic power values.

The participants selected for the exploratory study returned to the laboratory for a fourth visit. During that trial, subjects completed an additional 15-min, steady-state walk (4.8 $km.h^{-1}$, 0% gradient) with 50% of their body mass supported using a whole-body harness. By comparing those data with the standing and unsupported

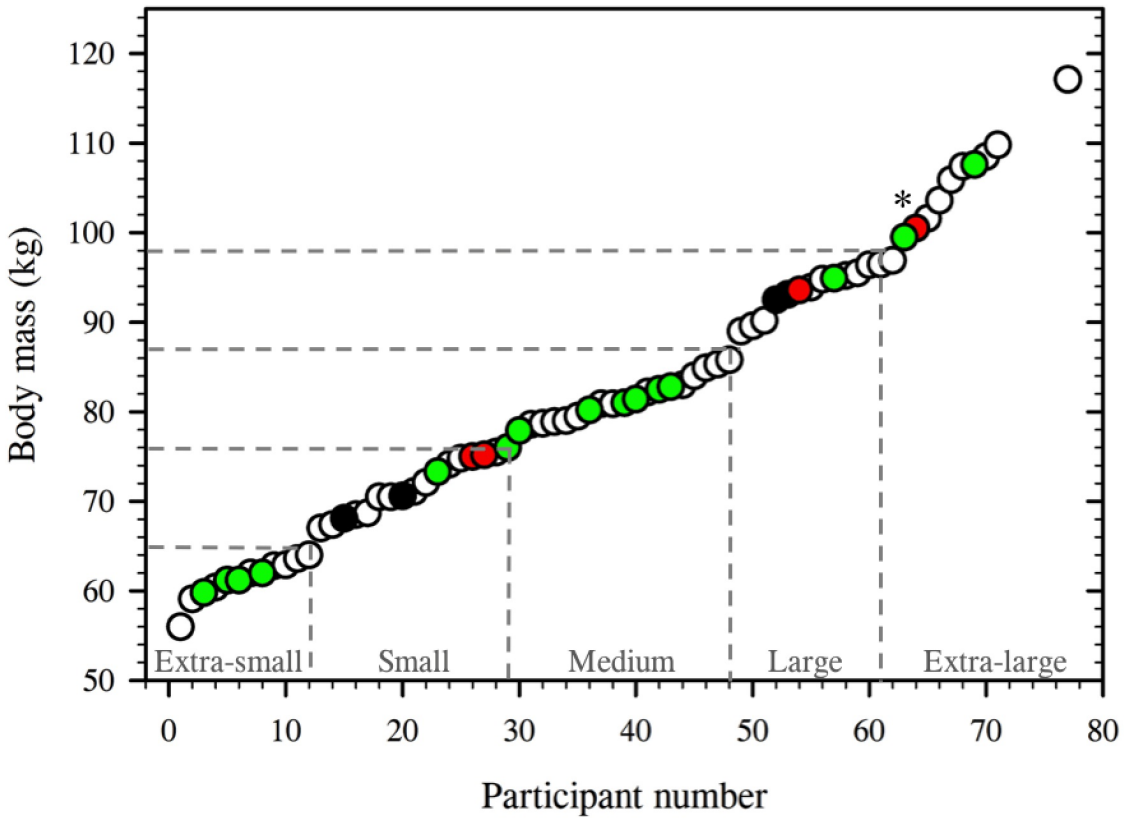

Figure 3.1: Scatter plot displaying the mass distribution of the participants tested within this project. Semi-nude body masses are displayed for 72 participants, representing the total number of participants tested between Chapter 2 and Chapter 5, with subjects arranged in ascending order of body mass. However, only 68 participants were tested within this experimental phase: 68 in the walking trial and 63 in the peak exercise test. Missing and partial datasets are identified by the black (not tested in this experimental phase: $N=4$) and red data points respectively (walking trial only: $N=4$). The green data points signify those participants who also completed the exploratory protocol ($N=15$), one of whom did not complete the peak exercise test (identified by the asterisk [*]). The dashed drop-lines identify the borders separating each of the five body-mass groups (Extra small: 55-65 kg; Small: 66-76 kg; Medium: 77-87 kg; Large: 88-98 kg; Extra large: ≥99 kg) and show the number of participants within each group.

walking trials, it was possible to partially isolate the metabolic cost of limb movement (mass-supported walking) without the body mass carriage associated with normal walking.

3.2.2.1 Experimental standardisation

Two sets of clothing were worn by participants during the testing. For all walking trials, clothing items were provided and pre-sized by the researchers (combat trousers, a shirt and thick socks: Figure 3.2A). However, during the walks, participants wore their own running shoes. As shoe sizes ranged from 4-13 within the sample, this resulted in individual shoe masses of ~250-500 g per foot. To minimised the known metabolic effect of loading at the foot (Soule and Goldman, 1969; Taylor *et al.,* 2012), shoe masses were standardised to 500 g by adding the mass difference to an ankle weight with sand (Figure 3.2B). The average mass added to each foot was ~150 g. During the peak exercise test, participants wore their own sports clothing (t-shirt, shorts and running shoes). Clothing masses were recorded to permit scaling to the total mass carried by each individual. All testing was conducted in an air conditioned laboratory (~23°C; ~50% humidity) at the same time of day (±1 h) per participant, to minimise any potential circadian rhythm affects. Prior to testing, participants were instructed to refrain from drinking caffeine for 6 h and to consume a meal high in carbohydrates and low in fats >2 h before the start of the test.

3.2.2.2 Measuring steady-state (walking) oxygen consumption

On arrival at the laboratory, semi-nude body mass was first recorded. A Polar cardiac frequency monitor (plug in receiver, Polar Electro, Kempele, Finland) and an oronasal mask (V-Mask 7400 series, oronasal mask, Hans Rudolph, Kansas City, U.S.A.) were then fitted to participants. The testing commenced with a 10-min stage, where the subject stood motionless next to the gas analysis system (TrueOne 2400, ParvoMedics Inc., Utah, U.S.A.: Crouter *et al.,* 2006). Participants then mounted a treadmill (Pulsar 3p Treadmill, H/P/Cosmos, Traunstein, Germany) and walked at the fixed velocity of 4.8 $km.h^{-1}$ (0% gradient) for 15 min.

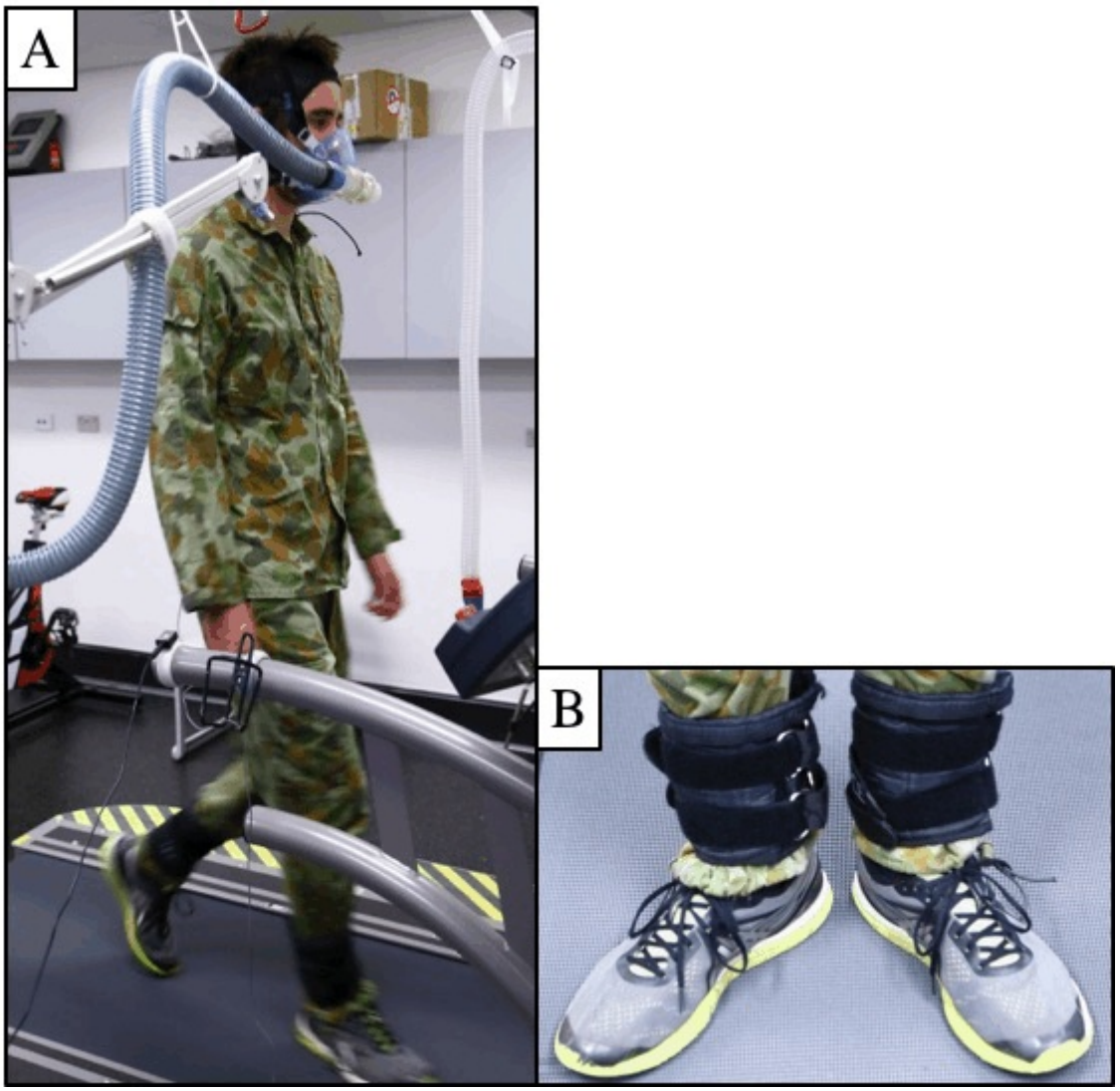

Figure 3.2: Clothing ensemble worn by participants during all walking trials, comprising of a t-shirt and combat trousers, pre-fitted by researchers, and their own running shoes (Figure 3.2A). Clothing items were selected to correspond with those worn by the Australian Defence Force, with the aim of determining the mass-independent oxygen cost of ambulatory activities for defence personnel. Figure 3.2B displays the sand-filled, ankle weights used to standardise the foot loading to 500 g (shoe plus ankle mass) during the walking trials.

3.2.2.3 Measuring mass-supported, walking oxygen consumption

On a separate day, a sub-sample of participants returned for an additional testing session completed as part of the exploratory investigation. Semi-nude body mass was taken before participants donned their usual, pre-fitted testing garments and pre-weighed ankle loads. The testing procedure for this trial replicated that used during the unaided walking condition (Section 3.2.2.2) with the exception that, during the walk, participants wore a whole-body harness. The harness was used to support 50% of the participant's body mass during walking. The harness was attached to an overhead beam, used to support the participant's mass at five points to encourage a normal walking posture: the top of both shoulders, the two most lateral points of the hips, and an attachment point at the centre of the back between the shoulders. The level of support was controlled manually, with the necessary rope tension determined using digital scales (MS3200, Medical Scale, Charder, Taichung, Taiwan). Neoprene foam was used to minimise the pressure applied by the harness.

3.2.2.4 Measuring peak oxygen consumption

Participants completed three peak oxygen consumption trials on separate days: two familiarisation sessions followed by the main trial, during which data were collected. The sessions commenced with subjects completing a self-paced warm up (10 min) on a treadmill (Pulsar 3p Treadmill, H/P/Cosmos, Traunstein, Germany), wearing their own sports clothing and instrumented with a Polar cardiac frequency monitor, mouth piece, nose clip and safety harness. Upon completion of the warm up, the incremental ramp test began. Participants ran at a fixed velocity between 8-12 $k.h^{-1}$, pre-determined by researchers during the familiarisation trials to ensure volitional exhaustion was achieved between 8-12 min. Work rate was increased each minute by raising the treadmill gradient in 1% increments (starting from 0%).

In addition to determining each participant's running speed, the familiarisation sessions were used to increase test reliability by introducing subjects to the testing protocol, experimental equipment and the feeling of running to the point of volitional failure. A preliminary pilot study was conducted to evaluate test reliability for the incremental ramp test, wherein 10 subjects visited the laboratory on three separate days to perform the test. No difference in peak aerobic power was observed across

the three trials (Table 3.2; $P > 0.05$). That outcome is atypical from other familiarisation literature (Shephard *et al.,* 1968; Jamnik *et al.,* 2013) and believed to be a result of the sample tested, who were all students experienced in participating in peak exercise testing. Accordingly, the two familiarisation sessions were kept within the testing protocol to ensure that all participants were accustomed with the peak exercise test, however, as the sample was drawn from a similar population, the peak-exercise data obtained were unlikely to increase with further test repetitions, thus, they were considered equivalent of maximal aerobic power values.

3.2.4 Experimental measurements

Oxygen consumption (open-circuit respirometry: TrueOne 2400, ParvoMedics Inc., Utah, U.S.A.: Crouter *et al.,* 2006) and cardiac frequency (ventricular depolarisation: Plug in receiver, Polar Electro, Kempele, Finland) data were measured continuously throughout the trials and recorded as 15-s averages using open-circuit respirometry and ventricular depolarisation. Steady-state data were collected and averaged during the last 5 min of the walk, while peak values were recorded during the peak-exercise test. Semi-nude and clothed (unshod) body masses (digital scales: MS3200, Medical Scale, Charder, Taichung, Taiwan) were recorded prior to the start of each trial. Anthropometric data (skinfold thicknesses [skinfold callipers: Eiken skinfold calliper, Meikosha, Tokyo, Japan] and standing, stretched stature [stadiometer: Harpenden Stadiometer, Holtain Ltd., Crymych, UK]) were measured on the participant's first visit at the laboratory (see Section 2.2.4 for details).

Variations in body size were controlled by adjusting morphometric data (sum of skinfolds and semi-nude body mass) for differences in standing height (Equation 2.3). Those height-adjusted measures were compared against age- and gender-specific, population normative data (Garrett and Kennedy, 1971; Wilmore and Behnke, 1969, 1970; Ross and Ward, 1985) to enable the identification of any non-proportional size variations. In addition, subcutaneous adiposity was controlled within the sample, due to its load-carriage effect on metabolism (Goldman and Iampietro, 1962). A criterion threshold of greater than the 60^{th} percentile (plus the measurement error) for height-adjusted adiposity was set (88 mm; Figure 2.7: Ross and Ward, 1985; Landers *et al.,* 2013), meaning that all participants were considered to have average to low adiposity

Table 3.2: Peak oxygen consumption data for ten subjects (24 y [SD 2]; 68.95 kg [SD 10.84]; 169.99 cm [SD 7.47]), measured across three separate laboratory visits, to evaluate the effect of familiarisation on the peak oxygen consumption data (see Section 3.2.2.4 for protocol). Two participants did not complete the third trial. The peak measurement observed during each trial is presented in the table below, along with mean group data with the standard error of those means in parentheses. Repeated measures analysis of variance revealed no difference in peak oxygen consumption among the three visits ($P > 0.05$).

	Peak oxygen consumption ($L.min^{-1}$)		
Participant	Trial 1	Trial 2	Trial 3
1	4.71	4.46	4.53
2	3.63	3.61	3.60
3	3.27	3.39	3.30
4	3.95	4.35	3.95
5	4.47	4.59	4.70
6	4.20	4.21	-
7	2.59	2.64	2.49
8	3.60	3.50	-
9	4.10	3.93	3.84
10	2.37	2.40	2.34
Mean	3.69 (0.24)	3.71 (0.24)	3.59 (0.30)

levels.

3.2.5 Design and analysis

3.2.5.1 Experimental design

This experimental stage was based on a five by three factorial design (Figure 3.3), with five levels of the first factor (body mass: extra-small, small, medium, large, extra-large) and three levels for the second factor (ambulatory intensity: peak, unaided walking, 50% mass-supported walking). The mass-supported level was conducted as part of an exploratory investigation conducted using a participant sub-sample. The experiment was based upon a repeated-measures design with participants acting as their own controls. Data are presented as means with data distributions described using standard deviations (SD) and standard errors of the mean ($\pm$) used to define the precision of the mean.

3.2.5.2 Data analysis

Sample homogeneity was assessed using raw and height-adjusted sum of skinfolds and semi-nude body masses. Between-group comparisons across the five body-mass groups[20] were performed using one-way analyses of variance. If differences remained among either height-adjusted measure, analysis of covariance was used to assess for a covariant effect in either of the two scaling relationships (walking and peak exercise).

Based upon the findings in Chapter 2 and the exercise-specific scaling literature, the assumption was made that the algebraic equations for both models would remain unchanged. Therefore, to confirm the regression shape for each metabolic intensity, linear (first-order polynomial with an intercept: $y=ax+c$) and non-linear (allometric: $y=ax^b$) regressions were applied to both datasets. The appropriateness of each model was evaluated using the steps outlined in Figure 2.8, where the assumptions of linear

[20] To permit size comparisons within the sample, the mass range was divided into five body-mass groups: Extra small ($\leq$65 kg), Small (66 kg - 76 kg), Medium (77 kg - 87 kg), Large (88 kg - 98 kg) and Extra large ($\geq$99 kg).

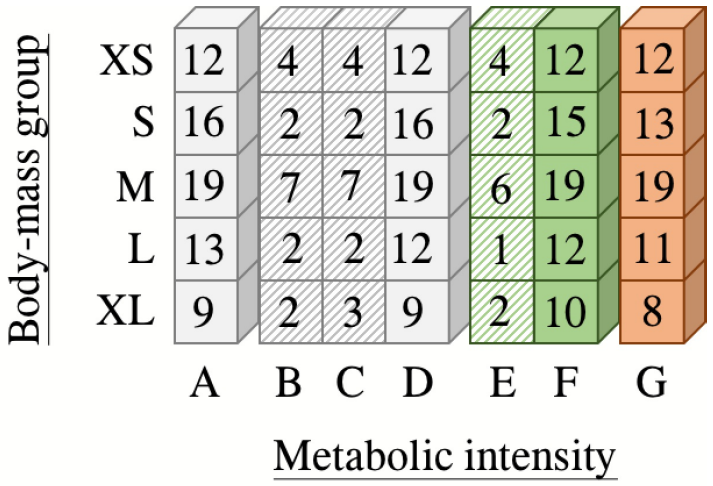

Figure 3.3: A schematic of the overall experimental design with sample sizes identified within each cell. The current research phase (coloured) consisted of a five (mass) by three (activity) factorial design, but was part of a wider research project which is partially depicted above (grey: Chapter 2) as a five by seven factorial design. The first factor (body mass) had five levels: extra-small (XS: ≤65 kg); small (S: 66-76 kg); medium (M: 77-87 kg); large (L: 88-98 kg); and extra-large (XL: ≥99 kg). The second factor (metabolic state) had seven levels: supine (Column A: basal, rest); 100% mass-supported standing (Column B: exploratory investigation); 50% mass-supported standing (Column C: Exploratory investigation); standing (Column D); 50% mass-supported walking (Column E: exploratory investigation); unsupported walking (Column F); peak exercise (Column G). Exploratory investigation trials are identified by the hashed fills.

regression[21] and the previously-determined biological assumptions[22] were assessed.

Before analysing the non-linear regressions, the datasets were log-transformed, using a Log_{10} base, to provide a linear function (Figure 2.9). All the regressions evaluated were bootstrapped (1000 re-sampled repetitions: Efron, 1979; Fox and Weisberg, 2017) to generate a mean and standard error of the mean for each regression coefficient.

Analysis of covariance was used to assess differences between regression slopes, for both between- and within-intensity differences. The latter comparison was performed within the exploratory sample to evaluate the similarity of the reduced-sample ($N=15$) regressions with those applied to the main cohort (standing: $N=67$; walking: $N=68$). A difference in regression slope was identified by a significant interaction effect. Such differences indicated the need to describe datasets using unique regression coefficients or mass exponents. Between-intensity differences were also compared using mean oxygen consumption and cardiac frequency using repeated-measures analysis of variance.

A Pearson's correlation coefficient test (Pearson, 1900, 1920) was performed on normalised oxygen consumption residuals, ordered by body mass, to determine whether a specific mass exponent (where the exponent equals one for a linear regression) could be used to generate mass-independent data. A *rho*[23] value approaching zero represented a successful attempt.

Potential outliers were identified using four assessments: raw and log-transformed scatter plots, box and whisker plots, Bonferroni test (Cook and Weisberg, 1982;

---

[21] The assumptions of linear regression: normality of variables, no autocorrelation among variables, a constant error variance among residuals (homeoscedasticity).

[22] The biological assumptions: a regression slope less than unity, as metabolic rate does not increase by a faster rate than body mass, even during peak exercise (Taylor *et al.*, 1981; Darveau *et al.,* 2002; Batterham and Jackson, 2003), and an origin intercept, for at zero mass it is not physiologically possible to have a non-zero metabolic rate.

[23] *Rho*, or the correlation coefficient, is the numerical measure for the strength and direction of any linear relationship between two variables ($-1 \leq rho \leq 1$).

Williams, 1987; Fox, 1997) and Cook's distance (Cook, 1977). Data points flagged in two or more tests were assessed by researchers and only removed if their omission significantly affected the shape of the regression or there was evidence of some experimental error (such as a leak in the mask; see Section 2.2.5.2 for further details on the data analysis methods).

3.3 RESULTS

3.3.1 Pre-experimental standardisation

Three objectives were investigated within this experimental phase. The first was to confirm whether the relationship between oxygen consumption and body mass was non-linear according to metabolic intensity (walking and peak exercise), thereby determining how best to derive mass-independent data during exercise across different intensities. The second objective was to identify whether the increase in intensity between the conditions significantly modified the regression shape, and thus the mass scaling exponent. The final objective was to perform a preliminary exploration of the individual effects of supporting the body's mass on scaling exponents. To effectively address those objectives it was necessary to ensure the sample homogeneity.

3.3.1.1 Evaluating the sample morphometry

Despite the small sample variations between Chapters 2 and 3 (Figure 3.1), six participants were still identified with height-adjusted sum of skinfold measures greater than 88 mm, and the larger three were outliers (extra-large group) when data were untransformed (Figure 2.11C). Inclusion of those data points was determined using analysis of covariance for each morphometric measure on the two scaling relationships (walking and peak exercise). No covariant relationship was realised for either measure during the walking condition ($P > 0.05$), however, a covariant effect was evident in the peak exercise dataset ($P < 0.05$). Fortunately, removal of the two largest outliers eliminated that relationship ($P > 0.05$). As a result, only those two data points were removed from the peak exercise trial.

Adjusting morphometric data for variations in standing height (Equation 2.3) reduced the pre-existing, between-group size differences in body mass and skinfold thickness ($P < 0.05$). However, size differences still remained among the extra-small group for

proportional mass ($P<0.05$), indicating that they carried less mass per unit of height, and the extra-large group for relative adiposity ($P<0.05$). Nevertheless, that difference for the extra-large group was removed when the two largest participants were temporarily removed ($P>0.05$). It was therefore concluded that Equation 2.3 was a successful method for comparing morphometric variables across varying body sizes and that, for the most part, the cohort was similar in morphology and any differences were proportional with body size.

3.3.2 Scaling oxygen consumption against body mass

The primary objective of this experimental phase was to establish whether the scaling relationship between oxygen consumption and body mass remained non-linear during exercising intensities (walking and peak exercise). The validity of that assumption was assessed by applying both a linear ($y=ax+c$) and a log-transformed, non-linear ($\text{Log}_{10}[y]= b \cdot \text{Log}_{10}[x]+\text{Log}_{10}[c]$)[24] regression to both datasets. Following the steps outlined in Figure 2.8, the fit of each regression was assessed against three criteria: satisfying the assumptions of linear regression[25], satisfying the two biological assumptions[26] and the ability to generate mass-independent oxygen-consumption data by normalising data using the regression equation. Prior to testing those assumptions, the two peak-exercise outliers were removed (Section 3.3.1.1). Accordingly, 68 participants were evaluated for the walking intensity and 61 for the peak-exercise test.

The assumptions of linear regression were met for all four regressions. Approximately normal distributions were evident among the eight regression-variable histogram plots (Figure 3.4 [walking] and Figure 3.5 [peak exercise]). Those observations were supported statistically, with neither the skewness and kurtosis *z*-scores nor the Shapiro-Wilk tests identifying any differences from a normal

---

[24] Log transformation of the non-linear, allometric equation $y=ax^b$ results in a linear, first-order polynomial equation with an intercept with the format $\text{Log}(y)= \text{Log}(a) + b \cdot \text{Log}(x)$. By transforming the data in that way, the non-linear regression can be assessed using the more robust linear assessment methods.

[25] The assumptions of linear regression: normality of variables, no autocorrelation among variables, a constant error variance among residuals (homeoscedasticity), and a linear relationship between both variables.

[26] The biological assumptions for the scaling relationship: a regression slope less than unity and an origin intercept.

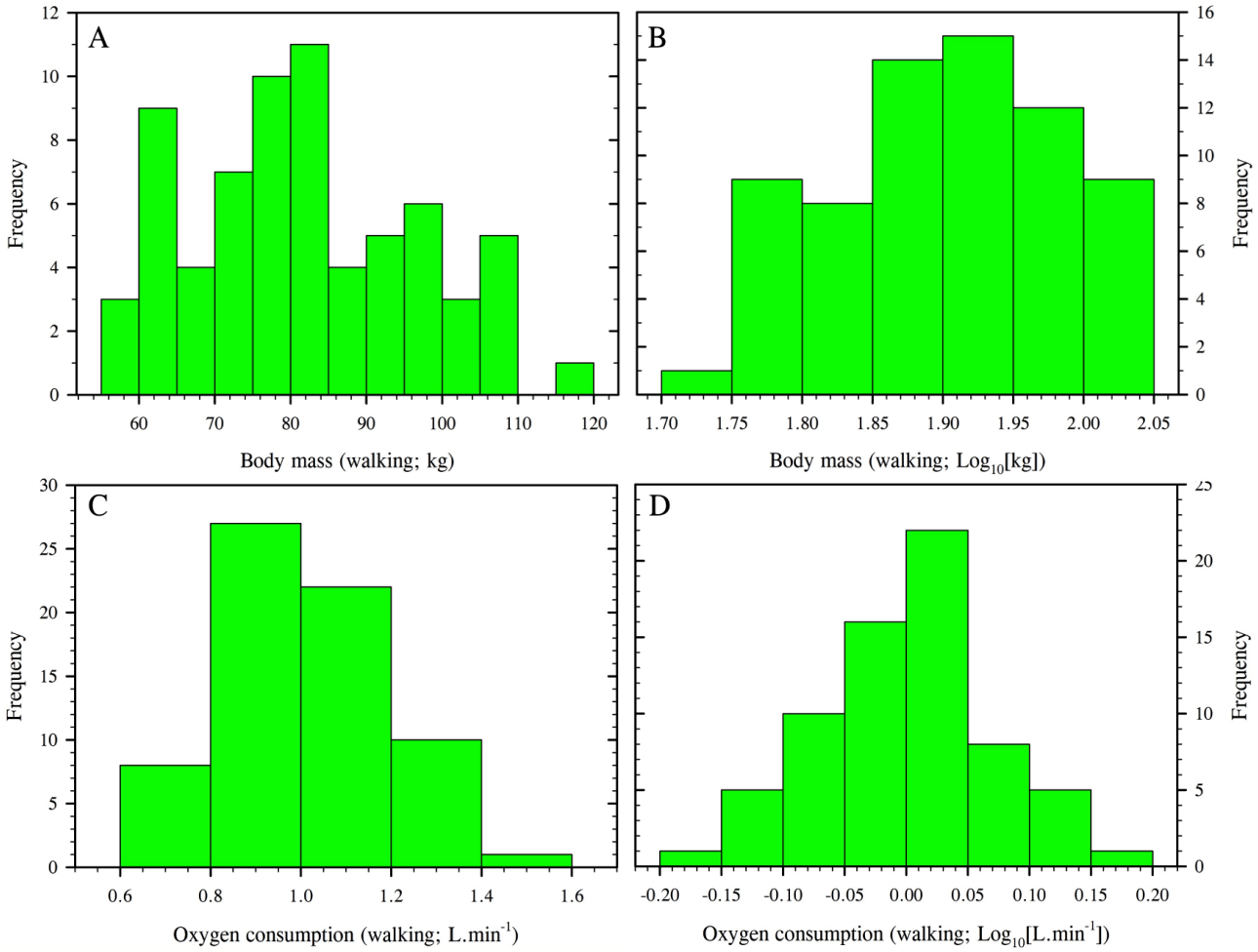

Figure 3.4: Frequency histogram displaying the data distributions of both regression variables (body mass and oxygen consumption) used for the steady-state walking relationship. Data are displayed for 68 adult men, in untransformed (Figure 3.4A and Figure 3.4C) and log-transformed (Figure 3.4B and Figure 3.4D) units to correspond with the linear and non-linear regressions, respectively.

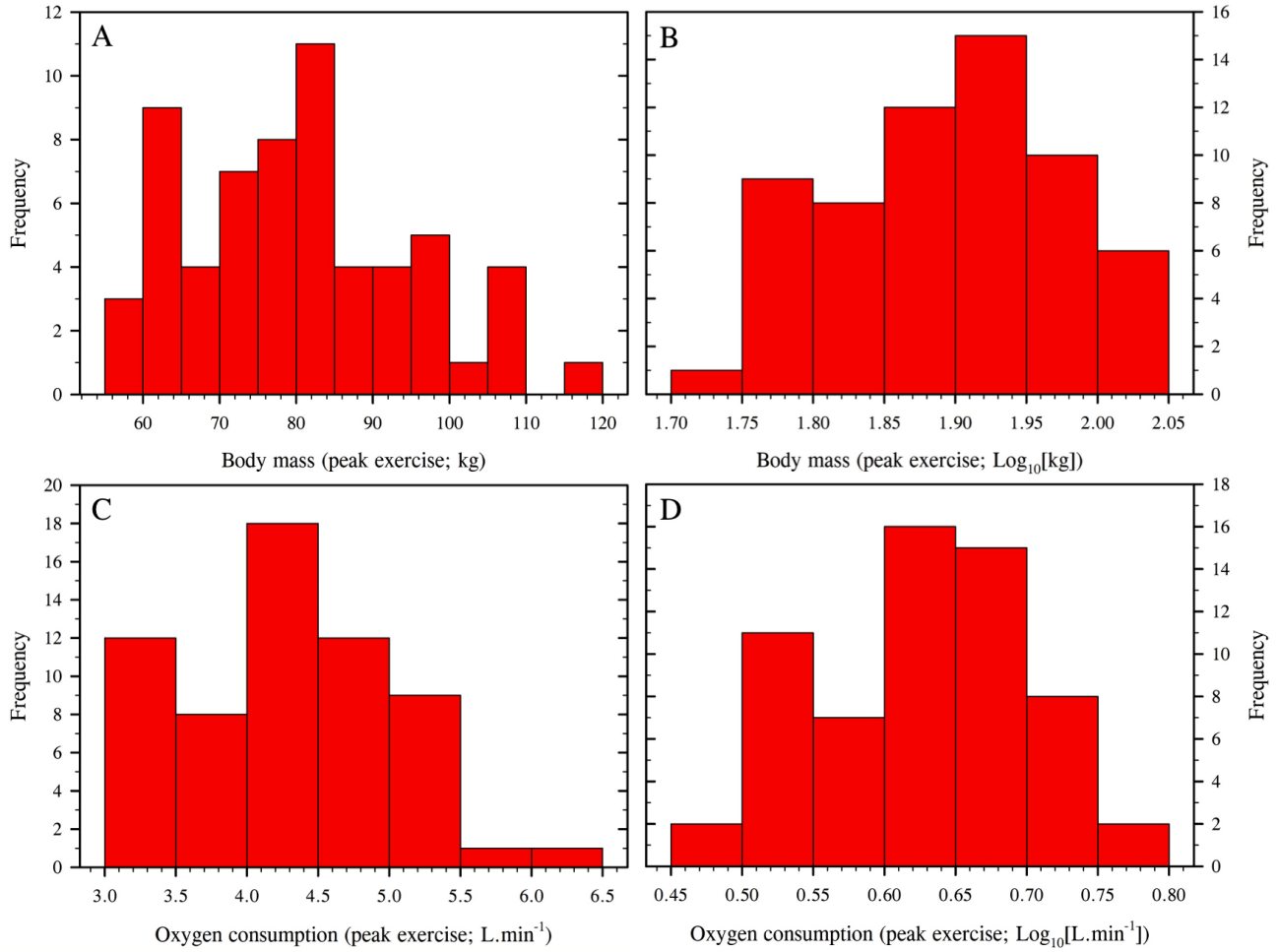

Figure 3.5: Frequency histograms of the peak exercise regression variables (body mass and oxygen consumption). Data are displayed for 61 adult men, in untransformed (Figure 3.5A and Figure 3.5C) and log-transformed (Figure 3.5B and Figure 3.5D) units to correspond with the linear and non-linear regressions, respectively.

distribution (Table 3.3; $P > 0.05$). Linearity was confirmed in the linear and non-linear regressions during both walking (Figure 3.6A and Figure 3.6C, respectively) and peak exercise (Figure 3.7A and Figure 3.7C, respectively). A small amount of heteroscedasticity was observed among the residuals for the walking condition (Figure 3.6B and Figure 3.6D), but not during the peak exercise (Figure 3.7B and Figure 3.7D). That variance in error was not corrected by the log transformation. It was considered that this observation was an artefact of having a reduced sample size in the extra-small ($N = 8$) when compared with the extra-large ($N = 12$) mass groups, causing the funnelling appearance, or perhaps that the two largest residuals at the lighter mass range were outliers, although they were not identified within any statistical testing ($P > 0.05$). While those observations were flagged in the initial analyses, removal of those individuals did not modify the regression equation ($P > 0.05$), therefore, they were kept within the dataset. Either way, the heteroscedasticity was considered to be a negligible amount of variance and was not further addressed. Lastly, no autocorrelation was realised among residuals in any of the regressions (Table 3.3; Figures 3.6B and 3.6D; Figures 3.7B and 3.7D; $P > 0.05$). Therefore, it was concluded that both the linear and non-linear scaling approaches were statistically suitable for scaling both walking and peak-exercise oxygen consumption against body mass (Figure 2.8).

Notwithstanding the statistical fit of both the linear and non-linear regressions, only the latter method satisfied the two biological assumptions (Figure 2.8). While all four regressions displayed slopes less than unity (Figure 3.8), satisfying the biological assumption that metabolic rate increases at a slower rate than body mass, an intercept significantly greater than zero was observed in the linear regressions for both exercise states (Figure 3.8 [dashed lines]; $P < 0.05$). As it is physiologically impossible for a hypothetical organism of zero mass to have anything other than zero oxygen consumption, those positive intercepts meant that the two linear regressions could not be considered suitable for describing the scaling relationships. On the other hand, an origin intercept was inherent within the constraints of a non-linear, allometric regression, meaning that the non-linear regressions were the only scaling approach to satisfy both the statistical and biological criteria for selection.

Table 3.3: The assumptions of linear regression were assessed for the walking and peak exercise scaling relationships between oxygen consumption and body mass using both linear ($y=ax+c$) and non-linear ($y=ax^b$) regressions. The table displays the test statistics and calculated *z*-scores for skewness and kurtosis, the Shapiro-Wilk test and the Durbin-Watson test used for those assessments. No significant values were found for any of those analyses ($P>0.05$).

	Regression variables						Regression residuals			
	Walking oxygen consumption ($L.min^{-1}$)		Peak oxygen consumption ($L.min^{-1}$)		Body mass (kg)		Walking		Peak exercise	
	Raw	Logged	Raw	Logged	Raw	Logged	Linear	Logged	Linear	Logged
Skewness statistic	0.29	-0.09	0.23	-0.11	0.33	0.03	0.30	-0.00	0.19	0.07
Z-score	1.01	-0.30	0.75	-0.37	1.16	0.10	1.02	-0.01	0.41	0.23
Kurtosis statistic	-0.46	0.49	-0.47	-0.80	-0.78	-0.93	-0.09	0.23	-0.66	-0.67
Z-score	-0.80	-0.86	-0.79	-1.34	-1.38	-1.64	-0.16	0.41	-1.09	-1.12
Shapiro-Wilk statistic	0.98	0.99	0.97	0.97	0.97	0.98	0.99	0.99	0.98	0.98
Durbin-Watson statistic	-	-	-	-	-	-	1.97	1.92	2.09	2.03

Notes: A Shapiro-Wilk test statistic of 1 would represent a perfectly normal distribution (Shapiro and Wilk, 1965), and a Durbin-Watson (1950; 1951) test statistic of 2 would identify a complete absence of autocorrelation between regression variables.

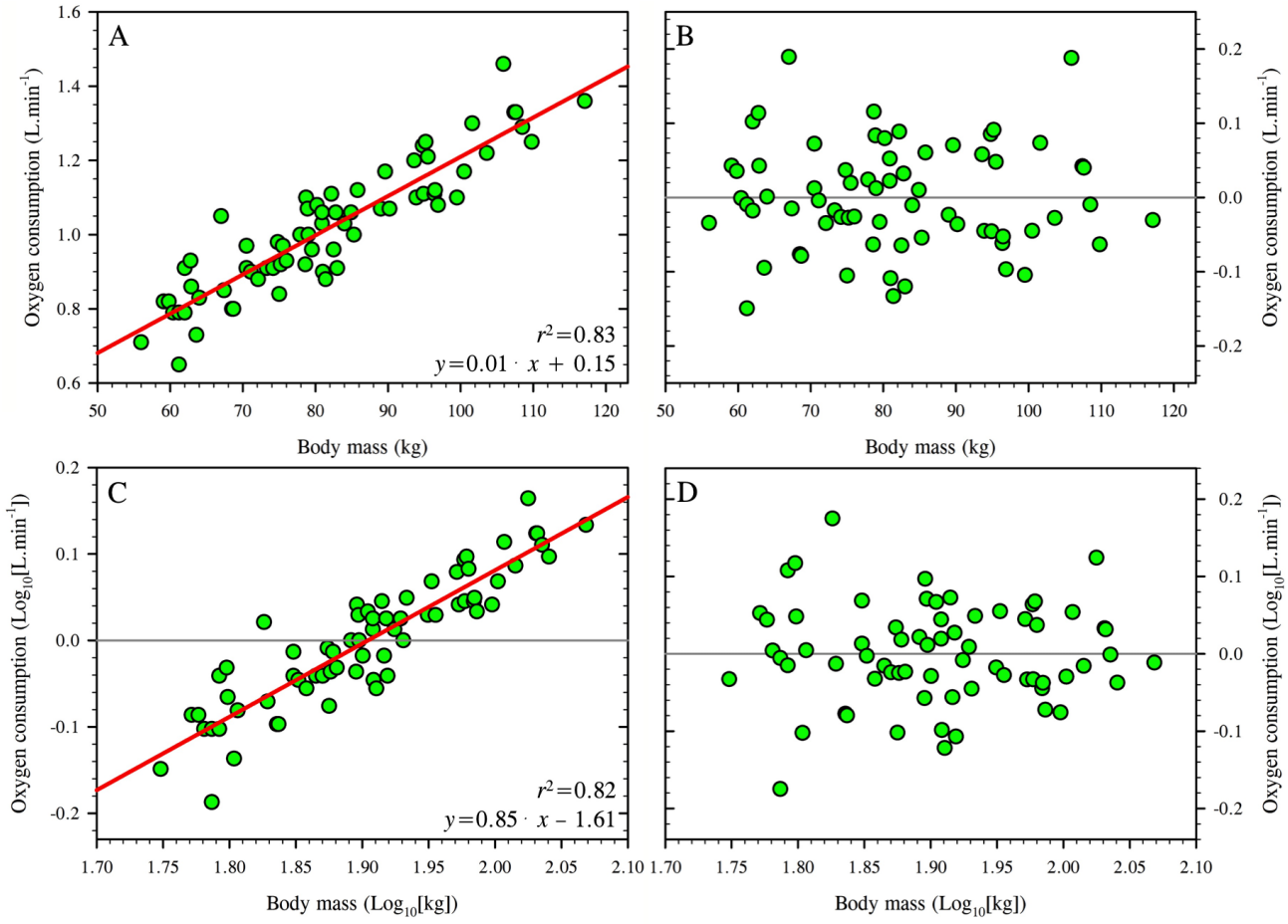

Figure 3.6: Scatter (Figure 3.6A and Figure 3.8C) and residual plots (Figure 3.6B and Figure 3.6D) used to assess the assumptions of linearity and homeoscedasticity, respectively, for the scaling relationship between oxygen consumption and body mass during the walking trial (N=68). Figures 3.6A and 3.6B correspond to the linear regression, whilst Figures 3.6C and 3.6D present the transformed, non-linear regression.

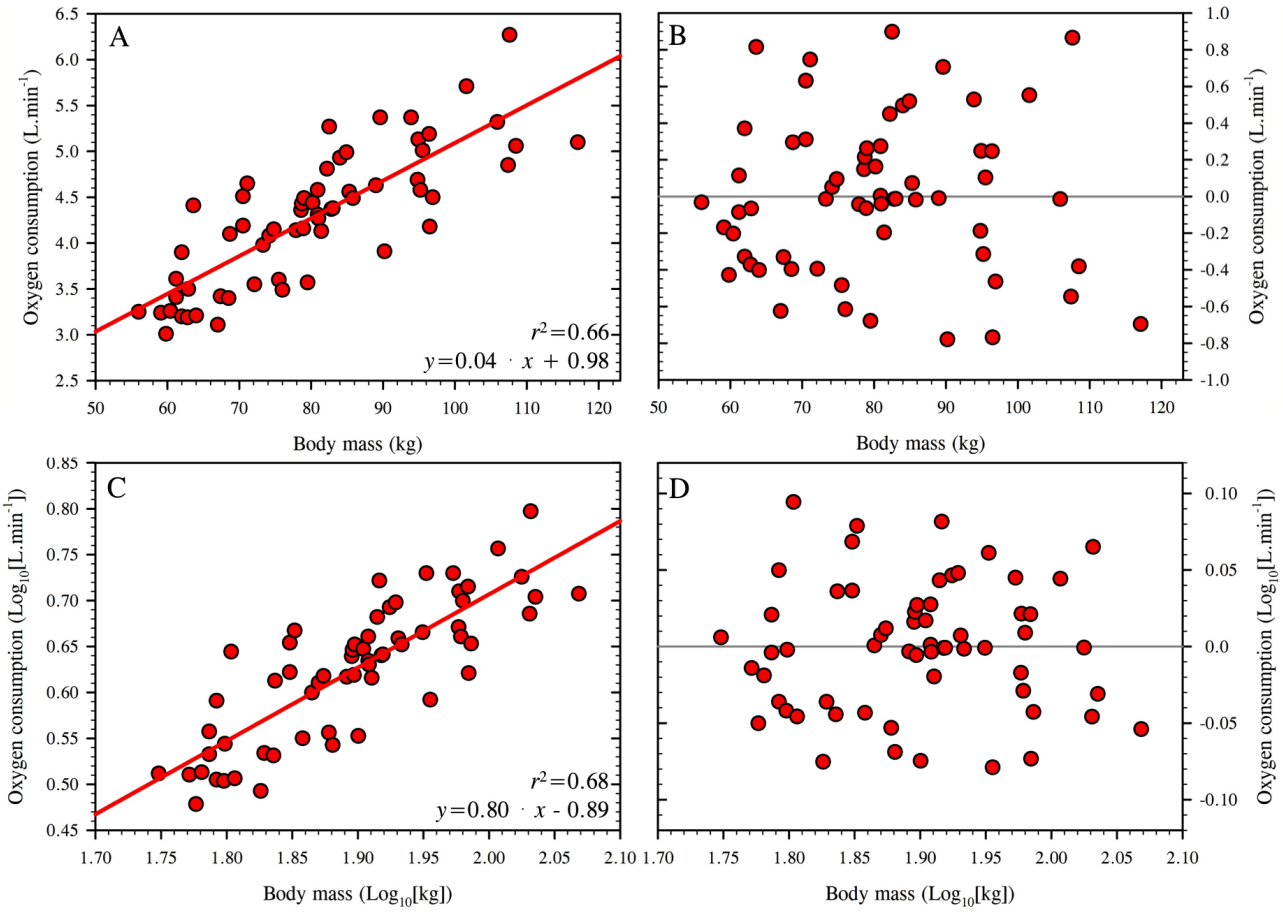

Figure 3.7: Peak exercise data presented in scatter (Figure 3.7A and Figure 3.7C) and residual plots (Figure 3.7B and Figure 3.7D) to assess the assumptions of linearity and homeoscedasticity, respectively, for the scaling relationship between oxygen consumption and body mass (N=61). Data for the linear regression are presented in Figures 3.7A and 3.7B, whilst the log-transformed data are displayed in Figures 3.7C and 3.7D.

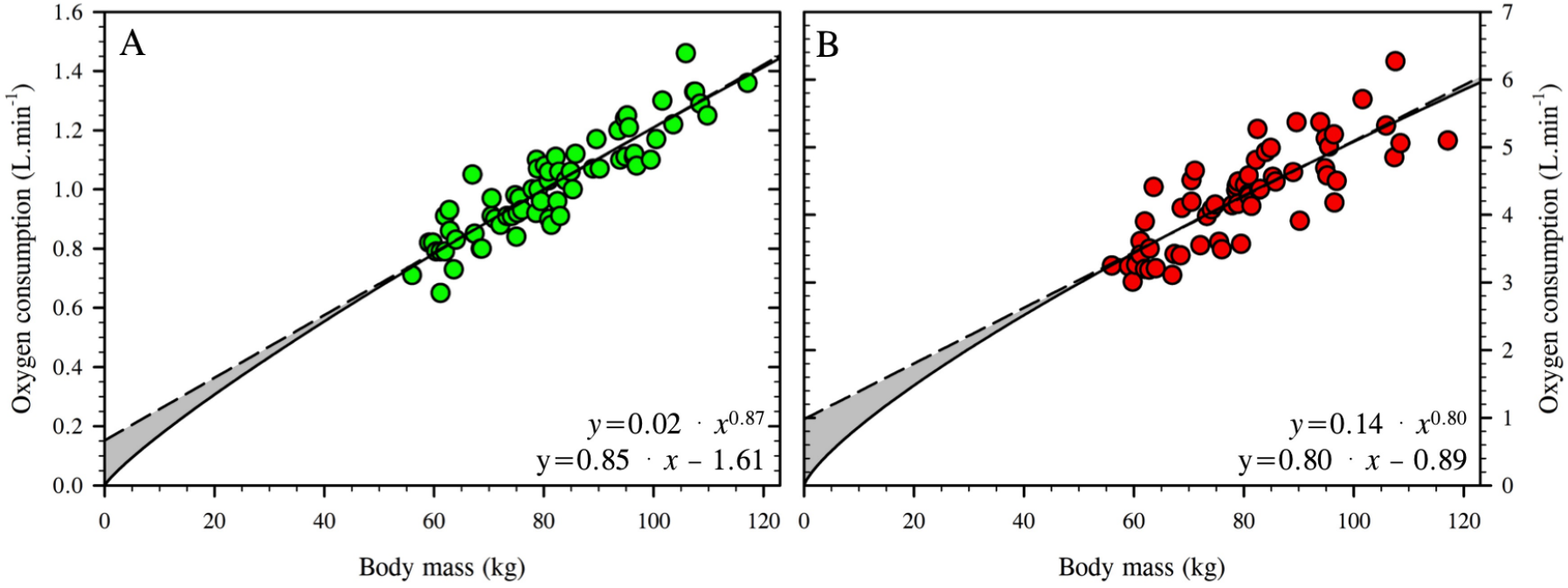

Figure 3.8: Scatter plot of the relationship between oxygen consumption and body mass during the walking (N=68; Figure 3.8A) and peak exercise (N=61; Figure 3.8B) trials. Linear (dashed line) and non-linear (solid line) scaling approaches have been applied to both datasets to demonstrate the fit of both regressions, with the difference between the regressions coloured in grey. All regressions have been extrapolated back to the ordinate so that the intercepts could be evaluated. Both linear regressions displayed an ordinate-intercept significantly different from zero (walking: 0.15 L.min^{-1} [±0.05]; peak exercise: 0.97 L.min^{-1} [±0.34]; P<0.05).

To evaluate the fit of those non-linear regressions, the untransformed data were normalised using the mass exponents and plotted in mass order (Figure 3.9). Providing the applied regression suitably described the dataset, a Pearsons' correlation coefficient would reveal no remaining mass correlation among the residuals. As no mass relationship was evident within the walking (Figure 3.9A; $r=0.08$; $P>0.05$) or peak exercise (Figure 3.9B; $r=0.02$; $P>0.05$) datasets, it was concluded that both regressions were a good fit for the two scaling relationships. Furthermore, the procedure confirmed that normalising exercise-intensity oxygen consumption data using $mass^{exponenet}$ successfully removes the mass-dependency present among absolute data.

3.3.3 Assessing the effect of metabolic intensity on the scaling relationships

After confirming that the two scaling relationships are non-linear, the next step was to determine whether or not they differed from each other. Specifically, whether metabolic intensity modified the shape of the regression during exercise. Moreover, as the experiment was a repeated-measures design, it was possible to extend that comparison across the four metabolic intensities tested so far, enabling comparisons across the entire physiological range: basal (supine), standing (rest), walking and peak exercise. If no difference was found between two or more scaling regressions, then oxygen consumption data from those states could be described and normalised using the same (common) mass exponent.

Among the four datasets, a significant increase in oxygen consumption ($P<0.05$) occurred with each metabolic intensity increase (basal: 0.27 $L.min^{-1}$ [$\pm$0.03]; standing: 0.33 $L.min^{-1}$ [$\pm$0.04]; walking: 1.02 $L.min^{-1}$ [$\pm$0.12]; peak exercise: 4.28 $L.min^{-1}$ [$\pm$0.55]; $P<0.05$), except between the basal and standing condition (Chapter 2; $P>0.05$). Those observations were mirrored in the cardiac frequency data, with a significant step-wise increase occurring among all trials (basal: 59 $b.min^{-1}$ [$\pm$1]; standing: 79 $b.min^{-1}$ [$\pm$2]; walking: 97 $b.min^{-1}$ [$\pm$2]; peak exercise: 195 $b.min^{-1}$ [$\pm$1]; $P<0.05$). Those data corresponded to similar observations for walking and peak exercise states within the literature (walking $\sim$4.8 $km.h^{-1}$: 1.03 $L.min^{-1}$, Rogers *et al.,* 1995; 1.40 $L.min^{-1}$, Markovic *et al.,* 2007; 0.89 $L.min^{-1}$, Taylor *et al.,* 2012; peak exercise: 4.30 $L.min^{-1}$, Rogers *et al.,* 1995; 4.50 $L.min^{-1}$, Markovic *et al.,*

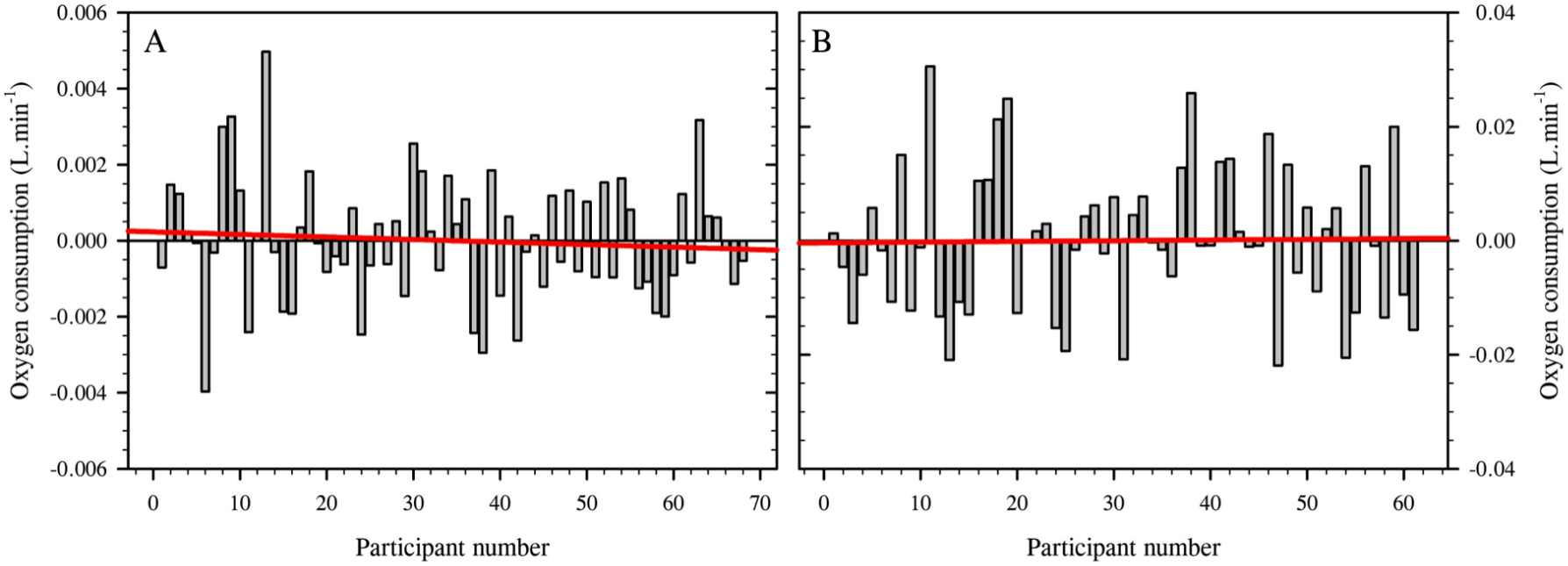

Figure 3.9: Residual plots of the normalised oxygen consumption data for the walking (Figure 3.9A; $N=68$; $r=0.08$; $P>0.05$) and peak exercise (Figure 3.9B; $N=61$; $r=0.02$; $P>0.05$) trials. Absolute oxygen consumption data were normalised using the two allometric scaling mass exponents (walking: $mass^{0.87}$; peak exercise: $mass^{0.80}$). Data are ordered by participant number along the abscissa, from lightest to heaviest.

2007; 3.40 L.min^{-1}, Taylor *et al.,* 2012). Thus, the observed increases in oxygen consumption were considered realistic and suitable for between-intensity comparisons.

Before comparing the four regressions, the distributions of the residuals from all four regressions were assessed, as an analysis of covariance requires regression residuals to be normally distributed to reduce interpretation errors. No difference from a normal distribution was found for any of the four regressions at the 5% probability level (supine [basal, Chapter 3]: W=0.98; standing [Chapter 3]: W=0.98,; walking: W=0.98; peak-exercise: W=0.98; $P>0.05$). Accordingly, all regressions could be compared statistically with one another.

The analysis of covariance revealed no difference between the mass exponents of the two exercise intensities tested within this experimental phase (walking: 0.85 [±0.05]; peak exercise: 0.80 [±0.07]; $P>0.05$; Figure 3.10). However, both exercise-intensity mass exponents were significantly greater than that applied to the basal dataset (log transformed: 0.55 [±0.05]; $P<0.05$), reflecting the increased activation of skeletal muscle tissue during those more active states. In contrast, the standing-intensity mass exponent only differed from that applied to the walking dataset (standing [log transformed]: 0.65 [±0.05]; $P<0.05$). Thus, it was considered that all non-basal, relative metabolic intensities would scale similarly. In review, a simple way to classify those differences in mass exponents was to separate resting (basal and standing) and exercising (walking and peak exercise) intensities so that two mass exponents could be used to describe aerobic power throughout the entire physiological range. Since the scaling exponent within mammals is intensity dependent (Darveau *et al.,* 2002), mass$^{0.80}$ was selected for use as the exercise-specific mass exponent as that intensity represents the maximum achievable rate of metabolism within the body, and, thus, the greatest possible scaling exponent achievable for the sample population. Although the exponent observed during the walking condition was numerically greater than mass$^{0.80}$, this was considered a possible artefact of the fixed-walking pace. Accordingly, the scaling relationship could be described by the untransformed exponents of mass$^{0.54}$ for resting states and mass$^{0.80}$ for exercising states. A summary of those regression equations can be found in Table 3.4.

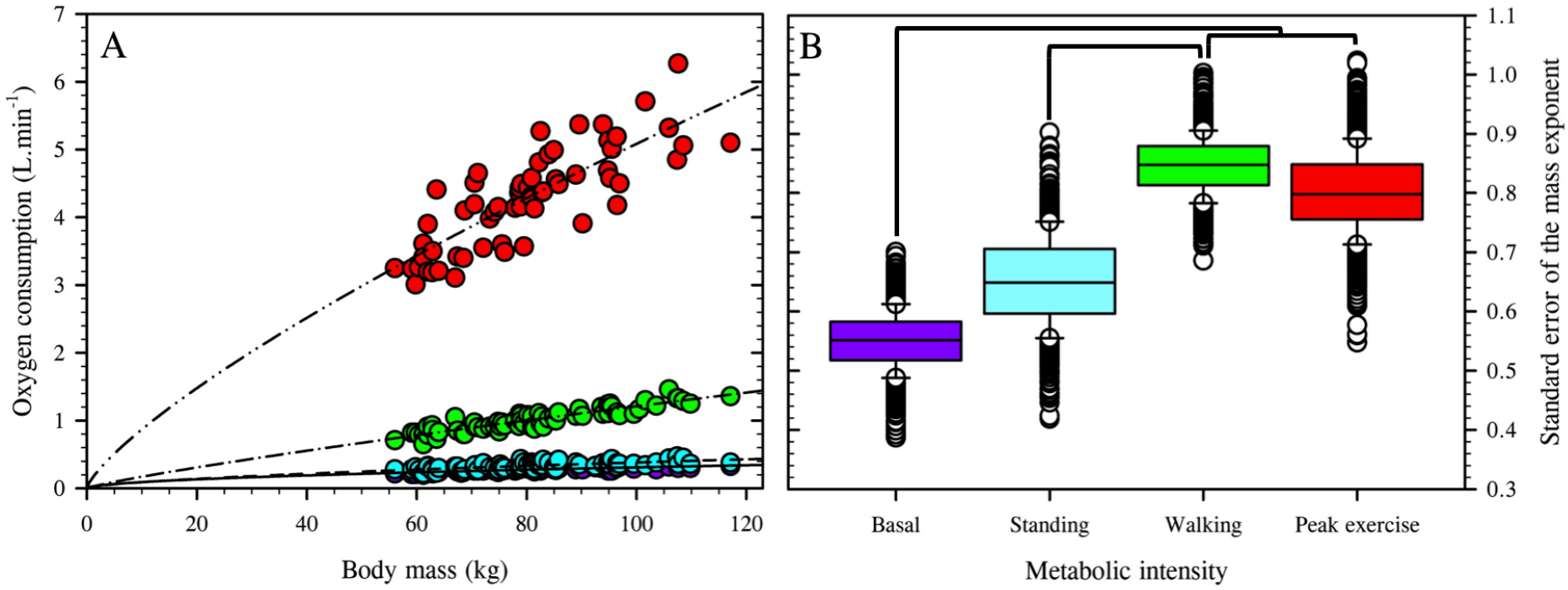

Figure 3.10: Figure 3.10A displays a scatter plot of the scaling relationships between oxygen consumption and body mass for four metabolic intensities (basal: $N=69$ [purple symbols, solid line]; standing: $N=67$ [blue symbols, dashed line]; walking: $N=68$ [green symbols, dash-dot line]; peak exercise: $N= 61$ [red symbols, dash-dot-dot line]). Figure 3.10B depicts the standard error of the mean for each of the four metabolic-intensity scaling exponents. Bootstrapping was used to generate those standard errors of the mean, whereby regressions were regenerated 1000 times using a re-sampling approach. Significant differences between exponent values are identified using brackets ($P<0.05$).

Table 3.4: A summary table of the raw ($y=ax^b$) and log-transformed (displayed as: $y= b \cdot x + a$) least-squares regression equations applied to the four metabolic states tested in Chapters 2 and 3. The equations below display the mean regression coefficients from the bootstrapped scaling relationships, with the mass exponents highlighted in bold. Data taken from Chapter 2 are for both resting states.

	Regression equation	
Metabolic intensity	Untransformed (allometric)	Log_{10}-transformed
Basal (supine)	$y=0.03 \cdot x^{\mathbf{0.54}}$	$y=\mathbf{0.55} \cdot x$ - 1.61
Standing (rest)	$y=0.02 \cdot x^{\mathbf{0.68}}$	$y=\mathbf{0.65} \cdot x$ - 1.72
Walking	$y=0.02 \cdot x^{\mathbf{0.87}}$	$y=\mathbf{0.85} \cdot x$ - 1.61
Peak exercise	$y=0.14 \cdot x^{\mathbf{0.80}}$	$y=\mathbf{0.80} \cdot x$ - 0.89

Notes: As logged mean values do not equal a log-transformed mean, a detransformed logarithmic regression will not identically equal its untransformed power regression (Jansson, 1985; Newman, 1993; Xiao *et al.,* 2011). Consequently, both untransformed and log-transformed regressions are presented to enable application to either data format.

3.3.3.1 Oxygen consumption during mass-supported walking

In the exploratory study, the independent effects of movement and carriage of the body's mass on the scaling relationship between oxygen consumption and body mass were investigated. By comparing scaling regressions across three sequentially increasing metabolic intensities (standing [Chapter 2], mass-supported walking, walking), it might be possible to isolate the impact of mass support, movement and load carriage on the scaling relationship. Thus, providing a more in-depth understanding of the mechanisms that affect the scaling relationship throughout a range of metabolic states. The three scaling relationships were compared using a repeated-measures approach, whereby data points were only included in the regressions if the corresponding participant completed all three trials ($N=15$). In this way, if any deviation in the shape of the scaling regression occurred as a result of the lower sample size, any within-sample trend across the exercise intensities could still be observed. As a non-linear scaling approach was deemed most suitable when applying a regression to the complete standing (Chapter 2: Section 2.3.3) and walking (Chapter 3: Section 3.3.2) datasets, the assumption was made that it would also apply to the regressions tested within the exploratory study. That assumption was tested in two ways: an evaluation of whether the exploratory regressions satisfied the assumptions of linear regression when log-transformed and a comparison with the full-sample regressions to determine whether the reduction in sample size modified the scaling shapes.

Evaluating whether non-linear regression was appropriate to describe the dataset

The distributions of the individual variables for the standing, body-mass supported walking and walking datasets were first evaluated. Frequency histograms of those log-transformed data displayed approximately normal distributions (Figure 3.11). Those observations were also supported statistically, with no difference from a normal distribution realised at the 5% probability level when calculated skewness and kurtosis *z*-scores were assessed, or when examined with the Shapiro-Wilk test (Table 3.5). As a result, data for those variables were all considered normally distributed when log-transformed (Shapiro and Wilk, 1965; Kim, 2013).

An assessment of the three exploratory scaling regressions (standing, mass-supported

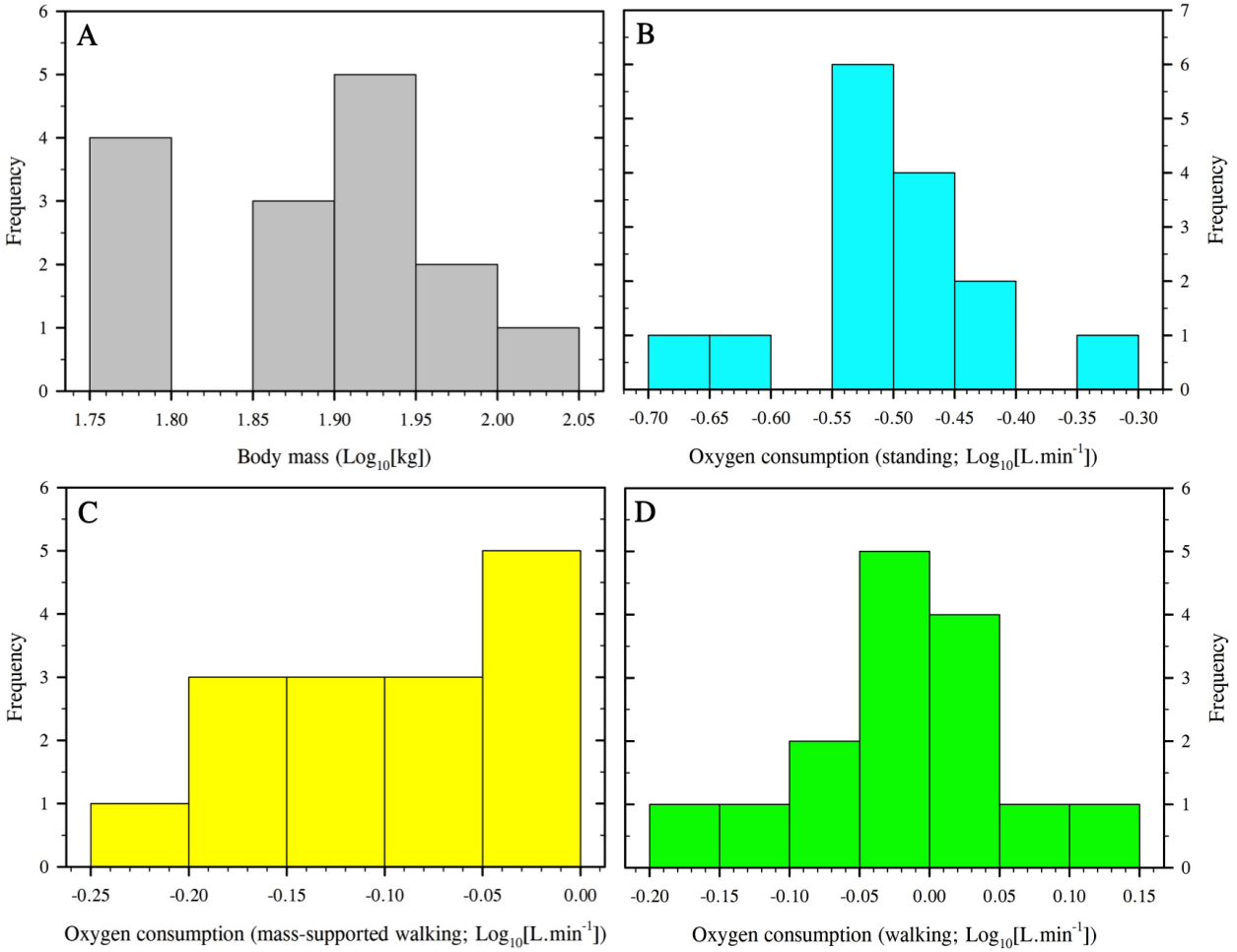

Figure 3.11: Frequency histogram distributions of the log-transformed regression variables used to generate the scaling relationships tested within the exploratory investigation ($N=15$). Data are displayed for body mass (Figure 3.11A) and oxygen consumption measured during the three metabolic intensities: standing (Figure 3.11B), mass-supported walking (Figure 3.11C) and walking (Figure 3.11D).

Table 3.5: Test statistics used to assess the assumptions of linear regression for data used in the exploratory investigation. Results are displayed for the variables and regression residuals of the three metabolic intensities tested: standing, mass-supported walking and walking ($N=15$). To permit comparisons between the exploratory and full-cohort results, data were taken from Table 3.3 (grey columns). All datasets conformed to a normal distribution when in the presented log-transformed units ($P>0.05$). Furthermore, model residuals showed no autocorrelation among variables ($P>0.05$).

	Regression variables				Regression residuals				
	Oxygen consumption (Log_{10}[L.min^{-1}])				Standing		Mass-supported walking	Walking	
	Standing	Mass-supported walking	Walking	Body mass (Log_{10}[kg])	$N=15$	$N=67$	$N=15$	$N=15$	$N=68$
Skewness statistic	-0.30	-0.23	-0.19	0.07	0.18	0.10	-0.64	-0.42	-0.03
Z-score	-0.52	-0.39	-0.33	0.11	-0.31	0.35	-1.10	-0.72	-0.01
Kurtosis statistic	0.00	-1.41	-0.36	-1.07	-1.23	-0.78	-0.37	-0.81	0.23
Z-score	0.00	-1.25	-0.32	-0.96	-1.09	-1.34	-0.33	-0.72	0.41
Shapiro-Wilk statistic	0.93	0.94	0.97	0.93	0.96	0.99	0.93	0.97	0.99
Durbin-Watson statistic	-	-	-	-	2.25	1.80	2.86	2.32	1.92

walking, walking) revealed approximate linearity when data were log-transformed (Figures 3.12A, 3.12B and 3.12C), with no evidence of heteroscedasticity or autocorrelation among the residuals (Figures 3.12D, 3.12E and 3.12F). The latter observation was further supported by the Durbin-Watson test statistics (Table 3.5; $P > 0.05$: Durbin and Watson 1950, 1951). Furthermore, the residuals from those three regressions displayed no evidence of a non-normal distribution (Table 3.5; $P > 0.05$: Shapiro and Wilk, 1965), indicating that, despite the low sample sizes, the three datasets were considered suitable for regression analysis.

Before investigating the scaling differences among those three metabolic states, within-intensity comparisons were made between the reduced- ($N = 15$) and full-sample scaling regressions (standing and walking) to determine whether reducing the sample size had any effect on each regression equation. Analysis of covariance was performed on those scaling regressions. No differences were realised between the full- and exploratory-cohort regression coefficients for either intensity (Table 3.5; $P > 0.05$). As a result, it was not necessary to perform further analyses for those data. Moreover, it meant that the reduced-cohort regressions provided valid representations of the full-cohort regressions, despite the lower sample sizes.

The effect of body support, movement and load carriage on the scaling regression
Analysis of covariance was performed on the three metabolic-intensity regressions: standing, mass-supported walking and unsupported walking. A significant difference was realised among all three regression intercepts (Figure 3.13; Table 3.6; $P < 0.05$), representing a step-wise increase in mean oxygen consumption with metabolic intensity (standing: 0.31 $L.min^{-1}$ [± 0.01]; mass-supported walking: 0.79 $L.min^{-1}$ [± 0.03]; walking: 0.96 $L.min^{-1}$ [± 0.04]; $P < 0.05$). Among the cardiac frequency data, significant differences were observed among all groups, except between the mass-supported walking and walking trials (standing: 75 $b.min^{-1}$ [± 3]; mass-supported walking: 92 $b.min^{-1}$ [± 4]; walking: 94 $b.min^{-1}$ [± 4]; $P < 0.05$). As such, the exploratory trial represented a metabolic state situated between that of standing and walking, as planned.

Despite those between-intensity differences in absolute oxygen consumption, no

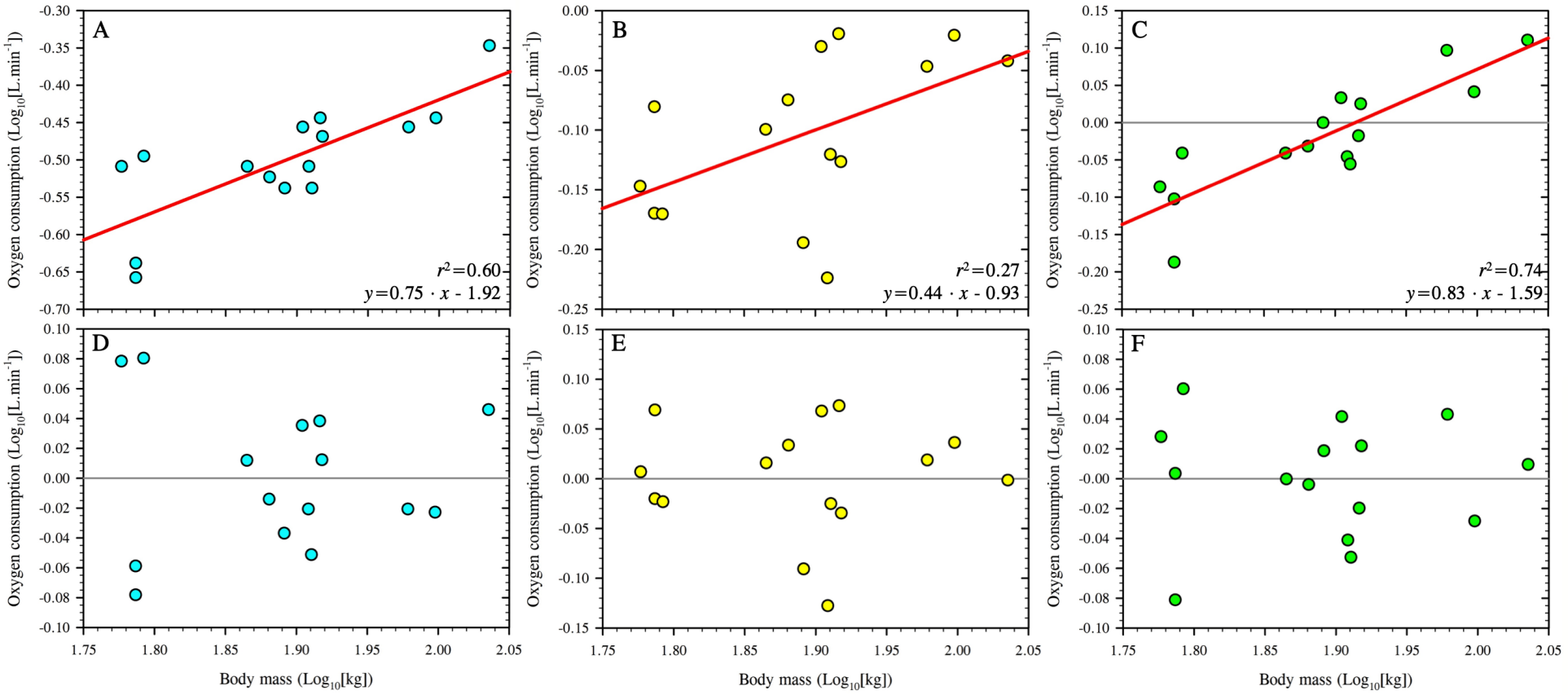

Figure 3.12: Scatter (Figures 3.12A, 3.12B and 3.12C) and residual (Figures 3.12D, 3.12E and 3.12F) plots of the relationship between oxygen consumption and body mass. Data are presented for the same sample (N=15; Figure 3.1) across three metabolic intensities, in log-transformed units: standing (Figures 3.12A and 3.12D), mass-supported walking (Figures 3.12B and 3.12E) and unsupported walking (Figures 3.12C and 3.12F). In this format, it was possible to assess the assumptions of linearity, homeoscedasticity and autocorrelation, and the regression fit using the coefficient of determination (r^2).

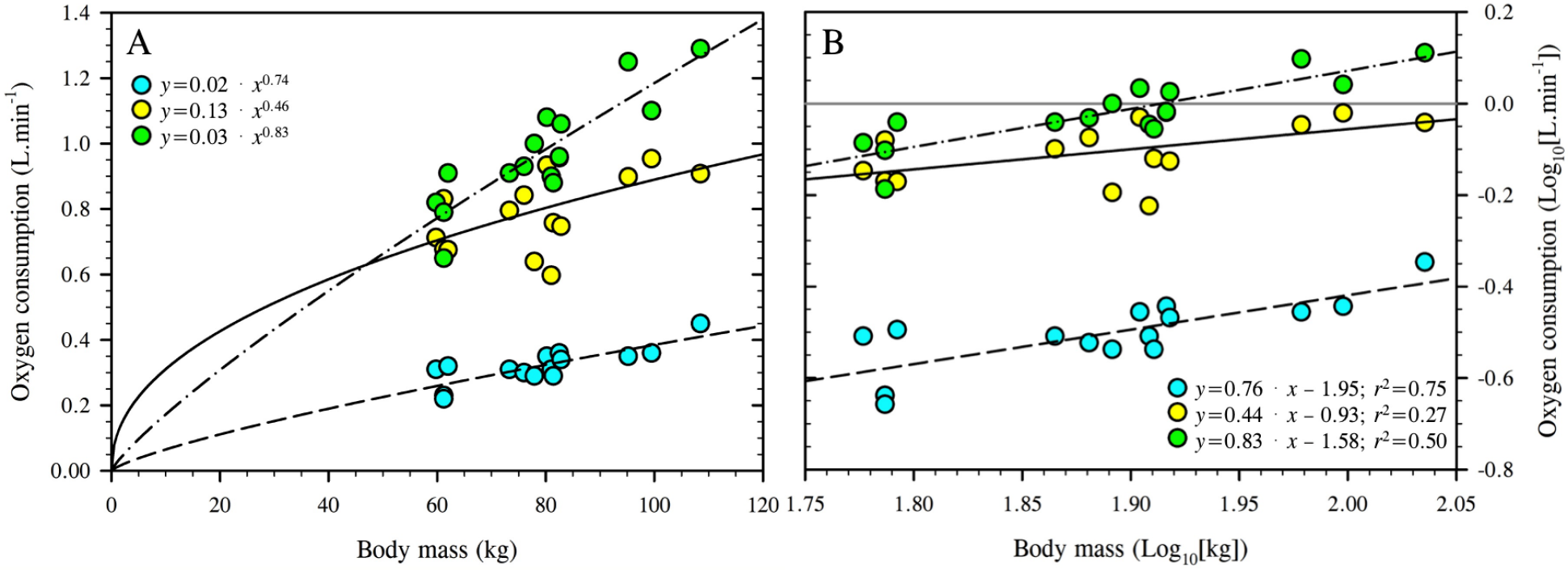

Figure 3.13: Scatter plots displaying the scaling relationships between oxygen consumption and body mass. Data are displayed for the 15 participants tested within the exploratory investigation, tested across three metabolic intensities: standing (blue, dashed line), mass-supported walking (yellow, solid line) and walking (green, dash-dot line). Figure 3.13A shows the untransformed relationships, while the log-transformed regressions are shown in Figure 3.13B to evaluate the model fit (coefficient of determination; r^2) and demonstrate differences in the regression equations.

Table 3.6: Bootstrapped regression coefficients for the log-transformed, non-linear regressions assessed in the exploratory ($N=15$; white columns) and full (standing: $N=67$; walking: $N=68$; grey columns) investigations. Data are presented as means with standard errors of the mean in parentheses. No differences were realised between the full- and exploratory-cohort regressions, within either intensity ($P>0.05$). However, across metabolic-intensity differences were found. Significant differences were realised between all model intercepts (a; $P<0.05$), however, the mass exponents (b) only differed between the two full-sample regressions ($P<0.05$).

	Reduced sample regressions		Full sample regressions	
Regression coefficient	*a*	*b*	*a*	*b*
Standing ($N=15$; $N=67$)	-1.93 (0.40)	0.76 (0.21)	-1.72 (0.15)	0.65 (0.08)
Mass-supported walking	-0.92 (0.26)	0.43 (0.14)	-	-
Walking	-1.59 (0.29)	0.83 (0.15)	-1.61 (0.09)	0.85 (0.05)

interaction effect was found between any of the three regression slopes (Table 3.6; $P > 0.05$). As such, the three mass exponents, while numerically different (standing: $mass^{0.75\ [\pm 0.21]}$; mass-supported walking: $mass^{0.44\ [\pm 0.14]}$; walking: $mass^{0.83\ [\pm 0.15]}$), were considered statistically equivalent. While the standing and walking regressions were not considered different from their full-sample versions, they did not demonstrate the between-group differences observed previously (Section 3.3.3), as the smaller sample sizes resulted in a greater standard error of the mean among the applied regression coefficients (Table 3.6), although a positive trend in mass exponents was still observed with intensity increase. Nevertheless, that relationship was not observed for the mass-supported trial. While the intensity had been established to reside between standing and walking conditions, the mass exponent observed was the lowest of all three metabolic intensities. Consequently, the expected increase in scaling exponent throughout the physiological range of aerobic power may not be purely intensity driven. It appears that the proportional relationship between metabolic intensity and the mass exponent is predominantly driven by the increase in oxygen consumption required to carry the body's mass. Indeed, movement of the body's mass at the same velocity, but with the mass load supported, demonstrated a flattening of the regression slope, indicating that the metabolic intensity was greater in the lighter mass ranges, as was the initial expectation for an absolute work rate.

3.4 DISCUSSION

During exercise, the most suitable method to describe the scaling of oxygen consumption against body mass in humans has remained a debated topic. The importance of understanding that relationship cannot be over-emphasised, for the applied regression determines how one both predicts and normalises oxygen consumption data. The present investigation is believed to be the first attempt to comprehensively address this question, by using an appropriately large sample that was diverse in body mass (Figure 3.1), but otherwise matched for morphological and physiological variables (Table 3.2; Figure 3.5; Figure 3.6). In this way, covariant influences on the observed regressions were minimised. Moreover, it is believed to be the first investigation in which the same participants were compared across the full range of metabolic intensities: basal (supine, fasted: Chapter 2), standing (rest: Chapter 2), walking (steady state, 4.8 $km.h^{-1}$) and peak exercise (running).

It was hypothesised that, during exercise, it would be more appropriate to describe the scaling relationship between oxygen consumption and body mass using a non-linear, simple allometric regression ($y = a \cdot x^b$: Hypothesis One), for which the mass exponent would increase stepwise with metabolic intensity (Hypotheses Two and Three). As anticipated, both walking and peak exercise intensities were best described using an allometric regression (Figure 3.10), supporting previously published work on both animals (Taylor *et al.,* 1970; 1974; Alexander 2005) and humans (Table 3.1). Furthermore, in accordance with the allometric cascade theory (Darveau *et al.*, 2002), a positive relationship between metabolic intensity and the mass exponent was observed (Figure 3.12). However, no difference in mass exponent was realised between the two exercise intensities (walking and peak exercise: Figure 3.12B). Thus, the scaling relationship was not modified whether exercising at a fixed-velocity (where the relative intensity may be variable across the sample) or at progressively increasing intensities. Incorporating those findings with the results from Chapter 2, it was concluded that, across the entire physiological range of metabolic intensity, the relationship between oxygen consumption and body mass could be described non-linearly by using either of two mass exponents: supine to standing (rest), $mass^{0.53}$; walking to peak exercise (exercise), $mass^{0.80}$. With $mass^{0.80}$ selected for this purpose as, physiologically, it represented the physiological maximum mass exponent for this sample population.

The scaling relationship was further evaluated using an exploratory investigation, conducted to isolate the separate effects of body mass support, movement (mass-supported walking) and unsupported walking. It was hypothesised that the mass exponent would increase stepwise when moving from standing to mass-supported walking and then to unsupported walking states (Hypothesis Four). However, that outcome was not observed, with no significant differences realised among the mass exponents ($N = 15$; $P > 0.05$). Moreover, the three mass exponents did not all increase with metabolic intensity (Figure 3.15), with the exponent for the mass-supported walking being the lowest value (standing: $mass^{0.74}$; mass-supported walking: $mass^{0.46}$; unsupported walking: $mass^{0.83}$; $P > 0.05$). As body mass was supported, the flattening (lower mass exponent) of that scaling curve is believed to represent the variable relative intensity of walking at the fixed velocity, where, to maintain the same pace,

smaller people were working harder than larger people. As a similar response was not observed during the unsupported walking, it was hypothesised that the mass carried represents the dominant variable when determining the shape of the scaling relationship during bipedal ambulation. Although that scaling outcome did not differ significantly from the other comparative states evaluated in the exploratory study, further testing into such mass-supported intensities may help expand our understanding of the scaling mechanics of bipedal locomotion, and aid in the analysis of oxygen consumption during rehabilitation walking states.

3.4.1 Determining the shape of the scaling regression during exercise

During exercising states, human oxygen consumption data have been scaled against body mass using both linear and non-linear regressions. Between both approaches, predicted values increase in difference as the mass range widens beyond the sampled range (Figure 3.10). Consequently, the accuracy of the two scaling methods was questioned. For that reason, the aim of this experimental phase was to identify which approach was more appropriate for describing such metabolic data, and whether the precise shape of that relationship changed with metabolic intensity.

The shape (linear or non-linear) of that scaling relationship was evaluated during walking and peak-exercise (running) states. Linear and non-linear regressions were applied to both datasets and the fit of each regression, and their appropriateness was assessed against the relevant statistical and biological assumptions (Figure 2.8; Section 3.3.2). For both metabolic intensities a non-linear, allometric approach demonstrated the superior fit (walking: $mass^{0.85}$; peak exercise: $mass^{0.80}$), and was the only approach to satisfy both the statistical and biological assumptions. Indeed, while the linear model satisfied the statistical assumptions for each state, a positive ordinate intercept, significantly greater than zero, was observed for both datasets (Figure 3.10). Since it is physically impossible to have a positive metabolic rate when body mass is zero, those positive intercepts invalidated the linear models, regardless of their simplicity and ubiquitous application, for they indicated the presence of a systematic error in each regression fit as the mass range was extended either side of the original data. As a result, non-linear (allometric) modelling was revealed to be more appropriate. Thus, Hypothesis One was accepted. Furthermore, when combined

with the results from Chapter 2 (basal and standing), it signified that oxygen consumption scaled non-linearly throughout the entire physiological range of metabolic intensity (Figure 3.12A).

Since the shape of the scaling relationship is dictated by the mass exponent, it was possible to evaluate the relationship between the steepness of the regression slope and metabolic intensity. In accordance with the allometric cascade theory (Darveau *et al.,* 2002), a stepwise increase in the exponent was observed with metabolic intensity (Figure 3.12). A similar response has been observed in both animals ($mass^{0.67}$: Sarrus and Rameaux, 1839 [basal]; $mass^{0.87}$: White and Seymour, 2003 [basal]; $mass^{0.87}$: Weibel and Hoppeler, 2005 [peak]; $mass^{0.87}$: White *et al.,* 2005 [peak]) and humans (Bergh *et al.,* 1991; Rogers *et al.,* 1995; Markovic *et al.,* 2007: Table 3.1). As previously expressed (Section 3.1), although those human studies displayed a step-wise increase in exponent value with metabolic rate, the samples used within those studies were not strictly controlled, unlike this project. Consequently, deviations in exponent values can be observed among those studies for any one state.

Howbeit, among the states tested within this project, the exponents did not all differ significantly. A significant difference was observed between the basal exponent and those of both exercise intensities (Figure 3.12B; $P < 0.05$), although only the walking exponent differed significantly from that of the standing state (Figure 3.12B; $P < 0.05$). Therefore, as there was no difference between the standing and peak-exercise regressions, Hypothesis Two was only partially accepted. However, it is possible that a biological difference still existed, due to the numerical differences in exponents and the noticeable change in physiological intensity. Therefore, it was considered important to separate the standing condition from the other exercising states and group it with the basal state.

The relationship between changes in the scaling exponent with variations in metabolic intensity is a likely consequence of changes that influence whole-body oxygen consumption. Oxygen consumption changes when the metabolic rate of a set mass of tissues changes, and when the volume of metabolically active tissues is varied. Skeletal muscle has the greatest metabolic reserve (peak less basal), ranging from

$\sim$0.26 mL.100 g^{-1}.min^{-1} (Andres *et al.,* 1956) to $\sim$385 mL.100 g^{-1}.min^{-1} (Richardson *et al.,* 1993), and thus the greatest capacity to influence whole-body oxygen consumption. Therefore, during non-basal states, both oxygen consumption and the scaling exponent are primarily influenced by the metabolic rate of the skeletal muscle. If skeletal muscle is considered, there is an increase in total muscle mass with size, yet percentage of total body mass actually decreases (Gallagher *et al.,* 1998; Müller *et al.,* 2011). At the same time, the percentage of bone (with a relatively low mass-specific metabolic rate) increases, presumably to support a heaver body mass (Prange *et al.,* 1979). As a result, non-linear relationships between skeletal muscle and bone masses and total body mass exist. This means that even if the entire skeletal muscle mass was working at its full metabolic capacity, the scaling relationship between oxygen consumption and body mass must remain non-linear, and a non-linear relationship should also hold for all other metabolic intensities, becoming less steep the closer one approaches to a basal state. Consequently, the relationships identified in this study (Figure 3.12) corresponded with these non-linear, theoretical constraints.

Notwithstanding the relationship between metabolic intensity and mass exponent, no significant difference was found between the two exercise-intensity mass exponents (Figure 3.12B; $P > 0.05$), thus Hypothesis Three was only partially accepted. In fact, the mass exponent observed for the walking trial was numerically higher than that of the peak-exercise state (walking: $mass^{0.85}$; peak exercise: $mass^{0.80}$). That deviation was not explained by the fixed walking velocity, which was expected to produce a non-constant, relative increase exercise intensity. If this had occurred, smaller individuals would have experienced a greater relative metabolic increase, flattening the regression slope and lowering the mass exponent. Therefore, it appears that some other mechanism, instead of metabolic intensity, exerted a greater influence on the scaling relationship.

That question was answered within the exploratory investigation (Section 3.3.3.1), the aim of which was to isolate the influence of body-mass support, movement and unsupported locomotion on the scaling relationship. The mass-supported intensity represented a metabolic state partway between standing and walking (Section 3.3.3.1), where participants were still able to complete a normal gait cycle, but were

just making contact with the treadmill surface. In this way, the scaling regression for that intensity could be interpreted as the oxygen uptake required to move the body without supporting the body mass. As such, it was expected that the mass exponent would fall between the standing and walking values. However, the value was both similar and lower than the standing condition (standing: $mass^{0.74}$; mass-supported walking: $mass^{0.46}$; $N=15$; $P>0.05$). Thus, during mass-supported walking the absolute cost of movement was more uniform across the body-mass range than when the body mass was not being supported, highlighting the previously-expected variances in relative intensity when walking at a fixed velocity. As the only difference between the mass-supported and unsupported walking trials was the body mass supported, then the different scaling response observed during the walking trial is likely to be the result of carrying a greater body mass.

That response was not dissimilar to the observed relationship for the cost of walking between unloaded and loaded states, where the nett metabolic rate increases proportionately with loading during moderate walking speeds, up to a load proportional to 30% of the body mass (Griffin *et al.,* 2003). During load carriage conditions, it is theorised that the oxygen cost to swing the leg remains constant, but oxygen uptake increases during the stance phases proportionally with the total mass being supported (Griffin *et al.,* 2003). Thus, it is likely that the primary variable associated with the scaling relationship during bipedal exercise is mass carriage and, as a result, fixed and variable intensity states can be treated similarly.

Although the mass-supported scaling relationship should be considered a preliminary finding, due to the small sample size, a more comprehensive investigation may provide useful information regarding rehabilitation walking and further our understanding of the scaling mechanisms during walking. From the experiences gained during this exploratory phase, and discussed within Chapter 2, it would be necessary to obtain an alternative method for suspending participants. The current technique proved to be uncomfortable for most participants, even with additional padding, inflating physiological variables within the standing stages, and potentially creating noise during the mass-supported walk.

It is, however, likely to provide only limited useful information when considering the scaling of other mass-supported exercises such as cycling or rowing. During such activities body mass is supported, but the participants are able to apply a far greater force than was possible during the mass-supported trial. Although body-size scaling has been performed during such mass-supported exercises, the research found scaled performance outcomes, such as time or power (Secher, 1983; Nevill *et al.,* 1992; Vanderburgh *et al.,* 1996; Vanderburgh *et al.,* 1998; Markovic and Jaric, 2004), rather than oxygen consumption. For such scaling purposes, either the exponent $mass^{0.67}$ was used to scale results for geometric changes in power (Secher, 1983; Nevill *et al.,* 1992; Jaric *et al.,* 2005; Vanderburgh *et al.,* 1998; Markovic and Jaric, 2004), or standing height was used (Vanderburgh *et al.,* 1996). As a result, it was not possible to directly compare the metabolic scaling of mass-supported walking with other exercise modes where body mass is supported.

Nevertheless, during bipedal exercise, unsupported mass is the dominant variable influencing the scaling relationship, regardless of metabolic intensity. From a physiological perspective, it appears that the step between standing and walking results in a greater change to the mass exponent than between walking and peak exercise (running). Therefore, once the body is in motion, the increase in skeletal muscle activation, while increasing absolute oxygen consumption, does not appear to further modify the scaling relationship. As the absolute oxygen consumption associated with walking at 4.8 $km.h^{-1}$ was only 24% of the peak oxygen consumption, it was a relatively low metabolic intensity. Thus, with no difference between the walking and peak exercise scaling exponents, it is reasonable to assume that data for all (bipedal) exercise, regardless of intensity, can be scaled using the same body-mass exponent. The peak-exercise exponent ($mass^{0.80}$) was chosen for this purpose, as it reflected the physiological maximum exponent achievable within adult humans (allometric cascade theory: Darveau *et al.,* 2002). Moreover, unlike the fixed-velocity walking, it was less likely to be influenced by other covariant factors, such as a non-constant relative intensity across the mass range. In addition, as a similar response was observed during the two resting states evaluated in Chapter 2, the entire physiological range can be divided into two categories for scaling purposes, which can be evaluated using either of two mass exponents: basal to standing (rest): $mass^{0.57}$;

walking to peak exercise (exercise) mass$^{0.80}$.

3.4.2 The pitfalls of scaling to lean-body mass

In an attempt to overcome the limitations associated with scaling to whole-body mass, when testing a heterogeneous sample, some researchers advocate scaling peak oxygen consumption against lean body mass (regularly interpreted as reflecting skeletal muscle mass; Toth *et al.,* 1993; Goran *et al.,* 2000; Lolli *et al.,* 2017). That approach is often favoured due to the strong relationship between skeletal muscle tissue and peak oxygen consumption (Hochachka, 1994; Hochachka and Somero, 2002), the linear relationship between mitochondrial volume and capillary erythrocyte volumes (Weibel *et al.,* 2004; Weibel and Hoppeler, 2005) and the low relative metabolic activity of adipose tissue during exercise (Elia, 1992; Pourhassan *et al.,* 2015). The method is typically applied when using ratiometric modelling. While it appears to reduce gender differences in peak oxygen consumption (Toth *et al.,* 1993; Vanderburgh and Katch, 1996; Neder *et al.,* 2001) that approach is dependent upon the verification of four assumptions. Firstly, the total skeletal muscle mass is recruited. Secondly, all muscles have been activated to their peak rate of oxygen consumption. Thirdly, no other (non-muscle) tissues are contributing to the whole-body oxygen consumption. Finally, it is assumed that the measurement technique used to quantify the lean body mass is free from error. There is ample justification to challenge the absolute validity of each of these assumptions.

This lean-mass normalisation method is used because skeletal muscle mass dictates ~90% of whole-body oxygen uptake during peak exercise (Hochachka, 1994; Hochachka and Somero, 2002). However, to selectively scale to that measure, the assumption is made that the entire skeletal muscle mass is contributing to oxygen consumption at a uniform metabolic rate. This assumption can be challenged in three ways. Firstly, during exercise, blood flow is shunted from the non-active tissues, increasing blood flow, and thus oxygen delivery, to the working muscle sites (Saltin and Strange, 1992). Therefore, some muscles will always be less active than others. Consequently, exercise mode will dictate muscle activation. In this way, oxygen consumption cannot be accurately normalised to lean body mass across exercise modes, forming the second challenge to this assumption. For instance, the greatest

peak oxygen consumption values are obtained on running and rowing ergometers (Shephard *et al.,* 1968; Yoshiga and Higuchi, 2003), whereas a 5-10% decrease is observed during cycle ergometry (Faulkner *et al.,* 1971; Miyamura and Honda, 1972; Miles *et al.,* 1980; Shephard *et al.,* 1968) and a further 15% reduction during arm cycle ergometry (Secher *et al.,* 1974) due to the reductions in recruited muscle mass. Finally, the suitability of that assumption during non-peak intensities must be considered. During submaximal states, as less power is required, the activated number of muscle fibres within the exercising muscles decreases (Miyashita *et al.,* 1971). Moreover, that value will be dependent upon body size, strength and aerobic fitness, depending upon the activity. As a result, while the total skeletal muscle mass is never simultaneously recruited, inducing some error into calculations, both a change in exercise mode or intensity will further modify that value.

The second assumption when normalising to lean body mass is that the active skeletal muscle mass is working at peak metabolic rate. While a larger activated muscle volume typically relates to a greater absolute metabolic rate, the mass-specific metabolic rate of a muscle will decrease as the demand for blood flow increases in other working muscles (Secher *et al.,* 1977; Saltin and Strange, 1992). Indeed, local muscle-specific blood flow and oxygen consumption can increase far greater than the rates observed during peak exercise (Andersen and Saltin 1985; Richardson *et al.* 1995; Rowell *et al.* 1986; Glazier, 2015). Such a paradox means that it is impossible for the entire skeletal-muscle mass to be sufficiently perfused to support work at localised peak metabolic rates during exercise. Furthermore, any decrease in metabolic intensity will reduce the volume and mass-specific metabolic rate of the skeletal-muscle tissues, thereby invalidating the association between oxygen consumption and lean body mass.

A further assumption when scaling to lean rather than whole body mass is that no other tissues are contributing towards oxygen consumption, or that their contribution is negligible. However, as the living body is never in a state where cellular metabolism ceases in the residual tissues (Pourhassan *et al.,* 2015), regardless of metabolic intensity, oxygen is still consumed by the other organs (*i.e.* peak exercise: Saltin and Strange, 1992). Moreover, the relative contribution to metabolism from

those organs will increase inversely with metabolic intensity, as muscle activation decreases. Consequently, to scale or normalise using lean body mass during resting states, such as basal, where the metabolic rate of four organs determines ~80% of energy expenditure (brain, liver, kidneys and heart: Holliday *et al.,* 1967; Elia, 1992; Müller *et al.,* 2013) and only ~20% from the skeletal muscle, would be imprudent. Therefore, while it may be possible to disregard the error associated with scaling against lean body mass during peak exercise, providing that the sample is proportionally similar (homogeneous), the variance of that error would increase if testing a heterogeneous sample, or during non-peak metabolic intensities.

The final assumption is that the measurement technique used to quantify lean body mass is free from error. As direct measurements taken from cadaver dissections are not appropriate for such comparative purposes, most measurement techniques rely on estimations of lean body mass, and thereby incur some level of error. The most readily available methods, such as skin folds (Durnin and Womersley, 1974; Jackson and Pollock, 1978) and hydrostatic weighing (Wellham and Behnke, 1942), use two-compartment models, whereby body fat is indirectly measured, and from that value a non-fat measure can be calculated. However, this non-fat measure includes all remaining tissues, not just skeletal muscle mass, and calculations assume that the proportion of those tissues are fixed (Brožek *et al.,* 1963). As such, two-compartment model calculations of lean body mass are based on proportionality assumptions and indirect estimations that are not free from error. To obtain skeletal muscle mass accurately a multi-compartment test is required (Lukaski, 1987; Roubenoff and Kehayias, 1991; Brodie *et al.,* 1998; Wells and Fewell, 2006).

Dual-energy X-ray absorptiometry, is becoming a popular body-composition measurement technique. Initially developed to accurately measure bone mineral density (Mazess *et al.,* 1981), it provides a three-compartment model: bone, bone-free lean and fat. However, despite it's popularity, it has some limitations when measuring lean body mass. Firstly, it assumes total weight and the composition of tissues based on pixel assessments of photon absorption, by assuming a uniform and fixed hydration of lean tissues. As such, the size of the pixels will alter the accuracy of the measurement, for instance, small amounts of bone may be interpreted as very

lean soft tissue. Secondly, soft-tissue readings are difficult in areas such as the thorax, arm and head, where there is a large proportion of bones. Thirdly, measurements are sensitive to anteriorposterior thicknesses (Johnson and Dawson-Hughes, 1991; Buhl *et al.,* 1991) and therefore error will vary with participant adiposity. Finally, it is unknown whether there is a discrepancy in readings for between-manufacturer equipment (Yasumura *et al.,* 1993; Pierson *et al.,* 1993), questioning between-equipment comparisons. As such, a four-compartment model is the only way to accurately measure lean (skeletal muscle) body mass at this time.

Magnetic resonance imagery provides a safe and accurate measurement of compartments within the body, including the trunk (Wells and Fewtrell, 2006), therefore a precise method to quantify skeletal muscle mass. However, the method is time consuming and requires skilled personnel to interpret the results. Moreover, the equipment is expensive and not readily available. Furthermore, most machines are not able to accommodate grossly obese individuals (Duren *et al.,* 2008). Consequently, while magnetic resonance imagery provides an accurate measurement of lean body mass, it is the least accessible. Therefore, most measurements of lean body mass will typically incur some error, which must be addressed during analyses and before any results are interpreted. Therefore, it does not appear possible to satisfy the four assumptions made when scaling oxygen consumption to lean body mass. Furthermore, it is not practical to adopt such an approach. Since, during ambulatory states the entire body mass must still be carried, despite the majority of work being performed by the lower-limb skeletal muscles. As evidenced within the exploratory investigation (Section 3.3.3.1), where the mass carried was supported, and in load-carriage states, where an external mass is placed on the body (Goldman and Iampietro, 1962; Taylor *et al.,* 2011, 2012), the mass carried directly impacts whole-body oxygen consumption. Indeed, if utilising the same principles, the mass of non-working portions of the body (like the head and hands) should also be removed. Therefore, by selecting only the skeletal muscle, information pertinent to the relationship between body size and oxygen consumption is overlooked.

Due to the imprecision of these assumptions, it is concluded that scaling to lean body mass, in preference to total mass, is lacking in justification. Indeed, it may actually

introduce more limitations and assumptions, particularly if a ratiometric approach is adopted. Thus, the question is raised whether scaling against lean-body mass is a practical method to pursue for most investigations, particularly when it is demonstrated within the present investigation that scaling against whole-body mass is both a practical and effective method. While some limitations exist when scaling against whole-body mass when using heterogeneous samples (Section 2.2.1), as demonstrated within this experiment, it is a suitable method for scaling and normalising oxygen consumption within a controlled sample. Nonetheless, until the covariant relationship between adipose tissue and the scaling relationship between oxygen consumption and whole-body mass is defined, scaling lean-body mass using a non-linear regression may help to reduce some of the error associated with scaling a sample with widely heterogeneous measures of subcutaneous adiposity (Lolli *et al.,* 2017).

3.5 CONCLUSION

To overcome the mass-dependent nature of oxygen consumption and permit data comparisons among individuals of different body sizes, it is important to understand how oxygen consumption scales with body size. Such comparisons are regularly performed using body mass as the morphological scaling variable, using either linear or non-linear modelling. In Chapter 2, the superiority of using a non-linear regression to describe that relationship was demonstrated during resting states, but it remained unclear whether or not a similar relationship would exist during exercise, and if the shape of that relationship would differ with a change in metabolic intensity. Although this is not a new topic, the few papers where these questions had been addressed (Table 3.1) had not used suitably large sample sizes that ranged widely in body mass but were otherwise matched for physiological and morphological variables that could influence oxygen consumption. To the author's best knowledge, this is the first experiment to satisfy those scaling requirements using a human population.

Non-linear scaling was found to remain the more appropriate method for describing the relationship between oxygen consumption and body mass during both walking and peak exercise intensities. Although absolute oxygen consumption increased significantly between the two states, the mass exponents were statistically equivalent.

This was an unexpected result, for it was anticipated that the walking state would scale by a mass exponent between that of standing and peak exercise. It appears as though the scaling relationship during bipedal ambulation is primarily influenced by the size of the supported mass, for when participants walked at the same velocity, but body mass was partially supported, the mass exponent was reduced, flattening the regression curve. It is believed that the observed increases in the mass exponent (when supporting one's own body mass), relative to metabolic activity, were driven by a change in the mass of the skeletal muscle activated, in turn, modifying the mass-specific metabolic rate of those tissues. This interpretation is based on the significant difference observed in mass exponents between the standing and walking states, as opposed to the walking and peak exercise (running) intensities. This has future applications, for it means that all bipedal states, where the entire body mass is carried, are likely to scale by a similar mass exponent. Consequently, it was concluded that, across the entire physiological range, oxygen consumption will scale by either of two mass exponents: $mass^{0.54}$ for resting states and $mass^{0.80}$ for exercising states.

3.6 REFERENCES

Abe, D., Muraki, S., and Yasukouchi, A. (2008). Ergonomic effects of load carriage on the upper and lower back on metabolic energy cost of walking. *Applied Ergonomics*. 39(3):392-398.

Alexander, R.M. (2005). Models and the scaling of energy costs for locomotion. *Journal of Experimental Biology*. 208(9):1645-1652.

Andersen, P., and Saltin, B. (1985). Maximal perfusion of skeletal muscle in man. *The Journal of Physiology*. 366(1):233-249.

Andres, R., Cader, G., and Zierler, K.L. (1956). The quantitatively minor role of carbohydrate in oxidative metabolism by skeletal muscle in intact man in the basal state. Measurements of oxygen and glucose uptake and carbon dioxide and lactate production in the forearm. *The Journal of Clinical Investigation*. 35(6):671-682.

Åstrand, P.O., and Rodahl, K. (1986). *Textbook of work physiology: physiological bases of exercise*. McGraw Hill, New York.

Batterham, A.M., and Jackson, A.S. (2003). Validity of the allometric cascade model at submaximal and maximal metabolic rates in exercising men. *Respiratory Physiology and Neurobiology*. 135(1):103-106.

Batterham, A.M., Vanderburgh, P.M., Mahar, M.T., and Jackson, A.S. (1999). Modeling the influence of body size on $\dot{V}O_2$ peak: effects of model choice and body composition. *Journal of Applied Physiology*. 87(4):1317-1325.

Bergh, U., Sjödin, B., Forsberg, A., and Svedenhag, J. (1991). The relationship between body mass and oxygen uptake during running in humans. *Medicine and Science in Sports and Exercise*. 23(2):205-211.

Brodie, D., Moscrip, V., and Hutcheon, R. (1998). Body composition measurement: a review of hydrodensitometry, anthropometry, and impedance methods. *Nutrition*. 14(3):296-310.

Brožek, J., and Henschel, A. (1963). *Techniques for measuring body composition*. National Academy of Sciences-National Research Council, Washington, DC.

Buhl, K., Heymsfield, S.B., Russell-Aulet, M., Wang, J., Pierson, R.N., and Lichtrnan, S. (1991). Effect of tissue thickness on bone density and bone mineral by dual energy x-ray absorptiometry. *The Federation of American Societies for Experimental Biology Journal*. 5(5):A924.

Cavagna, G.A., and Kaneko, M. (1977). Mechanical work and efficiency in level walking and running. *The Journal of Physiology*. 268(2):467-481.

Cook, R.D. (1977). Detection of influential observation in linear regression. *Technometrics*. 19(1):15-18.

Cook, R.D., and Weisberg, S. (1982). *Residuals and influence in regression*. Chapman and Hall, New York.

Crouter, S.E., Antczak, A., Hudak, J.R., DellaValle, D.M., and Haas, J.D. (2006). Accuracy and reliability of the ParvoMedics TrueOne 2400 and MedGraphics VO2000 metabolic systems. *European Journal of Applied Physiology*. 98(2):139-151.

Darveau, C.A., Suarez, R.K., Andrews, R.D., and Hochachka, P.W. (2002). Allometric cascade as a unifying principle of body mass effects on metabolism. *Nature*. 417(6885):166-170.

Durbin, J., and Watson, G.S. (1950). Testing for serial correlation in least squares regression: I. *Biometrika*. 37(3/4):409-428.

Durbin, J., and Watson, G.S. (1951). Testing for serial correlation in least squares regression. II. *Biometrika*. 38(1/2):159-177.

Duren, D.L., Sherwood, R.J., Czerwinski, S.A., Lee, M., Choh, A.C., Siervogel, R.M., and Chumlea, W.C. (2008). Body composition methods: comparisons and interpretation. *Journal of Diabetes Science and Technology*. 2(6):1139-1146.

Durnin, J.V.G.A., and Womersley, J. (1974). Body fat assessed from total body density and its estimation from skinfold thickness: measurements on 481 men and women aged from 16 to 72 years. *British Journal of Nutrition*. 32(1):77-97.

Efron, B. (1979). Computers and the theory of statistics: thinking the unthinkable. *SIAM review*. 21(4):460-480.

Elia, M. (1992). Organ and tissue contribution to metabolic rate. In: Kinney, J.H., and Tucker, H.N. (Ed.). *Energy metabolism: tissue determinants and cellular corollaries*. Raven Press, New York. Pp.61-80.

Faulkner, J.A., Roberts, D.E., Elk, R.L., and Conway, J. (1971). Cardiovascular responses to submaximum and maximum effort cycling and running. *Journal of Applied Physiology*. 30(4):457-461.

Fell, D., and Cornish-Bowden, A. (1997). *Understanding the Control of Metabolism*. Volume 2. Portland Press, London.

Fox, J. (1997). *Applied regression analysis, linear models, and related methods*. Sage, London.

Fox, J., and Weisberg, S. (2017). *An R Companion to Applied Regression.* Sage, London.

Gallagher, D., Belmonte, D., Deurenberg, P., Wang, Z., Krasnow, N., Pi-Sunyer, F.X., and Heymsfield, S.B. (1998). Organ-tissue mass measurement allows modeling of REE and metabolically active tissue mass. *American Journal of Physiology-Endocrinology And Metabolism*. 275(2):E249-E258.

Garrett, J.W., and Kennedy, K.W. (1971). *A collation of anthropometry*. Volume 1. Aerospace Medical Research Laboratory, Aerospace Medical Division.

Glazier, D.S. (2015). Is metabolic rate a universal 'pacemaker' for biological processes? *Biological Reviews*. 90(2):377-407.

Goldman, R.F., and Iampietro, P.F. (1962). Energy cost of load carriage. *Journal of Applied Physiology*. 17(4):675-676.

Goran, M., Fields, D.A., Hunter, G.R., Herd, S.L., and Weinsier, R.L. (2000). Total body fat does not influence maximal aerobic capacity. *International Journal of Obesity*. 24(7):841.

Griffin, T.M., Roberts, T.J., and Kram, R. (2003). Metabolic cost of generating muscular force in human walking: insights from load-carrying and speed experiments. *Journal of Applied Physiology*. 95(1):172-183.

Heil, D.P. (1997). Body mass scaling of peak oxygen uptake in 20-to 79-yr-old adults. *Medicine and Science in Sports and Exercise*. 29(12):1602-1608.

Hochachka, P.W. (1994). *Muscles as molecular and metabolic machines*. CRC Press, Boca Raton.

Hochachka, P.W., Darveau, C.A., Andrews, R.D., and Suarez, R.K. (2003). Allometric cascade: a model for resolving body mass effects on metabolism. *Comparative Biochemistry and Physiology Part A: Molecular and Integrative Physiology*. 134(4):675-691.

Hochachka, P.W., and Somero, G.N. (2002). *Biochemical Adaptation: Mechanism and Process in Physiological Evolution.* Oxford University Press, New York.

Holliday, M.A. (1986). Body composition and energy needs during growth. In: Falkner, F., and Tanner, J.M. (Ed.). *Postnatal Growth Neurobiology*. Springer, Boston, MA. Pp. 101-117.

Holliday, M.A., Potter, D., Jarrah, A., and Bearg, S. (1967). The relation of metabolic rate to body weight and organ size. *Pediatric Research*. 1(3):185.

Jackson, A.S., and Pollock, M.L. (1978). Generalized equations for predicting body density of men. *British Journal of Nutrition*. 40(3):497-504.

Jamnik, V., Gumienak, R., and Gledhill, N. (2013). Developing legally defensible physiological employment standards for prominent physically demanding public safety occupations: a Canadian perspective. *European Journal of Applied Physiology*. 113(10):2447-2457.

Jansson, M. (1985). A comparison of detransformed logarithmic regressions and power function regressions. *Geografiska Annaler: Series A, Physical Geography*. 67(1-2):61-70.

Jaric, S., Mirkov, D., and Markovic, G. (2005). Normalizing physical performance tests for body size: a proposal for standardization. *The Journal of Strength and Conditioning Research*. 19(2):467-474.

Jensen, K., Johansen, L., and Secher, N.H. (2001). Influence of body mass on maximal oxygen uptake: effect of sample size. *European Journal of Applied Physiology*. 84(3):201-205.

Johnson, J., and Dawson-Hughes, B. (1991). Precision and stability of dual-energy X-ray absorptiometry measurements. *Calcified Tissue International*. 49(3):174-178.

Kim, H.Y. (2013). Statistical notes for clinical researchers: assessing normal distribution (2) using skewness and kurtosis. *Restorative Dentistry and Endodontics*. 38(1):52-54.

Landers, G.J., Ong, K.B., Ackland, T.R., Blanksby, B.A., Main, L.C., and Smith, D. (2013). Kinanthropometric differences between 1997 World championship junior elite and 2011 national junior elite triathletes. *Journal of Science and Medicine in Sport*. 16(5):444-449.

Lolli, L., Batterham, A.M., Weston, K.L., and Atkinson, G. (2017). Size exponents for scaling maximal oxygen uptake in over 6500 humans: a systematic review and meta-analysis. *Sports Medicine*. 47(7):1405-1419.

Ludlow, L.W., and Weyand, P.G. (2017). Walking economy is predictably determined by speed, grade, and gravitational load. *Journal of Applied Physiology*. 123(5):1288-1302.

Lukaski, H.C. (1987). Methods for the assessment of human body composition: traditional and new. *The American Journal of Clinical Nutrition*. 46(4):537-556.

Markovic, G., and Jaric, S. (2004). Movement performance and body size: the relationship for different groups of tests. *European Journal of Applied Physiology*. 92(1-2):139-149.

Markovic, G., Vucetic, V., and Nevill, A.M. (2007). Scaling behaviour of in athletes and untrained individuals. *Annals of Human Biology*. 34(3):315-328.

Mazess, R.B., Peppler, W.W., Harrison, J.E., and McNeill, K.G. (1981). Total body bone mineral and lean body mass by dual-photon absorptiometry. *Calcified Tissue International*. 33(1):365-368.

Miles, D.S., Critz, J.B., and Knowlton, R.G. (1980). Cardiovascular, metabolic, and ventilatory responses of women to equivalent cycle ergometer and treadmill exercise. *Medicine and Science in Sports and Exercise*. 12(1):14-19.

Miyamura, M., and Honda, Y. (1972). Oxygen intake and cardiac output during treadmill and bicycle exercise. *Journal of Applied Physiology*. 32(2):185-188.

Miyashita, M., Matsui, H., and Miura, M. (1971). The relation between electrical activity in muscle and speed of walking and running. In: Vredenbregt, J., and Wartenweiler, J. (Ed.). *Biomechanics II. 2nd International Seminar on Biomechanics, Eindhoven, 1969. Medicine and Sport Science*. 6:192-196.

Müller, M.J., Langemann, D., Gehrke, I., Later, W., Heller, M., Glüer, C.C., Heymsfield, S.B., and Bosy-Westphal, A. (2011). Effect of constitution on mass of individual organs and their association with metabolic rate in humans—a detailed view on allometric scaling. *PloS one*. 6(7):e22732.

Müller, M.J., Wang, Z., Heymsfield, S.B., Schautz, B., and Bosy-Westphal, A. (2013). Advances in the understanding of specific metabolic rates of major organs and tissues in humans. *Current Opinion in Clinical Nutrition and Metabolic Care*. 16(5):501-508.

Neder, J.A., Nery, L.E., Peres, C., and Whipp, B.J. (2001). Reference values for dynamic responses to incremental cycle ergometry in males and females aged 20 to 80. *American Journal of Respiratory and Critical Care Medicine*. 164(8):1481-1486.

Nevill, A.M., Brown, D., Godfrey, R., Johnson, P.J., Romer, L., Stewart, A.D., and Winter, E.M. (2003). Modeling maximum oxygen uptake of elite endurance athletes. *Medicine and Science in Sports and Exercise*. 35(3):488-494.

Nevill, A.M., and Holder, R.L. (1994). Modelling maximum oxygen uptake-a case-study in non-linear regression model formulation and comparison. *Applied Statistics*. 653-666.

Nevill, A.M., Markovic, G., Vucetic, V., and Holder, R. (2004). Can greater muscularity in larger individuals resolve the 3/4 power-law controversy when modelling maximum oxygen uptake? *Annals of Human Biology*. 31(4):436-445.

Nevill, A.M., Ramsbottom, R., and Williams, C. (1992). Scaling physiological measurements for individuals of different body size. *European Journal of Applied Physiology and Occupational Physiology*. 65(2):110-117.

Newman, M.C. (1993). Regression analysis of log transformed data: Statistical bias and its correction. *Environmental Toxicology and Chemistry*. 12(6):1129-1133.

Pearson, K. (1900). Mathematical contributions to the theory of evolution. VIII. On the correlation of characters not quantitatively measurable. *Proceedings of the Royal Society of London*. 66(424-433):241-244.

Pearson, K. (1920). Notes on the history of correlation. *Biometrika*. 13(1):25-45.

Pierson, R.N., Russell, M., Wang, J., Thornton, J.C., Ma, R.M., and Weber, D.A. (1993). Body calcium by in-vivo neutron activation analysis is predicted by dual photon absorptiometry: comparisons by three DPA methods. *The Federation of American Societies for Experimental Biology Journal*. 7:A68.

Pourhassan, M., Eggeling, B., Schautz, B., Johannsen, M., Kiosz, D., Glüer, C.C., Bosy-Westphal, A., and Müller, M.J. (2015). Relationship between submaximal oxygen uptake, detailed body composition, and resting energy expenditure in overweight subjects. *American Journal of Human Biology*. 27(3):397-406.

Prange, H.D., Anderson, J.F., and Rahn, H. (1979). Scaling of skeletal mass to body mass in birds and mammals. *The American Naturalist*. 113(1):103-122.

Richardson, R.S., Kennedy, B., Knight, D.R., and Wagner, P.D. (1995). High muscle blood flows are not attenuated by recruitment of additional muscle mass. *American Journal of Physiology-Heart and Circulatory Physiology*. 269(5):H1545-H1552.

Richardson, R.S., Poole, D.C., Knight, D.R., Kurdak, S.S., Hogan, M.C., Grassi, B.R., Johnson, E.C., Kendrick, K.F., Erickson, B.K. and Wagner, P.D. (1993). High muscle blood flow in man: is maximal O_2 extraction compromised? *Journal of Applied Physiology*. 75(4):1911-1916.

Rogers, D.M., Olson, B.L., and Wilmore, J.H. (1995). Scaling for the $\dot{V}O_2$-to-body size relationship among children and adults. *Journal of Applied Physiology*. 79(3):958-967.

Ross, W.D., and Ward, R. (1985). *The O-scale system*. Rosscraft, Surrey, BC.

Roubenoff, R., and Kehayias, J.J. (1991). The meaning and measurement of lean body mass. *Nutrition Reviews*. 49(6):163-175.

Rowell, L.B., Saltin, B., Kiens, B., and Christensen, N.J. (1986). Is peak quadriceps blood flow in humans even higher during exercise with hypoxemia? *American Journal of Physiology-Heart and Circulatory Physiology*. 251(5):H1038-H1044.

Rubenson, J., Heliams, D.B., Maloney, S.K., Withers, P.C., Lloyd, D.G., and Fournier, P.A. (2007). Reappraisal of the comparative cost of human locomotion using gait-specific allometric analyses. *Journal of Experimental Biology*. 210(20):3513-3524.

Saltin, B., and Strange, S. (1992). Maximal oxygen uptake:" old" and" new" arguments for a cardiovascular limitation. *Medicine and Science in Sports and Exercise*. 24(1):30-37.

Sarrus, F., and Rameaux, J.F. (1839). Mathématique appliquée à la physiologie. *Bulletin de l'Academie Royale de Medicine de Paris*. 3:1094-1100.

Secher, N.H., Clausen, J.P., Klausen, K., Noer, I., and Trap-Jensen, J. (1977). Central and regional circulatory effects of adding arm exercise to leg exercise. *Acta Physiologica*. 100(3):288-297.

Secher, N.H., Ruberg-Larsen, N.S., Binkhorst, R.A., and Bonde-Petersen, F. (1974). Maximal oxygen uptake during arm cranking and combined arm plus leg exercise. *Journal of Applied Physiology*. 36(5):515-518.

Secher, N.H., Vaage, O., Jensen, K., and Jackson, R.C. (1983). Maximal aerobic power in oarsmen. *European Journal of Applied Physiology and Occupational Physiology*. 51(2):155-162.

Shapiro, S.S., and Wilk, M.B. (1965). An analysis of variance test for normality (complete samples). *Biometrika*. 52(3/4), 591-611.

Shephard, R.J., Allen, C., Benade, A.J.S., Davies, C.T.M., Di Prampero, P.E., Hedman, R., Merriman, J.E., Myhre, K., and Simmons, R. (1968). The maximum oxygen intake: an international reference standard of cardio-respiratory fitness. *Bulletin of the World Health Organization*. 38(5):757.

Soule, R.G., and Goldman, R.F. (1969). Energy cost of loads carried on the head, hands, or feet. *Journal of Applied Physiology*. 27(5):687-690.

Taylor, C.R., Heglund, N.C., and Maloiy, G.M.O. (1982). Energetics and mechanics of terrestrial locomotion. I. Metabolic energy consumption as a function of speed and body size in birds and mammals. *Journal of Experimental Biology*. 97(1):1-21.

Taylor, C.R., Maloiy, G.M.O., Weibel, E.R., Langman, V.A., Kamau, J.M., Seeherman, H.J., and Heglund, N.C. (1981). Design of the mammalian respiratory system. III. Scaling maximum aerobic capacity to body mass: wild and domestic mammals. *Respiration Physiology*. 44(1):25-37.

Taylor, C.R., Schmidt-Nielsen, K., and Raab, J.L. (1970). Scaling of energetic cost of running to body size in mammals. *American Journal of Physiology-Legacy Content*. 219(4):1104-1107.

Taylor, C.R., Shkolnik, A., Dmi'el, R., Baharav, D., and Borut, A. (1974). Running in cheetahs, gazelles, and goats: energy cost and limb configuration. *American Journal of Physiology-Legacy Content*. 227(4):848-850.

Taylor, N.A.S., Lewis, M.C., Notley, S.R., and Peoples, G.E. (2011). The Oxygen Cost of Wearing Firefighters' Personal Protective Equipment: Ralph Was Right. In: *ICEE 2011 XIV International Conference on Environmental Ergonomics: Book of Abstracts*. 236-239.

Taylor, N.A.S., Lewis, M.C., Notley, S.R., and Peoples, G.E. (2012). A fractionation of the physiological burden of the personal protective equipment worn by firefighters. *European Journal of Applied Physiology*. 112(8):2913-2921.

Toth, M.J., Gardner, A.W., Ades, P.A., and Poehlman, E.T. (1994). Contribution of body composition and physical activity to age-related decline in peak $\dot{V}O_2$ in men and women. *Journal of Applied Physiology*. 77(2):647-652.

Toth, M.J., Goran, M.I., Ades, P.A., Howard, D.B., and Poehlman, E.T. (1993). Examination of data normalization procedures for expressing peak $\dot{V}O_2$ data. *Journal of Applied Physiology*. 75(5):2288-2292.

Vanderburgh, P.M. (1998). Two important cautions in the use of allometric scaling: the common exponent and group difference principles. *Measurement in Physical Education and Exercise Science*. 2(3):153-163.

Vanderburgh, P.M., and Katch, F.I. (1996). Ratio scaling of $\dot{V}O_2$max penalizes women with larger percent body fat, not lean body mass. *Medicine and Science in Sports and Exercise*. 28(9):1204-1208.

Wang, Z., Ying, Z., Bosy-Westphal, A., Zhang, J., Schautz, B., Later, W., Heymsfield, S.B., and Müller, M.J. (2010). Specific metabolic rates of major organs and tissues across adulthood: evaluation by mechanistic model of resting energy expenditure. *The American Journal of Clinical Nutrition*. 92(6):1369-1377.

Weibel, E.R., Bacigalupe, L.D., Schmitt, B., and Hoppeler, H. (2004). Allometric scaling of maximal metabolic rate in mammals: muscle aerobic capacity as determinant factor. *Respiratory Physiology and Neurobiology*. 140(2):115-132.

Weibel, E.R., and Hoppeler, H. (2005). Exercise-induced maximal metabolic rate scales with muscle aerobic capacity. *Journal of Experimental Biology*. 208(9):1635-1644.

Welham, W.C., and Behnke, A.R. (1942). The specific gravity of healthy men: body weight ÷ volume and other physical characteristics of exceptional athletes and of naval personnel. *Journal of the American Medical Association*. 118(7):498-501.

Wells, J.C.K., and Fewtrell, M.S. (2006). Measuring body composition. *Archives of disease in childhood.* 91(7):612-617.

Welsman, J.R., Armstrong, N., Nevill, A.M., Winter, E.M., and Kirby, B.J. (1996). Scaling peak $\dot{V}O_2$ for differences in body size. *Medicine and Science in Sports and Exercise*. 28(2):259-265.

Weyand, P.G., Smith, B.R., Puyau, M.R., and Butte, N.F. (2010). The mass-specific energy cost of human walking is set by stature. *Journal of Experimental Biology*. 213(23):3972-3979.

White, C.R., and Seymour, R.S. (2003). Mammalian basal metabolic rate is proportional to body mass$^{2/3}$. *Proceedings of the National Academy of Sciences*. 100(7):4046-4049.

White, C.R., and Seymour, R.S. (2005). Allometric scaling of mammalian metabolism. *Journal of Experimental Biology*. 208(9):1611-1619.

Williams, D.A. (1987). Generalized linear model diagnostics using the deviance and single case deletions. *Applied Statistics*. 36(2):181-191.

Wilmore, J.H., and Behnke, A.R. (1969). An anthropometric estimation of body density and lean body weight in young men. *Journal of Applied Physiology*. 27(1):25-31.

Wilmore, J.H., and Behnke, A.R. (1970). An anthropometric estimation of body density and lean body weight in young women. *The American Journal of Clinical Nutrition*. 23(3):267-274.

Xiao, X., White, E.P., Hooten, M.B., and Durham, S.L. (2011). On the use of log transformation vs. nonlinear regression for analyzing biological power laws. *Ecology*. 92(10):1887-1894.

Yasumura, S., Chalif, P., Ma, R., Dilmanian, F.A., Pierson, R.N., Aulet, M., and Weber, D. (1993). The effect of changes in body size on total body bone mineral content as assessed by dual x-ray absorptiometry in phantoms. *The Federation of American Societies for Experimental Biology Journal*. 7(3):A85.

Yoshiga, C.C., and Higuchi, M. (2003). Oxygen uptake and ventilation during rowing and running in females and males. *Scandinavian Journal of Medicine and Science in Sports*. 13(6):359-363.

4: SCALING STEADY-STATE OXYGEN CONSUMPTION DURING WALKING ON DIFFERENT GRADIENTS

4.1 INTRODUCTION

In exercising adult humans, oxygen consumption scales allometrically against body mass, by the exponent mass$^{0.80}$ (Chapter 3). That relationship persists for metabolic rates from standing to peak exercise, including the commonly used (Wyndham *et al.,* 1971; Rogers *et al.,* 1995; Taylor *et al.,* 2012) absolute walking velocity of 4.8 km.h^{-1} (0% gradient: Chapter 3). That walking pace was expected to modify the shape of the regression slope[27], as the application of a fixed, absolute work rate typically elicits responses that vary with body-size differences. However, this was not found to be the case. A possible reason for that response, in this instance, was that all participants were walking at approximately 24% of their peak aerobic power, with body mass (load) carriage displaying a greater impact on the scaling relationship than any other size-specific response. Nevertheless, it still cannot be concluded that all absolute exercise intensities will scale by that same mass exponent. If a condition does exist where those mass differences are significantly exaggerated, applying a fixed-mass exponent would result in spurious normative data. Whether this occurs during human, bipedal locomotion is currently unknown. However, a change in walking gradient may be a sufficient modification to that absolute intensity and induce such a body-size response, for the additional energy required to overcome gravity during gradient walking is also mass dependent[28] (Taylor *et al.,* 1972; Borghols *et al.,* 1978).

How a gradient change will influence the scaling regression remains unclear. Only one study was found where graded walking was scaled in humans (2.4 km.h^{-1}, 10% gradient, mass$^{0.83}$: Batterham and Jackson, 2003), and due to methodological limitations (*i.e.* no comparison to a level condition, use of an heterogeneous sample,

---

[27] Non-linear, allometric regression is plotted using the following equation $y = ax^b$, where, within this project, y is oxygen consumption (L.min^{-1}), a is the proportionality constant (non-dimensional), x is body mass (kg) and b is the mass exponent (non-dimensional). For scaling purposes, the shape of the regression curve is dictated by the mass exponent.

[28] Potential energy is gained during ascents and lost during descents, relative to the body's original position. Potential energy is the product of the body's mass and its vertical displacement: $E_p = mgh$, where E_p is potential energy (J), m is body mass (kg), g is the gravitational constant (N) and h is the distance of the body's displacement (m).

short-duration stages [unclear if a steady state was achieved by all participants: 3-min stages]) those findings could not be directly applied to the present research theme. Nevertheless, it did demonstrate that the scaling relationship is likely to remain non-linear. Thus, if graded walking does modify the scaling relationship, the important change to the regression will occur in the mass exponent.

It is plausible that the mass exponent will be modified relative to the change in gradient direction. Compared with level walking, nett oxygen consumption is greater on an uphill slope due to the additional mechanical work required to overcome the force of gravity (total less resting values: Hill, 1927; Workman and Armstrong, 1963; Johnson *et al.,* 2002). That increase in oxygen consumption is relatively uniform per unit of mass (Halsey and White, 2017), with the isolated cost of pure vertical ascent (primary difference between level and uphill walking) approximately 2 $mL.kg^{-1}.m^{-1}$ (1.48 $mL.kg^{-1}.m^{-1}$ [Dill, 1965]; 2.17 $mL.kg^{-1}.m^{-1}$ [Taylor *et al.,* 1970]; 1.36 $mL.kg^{-1}.m^{-1}$ [Cohen *et al.,* 1978]). Therefore, absolute nett oxygen consumption will increase with either a change in gradient (Laursen *et al.,* 2000; Johnson *et al.,* 2002) or the total mass carried (Goldman and Iampietro, 1962; Workman and Armstrong, 1963; Taylor *et al.,* 1972). Accordingly, at a fixed, uphill gradient, nett absolute oxygen consumption will increase by a ratiometric relationship with body mass. Applying that ratiometric scaling regression on top of the non-linear level walking regression (Chapter 3), would result in a steeper, non-linear relationship, providing that the human mass range is wide enough to observe a significant size-relationship among those nett data.

In contrast, oxygen consumption is reduced during downhill walking, with values reportedly half of those measured on equivalent uphill gradients (Johnson *et al.,* 2002). The downwards displacement of body mass releases potential energy, which, as it works on the body, is transferred into some thermal energy within the eccentrically activated muscles (Nadel *et al,.* 1972) and the rest as kinetic energy, which reduces the mechanical work (muscular contractions) required to maintain walking velocity (Margaria, 1968; Cavagna *et al.,* 1977). Although no research has been found wherein the scaling relationship between whole-body oxygen consumption and body mass was evaluated during downhill walking, it is proposed that since

potential energy is mass dependent, heavier individuals should experience a greater decrease in absolute oxygen consumption. That response, if pronounced enough, would flatten the regression slope, reducing the mass exponent compared with level and uphill values.

Accordingly, the focus within this experimental phase was to evaluate the effect of uphill and downhill walking on the scaling relationship between whole-body oxygen uptake and body mass. Specifically, the relationship was investigated within the mass range of adult humans with the purpose of identifying whether the scaling regression applied to level walking at the same velocity is modified by a change in gradient. To effectively assess that aim, three experimental hypotheses were developed, and based on the assumption that oxygen consumption during gradient walking will scale allometrically.

Hypothesis Four-One: The mass exponent applied to the scaling relationship between oxygen consumption and body mass during uphill walking will be significantly greater than that observed during level walking.
Hypothesis Four-Two: The downhill walking mass exponent will be numerically smaller than that observed during level walking, but not significantly different.
Hypothesis Four-Three: The mass exponent applied to the uphill walking scaling relationship will be significantly greater than that applied in the downhill walking condition.

4.2 METHODS

4.2.1 Subjects

The effect of surface gradient on the scaling relationship between oxygen consumption and body mass during walking was assessed using 64 healthy and physically active men (N=63, uphill; N=62, downhill: Figure 4.1), most of whom also completed the level walk in Chapter 3 (N=68). To permit scaling analyses, subjects were evenly recruited across a two-fold mass range (56.0-117.1 kg: Figure 4.1), but were otherwise matched for physiological and morphological variables that could influence whole-body oxygen consumption (Section 2.2.1; Table 2.2). Morphometric comparisons were again made by splitting the sample into five

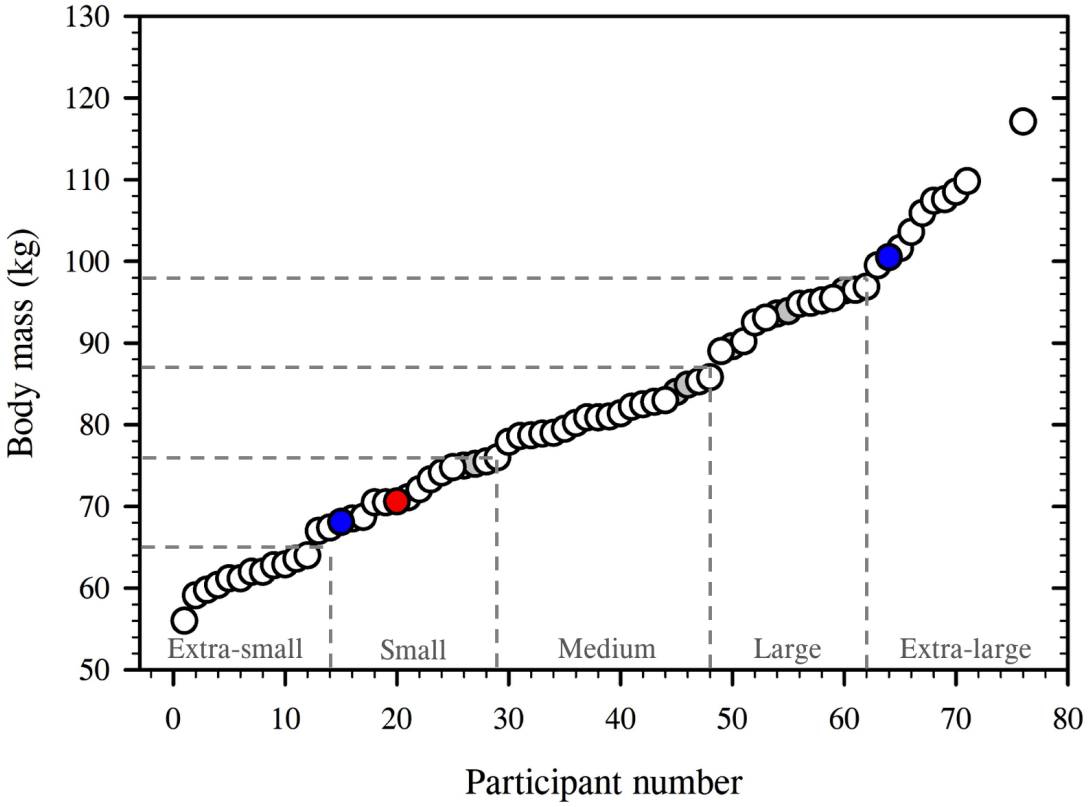

Figure 4.1: Scatter plot displaying the mass distribution for the full 72 participants that were tested between Chapters 2 and 6, with subjects arranged in ascending order of body mass. Of those 72 participants, 64 completed testing within this present investigation (uphill: $N=63$; downhill: $N=62$). Partial (uphill only: $N=2$ [blue]; downhill only: $N=1$ [red]) and missing ($N=8$ [grey]) datasets are identified by the coloured symbols. The drop-lines signify the borders separating each of the five body-mass groups and show the number of participants within each group.

body-mass groups (Figure 4.1), among which participants were relatively similar with regard to height-adjusted sum of skinfold thickness and height-adjusted body mass (Figures 2.10 and 2.11).

The subjects were recruited from the local university population and nearby sports teams, and screened to eliminate those with a history of cardiovascular, respiratory or musculo-skeletal pathologies contraindicative of participation in this experiment. Before testing, participants were supplied with an information package and provided written, informed consent. The experimental procedures performed within this experimental phase were approved by the Human Research Ethics Committee (University of Wollongong; HE14/469).

4.2.2 Procedural overview

The influence of walking gradient on the scaling relationship between oxygen consumption and body mass was investigated during both uphill (5%) and downhill (-5%) walking, and then compared against the level-walking data collected in Chapter 3. It has been found that grades steeper than a -5% to -10% range result in a proportional increase in oxygen consumption (Pivarnik and Sherman, 1990; Minetti *et al.,* 1993; Johnson *et al.,* 2002), due to an increase in breaking forces (Franz *et al.,* 2012), a decrease in postural stability (Hunter *et al.,* 2010; Monsch *et al.,* 2012; Scaglioni-solano and Arago, 2015) and consequently an increase in stride frequency (Pinch and Claussen 2003; Hunter *et al.,* 2010). Thus, a $\pm$5% gradient was used during testing to minimise the additional variables influencing the scaling relationship at this preliminary investigative stage. All trials were conducted at the same absolute velocity (4.8 $km.h^{-1}$) and, where possible, all participants completed all three walking trials. Each trial was completed on a separate visit at the laboratory, with the trial order balanced across participants using a Latin Square design. Each trial commenced with a 10-min standing (stationary) stage, followed by a 15-min treadmill walk. Prior to these trials, all participants completed two familiarisation visits. During those visits, participants were equipped with the testing equipment and asked to walk uphill and downhill for 10 min to get them used to the testing requirements, thereby increasing test reliability (Jamnik *et al.,* 2013).

4.2.2.1 Measuring oxygen consumption during steady-state walking

Participants instrumented with a cardiac frequency monitor and an oronasal mask. Then, wearing laboratory-provided clothing (combat trousers, shirt and thick socks: Figure 3.2A) and their own running shoes, subjects mounted a treadmill (Pulsar 3p Treadmill, H/P/Cosmos, Traunstein, Germany) and stood motionless, whereupon a 10-min baseline data collection period began. Subsequently, walking at 4.8 $km.h^{-1}$ for 15 min commenced, with the treadmill set to either the uphill or downhill gradient (5% or -5%).

4.2.3 Experimental standardisation

All clothing worn by participants was sized by the researchers prior to commencing. Clothing items were selected to correspond with those worn by the Australian Defence Force, with the secondary aim of determining the mass-independent oxygen cost of ambulatory activities for defence personnel. Furthermore, participants wore their own running shoes, which varied in model and size. To minimise the known magnified metabolic effect of loading the foot (Soule and Goldman, 1969; Taylor *et al.,* 2012), the mass of each shoe was brought up to 500 g by adding the difference to each ankle with a weighted ankle strap (Figure 3.2B). All testing was conducted in an air-conditioned laboratory ($\sim$23°C; $\sim$50% humidity) and at the same time of day ($\pm$1 h) within participants, to minimise potential circadian effects. Prior to testing, participants were instructed to refrain from drinking caffeine for 6 h and to consume a pre-experimental meal high in carbohydrates and low in fats $>$2 h before starting the test.

4.2.4 Experimental measurements

Oxygen consumption (open-circuit respirometry: TrueOne 2400, ParvoMedics Inc., Utah, U.S.A.: Crouter *et al.,* 2006; see Section 2.2.4.1 for details) and cardiac frequency (ventricular depolarisation: Plug in receiver, Polar Electro, Kempele, Finland; see Section 2.2.4.3 for details) were measured continuously as 15-s averages (respiratory measures) and intervals (cardiac frequency), and sampled during the last 5 min of each stage. Semi-nude and clothed (unshod) body masses were measured at the start of each laboratory visit (digital scales: MS3200, Medical Scale, Charder, Taichung, Taiwan: see Section 2.2.4.4 for details). Anthropometric data were

collected during the first visit at the laboratory (standing stretched-stature: Harpenden Stadiometer, Holtain Ltd., Crymych, UK; six-site sum of skinfolds: Eiken skinfold calliper, Meikosha, Tokyo, Japan; see Section 2.2.4.4 for details). To control size-related morphometric differences, sum of skinfold and body mass data were normalised to a common standing height using Equation 2.5 (170.18 cm; Ross and Wilson, 1974), and a criterion height-adjusted adiposity threshold of 88 mm was set for participant selection (60^{th} percentile: Ross and Ward, 1985; Landers *et al.,* 2013: see Section 2.2.1).

4.2.5 Design and analysis

4.2.5.1 Experimental design

The two experimental conditions tested within this stage (uphill and downhill walking: Figure 4.2 [coloured cells]) were combined with level walking (Chapter 3) to evaluate the effect of gradient on the scaling regression. This yielded an experiment that was based on a five by three factorial design, with five levels of the first factor (body mass: extra-small, small, medium, large, extra-large]). and three levels for the second factor (gradient: level, incline, decline). Participants acted as their own controls using a repeated-measures design. Data are presented as means with standard deviations (SD) used to describe data distributions and the accuracy of the mean described using standard errors of the mean ($\pm$).

4.2.5.2 Data analysis

Both uphill and downhill walking datasets were assessed using the schematic decision making chart (Figure 2.8) to confirm whether the scaling relationships remained non-linear. Data were then temporarily $\log_{10}$ transformed (Figure 2.9) to generate a linear regression format before performing statistical comparisons. As a result, two regression equations are presented for both metabolic intensities: allometric and $\log_{10}$ transformed, with each serving a different purpose. The untransformed (allometric) exponent should be adopted when predicting or normalising untransformed oxygen consumption data. As a result, any in-text references to exponent values will correspond to the untransformed exponent, unless directly stated. The log-transformed regression equations have been reported to display the exponents used during the statistical comparisons and for possible future reference, if regression

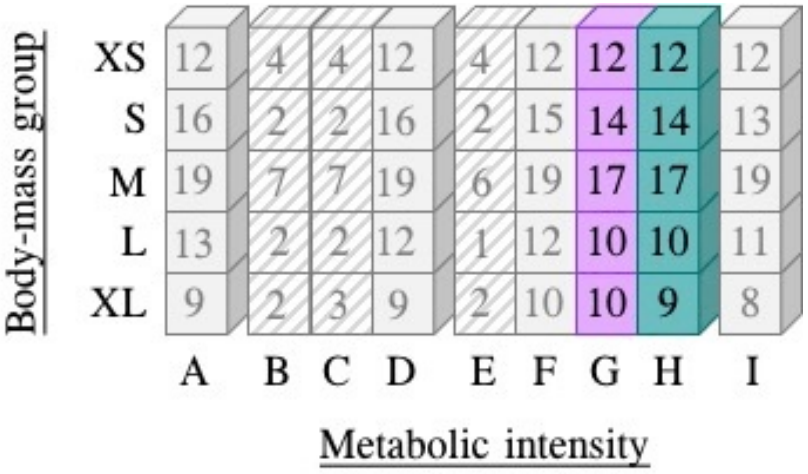

Figure 4.2: A schematic of the experimental design from Chapters 2 through to 4. Exploratory trials are identified by the hashed fills. Sample sizes are identified within each cell. The wider research phase consisted of a five by nine factorial design, with those factors measured within the current experimental phase identified by the coloured cells. The first factor (body mass) had five levels: extra-small (XS); small (S); medium (M); large (L); extra-large (XL). The second factor (metabolic intensity) had nine levels: supine (Column A: basal, rest); 100% mass-supported standing (Column B: exploratory investigation); 50% mass-supported standing (Column C: exploratory investigation); standing (Column D); 50% mass-supported walking (Column E: exploratory investigation); level walking (Column F); uphill walking (Column G); downhill walking (Column H); peak exercise (Column I).

analyses are required. In some cases the exponents stated for both data formats (untransformed and log-transformed) differ, this is a consequence of the transformation process and its effect on the distribution of residuals[29] (Jansson, 1985; Newman, 1993; Xiao *et al.,* 2011).

The effect of gradient (level, uphill and downhill walking) was compared among the $\log_{10}$-transformed scaling regressions using analysis of covariance to identify any significant changes to the mass exponents. A significant interaction effect identified statistically different mass exponents. For those comparisons, the level scaling regressions observed in Chapter 3 were used (Equations 4.1 and 4.2), where y is absolute oxygen consumption ($L.min^{-1}$), x is body mass (kg) and the exponents have been highlighted in bold. Although a single exercise-intensity exponent was determined within Chapter 3 ($mass^{0.80}$), the effect of gradient was initially compared against the level-walking value ($mass^{0.85}$), to permit quantification of the effect of a gradient change on the scaling relationship. The gradient exponents were then compared against $mass^{0.80}$ to assess the feasability of describing both states using that single exercise-intensity exponent. This latter comparison was conducted using a null-hypothesis t-test (Equation 4.3), where a non-significant result would indicate that a condition could be described using $mass^{0.80}$.

Level walking, untransformed

Equation 4.1

$$y = 0.02 \cdot x^{\mathbf{0.85}}$$

Level walking, log_{10} transformed

Equation 4.2

$$\mathrm{Log}_{10}(y) = \mathbf{0.85} \cdot \mathrm{Log}_{10}(x) - 1.61$$

[29] Since the logged mean of the untransformed data does not equal the mean of the log-transformed data (Jansson, 1985; Newman, 1993; Xiao *et al.*, 2011), error would be introduced if using a regression coefficient from the log-transformed data on the untransformed dataset. Consequently, both allometric and log-transformed regressions have been presented .

Null-hypothesis t-test

$$T_1 = (\hat{\beta}_1 - 0.80) / SEM(\hat{\beta}_1) \qquad \textbf{Equation 4.3}$$

where:

T_1 = test statistic [non-dimensional units]

$\hat{\beta}_1$ = mass exponent (slope) [morphological units]

0.80 = exercise-intensity mass exponent [morphological units]

$SEM(\hat{\beta}_1)$ = standard error of the mean for the mass exponent [morphological units]

Means and standard errors of the mean were estimated for each regression coefficient using bootstrapping[30] (Efron, 1979; Fox and Weisberg, 2017). As per previous Chapters, potential regression outliers were identified prior to scaling analyses, using scatter plots, box plots, the Bonferroni test (Cook and Weisberg, 1982; Williams, 1987; Fox, 1997) and Cook's distance (Cook, 1977; Fox, 1991; Hair *et al.,* 1998; see Section 2.2.5.2 for details).

A Pearson's correlation coefficient test (Pearson, 1896, 1920) was performed on the normalised oxygen consumption data to assess the ability to generate mass-independent oxygen consumption data using a specific mass exponent. As per Chapters 2 and 3, data were plotted in mass order to remove the original distribution of the data points, and the test was deemed successful if *rho*[31] approached zero.

The relative effect of a change in ambulatory gradient from level walking was evaluated for oxygen consumption. This was compared between extreme body-mass groups (10 lightest and heaviest participants) using two-way factorial analysis of variance. A significant interaction effect would identify a body-size relationship to the relative change in oxygen consumption, compared with level walking. Additionally, differences in mean oxygen consumption and cardiac frequency were compared

[30] Each model was generated 1000 times using a re-sampling approach from the original dataset.

[31] *Rho*, or the correlation coefficient, is the numerical measure for the strength and direction of any linear relationship between two variables ($-1 \leq rho \leq 1$).

between conditions using repeated-measures analysis of variance.

Mean body-mass group differences in morphometric and physiological variables were compared using one-way analysis of variance. Analysis of covariance was performed when size-differences remained among height-adjusted measures. However, as no significant interaction effect was realised between those measures and the scaling regressions, the morphometric data were not considered necessary covariant variables for the scaling regressions.

4.3 RESULTS

4.3.1 Pre-experimental standardisation

Before performing any scaling analyses, the morphometric homogeneity of the sample was assessed. The partial datasets within this Chapter (Figure 4.1) did not modify the size-specific morphometric differences observed in Chapter 2 (Section 2.3.1.1). However, this meant that some size-differences still remained among the height-adjusted data (Figures 2.10 and 2.11; $P < 0.05$). Analysis of covariance was performed using both height-adjusted measures for both gradient walking datasets to identify whether either variable influenced the scaling regressions. However, no significant covariant effect was observed during either metabolic intensity, for either measure ($P > 0.05$). Thus the morphometric data was not included in the scaling regressions, and the sample were considered morphometrically homogeneous.

The decision making flow chart (Figure 2.8) was used to assess whether oxygen consumption during the two graded walking states still scales nonlinearly against body mass. When a linear regression was applied to either untransformed dataset a positive intercept, significantly greater than zero was observed (uphill: 0.26 $L.min^{-1}$; downhill: 0.21 $L.min^{-1}$; $P < 0.05$), thus confirming that a linear model was unsuitable

to describe those data. However, when data were $\log_{10}$ transformed[32], linearity was observed (uphill: $r^2=0.90$; downhill: $r^2=0.60$; $P<0.05$), and the regression residuals were considered normally distributed using skewness and kurtosis z-scores ($<\pm3.26$; Kim, 2013; $P>0.05$) and the Shapiro-Wilk test (1965; $P>0.05$). Moreover, no autocorrelation was observed among any model residuals using the Durbin-Watson test (1950, 1951: $P>0.05$). Consequently, both graded-walking datasets were deemed non-linear, and the regressions could be confidently compared with the level walking condition (Chapters 3) when $\log_{10}$ transformed.

4.3.2 Comparing the effect of walking gradient on the scaling relationships

Mean absolute oxygen consumption differed significantly among all three walking gradients (level: 1.02 L.min^{-1} [±0.02]; uphill: 1.46 L.min^{-} [±0.03] ^{1}; downhill: 0.73 L.min^{-1} [±0.02]; $P<0.05$). Those responses followed the expected outcomes, whereby, the change in metabolic intensity matched the gradient direction (Minetti *et al.*, 1993; Johnson *et al.,* 2002). Furthermore, it demonstrated that each gradient represented a unique metabolic load, despite only varying by $\pm5\%$. As a result, it was possible that each metabolic intensity would also scale against a different mass exponent.

To identify whether the relative change in oxygen consumption was influenced by body mass, two-way factorial analysis of variance was performed using the 10 lightest and heaviest individuals and the three gradient conditions. No effect of body mass was identified between level and uphill walking conditions, with oxygen consumption increasing by a similar amount in both body-mass groups (lightest: 45%; heaviest: 44%; Figure 4.3; $P>0.05$). As such, the nett increase in oxygen consumption for vertical ascent was considered proportional with body mass. However, during downhill walking, a greater decrease in oxygen consumption was observed in the heavier group (lightest: 22%; heaviest: 28%; $P<0.05$).

Analysis of covariance was performed to assess whether those metabolic responses to

[32] Allometric equations were log transformed, producing a linear equation. In this way, the non-linear regressions could be assessed using robust statistical tests that assume a linear relationship among variables.

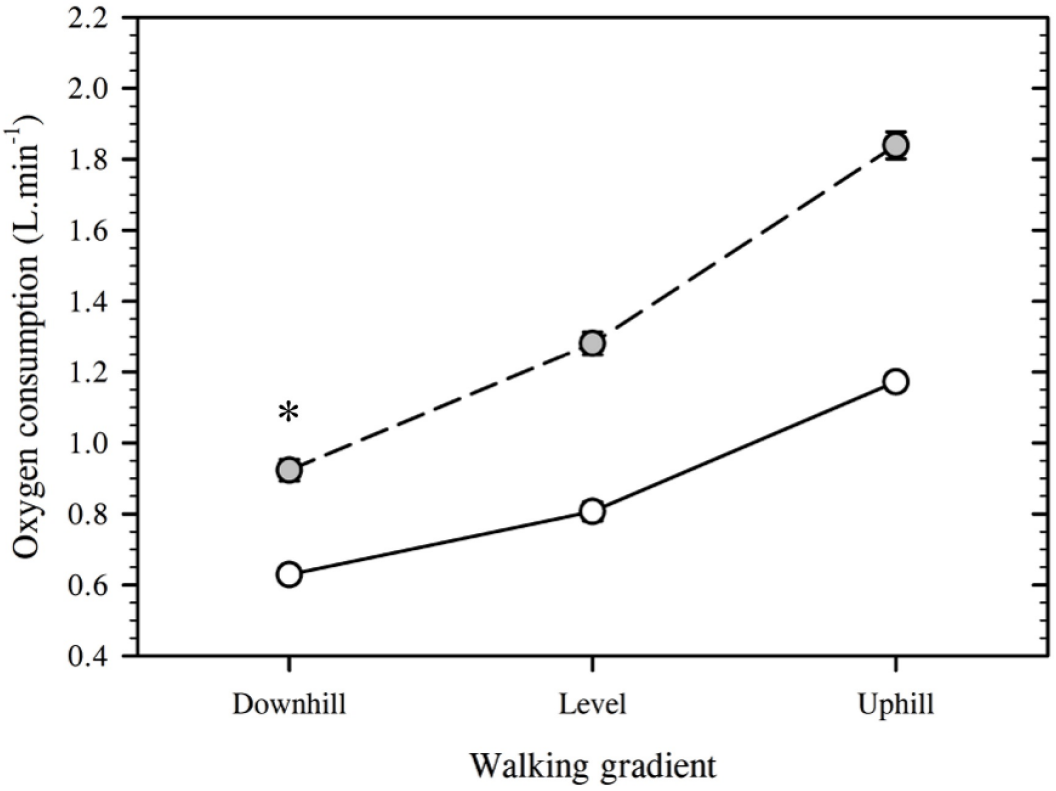

Figure 4.3: Line and scatter plot displaying the mean change in oxygen consumption between changes in walking gradient (-5%, 0%, 5%). Data are presented for the 10 smallest (56.0-62.9 kg [white symbols]) and heaviest (99.5-117.1 kg [grey symbols]) individuals in the sample. A significant difference in the percentage change of oxygen consumption was realised among body-mass groups between level and downhill walking (*; $P < 0.05$).

graded walking modified the regression exponent from that of level walking. However, while each gradient condition were considered separate metabolic intensities, no difference in mass exponents was observed among the log-transformed scaling regressions for level ($mass^{0.85}$), uphill ($mass^{0.81}$) and downhill ($mass^{0.71}$) walking (Figure 4.4; Table 4.1; $P > 0.05$), leading to the rejection of Hypotheses Four-One and Four-Three but the acceptance of Hypothesis Four-Two. Furthermore, neither gradient exponent differed significantly from the exercise-specific exponent (Chapter 3; $P > 0.05$). As a result, it is possible to describe both uphill and downhill walking using that same mass exponent ($mass^{0.80}$; Figure 4.5; $P > 0.05$).

4.4 DISCUSSION

The purpose of this Chapter was to quantify the effect of walking gradient on the scaling relationship between oxygen consumption and body mass in humans. Prior to this investigation, that relationship had only been explored in one paper, during uphill locomotion (2.74 $km.h^{-1}$; 10% gradient: Batterham and Jackson, 2003). However, due to sample and method limitations[33], those results could not be used to derive the effect of a change in surface gradient. Therefore, this experimental phase represented the first study to define the effect of gradient change on the scaling relationship of level walking. Moreover, that aim was explored using a repeated measures design, across uphill (5%), downhill (-5%) and level (Chapter 3) grades (Figure 4.5), using an appropriate sample for scaling analyses (Section 4.2.1; see Section 2.2.1 for sample requirements).

The shape of the scaling relationship remained non-linear for both uphill and downhill grades (Table 4.1; $P > 0.05$), confirming the continuity of non-linear scaling throughout the physiological range. During uphill walking, it was hypothesised that the increase in oxygen consumption associated with a gain in potential energy would steepen the regression slope (larger mass exponent) compared with level (Hypothesis Four-One) and downhill (Hypothesis Four-Three) grades. However, no statistical

[33] Batterham and Jackson (2003) used a heterogeneous sample, varying in age, gender, mass, adiposity and fitness. Consequently, their sample contains many potential covariant variables that may introduce an uncontrolled error when determining the mass exponent for that scaling relationship. Furthermore, their steady-state walking stage was only sampled for 3 min. As a result, it is possible that not all participants had obtained a steady state. Therefore, for comparative purposes, the accuracy of their scaling exponent is unclear.

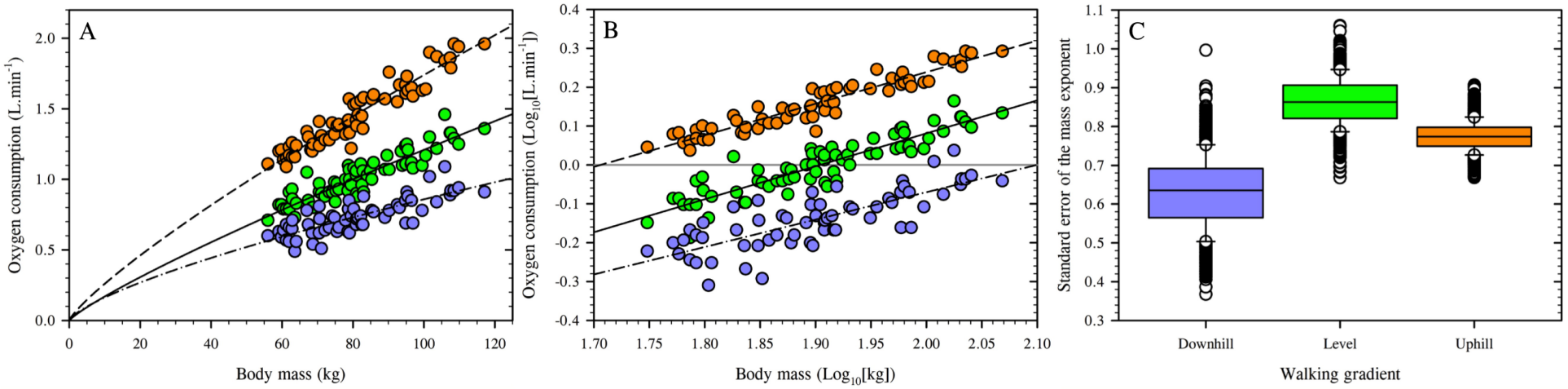

Figure 4.4: Figures 4.4A and 4.4B display the untransformed (allometric) and $\log_{10}$-transformed scatter plots for the three scaling relationships between oxygen consumption and body mass. Data are presented for uphill (N=63 [orange symbols]), downhill (N=62 [purple symbols]) and level (N=68 [green symbols]) walking conditions. The box plot displays the bootstrapped (generated 1000 times using re-sampling) untransformed mass exponents (uphill: $mass^{0.77\ [\pm 0.04]}$; downhill: $mass^{0.63\ [\pm 0.10]}$; level: $mass^{0.86\ [\pm 0.06]}$) and their respective standard errors of the mean for each of the three walking gradients (Figure 4.4C).

Table 4.1: A summary table of the allometric and $\log_{10}$-transformed regression equations applied to the level (Equations 4.1 and 4.2; Chapter 3), uphill and downhill walking datasets. Regression coefficients are displayed as bootstrapped means, with the mass exponents highlighted in bold. No differences were found among the three $\log_{10}$-transformed regression equations ($P > 0.05$).

	Regression equation	
Metabolic intensity	Power (untransformed)	Log_{10} transformed
Level walking	$y = 0.02 \cdot x_B^{\mathbf{0.86}}$	$y = \mathbf{0.85} \cdot x_B$ - 1.61
Uphill walking	$y = 0.04 \cdot x_B^{\mathbf{0.77}}$	$y = \mathbf{0.81} \cdot x_B$ - 1.38
Downhill walking	$y = 0.03 \cdot x_B^{\mathbf{0.63}}$	$y = \mathbf{0.71} \cdot x_B$ - 1.48

Notes: As logged mean values do not equal a log-transformed mean, a de-transformed logarithmic regression will not identically equal its untransformed power regression (Jansson, 1985; Newman, 1993; Xiao *et al.,* 2011). Consequently, both regressions are presented.

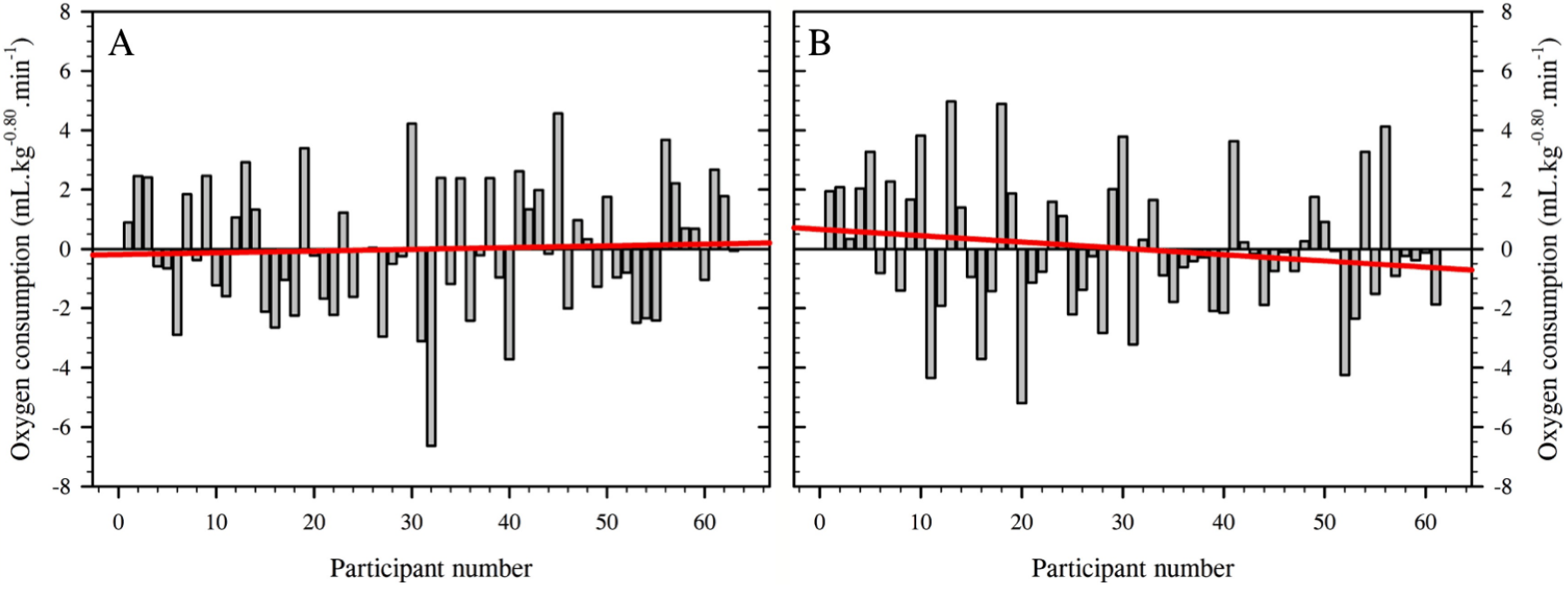

Figure 4.5: Residual plots for the difference in the actual and predicted data points for uphill (Figure 4.5A; $r=0.05$; $P>0.05$) and downhill (Figure 4.5B; $r=0.17$; $P>0.05$) walking, when data were normalised to mass$^{0.80}$. The normalised residuals are ordered from lightest to heaviest across the abscissa, so that the data could be assessed independently from their original regression distributions. Pearson's correlation coefficient was used to evaluate any remaining mass relationship among those data, where a *rho* approaching zero identified a successful normalisation outcome.

difference was observed among any of the three mass exponents (uphill: $mass^{0.77}$; downhill: $mass^{0.63}$; level: $mass^{0.86}$; Table 4.1; Figure 4.4; $P > 0.05$). Therefore, both Hypotheses Four-One and Four-Three were rejected. Although the increase in oxygen consumption was closely related to the total mass carried uphill, it appeared that the human mass range was not wide enough to observe the expected change in mass exponent.

In contrast, the non-significant decrease in the downhill exponent (Hypothesis Four-Two accepted) highlighted a significant mass-response for the change in absolute oxygen consumption. That is, downhill walking became significantly more efficient with an increase in body mass (10 smallest: 22%; 10 largest: 28%; $P < 0.05$). The influence of this relationship was not realised during uphill walking (10 smallest: 45%; 10 largest: 44%; Figure 4.3; $P > 0.05$), and so it was suspected that an additional variable influenced the downhill scaling relationship. It was theorised that the heavier individuals became more economical due to a greater pre-stretching of their eccentrically activated muscles, as a result of greater mass-induced landing forces.

This possibility is important, for it demonstrates a mass-dependent energy-saving mechanism during downhill walking not present on an incline. Such information could inform rehabilitative and performance estimations. Moreover, the fact that all three gradient conditions could be scaled using the same mass exponent simplifies comparison practices during walking on moderate gradients. That is, both gradient-walking mass exponents were statistically similar with the exercise-intensity mass exponent derived in Chapter 3 ($mass^{0.80}$; $P > 0.05$), meaning that one mass exponent can be used to describe walking and peak exercise oxygen consumption, despite moderate gradient changes.

During uphill walking, oxygen consumption increased by $\sim 45\%$ (level: 1.02 $L.min^{-1}$ [± 0.02]; uphill: 1.46 $L.min^{-1}$ [± 0.03]; $P < 0.05$) and cardiac frequency by $\sim 18\%$ (level: 97 $b.min^{-1}$ [± 2]; incline: 115 $b.min^{-1}$ [± 2]; $P < 0.05$), compared with the level trial. Such a response is typical of a moderate increase in walking gradient (Sagiv *et al.,* 2000: 1.10 $L.min^{-1}$, 111 $b.min^{-1}$ [± 2]; Johnson *et al.,* 2002: 1.06 $L.min^{-1}$

[±0.24]; Pal *et al.,* 2014: 1.28 L.min^{-1}, 111 b.min^{-1} [±4]), and represents the greater physiological strain associated with a vertical ascent. Indeed, oxygen consumption increased by approximately 1.40 mL.kg^{-1}.m^{-1}, per vertical metre of ascent.[34] That value was similar to those identified within the literature (Dill, 1965: 1.48 mL.kg^{-1}.m^{-1}; Taylor *et al.,* 1970: 2.17 mL.kg^{-1}.m^{-1}; Cohen *et al.,* 1978: 1.36 mL.kg^{-1}.m^{-1}), demonstrating a consistency in the cost of vertical movement.

Despite the significant increase in absolute oxygen consumption during uphill walking, the gradient change did not significantly modify the mass exponent compared with level walking (uphill: mass$^{0.77}$ [untransformed]; level: mass$^{0.86}$ [untransformed]; Figure 4.4; $P > 0.05$). Therefore, Hypothesis Four-One was rejected. The similarity in mass exponents reflects the uniform percentage increase in oxygen consumption across the sample mass range (10 lightest participants: 45%; 10 heaviest participants: 44%; Figure 4.3; $P > 0.05$). The fact that the greater increase in absolute oxygen uptake among the heavier individuals did not increase the mass exponent indicates that, compared with animals (Taylor *et al.,* 1972), the adult human mass range may have been too narrow to observe that effect. Moreover, that homogeneous response demonstrates the mass-dependent nature of the relationship between oxygen consumption and uphill walking, whereby the increase in oxygen uptake was directly related to the total mass displaced. This is a possible explanation for the equivalent scaling response observed by Batterham and Jackson (mass$^{0.83}$: 2003) when scaling uphill walking using a heterogeneous sample (Table 3.1). Such a response would indicate that all uphill walking should scale similarly. While at present that conclusion remains unconfirmed, it could easily be explored using a range of uphill gradients or with external loading. The latter is investigated in Chapter 5.

In contrast, mean absolute oxygen consumption during downhill walking decreased by ~27% from level walking (level: 1.02 L.min^{-1}; downhill: 0.73 L.min^{-1}; $P < 0.05$) and ~50% from the uphill condition (1.46 L.min^{-1}; $P < 0.05$). Those reductions in

[34] The oxygen cost of vertical ascent (mL.kg^{-1}.m^{-1}) was calculated by dividing the mean nett oxygen consumption (uphill less level; mL.min^{-1}) by the vertical ascent per minute (4 m.min^{-1}). That value was then divided by the participant's mass (kg) to provide the mass-specific cost of vertical ascent.

oxygen consumption between gradients were consistent with those reported within the literature (~50% of uphill and ~25% of level: Lloyd and Cooke, 2000; Johnson *et al.,* 2002). A similar, but reduced, response was also observed among the cardiac frequency data (downhill: 91 b.min^{-1} [±2]: 6% less than level; 21% less than uphill; $P<0.05$), consistent with the literature (Johnson *et al.,* 2002: 0.61 L.min^{-1} [±0.20]; Lloyd and Cooke, 2000: 89 b.min^{-1}), reflecting the reduction in oxygen demand during downhill walking as a result of the increased transfer of potential to kinetic energy. Within this investigation, the reduction in oxygen consumption did not remain constant with changes in body mass, with heavier individuals experiencing a greater reduction in oxygen uptake (percentage change from level walking: 10 lightest: 22% reduction [178 mL.min^{-1}]; 10 heaviest: 28% reduction [358 mL.min^{-1}]; Figure 4.3; $P<0.05$). A similar observation had not been found reported within the literature, and may be a novel observation due to the mass range tested in this investigation.

The mass-dependent decrease in oxygen consumption during downhill walking is believed to be an artefact of the reduction in concentric energy required to lift the body's mass (Minetti *et al.,* 2002; Gottschall and Kram, 2006) and the increase in eccentric muscle activation during the gait cycle (Minetti *et al.,* 1993). During eccentric work, elastic strain energy is stored within the muscle fascicles, tendons (Asmussen and Bonde-Petersen, 1974; Alexander and Bennet-Clark, 1977; Blickhan, 1989) and the titin proteins of the sarcomere (Herzog, 2014; Monroy *et al.,* 2017) which produces an elastic recoil when the force direction changes. In this way, the muscle-fibre cross bridges develop tension while stretching without the production of adenosine triphosphate (Davies, 1971; Curtin and Davies, 1975). That stored energy is released back into the gait cycle as kinetic energy, reducing oxygen consumption (Aura and Komi, 1986; Herzog, 2018) and thereby decreasing the metabolic cost of movement. The magnitude of energy transferred during that process is proportional to the pre-stretch load. Since the pre-stretch is increased by the carriage of a greater load (mass; Abe *et al.,* 2008), it is possible that within the present investigation, a similar response was observed among the heavier participants, resulting in a more economical gait cycle. Such a response could be used to inform rehabilitative prescriptions, where eccentric loading is used to rebuild muscle strength without overloading the cardiovascular system, or, be used to increase the accuracy of predicted energy

expenditure during walking.

It was initially anticipated that, in accordance with the allometric cascade theory[35] (Darveau *et al.,* 2002), the mass exponent for each gradient would be modified according to the respective change in metabolic intensity. However, the relationship between metabolic intensity and the mass exponent does not appear to be as sensitive in humans as initially expected. Although walking oxygen consumption decreased by a greater percentage during downhill walking, thereby resulting in significantly lower mean absolute oxygen consumption compared with level and uphill walking (Section 4.3.2; $P<0.05$), the mass exponent was not significantly modified (Hypothesis Four-Three rejected; Figure 4.4; $P>0.05$). However, there was a non-significant decrease in the mass exponent (uphill: mass$^{0.77}$ [untransformed]; downhill: mass$^{0.63}$ [untransformed]; level: mass$^{0.86}$ [untransformed]; Figure 4.4; $P>0.05$; Hypothesis Four-Two accepted), which resulted in the disproportionate decreases in oxygen consumption across the body-mass range ($P<0.05$). Therefore, in this instance, there is a biologically-meaningful change in oxygen consumption that was not statistically evident between scaling regressions. This warrants further investigations. Nevertheless, statistically, the outcomes indicated that three unique metabolic intensities could all be scaled using the same mass exponent, even though the relative change in oxygen consumption was not consistent between conditions (Figure 4.3; $P<0.05$). Moreover, as neither gradient exponent differed from mass$^{0.80}$ (Chapter 3; $P>0.05$), both conditions could be described using this same universal exercise-intensity exponent. It is hypothesised that, once exercising, a relative change in metabolic intensity may not further modify the mass exponent. However, it remains uncertain whether a stronger mass response, and thus a non-relative change in oxygen consumption, would be observed at a steeper gradient.

4.5 CONCLUSION

This was the first investigation where the scaling regressions for uphill, downhill and level walking were individually determined using a controlled sample, and

[35] The allometric cascade theory details an increase in mass exponent value as metabolic intensity increases, due to the shift in cellular respiration pathways and transition from an energy demand to energy supply state (Darveau *et al.,* 2002).

subsequently compared to identify the effect of a gradient change. Prior to this experiment, it was uncertain whether a change in walking gradient would exaggerate any size-dependent responses to walking at a fixed velocity, and thereby modify the mass exponent observed during level walking. Among the three conditions, mean oxygen consumption and cardiac frequency data differed significantly. However, the three mass exponents did not reflect those mean responses, and, unexpectedly, did not differ significantly, despite the moderate mass-response observed during downhill walking. Moreover, those mass exponents were not dissimilar to the universal exponent derived for metabolic data during exercise in Chapter 3 ($mass^{0.80}$). It is hypothesised that a similar scaling response would be observed among all exercise intensities, providing that the condition does not exaggerate any mass response.

4.6 REFERENCES

Abe, D., Muraki, S., and Yasukouchi, A. (2008). Ergonomic effects of load carriage on energy cost of gradient walking. *Applied Ergonomics*. 39(2):144-149.

Alexander, R.M., and Bennet-Clark, H.C. (1977). Storage of elastic strain energy in muscle and other tissues. *Nature*. 265(5590):114.

Asmussen, E., and Bonde-Petersen, F. (1974). Storage of elastic energy in skeletal muscles in man. *Acta Physiologica*. 91(3):385-392.

Aura, O., and Komi, P.V. (1986). The mechanical efficiency of locomotion in men and women with special emphasis on stretch-shortening cycle exercises. *European Journal of Applied Physiology and Occupational Physiology*. 55(1):37-43.

Batterham, A.M., and Jackson, A.S. (2003). Validity of the allometric cascade model at submaximal and maximal metabolic rates in exercising men. *Respiratory Physiology and Neurobiology*. 135(1):103-106.

Blickhan, R. (1989). The spring-mass model for running and hopping. *Journal of Biomechanics*. 22(11-12):1217-1227.

Borghols, E.A.M., Dresen, M.H.W., and Hollander, A.P. (1978). Influence of heavy weight carrying on the cardiorespiratory system during exercise. *European Journal of Applied Physiology and Occupational Physiology*. 38(3):161-169.

Cavagna, G.A., Heglund, N.C., and Taylor, C.R. (1977). Mechanical work in terrestrial locomotion: two basic mechanisms for minimizing energy expenditure. *American Journal of Physiology-Regulatory, Integrative and Comparative Physiology*. 233(5):R243-R261.

Cohen, Y., Robbins, C.T., and Davitt, B.B. (1978). Oxygen utilization by elk calves during horizontal and vertical locomotion compared to other species. *Comparative Biochemistry and Physiology--Part A: Physiology*. 61(1):43-48.

Cook, R.D. (1977). Detection of influential observation in linear regression. *Technometrics*. 19(1):15-18.

Cook, R.D., and Weisberg, S. (1982). *Residuals and influence in regression*. Chapman and Hall, New York.

Curtin, N.A., and Davies, R.E. (1975). Very high tension with very little ATP breakdown by active skeletal muscle. *Journal of Mechanochemistry and Cell Motility*. 3(2):147-154.

Darveau, C.A., Suarez, R.K., Andrews, R.D., and Hochachka, P.W. (2002). Allometric cascade as a unifying principle of body mass effects on metabolism. *Nature*. 417(6885):166-170.

Davies, W.E.A. (1971). The elastic constants of a two-phase composite material. *Journal of Physics D: Applied Physics*. 4(8):1176.

Dill, D.B. (1965). Oxygen used in horizontal and grade walking and running on the treadmill. *Journal of Applied Physiology*. 20(1):19-22.

Durbin, J., and Watson, G.S. (1950). Testing for serial correlation in least squares regression: I. *Biometrika*. 37(3/4):409-428.

Durbin, J., and Watson, G.S. (1951). Testing for serial correlation in least squares regression. II. *Biometrika*. 38(1/2):159-177.

Efron, B. (1979). Computers and the theory of statistics: thinking the unthinkable. *SIAM review*. 21(4):460-480.

Fox, J. (1991). *Regression diagnostics: An introduction*. Volume 79. Sage, London.

Fox, J. (1997). *Applied regression analysis, linear models, and related methods*. Sage, London.

Fox, J., and Weisberg, S. (2017). *An R Companion to Applied Regression.* Sage, London.

Franz, J.R., Lyddon, N.E., and Kram, R. (2012). Mechanical work performed by the individual legs during uphill and downhill walking. *Journal of Biomechanics*. 45(2):257-262.

Goldman, R.F., and Iampietro, P.F. (1962). Energy cost of load carriage. *Journal of Applied Physiology*. 17(4):675-676.

Gottschall, J.S., and Kram, R. (2006). Mechanical energy fluctuations during hill walking: the effects of slope on inverted pendulum exchange. *Journal of Experimental Biology*. 209(24):4895-4900.

Hair, J.F., Anderson, R.E., Tatham, R.L., and Black, W.C. (1998). *Multivariate data analysis*. Prentice-Hall International, Upper Saddle River, NJ.

Halsey, L.G., and White, C.R. (2017). A different angle: comparative analyses of whole-animal transport costs when running uphill. *Journal of Experimental Biology*. 220(2):161-166.

Herzog,W. (2014). The role of titin in eccentric muscle contraction. *Journal of Experimental Biology*. 217(16):2825-2833.

Herzog, W. (2018). Why are muscles strong, and why do they require little energy in eccentric action? *Journal of Sport and Health Science*. 7(3):255-264.

Hill, A.V. (1927). *Muscular Movement in Man: The Factors Governing Speed and Recovery from Fatigue*. McGraw-Hill, New York.

Hunter, L.C., Hendrix, E.C., and Dean, J.C. (2010). The cost of walking downhill: is the preferred gait energetically optimal? *Journal of Biomechanics*. 43(10):1910-1915.

Jamnik, V., Gumienak, R., and Gledhill, N. (2013). Developing legally defensible physiological employment standards for prominent physically demanding public safety occupations: a Canadian perspective. *European Journal of Applied Physiology*. 113(10):2447-2457.

Jansson, M. (1985). A comparison of detransformed logarithmic regressions and power function regressions. *Geografiska Annaler: Series A, Physical Geography*. 67(1-2):61-70.

Johnson, A.T., Benjamin, M.B., and Silverman, N. (2002). Oxygen consumption, heat production, and muscular efficiency during uphill and downhill walking. *Applied Ergonomics*. 33(5):485-491.

Landers, G.J., Ong, K.B., Ackland, T.R., Blanksby, B.A., Main, L.C., and Smith, D. (2013). Kinanthropometric differences between 1997 World championship junior elite and 2011 national junior elite triathletes. *Journal of Science and Medicine in Sport*. 16(5):444-449.

Laursen, B., Ekner, D., Simonsen, E.B., Voigt, M., and Sjøgaard, G. (2000). Kinetics and energetics during uphill and downhill carrying of different weights. *Applied Ergonomics*. 31(2):159-166.

Lloyd, R., and Cooke, C.B. (2000). Kinetic changes associated with load carriage using two rucksack designs. *Ergonomics*. 43(9):1331-1341.

Maloiy, G.M.O., Heglund, N.C., Prager, L.M., Cavagna, G.A., and Taylor, C.R. (1986). Energetic cost of carrying loads: have African women discovered an economic way? *Nature*. 319(6055):668-669.

Margaria, R. (1968). Positive and negative work performances and their efficiencies in human locomotion. *Internationale Zeitschrift für angewandte Physiologie einschließlich Arbeitsphysiologie*. 25(4):339-351.

Minetti, A.E., Ardigo, L.P., and Saibene, F. (1993). Mechanical determinants of gradient walking energetics in man. *The Journal of Physiology*. 472(1):725-735.

Minetti, A.E., Moia, C., Roi, G.S., Susta, D., and Ferretti, G. (2002). Energy cost of walking and running at extreme uphill and downhill slopes. *Journal of Applied Physiology*. 93(3):1039-1046.

Monroy, J.A., Powers, K.L., Pace, C.M., Uyeno, T., and Nishikawa, K.C. (2017). Effects of activation on the elastic properties of intact soleus muscles with a deletion in titin. *Journal of Experimental Biology*. 220(5):828-836.

Monsch, E.D., Franz, C.O., and Dean, J.C. (2012). The effects of gait strategy on metabolic rate and indicators of stability during downhill walking. *Journal of Biomechanics*. 45(11):1928-1933.

Nadel, E.R., Bergh, U., and Saltin, B. (1972). Body temperatures during negative work exercise. *Journal of Applied Physiology*. 33(5):553-558.

Newman, M.C. (1993). Regression analysis of log transformed data: Statistical bias and its correction. *Environmental Toxicology and Chemistry*. 12(6):1129-1133.

Pal, M.S., Majumdar, D., Pramanik, A., Chowdhury, B., and Majumdar, D. (2014). Optimum load for carriage by Indian soldiers on different uphill gradients at specified walking speed. *International Journal of Industrial Ergonomics*. 44(2):260-265.

Pearson, K. (1900). Mathematical contributions to the theory of evolution. VIII. On the correlation of characters not quantitatively measurable. *Proceedings of the Royal Society of London*. 66(424-433):241-244.

Pearson, K. (1920). Notes on the history of correlation. *Biometrika*. 13(1):25-45.

Pinch, F.C., and Claussen, D.L. (2003). Effects of temperature and slope on the sprint speed and stamina of the Eastern Fence Lizard, Sceloporus undulatus. *Journal of Herpetology*. 37(4):671-679.

Pivarnik, J.M., and Sherman, N.W. (1990). Responses of aerobically fit men and women to uphill/downhill walking and slow jogging. *Medicine and Science in Sports and Exercise*. 22(1):127-130.

Rogers, D.M., Olson, B.L., and Wilmore, J.H. (1995). Scaling for the $\dot{V}O_2$-to-body size relationship among children and adults. *Journal of Applied Physiology*. 79(3):958-967.

Ross, W.D., and Ward, R. (1985). *The O-scale system*. Rosscraft, Surrey, BC.

Ross, W.D., and Wilson, N.C. (1974). A stratagem for proportional growth assessment. *Acta Paediatrica Belgica*. 28:169-182.

Sagiv, M., Ben-Gal, S., and Ben-Sira, D. (2000). Effects of gradient and load carried on human haemodynamic responses during treadmill walking. *European Journal of Applied Physiology*. 83(1):47-50.

Scaglioni-Solano, P., and Aragón-Vargas, L.F. (2015). Age-related differences when walking downhill on different sloped terrains. *Gait and Posture*. 41(1):153-158.

Shapiro, S.S., and Wilk, M.B. (1965). An analysis of variance test for normality (complete samples). *Biometrika*. 52(3/4):591-611.

Soule, R.G., and Goldman, R.F. (1969). Energy cost of loads carried on the head, hands, or feet. *Journal of Applied Physiology*. 27(5):687-690.

Taylor, C.R., Caldwell, S.L., and Rowntree, V.J. (1972). Running up and down hills: some consequences of size. *Science*. 178(4065):1096-1097.

Taylor, C.R., Schmidt-Nielsen, K., and Raab, J.L. (1970). Scaling of energetic cost of running to body size in mammals. *American Journal of Physiology-Legacy Content*. 219(4):1104-1107.

Taylor, N.A.S., Lewis, M.C., Notley, S.R., and Peoples, G.E. (2012). A fractionation of the physiological burden of the personal protective equipment worn by firefighters. *European Journal of Applied Physiology*. 112(8):2913-2921.

Xiao, X., White, E.P., Hooten, M.B., and Durham, S.L. (2011). On the use of log transformation vs. nonlinear regression for analyzing biological power laws. *Ecology*. 92(10):1887-1894.

Williams, D.A. (1987). Generalized linear model diagnostics using the deviance and single case deletions. *Applied Statistics*. 36(2):181-191.

Workman, J.M., and Armstrong, B.W. (1963). Oxygen cost of treadmill walking. *Journal of Applied Physiology*. 18(4):798-803.

Wyndham, C.H., Van der Walt, W.H., Van Rensburg, A.J., Rogers, G.G., and Strydom, N.B. (1971). The influence of body weight on energy expenditure during walking on a road and on a treadmill. *Internationale Zeitschrift für Angewandte Physiologie Einschließlich Arbeitsphysiologie*. 29(4):285-292.

CHAPTER 5: SCALING STEADY-STATE, STANDING AND AMBULATORY OXYGEN CONSUMPTION DURING TORSO-BORNE LOAD CARRIAGE

5.1 INTRODUCTION

Throughout the physiological range of metabolic intensity (basal [supine] to peak exercise [running]), oxygen consumption scales by a non-linear, allometric[36] regression against body mass (Chapters 2-4). In humans, the slope of that relationship can be described using either of two intensity-specific body-mass exponents: $mass^{0.54}$ (rest: Chapter 2) and $mass^{0.80}$ (exercise: Chapters 3 and 4)[37]. However, since the scaling exponent can be influenced by a change in metabolic intensity, it might be affected by other variables that might modify oxygen consumption. Load carriage is one such stimulus, wherein oxygen consumption increases with the mass (load) carried (Pandolf *et al.,* 1977; Soule *et al.,* 1978; Taylor *et al.,* 2016). Although much work has been performed exploring the mean effects of load carriage (Goldmand and Iampietro, 1962; Datta and Ramanathan, 1971; Taylor *et al.,* 2012), this theme has yet to be extended to a whole-body scaling context in humans. Accordingly, the primary aim within this investigation was to explore how load carriage might modify the mass exponent during steady-state metabolic intensities.

Load carriage has a mass-dependent relationship with oxygen consumption, whereby its relative metabolic impact is proportional to the change in total mass (Goldman and Iampietro, 1962; Taylor *et al.,* 1980; Taylor *et al.,* 2016). Consequently, the metabolic response to load carriage across a wide body-mass range will vary depending upon whether that load is a relative (percentage of body mass) or fixed mass. The former loading strategy was anticipated to have minimal effect on the mass exponent, producing a similar elevation in oxygen consumption across the body-mass range (Taylor *et al.,* 1980; Maloiy *et al.,* 1986; Silder *et al.,* 2013), which, when plotted, is unlikely to change the regression shape, only shift it upwards on the

[36] The allometric regression for the scaling relationship between oxygen consumption ($L.min^{-1}$) and body mass (kg) is defined using the equation $y = ax^b$, where y is oxygen consumption, a is the multiplicative constant, x is body mass and b is the mass exponent. The mass exponent "b" determines the shape of the regression curve. Consequently, differences in this value can be used to identify changes in regression models between conditions.

[37] Both body-mass exponents stated are taken from the untransformed, non-linear models, and can, therefore, be directly applied to raw oxygen consumption data ($L.min^{-1}$).

ordinate. In contrast, when a fixed-mass load is applied to a sample that varies in body mass, the lightest individuals must work relatively harder than the heaviest individuals, as they are carrying a greater percentage of their unloaded body mass (Soule *et al.,* 1978; Taylor *et al.,* 1980; Taylor *et al.,* 2016). This response would produce a greater relative increase in nett oxygen consumption (loaded less unloaded) as body mass decreases, which, when plotted, may flatten the regression, possibly reducing the body-mass exponent. Accordingly, when considering the potential effects of load carriage on the scaling exponent, the exponent is more likely to be influenced by fixed- rather than relative-mass loading. As this was a novel research theme, the loading strategy deemed more likely to modify the scaling exponent was selected for the investigation; thus, fixed-mass loading was selected.

In relation to this investigation, the mean metabolic response to load carriage can be influenced by two changes to metabolic intensity: movement and the mass of the load carried. During standing, providing that any external mass is carried close to the body, the total mass is carried relatively passively by the skeletal structure of the body (Kinoshita, 1985; Abe *et al.,* 2004, 2008; Attwells *et al.,* 2006). As a result, it is not anticipated that load carriage will modify the mass exponent during this metabolic intensity. However, with the introduction of movement (ambulation), a significant increase in oxygen consumption can be observed, reflecting the energy required to both support and move the body (Taylor *et al.,* 1970, 1974, 1982; Cavagna and Kaneko, 1977; Abe *et al.,* 2008), as discussed above. That metabolic response increases further with an increase in total mass (Goldman and Iampietro, 1962; Griffin *et al.,* 2003; Grabowski *et al,.* 2005). As a stepwise relationship was realised between the scaling exponent and metabolic intensity during unloaded states (Section 3.3.3; $P < 0.05$), it is anticipated that with the greater increase in oxygen consumption during loaded ambulation, a similar outcome will be observed between those two loaded metabolic intensities (standing and walking).

In addition to load carriage during level walking, the effect of the ambulatory gradient was also considered. Although the body-mass exponent was not modified by a $\pm 5\%$ gradient change during unloaded walking (Chapter 4), it was important to consider how an increase in total mass might influence that outcome. Such a consideration has

both basic and applied physiological outcomes.

The increase in oxygen consumption during uphill walking is associated with the greater mechanical work required to overcome the force of gravity (Hill, 1927; Workman and Armstrong, 1963; Johnson *et al.,* 2002): a gain in potential energy[38]. That relationship is mass-dependent (Dill, 1965; Taylor *et al.,* 1970; Cohen *et al.,* 1978), with nett absolute oxygen consumption increasing with the total mass carried (Goldman and Iampietro, 1962; Workman and Armstrong, 1963; Taylor *et al.,* 1972). During unloaded walking, the mass-specific oxygen cost of vertical ascent is constant across the human mass range (1.40 $mL.kg^{-1}.m^{-1}$: Chapter 4). Accordingly, since the mechanical cost of movement remains consistent with a change in total mass (Heglund, 1979; Halsey and White, 2017), it is expected that the mass-specific cost of vertical movement will remain consistent with a change in total mass. Therefore, it is not expected that the mass exponent will be modified during loaded walking by changes in the ambulatory gradient, for the relative change in regression models will be comparable to the unloaded trials (Chapter 4).

In contrast, oxygen consumption decreases during downhill walking (Minetti *et al.,* 1993; Johnson *et al.,* 2002). The downwards displacement of the body, assisted by the force of gravity, transfers energy into the body: some thermal energy accumulates within the eccentrically activated muscles (Nadel *et al,.* 1972), and, the rest, appears as energy within the gait cycle (kinetic energy), reducing the demand for mechanical work (Margaria, 1968; Cavagna *et al.,* 1977). In Chapter 4, an energy-saving mechanism was observed in the heavier participants during downhill-walking. It was speculated that the increase in mass resulted in a greater pre-stretch load during the eccentric muscle activation phase (Abe *et al.,* 2008), thus storing more strain energy that can be reused (Asmussen and Bonde-Petersen, 1974; Alexander and Bennet-Clark, 1977; Blickhan, 1989). However, the extent of that potential mechanism on the kinetics of downhill walking remains uncertain. It is possible that a similar relationship will be observable with an increase in total mass (load carriage),

[38] Potential energy is gained during ascents and lost during descents, relative to the body's original position. Potential energy is the product of the body's mass and its vertical displacement: $E_p = mgh$, where E_p is potential energy (J), m is body mass (kg), g is the gravitational constant (N) and h is the distance of the body's displacement (m).

with the most pronounced response occurring among the lightest individuals due to the relative physiological strain of carrying a fixed-mass. Nevertheless, it is important to remember that even though this response was observed during the unloaded trials, that change in walking energy expenditure did not translate to a change in the scaling exponent (Chapter 4). Therefore, it is also unlikely that a change to the mass exponent will be observed during loaded downhill walking.

An alternative method to describe the oxygen cost of load carriage is to consider the total mass[39] carried by an individual (Taylor *et al.,* 2011, 2012, 2016). During loaded ambulatory states, the mechanical work of walking increases to maintain the vertical and horizontal movement of the gait cycle while supporting the mass carried (Cavagna and Kaneko, 1977; Gottschall and Kram, 2005). This increases the demand for oxygen consumption at the working muscles, and thus the metabolic cost of walking. Thus, oxygen consumption is determined by the total mass supported by the legs, rather than just the metabolically active tissues of the body (Goldman and Iampietro, 1962; Soule *et al.,* 1978; Taylor *et al.,* 2016). As a result, scaling against body mass alone may not provide a true representation of the scaling relationship during the test condition, for the metabolic rate of those tissues will appear elevated in comparison to the unloaded trials (Taylor *et al.,* 2012, 2016).

It has been demonstrated that, per kilogram of mass, the mechanical cost of walking remains constant with an increase in total mass (Heglund, 1979). A similar observation has been reported for the mass-specific increase in nett oxygen consumption with load carriage relative to an unloaded state (mL oxygen per kilogram of added mass: Goldman and Iampietro, 1962; Soule *et al.,* 1978; Taylor *et al.,* 2012). Therefore, when considering the mean response to load carriage, it is plausible to accept a proportional relationship between total mass and oxygen consumption during ambulation, whether it is due to growth (increase in body mass) or external load carriage. Whether or not these relationships change across the body-mass range remains unclear; however, they demonstrate a strong relationship between total mass and ambulatory oxygen consumption. Consequently, if the body-mass exponent is

[39] The term "total mass" has been used to refer to the sum of a subject's body mass, clothing and all external loads worn or carried by the body.

expected to be influenced by load carriage, it may be more appropriate to scale oxygen consumption during loaded ambulation against total mass instead. If applicable, this scaling option could simplify the way that ambulatory oxygen consumption during loaded states is described and normalised, and this possibility was also explored.

Accordingly, within this phase, the effect of load carriage (total mass change) on the mass exponents used to describe the relationship between oxygen consumption and body mass was explored. This was achieved by placing a fixed-mass load about the torso of a large sample of individuals, who varied in body mass from 56 kg to 117 kg. Such loading simulates both an increase in body mass and external load carriage. By using the same sample tested in Chapters 2-4 (unloaded trials), it was possible to maintain a repeated-measures design to the project. Trials were conducted during standing, level walking, uphill walking and downhill walking conditions. Oxygen consumption was scaled against both body mass and total mass to determine which mass exponent was most appropriate during those loaded states. To effectively assess that aim, four experimental hypotheses were developed, based on the assumption that the relationship between oxygen consumption and body mass would remain non-linear (allometric) during load carriage.

Hypothesis Five-One: During standing (rest), the unloaded body-mass exponent will not be significantly modified during fixed-mass, torso-borne load carriage.
Hypothesis Five-Two: During steady-state walking, the unloaded body-mass exponent will be significantly decreased during fixed-mass, torso-borne load carriage during both uphill and downhill ambulatory gradients.
Hypothesis Five-Three: Oxygen consumption during loaded steady-state walking will more precisely scale against the total mass (body mass, clothing and all external loads) than body mass, regardless of the ambulatory gradient.
Hypothesis Five-Four: During torso-borne load carriage (walking), the mass exponent (body or total mass) will not be modified by a change in ambulatory gradient (-5%, 0%, 5%).

5.2 METHODS

5.2.1 Subjects

The sample used to explore the scaling response to torso loading consisted of 72 healthy and physically active men across four variations in metabolic intensity (standing: $N=67$; level walking: $N=67$; uphill walking: $N=62$; downhill walking: $N=61$; Figure 5.1). Subjects were recruited from the local university population and nearby sports teams. This was the same sample tested in Chapters 2-4 with the exception of one participant, who, due to a previous injury, could not wear the torso load. Those participants had been evenly recruited across a two-fold mass range (56.0-117.1 kg) to permit scaling analyses. Furthermore, the sample was matched for physiological and morphological variables that could influence whole-body oxygen consumption (Section 2.2.1; Table 2.2; Figures 2.10 and 2.11). This included subcutaneous adiposity which has a similar effect on oxygen consumption as external, torso-borne load carriage (Goldman and Iampietro, 1962).

Subjects were screened to eliminate those with a history of cardiovascular, respiratory or musculo-skeletal pathologies contraindicative of participation in this experiment. Participants were supplied with an information package and provided written, informed consent before commencing the trials. The experimental procedures performed within this experimental phase were approved by the Human Research Ethics Committee (University of Wollongong; HE14/469).

5.2.2 Procedural overview

To compare the effect of torso loading on the scaling relationship between oxygen consumption and body mass, participants were tested across four submaximal, bipedal intensities: standing, level walking, uphill walking (5%) and downhill walking (-5%). Those four conditions corresponded with states tested within Chapters 2-4 (unloaded), therefore, within this experimental phase, data were only collected while participants wore the torso loads (25-kg weighted vest: Figure 5.2A), then were compared with the previously-tested unloaded datasets. Each metabolic intensity was tested on a separate visit at the laboratory, with both loading conditions (unloaded and loaded) completed during the same visit. The trial and load-configuration orders were balanced across participants using a Latin Square design. During each of these trials,

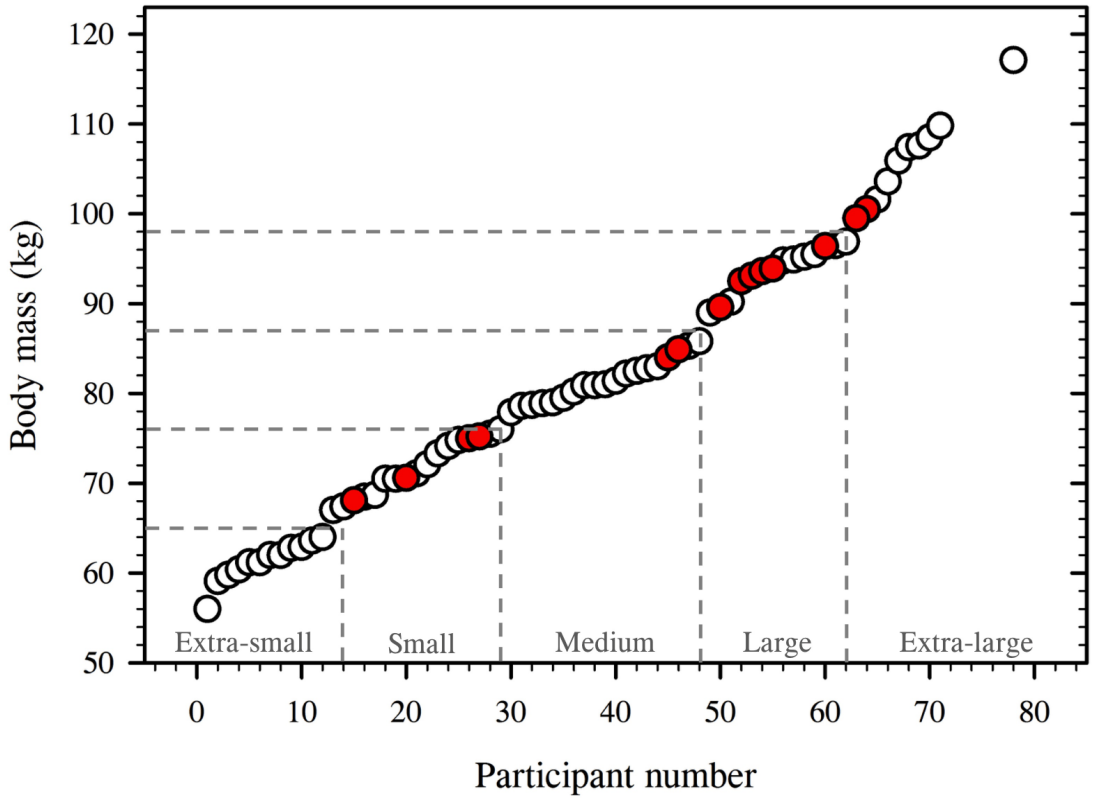

Figure 5.1: Scatter plot displaying the mass distribution of the sample, with participants arranged in ascending order of body mass. Data points are displayed for the full 72 participants who completed testing in the wider project (standing: $N=67$; level walking: $N=67$; uphill walking: $N=62$; downhill walking: $N=61$). Partial datasets are identified using the red symbols. The drop-lines signify the borders separating each of the five body-mass groups and their sample sizes.

Figure 5.2: (Figure 5.2A) During the loaded trials, participants wore a 25-kg weighted vest over a standardised clothing ensemble (t-shirt and combat trousers, pre-fitted by researchers, and their own running shoes). The mass of the vest was evenly balanced between front and back panels to minimise postural changes. Movement of the load was minimised using Velcro adjustment waist-straps to comfortably secure the vest to the torso. A load of 25 kg was selected as it corresponded with the mass carried on the torso by the Riflemen in the Australian Defence Force[40]. Figure 5.2B displays the adjustable ankle weights worn by participants, in addition to their own running shoes, to standardise load carriage at the feet.

[40] This project was funded by the Defence Science and Technology group, with the secondary aim of exploring the interactions between load carriage and body size in a military context.

subjects wore standardised clothing (t-shirt and combat trousers) and wore their own running shoes. In addition, due to differences in the mass of those shoes, ankle weights were worn to standardise the load worn at each limb to 500 g (Figure 5.2B).

The trial procedures can be separated into two main testing states: standing and walking. Standing data were collected during a 10-min (stationary) stage, immediately following the basal trial (Section 2.2.3.1). For each walking trial, baseline data were first collected during a 10-min standing stage, followed by a 15-min treadmill walk at the respective gradient (4.8 $km.h^{-1}$). Subjects had a 5-min rest between loaded and unloaded conditions in all trials. Before commencing the walking trials, participants completed two familiarisation sessions equipped with the testing equipment and torso load, and they were asked to walk at each of the three gradients for 10 min, to familiarise them with the testing requirements, thereby increasing test reliability (Jamnik *et al.,* 2013).

5.2.2.1 Measuring oxygen consumption

On arrival at the laboratory, both semi-nude and clothed (unshod) body masses were recorded, then, a cardiac frequency monitor and an oronasal mask (Figure 2.4B) were positioned. For the standing trial, subjects had first completed the basal condition (Section 2.2.3.1). Due to the carefully applied standardisation procedures (Section 2.2.4), they were in a well-rested and fasted state. Between the basal and standing states, participants had a 5-min rest, before the upright oxygen consumption measurement commenced. Both unloaded (Chapter 2) and loaded (25-kg weighted vest: Figure 5.2A) standing were completed on the same day, with a 5-min rest between conditions.

All walking trials started with a 10-min standing (stationary) baseline stage, after which, walking commenced. Participants walked on a treadmill (Pulsar 3p Treadmill, H/P/Cosmos, Traunstein, Germany) at 4.8 $km.h^{-1}$ for 15 min at their respective gradient during both unloaded (Chapters 3 and 4) and loaded (weighted vest) conditions, with a 5-min seated rest between successive stages.

5.2.3 Experimental standardisation

All testing was conducted in an air-conditioned laboratory (~23°C; ~50% humidity). Walking trials commenced at the same time of day (±1 h) within participants, to minimise potential circadian effects. Prior to those tests, participants were instructed to refrain from drinking caffeine for 6 h and to consume a pre-experimental meal high in carbohydrates and low in fats >2 h before starting the test. In contrast, the standing trials immediately followed the basal trial (~8am; Section 2.2.3.1), so the pre-test standardisation was more rigid (Section 2.2.4), resulting in participants being well rested, but also in a fasted (water only) state.

5.2.4 Experimental measurements

Oxygen consumption was estimated using open-circuit respirometry (TrueOne 2400, ParvoMedics Inc., Utah, U.S.A.: Crouter *et al.,* 2006; see Section 2.2.4.1 for details). Cardiac frequency was measured from ventricular depolarisation, using a cardiac frequency monitor (Plug in receiver, Polar Electro, Kempele, Finland: see Section 2.2.4.3 for details). Data were measured continuously as 15-s averages (respiratory measures) and intervals (cardiac frequency), and sampled during the last 5 min of each testing stage. Semi-nude and clothed (unshod) body masses were measured at the start of each testing session (MS3200, Medical Scale, Charder, Taichung, Taiwan: see Section 2.2.4.4 for details), while standing stretched-stature (Harpenden Stadiometer, Holtain Ltd., Crymych, UK) and six-site (triceps, subscapular, supraspinale, abdominal, anterior thigh, medial calf: Figure 2.6) subcutaneous adiposity (skinfolds: Eiken skinfold calliper, Meikosha, Tokyo, Japan) were measured once, on the subject's first visit at the laboratory (see Section 2.2.4.4 for details). To minimise size-related differences in absolute morphometric measurements, sum of skinfold and body mass data were normalised to a common standing height using Equation 2.5 (170.18 cm; Ross and Wilson, 1974). A criterion height-adjusted adiposity threshold of 88 mm was set for participant selection to control for variations in subcutaneous adiposity (60^{th} percentile: Ross and Ward, 1985; Landers *et al.,* 2013: see Section 2.2.1).

5.2.5 Design and analysis

5.2.5.1 Experimental design

The effect of load carriage was tested across four experimental conditions: standing, level walking, uphill walking and downhill walking (Figure 5.3 [coloured cells]). When combined with the respective unloaded trials (Chapters 2-4), this yielded an experiment that was based on a three-way, repeated-measures factorial design, with five levels of the first factor (body mass: extra-small, small, medium, large, extra-large]), four levels for the second factor (metabolic intensity: standing, level walking, uphill walking, downhill walking) and two levels of the third factor (load: unloaded and loaded). Participants acted as their own controls using a repeated-measures design. Data are presented as means with standard deviations (SD) standard errors of the mean ($\pm$) used to provide information regarding the data distribution and precision of the mean, respectively.

5.2.5.2 Data analysis

To confirm whether or not the scaling relationships remained non-linear (allometric: Equation 2.5) during load-carriage states, each dataset was assessed using the steps outlined in the decision-making chart (Figure 2.8). Specifically, for a model to be considered appropriate it had to satisfy the assumptions of linearity[41], thereby confirming the statistical fit of the regression (Poole and O'Farrell, 1971; Weisberg, 2014), as well as the biological assumption of an origin intercept (Sholl, 1948). The origin intercept demonstrates the ability for the model to describe the relationship between oxygen consumption and body mass beyond the tested mass range. Before performing these analyses on the non-linear models, data were first $\log_{10}$ transformed to generate a temporary linear relationship (Equation 2.6; Figure 2.9)[42].

[41] The assumptions of linearity: normal distribution, linearity, homeoscedasticity and no autocorrelation among variables.

[42] Due to the inherent error in applying a transformed regression equation to an untransformed dataset (Jansson, 1985; Newman, 1993; Xiao *et al.,* 2011), both $\log_{10}$-transformed and non-linear (allometric) regression coefficients are presented throughout this Chapter. The non-linear, allometric regression is the more appropriate method to use when predicting or normalising raw oxygen consumption data.

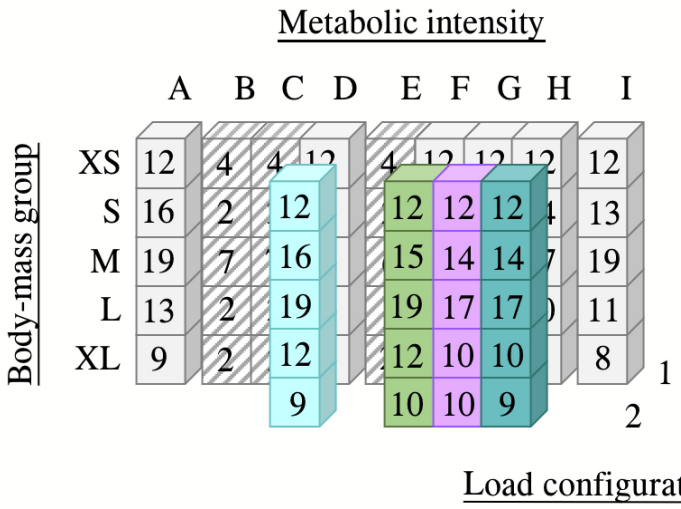

Figure 5.3: A schematic of the experimental design from Chapters 2 through to 5. Sample sizes are identified within each cell. The wider research phase consisted of a five by nine by two factorial design, with those factors measured within the current experimental phase identified by the coloured cells. The first factor (body mass) had five levels: extra-small (XS: $<$65 kg); small (S: 66-76 kg); medium (M: 77-87 kg); large (L: 88-98 kg); and extra-large (XL: $>$99 kg). The second factor (metabolic intensity) had nine levels: supine (Column A: basal, rest); 100% mass-supported standing (Column B: exploratory investigation); 50% mass-supported standing (Column C: exploratory investigation); standing (Column D); 50% mass-supported walking (Column E: exploratory investigation); level walking (Column F); uphill walking (Column G); downhill walking (Column H); peak exercise (Column I). The third factor (load configuration) had two levels: unloaded (1) and loaded (2: 25-kg weighted vest).

Bootstrapping[43] (Efron, 1979; Fox and Weisberg, 2017) was performed on each regression equation to generate means and standard errors of the mean for each regression coefficient. In this way, the regression equations assessed were considered the most likely fit for each metabolic intensity. To compare the effect of load carriage on the relationship between oxygen consumption and body mass, the regressions applied within this experimental phase were compared with those obtained during the unloaded trials performed in Chapters 2-4 (Table 5.1). Analyses of covariance were used to compare mass exponents between trials or mass-exponents (body mass and total mass). A null-hypothesis t-test was used to compare generated exponents against the exercise-specific exponent of mass$^{0.80}$. A significant interaction effect indicated the requirement to use different mass exponents between conditions. For the standing condition, shoe mass was not included in the calculation for total mass, as it was not supported by the body. As per previous Chapters, potential outliers that could influence the mass exponent were identified prior to scaling analyses using four separate tests: scatter plots, box plots, the Bonferroni test (Cook and Weisberg, 1982; Williams, 1987; Fox, 1997) and Cook's distance (Cook, 1977; Fox, 1991; Hair *et al.,* 1998; see Section 2.2.5.2 for details). Outliers that were flagged in two or more tests were highlighted for review by the researchers.

Mean morphological and physiological differences were compared between conditions using repeated-measures analyses of variance and within conditions among body-mass groups using one-way analysis of variance. Remaining differences in height-adjusted morphometric data (sum of skinfolds and body mass) were analysed using analysis of covariance to determine whether or not those variations influenced the mass exponent for each metabolic intensity tested.

5.3 RESULTS

5.3.1 Pre-experimental standardisation

Before performing any scaling analyses in this experimental phase, the morphometric homogeneity of the sample was assessed. The sample tested in this experiment was statistically similar to that used in Chapter 2 (Table 2.2; Figure 2.10; Figure 2.11),

[43] Each model was generated 1000 using a re-sampling approach from the original dataset.

Table 5.1: A summary table, extracted from Chapters 2-4 (Table 5.1A), of the unloaded, steady-state regression equations used to assess the effect of load carriage on the body-mass exponent. Table 5.1B: Intensity-specific body-mass exponents than can be used to describe oxygen consumption data throughout the physiological range of metabolic intensity (basal [supine] to peak exercise [running]).

Table 5.1A

	Non-linear regression equation	
Metabolic intensity	Untransformed	Log_{10} transformed
Standing (rest) [Chapter 2]	$y = 0.02 \cdot x^{\mathbf{0.68}}$	$y = \mathbf{0.65} \cdot x$ - 1.72
Level walking [Chapter 3]	$y = 0.02 \cdot x^{\mathbf{0.87}}$	$y = \mathbf{0.85} \cdot x$ - 1.61
Uphill walking [Chapter 4]	$y = 0.04 \cdot x^{\mathbf{0.83}}$	$y = \mathbf{0.81} \cdot x$ - 1.38
Downhill walking [Chapter 4]	$y = 0.03 \cdot x^{\mathbf{0.72}}$	$y = \mathbf{0.71} \cdot x$ - 1.48

Table 5.1B

	Untransformed exponents
Resting intensities [Chapter 2]	$x^{\mathbf{0.54}}$
Exercising intensities [Chapters 3 and 4]	$x^{\mathbf{0.80}}$

despite the missing participant (Figure 5.1). This meant that some differences still remained among the height-adjusted measures: two outliers for body mass (Figure 2.10C; $P<0.05$) and three outliers for sum of skinfolds (Figure 2.11C; $P<0.05$). Nevertheless, no significant interaction effect was realised for either height-adjusted measure in any of the scaling relationships tested in this phase ($P>0.05$). Since those remaining morphometric variations did not modify the observed mass exponents for the relationship between oxygen consumption and body mass, in any trial, it was not necessary to include those data as covariant variables when generating the scaling regressions. Therefore, for scaling purposes, the sample could be considered morphometrically homogeneous.

5.3.2 Assessing the regression assumptions

To test the hypothesis that the scaling relationship remained non-linear during load carriage, each dataset was evaluated using the decision-making flow chart (Figure 2.8). For either scaling model (linear or non-linear) to be considered suitable to describe the relationship between oxygen consumption and body mass, it had to satisfy the assumptions of linearity, equal error variance of the residuals, normality of the variables and no autocorrelation between these variables. Finally, the biological assumption of an origin intercept must be satisfied so that a realistic prediction of oxygen consumption could be obtained when body mass was equal to zero (Sholl, 1948).

Both linear and $\log_{10}$-transformed non-linear regressions were evaluated against these model assumptions, with only the latter satisfying both the statistical and biological assumptions. That is, a positive origin intercept was observed for all four linear regressions (standing: 0.11 L.min^{-1}; level walking: 0.42 L.min^{-1}; uphill walking: 0.54 L.min^{-1}; downhill walking: 0.40 L.min^{-1}; $P<0.05$). In contrast, when $\log_{10}$-transformed, all non-linear models displayed a linear relationship (Figures 5.4; $P<0.05$) with an equal error variance among those residuals (Figure 5.5). Moreover, the variables and model residuals were considered normally distributed at the 5% probability level, with skewness and kurtosis z-scores less than ± 3.26 (Kim, 2013; $P>0.05$) and a non-significant Shapiro-Wilk test (1965; $P>0.05$). Finally, no autocorrelation was observed (Durbin-Watson test 1950, 1951: $P>0.05$).

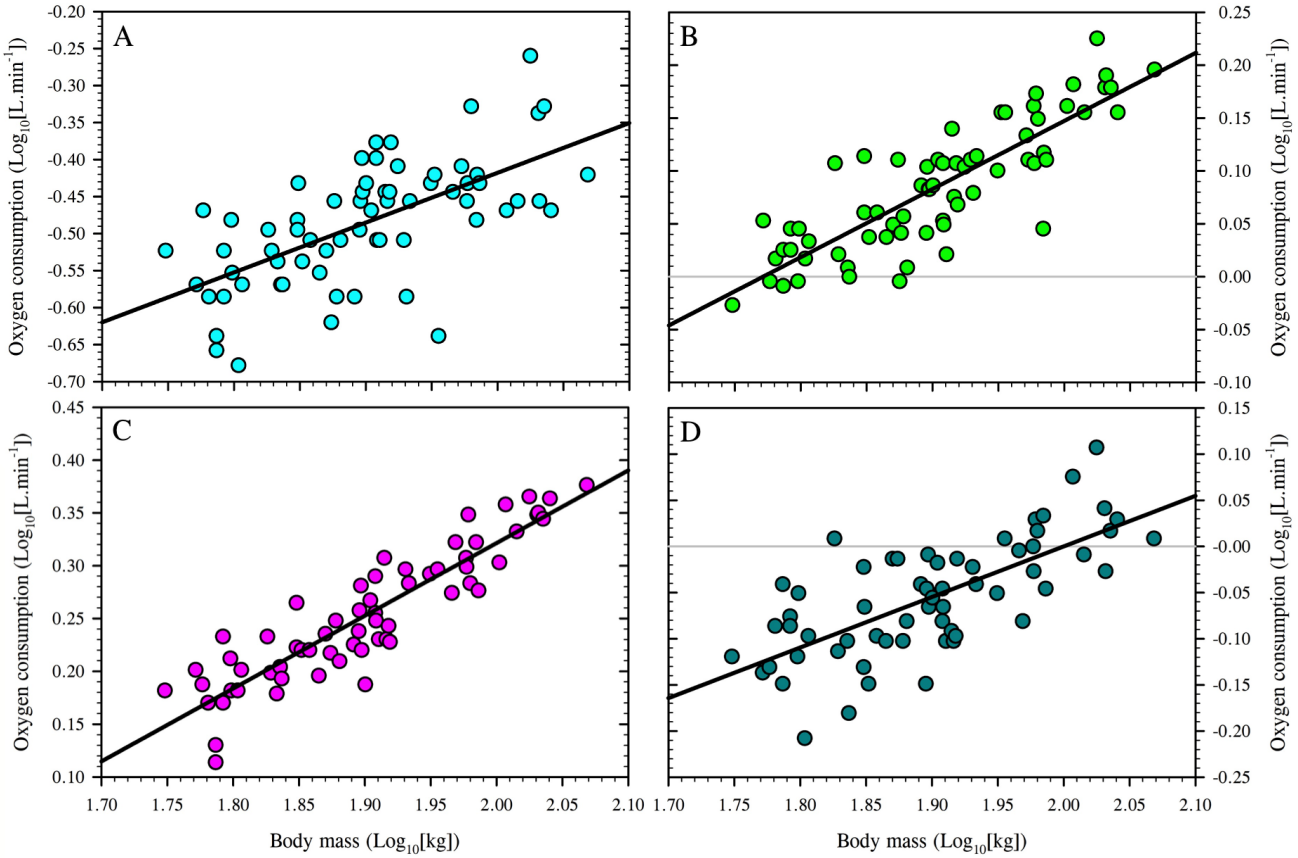

Figure 5.4: Scatter plots of the $\log_{10}$-transformed datasets for the four submaximal, bipedal metabolic intensities during torso loading (25-kg weighted vest): standing (N=67; r^2=0.41; Figure 5.4A), level walking (N=67;r^2=0.71; Figure 5.4B), uphill walking (N=62; r^2=0.82; Figure 5.4C) and downhill walking (N=61; r^2=0.49; Figure 5.4D).

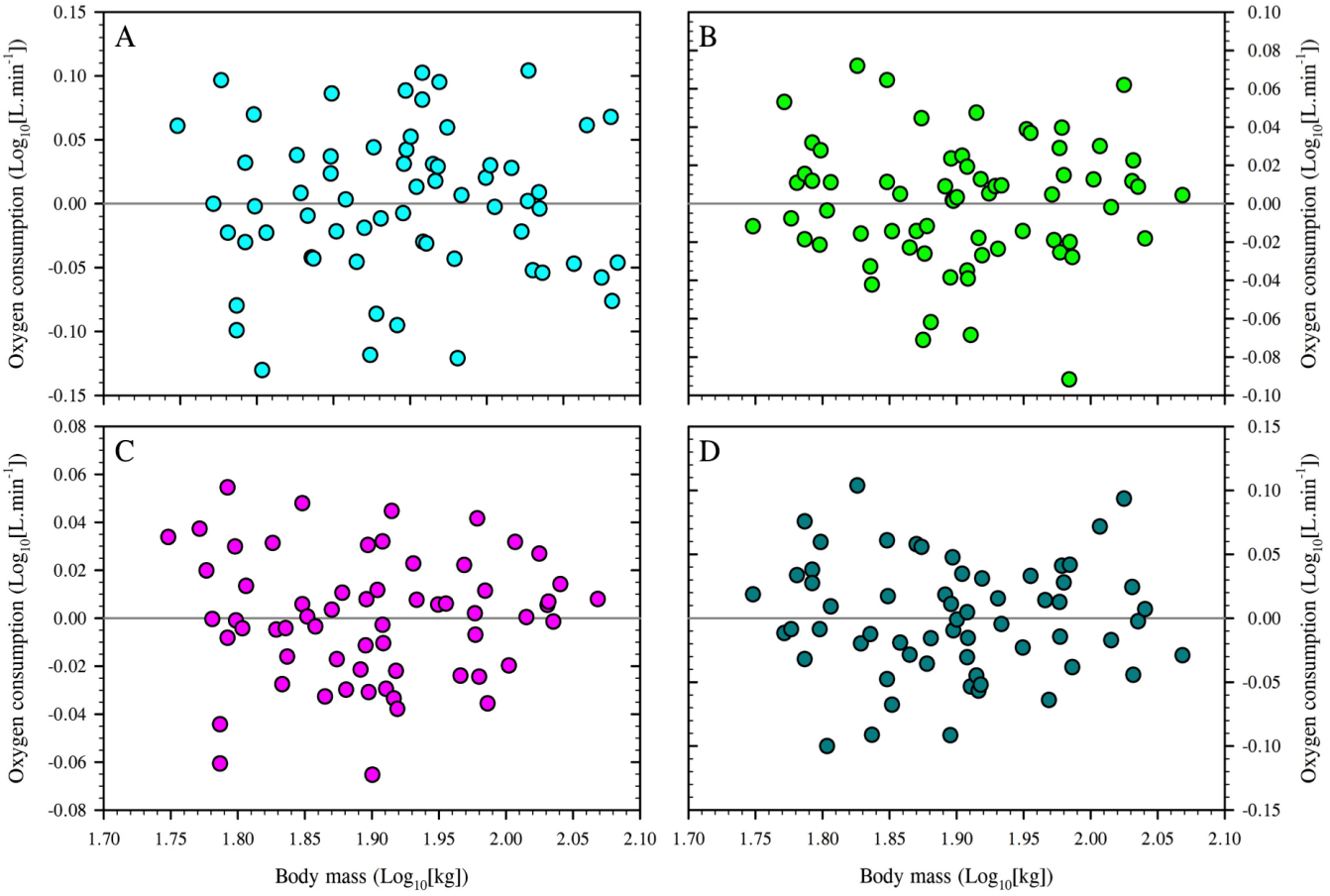

Figure 5.5: Residual plots used to assess the assumption of homeoscedasticity for the $\log_{10}$-transformed models. Data are presented for the four submaximal bipedal states during torso loading: standing (N=67; Figure 5.5A), level walking (N=67; Figure 5.5B), uphill walking (N=62; Figure 5.5C) and downhill walking (N=61; Figure 5.5D).

Consequently, non-linear scaling was the more suitable model to describe the four metabolic intensities, and, as the regression residuals were normally distributed, analysis of covariance could be confidently used to compare the mass exponents between trials.

5.3.3 Comparing the effect of load carriage on the body-mass exponent

During the standing trial, load carriage significantly increased cardiac frequency (Table 5.2; $P<0.02$) but had no significant impact on oxygen consumption (Table 5.2; $P>0.02$). Since oxygen consumption did not change between trials, the scaling regression and its corresponding body-mass exponent remained unchanged (Table 5.3; Figure 5.6; $P>0.05$). This led to the acceptance of Hypothesis Five-One.

During all three walking trials, both oxygen consumption and cardiac frequency significantly increased with load carriage (Table 5.2; $P<0.05$), indicating that while load carriage increased physiological strain during both standing and walking conditions, locomotion was required to significantly increase oxygen demand. As anticipated, the increase in oxygen consumption varied systematically across the body-mass range (Figure 5.7; $P<0.05$), increasing by a greater relative amount in the lightest individuals. Compared with unloaded walking, these increases in oxygen consumption resulted in a significantly smaller body-mass exponent during the loaded trials, regardless of the ambulatory gradient (Table 5.3; Figure 5.6; $P<0.05$). This outcome led to the acceptance of Hypothesis Five-Two.

5.3.3.1 Comparing the effect of gradient

During loaded ambulation, mean absolute oxygen consumption and cardiac frequency differed significantly among all three gradient conditions. Therefore, each ambulatory gradient represented a unique metabolic intensity. However, despite those differences in physiological strain, no interaction effect was observed for gradient among the three scaling models (Table 5.3; Figure 5.6; $P>0.05$). This led to the acceptance of Hypothesis Five-Four. Thus, a single scaling exponent could be used to describe oxygen consumption during the three trials. Accordingly, the level body-mass exponent was selected to describe that scaling relationship, as it was the central gradient in the range tested, and represented a commonly-tested walking condition.

Table 5.2: Mean oxygen consumption and cardiac frequency responses during standing and walking trials, with standard errors of the mean in parenthesis. Data are presented for unloaded (Chapters 2-4) and loaded (25-kg weighted vest) conditions. Sample sizes are presented for the unloaded conditions first (unloaded; loaded). Significant between-group differences are identified by the symbol (*; $P<0.05$). The Chapters from which those unloaded data are taken are identified using the abbreviations, whereby "C2" indicates Chapter 2.

Oxygen consumption ($L.min^{-1}$)	Standing ($N=68$; $N=67$)	Level walking ($N=68$; $N=67$)	Uphill walking ($N=63$; $N=62$)	Downhill walking ($N=62$; $N=61$)
Unloaded	0.33 (0.01) [C2]	1.02 (0.02) [C3]	1.46 (0.03) [C4]	0.73 (0.02) [C4]
Loaded	0.33 (0.01)	1.23 (0.02)*	1.81 (0.03)*	0.89 (0.02)*
Cardiac frequency ($b.min^{-1}$)				
Unloaded	80 (2) [C2]	97 (2) [C3]	115 (2) [C4]	91 (2) [C4]
Loaded	82 (2)*	107 (2)*	135 (2)*	99 (2)*

Table 5.3: Summary of scaling regressions for unloaded and loaded trials. The unloaded data have been taken from Chapters 2-4 (identified as C2-C4). Mean regression coefficients (generated using bootstrapping) are displayed for log_{10}-transformed and untransformed (allometric) equations. Body-mass and total-mass exponents are highlighted in bold. Sample sizes are displayed as unloaded then loaded conditions. Significant within-intensity differences for the effect of load carriage (25-kg weighted vest) are identified (*; $P<0.05$) for the log_{10}-transformed equations only.

	Unloaded trials	Loaded trials	
Log_{10}-transformed	Body-mass exponent	Body-mass exponent	Total-mass exponent
Standing (N=68; N=67)	$y=\mathbf{0.63} \cdot x$ - 1.68 [C2]	$y=\mathbf{0.67} \cdot x$ - 1.77	$y=\mathbf{0.90} \cdot x$ - 2.30
Level walking (N=68; N=67)	$y=\mathbf{0.85} \cdot x$ - 1.62 [C3]	$y=\mathbf{0.65} \cdot x$ - 1.15*	$y=\mathbf{0.87} \cdot x$ - 1.67
Uphill walking (N=63; N=62)	$y=\mathbf{0.81} \cdot x$ - 1.38 [C4]	$y=\mathbf{0.69} \cdot x$ - 1.06*	$y=\mathbf{0.92} \cdot x$ - 1.62
Downhill walking (N=62; N=61)	$y=\mathbf{0.71} \cdot x$ - 1.06 [C4]	$y=\mathbf{0.55} \cdot x$ - 1.10*	$y=\mathbf{0.74} \cdot x$ - 1.55
Untransformed			
Standing	$y=0.02 \cdot x^{\mathbf{0.66}}$ [C2]	$y=0.02 \cdot x^{\mathbf{0.63}}$	$y=0.00 \cdot x^{\mathbf{-0.67}}$
Level walking	$y=0.02 \cdot x^{\mathbf{0.86}}$ [C3]	$y=0.07 \cdot x^{\mathbf{0.66}}$	$y=0.02 \cdot x^{\mathbf{0.89}}$
Uphill walking	$y=0.05 \cdot x^{\mathbf{0.78}}$ [C4]	$y=0.11 \cdot x^{\mathbf{0.65}}$	$y=0.03 \cdot x^{\mathbf{0.88}}$
Downhill walking	$y=0.05 \cdot x^{\mathbf{0.64}}$ [C4]	$y=0.10 \cdot x^{\mathbf{0.52}}$	$y=0.04 \cdot x^{\mathbf{0.70}}$

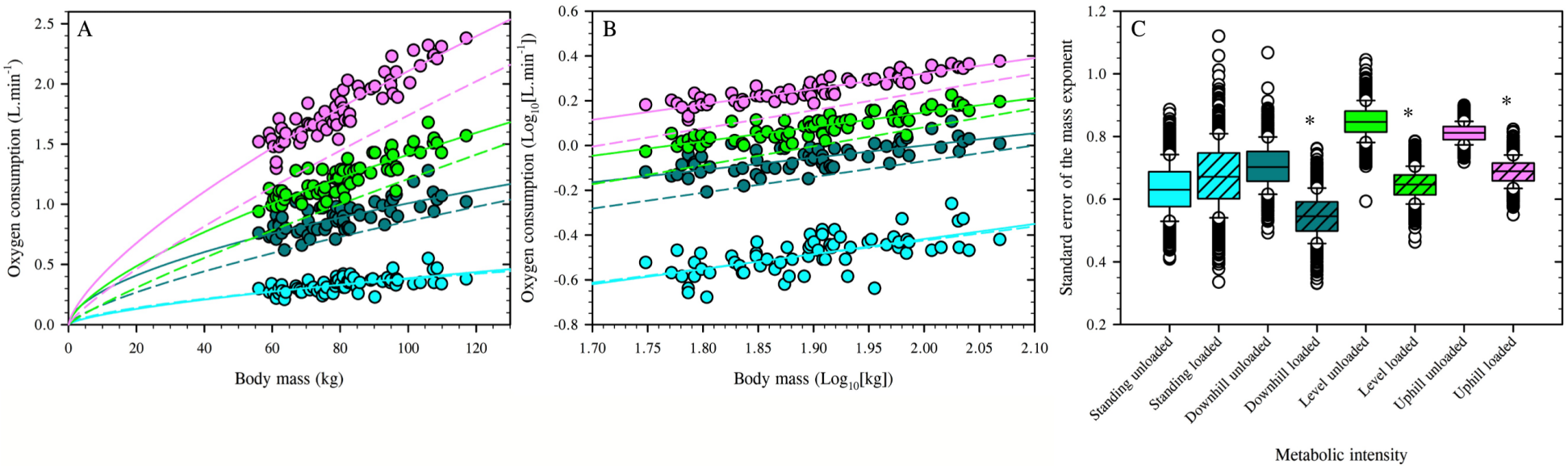

Figure 5.6: Scatter plots of the scaling relationships between oxygen consumption and body mass in untransformed (allometric: Figure 5.6A) and $\log_{10}$-transformed formats (Figure 5.6B). Data are presented for the load-carriage states during standing (N=67 [light blue]), downhill (N=61 [dark blue]), level (N=67 [green]) and uphill walking (N=62 [pink]) trials. The applied (load carriage) scaling regressions are identified by the solid lines. The respective unloaded regressions (dashed lines) have been superimposed for comparison. Figure 5.6C displays the bootstrapped means and standard errors of the means for each body-mass exponent. Significant, within-intensity, differences are highlighted (*; $P<0.05$).

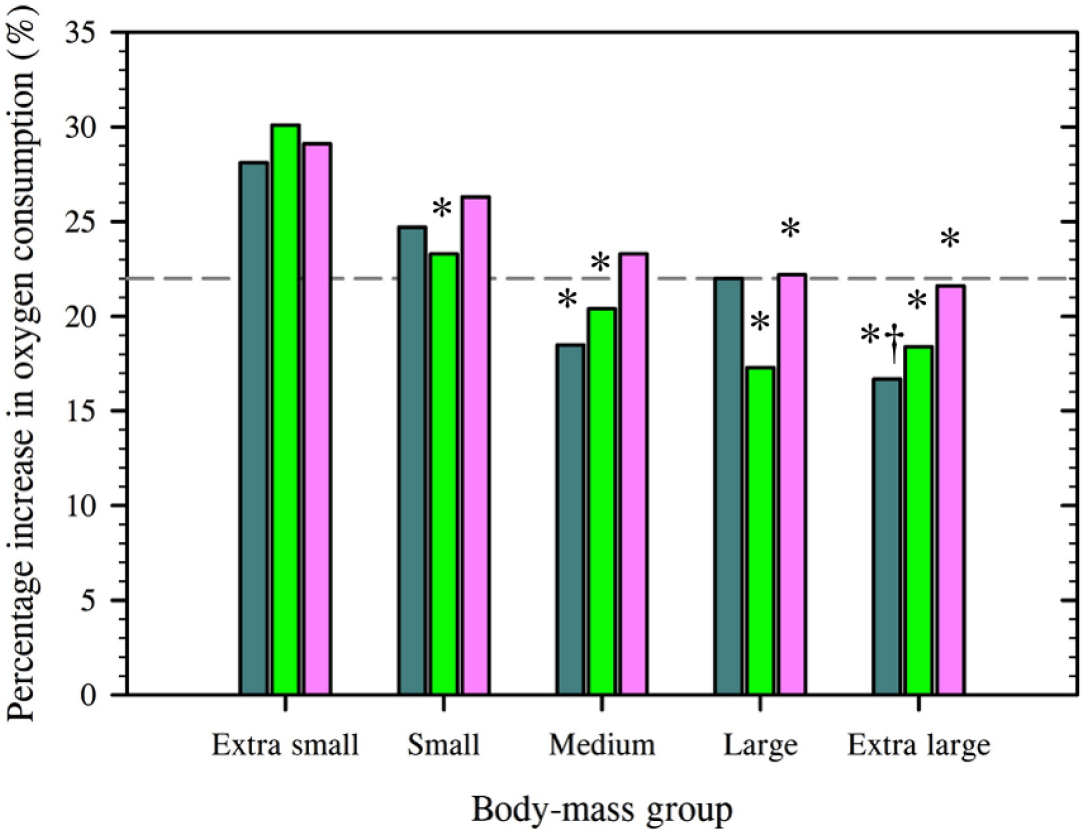

Figure 5.7: Percentage increases in oxygen consumption, relative to the unloaded state, associated with load carriage (25-kg weighted vest) for each body-mass group (Extra small: <65 kg; Small: 66-76 kg; Medium: 77-87 kg; Large: 88-98 kg; Extra large: >99 kg), during the three walking trials (downhill: $N=61$ [dark green bars]; level: $N=67$ [light green bars]; uphill: $N=62$ [pink bars]). The grey dashed line represents the mean increase in oxygen consumption across all participants. Within-gradient significant differences are identified within the Figure using the symbols (*: significantly different from the extra-small group; †: significantly different from the small group; $P<0.05$).

During unloaded walking (Chapter 4), the 10 heaviest individuals (106.2 kg: 99.5-117.1 kg) experienced a significantly greater decrease in oxygen consumption between level and downhill gradients than the lightest individuals (60.7 kg: 56.0-62.9 kg). A potential mechanism identified for this response was a greater pre-stretch occurring with an increase in body mass. To explore this theory, two-way repeated measures analysis of variance was performed on a sub-sample of participants ($N=10$; 60.7 kg: 56.0-62.9 kg) with and without the torso load (25-kg weighted vest), to simulate a change in body mass. However, no significant interaction effect was realised between those conditions (Figure 5.8; $P>0.05$). To identify whether or not this outcome was an effect of wearing the torso load, rather than an increase in body mass, the test was repeated using a second sample of participants who were unloaded but matched to be $\sim$25 kg heavier than the first group (82.6 kg: 80.9-85.8 kg). In this way, the heavier group simulated the total mass of the lighter group plus the torso load, but now without the external load actually being added. Again, no interaction effect was observed ($P>0.05$). Thus, the relationship observed in Chapter 4 was not repeated.

5.3.3.2 Scaling oxygen consumption against total mass

Each of the four regressions were regenerated by scaling oxygen consumption against total mass (body mass, clothing [$\sim$1 kg] and all external loads [shoes: 1 kg])[44] rather than body mass alone (Table 5.3). Analysis of covariance revealed no difference between the two standing mass exponents (body mass and total mass (Table 5.3; $P>0.05$). This was an unexpected outcome, since absolute oxygen consumption, which remained unchanged from the unloaded trial, was now regressed against a heavier mass. The same response was not observed during loaded walking. Instead, across all gradients, the derived total-mass exponents were significantly larger than the body-mass exponents (Table 5.3; $P<0.05$).

Nonetheless, no significant difference was observed between those loaded total-mass exponents and the unloaded body-mass exponents during walking at the same gradient (Table 5.2; Table 5.3; $P>0.05$), leading to the acceptance of Hypothesis Five-Three.

[44] Shoe masses were not included when calculating total mass for the standing trials since those loads were not supported by the body.

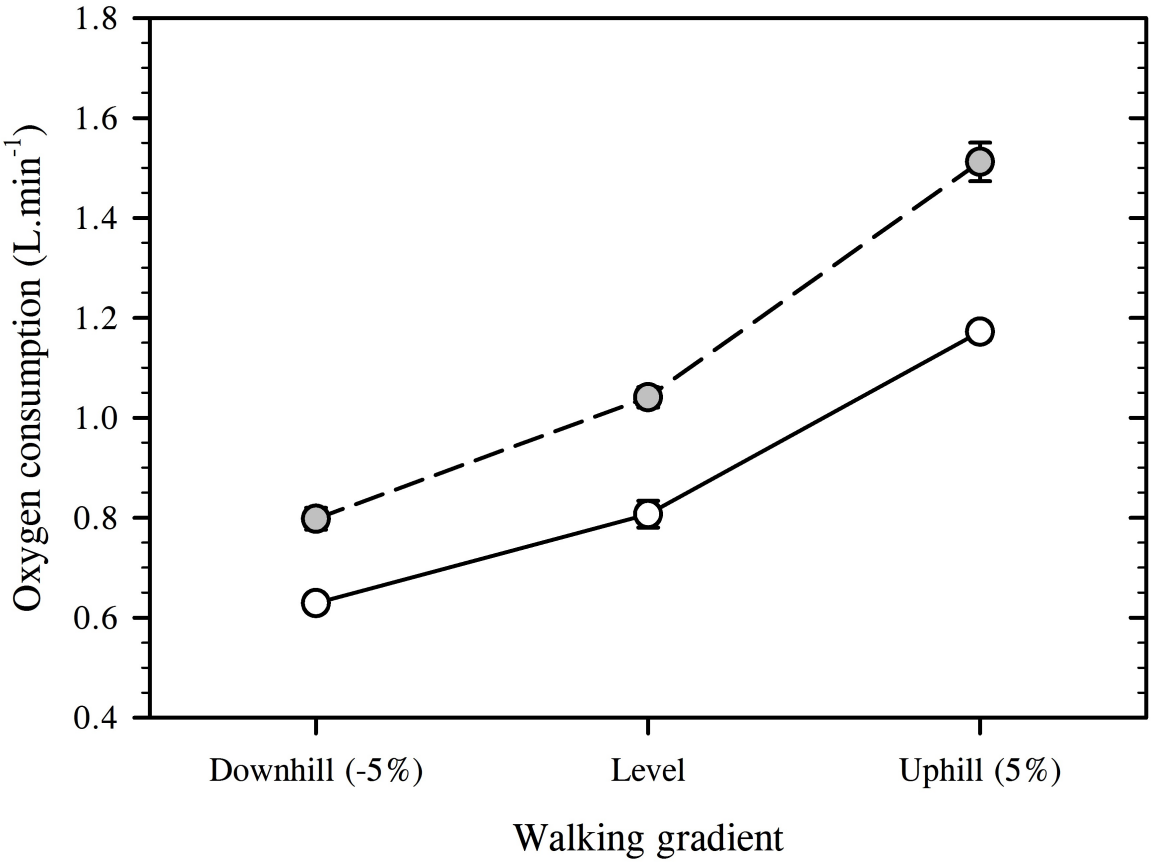

Figure 5.8: Variations in oxygen consumption with changes in walking gradient. Data are presented for the 10 smallest individuals in the sample (56.0-62.9 kg) with (grey symbols) and without torso loading (white symbols). No significant interaction effect was observed within or between conditions.

As a result, the same scaling model could be used to describe both datasets, provided that oxygen consumption was scaled against the total mass carried. Moreover, no significant difference was observed between those three total-mass exponents and the exercise-specific exponent derived in Chapters 3 and 4 ($mass^{0.80}$; $P > 0.05$). Accordingly, this universal exercise-intensity exponent was selected for this purpose, as it accurately described the relationship between oxygen consumption and body mass, regardless of the ambulatory gradient ($\pm 5\%$): $mass_{total}^{0.80}$.

5.4 DISCUSSION

This is the first investigation where the scaling of oxygen consumption against body mass has been extended to load-carriage states in humans. During unloaded states, that relationship can be described using either of two body-mass exponents, throughout the physiological range of metabolic intensity: $mass_{body}^{0.54}$ (rest) and $mass_{body}^{0.80}$ (exercise; Chapters 2-4). However, since absolute oxygen consumption is heavily influenced by the total mass carried (Goldman and Iampietro, 1962; Soule and Goldman, 1969; Soule *et al.,* 1978), it remained unclear how fixed-mass load carriage would influence those scaling exponents and whether or not they could be applied to oxygen consumption during load-carriage states.

To investigate this relationship, the experiment was designed to evaluate four hypotheses. Firstly, that load carriage would significantly reduce the body-mass exponent during walking (Hypothesis Five-Two), but not during standing states (Hypothesis Five-One). Building from the results of Chapter 4, it was hypothesised there would be no effect of ambulatory gradient on the scaling exponent during walking (Hypothesis Five-Four). Finally, it was hypothesised that it would be more appropriate to scale loaded-walking oxygen consumption against the total mass carried, rather than body mass alone (Hypothesis Five-Three). Accordingly, there were two primary objectives within this experiment. The first was to explore the effect of load carriage on the scaling exponent, and the second was to determine whether or not it was more appropriate to describe those relationships using total mass. These objectives were explored, in part, by comparing data from this experiment against the unloaded datasets in Chapters 2-4.

5.4.1 The effect of torso loading during a standing state

Even though torso loading (25-kg weighted vest) increased total mass by almost 50% amongst the lightest individuals, during standing, the loaded state did not represent a unique metabolic intensity (unloaded: 0.33 $L.min^{-1}$ [$\pm$0.01]; loaded: 0.33 $L.min^{-1}$ [$\pm$0.01]; $P > 0.05$). During loaded standing (stationary), muscle activation mainly occurs for postural support (Danna-Dos-Santos *et al.,* 2014; Hellebrandt *et al.,* 1940) because the body's mass is supported by the rigid structure of the skeletal frame; this is also true for any centrally-placed loads (Carlsöö, 1964; Schiffman *et al.,* 2006). Accordingly, the metabolic rate of the skeletal-muscle tissues, and thus whole-body oxygen consumption remains relatively unchanged. Therefore, it was not surprising that there was no difference between the unloaded and loaded body-mass exponents (Hypothesis Five-One accepted: Table 5.3; Figure 5.6; $P > 0.05$). This outcome meant that it was possible to scale both unloaded and loaded standing states using the same mass exponent, the resting exponent from Chapter 2 was selected for this purpose ($mass^{0.54}$). It is anticipated that this scaling relationship will remain appropriate for loaded standing conditions up to 40 kg (Borghols *et al.,* 1978; Pimental and Pandolf, 1979; Pierrynowski *et al.,* 1981; Holewijn, 1990; Peoples *et al.,* 2016), for only loads above this mass have been shown to significantly increase standing oxygen consumption (Phillips *et al.,* 2016 [45 kg]).

5.4.2 Scaling oxygen consumption against body mass during loaded walking

In contrast to the standing condition, during locomotion, the 25-kg load resulted in a significantly greater metabolic intensity, across all ambulatory gradients. Load carriage significantly increased oxygen consumption by an average of 22% (level: 21%; uphill: 24%; downhill: 21%), and cardiac frequency by $\sim$12% (level: 10%; uphill: 17%; downhill: 9%; Table 5.2; $P < 0.05$). This physiological response was associated with the increased mechanical work required to lift and carry the greater mass loaded on the body during this condition (Cavagna and Kaneko, 1977; Minetti *et al.,* 1993; Huang and Kuo, 2014). Therefore, load carriage resulted in a significantly higher metabolic intensity compared with unloaded walking at each ambulatory gradient, and therefore could potentially scale against a different mass exponent (Taylor *et al.,* 1980; Darveau *et al.,* 2002).

Per kilogram of added mass, that increase in oxygen consumption was uniform across the sample population ($\sim$8.68 mL.kg^{-1}.min^{-1}; level walking; $P > 0.05$). This outcome was consistent with previous observations (Goldman and Iampietro, 1962; Soule *et al.,* 1978) and confirmed that relationship across a greater mass range (double) than those originally tested. Therefore, nett oxygen consumption during loaded ambulation is not modified by body size. Collectively, these outcomes confirmed the underlying principle that the mechanical cost of walking remains constant per kilogram of mass, regardless of its tissue composition (Heglund, 1979). Thus, regardless of body size, or the mass added, a similar increase in oxygen consumption should be observed for each kilogram of mass carried (whether from growth or external load carriage). These relationships are important to remember when the scaling relationship is discussed in relation to total mass (below). Nevertheless, comparing the effect of load carriage using nett or mass-specific data alone masks the mass-dependent change in relative oxygen consumption, which is directly related to the body-mass exponent.

When that uniform nett oxygen uptake associated with load carriage (*i.e.* $\sim$8.68 mL.kg^{-1}.min^{-1}; level walking) was applied to the underlying non-linear relationship observed during unloaded walking (Chapters 3 and 4), a greater relative increase in oxygen consumption was observed among the lightest individuals (Figure 5.7; $P < 0.05$), confirming that oxygen consumption increases proportionally with the total-mass change (Goldman and Iampietro, 1962; Taylor *et al.,* 1980; Lyons *et al.,* 2005; Pal *et al.,* 2014). This demonstrates the importance of body mass when exploring the impact of load carriage on oxygen consumption, particularly if the load is a fixed mass (as it might be within all applied settings). To highlight this bias, the mean response shown above did not reflect the physiological burden of individuals at either end of the mass range. For instance, the extra small subjects experienced a 30% increase while for the extra large, it was only 18% (Figure 5.7; $P < 0.05$).

That mass-dependent response to load carriage had an observable impact on the scaling model. When plotted against the unloaded condition, the loaded scaling model was flatter, as nett oxygen consumption increased by a greater relative amount as body mass decreased (Figures 5.6A and 5.6B). This change to the regression slope significantly decreased the body-mass exponent compared with the unloaded

condition, and occurred regardless of the ambulatory gradient (Table 5.3; Figure 5.6C; $P < 0.05$; Hypothesis Five-Two accepted). Consequently, it was not appropriate to scale oxygen consumption against the unloaded body-mass exponent during loaded ambulation, and doing so would produce a systematic error among predictive and normalised data.

5.4.3 Scaling oxygen consumption against total mass during loaded walking

While it was possible to use the derived body-mass exponent to accurately describe the scaling relationship between oxygen consumption and body mass during the loaded walking states, it was uncertain whether or not that mass exponent would change with an increase in the load carried. Indeed, the observed change to the body-mass exponent was determined by the relative increase in absolute oxygen consumption across the body-mass range. Therefore, it is possible that a heavier load would further reduce the body-mass exponent. This outcome would complicate the application of a mass exponent during loaded states, for multiple load-specific values would be required. Thus, an alternative approach was explored.

It was possible to minimise the effect of load carriage on the scaling relationship by changing the morphometric scaling variable from body mass to total mass (body mass plus all external masses worn). By scaling oxygen consumption in this way, the derived scaling exponents for the load-carriage states did not differ from their respective unloaded conditions (Table 5.3; $P > 0.05$). Accordingly, a single mass exponent could be used to describe both states, providing that total mass was considered. Rather than using the level-walking exponent ($mass^{0.85}$), the exercise-specific exponent ($mass_{total}^{0.80}$: Chapters 3 and 4) was selected for this purpose. Since $mass^{0.80}$ was statistically similar among all conditions, the adoption of a single mass exponent was deemed preferable compared with many condition-specific values.

With this outcome a consistent relationship between oxygen consumption and the total mass carried was demonstrated, supporting the observations of previous researchers (Goldman and Iampietro, 1962; Borghols *et al.,* 1978; Heglund, 1979; Taylor *et al.,* 2016), but extending that research across a wide mass range to reveal a non-linear model. Accordingly, regardless of the change in total mass (growth or load carriage),

it is possible to predict and normalise oxygen consumption across a body-mass range using a single mass exponent, providing that those data are scaled against the total mass. To demonstrate that relationship, data were extracted during level walking for the 10 lightest individuals and 10 participants matched to be 25 kg heavier. When the total mass carried was matched, absolute oxygen consumption did not differ between groups (lighter group wearing 25-kg load: 1.04 $L.min^{-1}$ [$\pm$0.02]; heavier group unloaded: 1.00 $L.min^{-1}$ [$\pm$0.03]; $P > 0.05$).

It is anticipated that this relationship will remain constant providing that the increase in oxygen consumption remains proportional to the load carried. Instances where this relationship might be violated include very heavy (Soule *et al.,* 1978; Phillips *et al.,* 2016), asymmetrically placed (Bloswick *et al.,* 1994; Laursen *et al.,* 2000) and distally placed loads (Soule and Goldman, 1969; Datta and Ramanathan, 1971; Schertzer and Riemer, 2014). The threshold for heavy load carriage, after which an increase in external load causes a disproportionate increase in oxygen consumption, could be easily tested using a homogeneous sample and applying an increasing external mass to determine the point of inflection in their nett oxygen consumption. However, it remained unclear whether loads placed away from the centre of the body would modify that response, since they are known to magnify the mass-specific increase in nett oxygen consumption (Soule and Goldman, 1969; Datta and Ramanathan, 1971; Taylor *et al.,* 2012; Shertzer and Riemer, 2014), and so this was investigated in Chapter 6.

5.4.4 The effect of ambulatory gradient during loaded walking

As expected, mean absolute oxygen consumption significantly changed with the gradient direction (Table 5.2; $P < 0.05$), resulting in three separate metabolic intensities. However, neither the body-mass nor the total-mass scaling exponents were influenced by those gradient-specific variations in oxygen consumption (Figure 5.7; Table 5.1; Table 5.3; $P > 0.05$; Hypothesis Five-Four accepted). This observation was consistent with the relationship between gradient and the unloaded walking exponents (Chapter 4). Therefore, a change in ambulatory gradient did not modify the scaling outcomes previously reports. Accordingly, the same total-mass exponent could be used to describe both unloaded and loaded walking, across all three

ambulatory gradients ($\pm 5\%$; $mass_{total}^{0.80}$; $P > 0.05$).

During uphill walking, the addition of the external load did not modify the mass-specific oxygen cost of purely vertical movement[45] from that observed during the unloaded trial (unloaded: 1.40 $mL.kg^{-1}.m^{-1}$ [± 0.03]; loaded: 1.37 $mL.kg^{-1}.m^{-1}$ [± 0.03]; $P > 0.05$). Accordingly, the oxygen uptake required for vertical movement was proportional to the total mass, and apparently not influenced by the composition of that mass. For this reason, it is anticipated that a further increase in the total mass carried during uphill walking will not modify the mass exponent. Instead, that increase in total mass will generate similar metabolic values as an unloaded person of the same total mass. That relationship is anticipated to remain constant with a mass change, providing that an individual's posture or gait is not modified by that load, which could disproportionally increase oxygen consumption (Abe *et al.,* 2004; Birrell and Haslam, 2008; Schertzer and Riemer, 2014).

During the unloaded gradient-walking trials (Chapter 4), while the body-mass exponent was not modified, a significant body-mass dependent response was observed between level and downhill walking. Specifically, oxygen consumption decreased by a greater percentage in the heaviest 10 participants (106.2 kg: 99.5-117.1 kg) compared with the 10 lightest participants (60.7 kg: 56.0-62.9 kg). A potential mechanism identified for this outcome was a greater pre-stretch occurring with an increase in body mass. This theory was explored within the present study using two, similar investigations. The first was a repeated-measures test using the same lightest 10 participants as tested previously, both with and without the torso load. In the second test, the loaded condition was replaced with an unloaded sample matched for total mass (82.6 kg: 80.9-85.8 kg [$\sim$25 kg heavier]). However, no significant difference was observed in the decrease in oxygen consumption between those conditions ($P > 0.05$). Therefore, it was concluded that energy-saving response is related to a change in pre-stretch load, but a 25-kg increase in total mass was not sufficient to observe that outcome.

[45] The oxygen cost of vertical ascent ($mL.kg^{-1}.m^{-1}$) was calculated by dividing the mean nett oxygen consumption (uphill less level; $mL.min^{-1}$) by the vertical ascent per minute (4 $m.min^{-1}$). That value was then divided by the total mass carried by participants (kg) to provide the mass-specific cost of vertical ascent.

5.5 CONCLUSION

In summary, this was the first experiment designed to evaluate the effect of load carriage on the scaling relationship between oxygen consumption and body mass in humans. Compared with the unloaded models, load carriage had a significant effect on the scaling exponent during walking, but not standing states. Therefore, it remained more appropriate to scale standing oxygen consumption by the resting body-mass exponent derived in Chapter 2 ($mass_{body}^{0.54}$). During steady-state walking, at any ambulatory gradient within the range of $\pm 5\%$, load carriage significantly reduced the exponent when scaling against body mass. The shape of that regression was influenced by the mass-dependent increase in relative oxygen consumption during fixed-mass load carriage. Nevertheless, the effect of that relationship could be minimised if oxygen consumption data were scaled against total mass, rather than body mass alone. This is because oxygen consumption is heavily influenced by the total mass carried, for which a proportional relationship was observed between body mass and external load carriage. Accordingly, it was possible to describe the scaling relationship between oxygen consumption and body mass, regardless of ambulatory gradient and the load carried. The exercise-specific exponent derived in Chapters 3 and 4 was selected for this purpose: $mass_{total}^{0.80}$.

5.6 REFERENCES

Abe, D., Muraki, S., and Yasukouchi, A. (2008). Ergonomic effects of load carriage on energy cost of gradient walking. *Applied Ergonomics*. 39(2):144-149.

Abe, D., Yanagawa, K., and Niihata, S. (2004). Effects of load carriage, load position, and walking speed on energy cost of walking. *Applied Ergonomics*. 35(4):329-335.

Alexander, R.M., and Bennet-Clark, H.C. (1977). Storage of elastic strain energy in muscle and other tissues. *Nature*. 265(5590):114.

Asmussen, E., and Bonde-Petersen, F. (1974). Storage of elastic energy in skeletal muscles in man. *Acta Physiologica*. 91(3):385-392.

Attwells, R.L., Birrell, S.A., Hooper, R.H., and Mansfield, N.J. (2006). Influence of carrying heavy loads on soldiers' posture, movements and gait. *Ergonomics*. 49(14):1527-1537.

Birrell, S.A., and Haslam, R.A. (2008). The influence of rifle carriage on the kinetics of human gait. *Ergonomics*. 51(6):816-826.

Blickhan, R. (1989). The spring-mass model for running and hopping. *Journal of Biomechanics*. 22(11-12):1217-1227.

Bloswick, D.S., Gerber, A., Sebesta, D., Johnson, S., and Mecham, W. (1994). Effect of mailbag design on musculoskeletal fatigue and metabolic load. *Human Factors*. 36(2):210-218.

Borghols, E.A.M., Dresen, M.H.W., and Hollander, A.P. (1978). Influence of heavy weight carrying on the cardiorespiratory system during exercise. *European Journal of Applied Physiology and Occupational Physiology*. 38(3):161-169.

Carlsöö, S. (1961). The static muscle load in different work positions: an electromyographic study. *Ergonomics*. 4(3):193-211.

Cavagna, G.A., Heglund, N.C., and Taylor, C.R. (1977). Mechanical work in terrestrial locomotion: two basic mechanisms for minimizing energy expenditure. *American Journal of Physiology-Regulatory, Integrative and Comparative Physiology*. 233(5):R243-R261.

Cavagna, G.A., and Kaneko, M. (1977). Mechanical work and efficiency in level walking and running. *The Journal of Physiology*. 268(2):467-481.

Cohen, Y., Robbins, C.T., and Davitt, B.B. (1978). Oxygen utilization by elk calves during horizontal and vertical locomotion compared to other species. *Comparative Biochemistry and Physiology--Part A: Physiology*. 61(1):43-48.

Cook, R.D. (1977). Detection of influential observation in linear regression. *Technometrics*. 19(1):15-18.

Cook, R.D., and Weisberg, S. (1982). *Residuals and influence in regression*. Chapman and Hall, New York.

Crouter, S.E., Antczak, A., Hudak, J.R., DellaValle, D.M., and Haas, J.D. (2006). Accuracy and reliability of the ParvoMedics TrueOne 2400 and MedGraphics VO2000 metabolic systems. *European Journal of Applied Physiology*. 98(2):139-151.

Danna-Dos-Santos, A., Boonstra, T.W., Degani, A.M., Cardoso, V.S., Magalhaes, A.T., Mochizuki, L., and Leonard, C.T. (2014). Multi-muscle control during bipedal stance: an EMG–EMG analysis approach. *Experimental Brain Research*. 232(1):75-87.

Darveau, C.A., Suarez, R.K., Andrews, R.D., and Hochachka, P.W. (2002). Allometric cascade as a unifying principle of body mass effects on metabolism. *Nature*. 417(6885):166-170.

Datta, SR., a nd Ramanathan, N.L. (1971). Ergonomic comparison of seven modes of carrying loads on the horizontal plane. *Ergonomics*. 14(2):269-278.

Dill, D.B. (1965). Oxygen used in horizontal and grade walking and running on the treadmill. *Journal of Applied Physiology*. 20(1):19-22.

Durbin, J., and Watson, G.S. (1950). Testing for serial correlation in least squares regression: I. *Biometrika*. 37(3/4):409-428.

Durbin, J., and Watson, G.S. (1951). Testing for serial correlation in least squares regression. II. *Biometrika*. 38(1/2):159-177.

Efron, B. (1979). Computers and the theory of statistics: thinking the unthinkable. *SIAM review*. 21(4):460-480.

Fox, J. (1991). *Regression diagnostics: An introduction*. Volume 79. Sage, London.

Fox, J. (1997). *Applied regression analysis, linear models, and related methods*. Sage, London.

Fox, J., and Weisberg, S. (2017). *An R Companion to Applied Regression.* Sage, London.

Goldman, R.F., and Iampietro, P.F. (1962). Energy cost of load carriage. *Journal of Applied Physiology*. 17(4):675-676.

Gottschall, J.S., and Kram, R. (2005). Energy cost and muscular activity required for leg swing during walking. *Journal of Applied Physiology*. 99(1):23-30.

Grabowski, A., Farley, C.T., and Kram, R. (2005). Independent metabolic costs of supporting body weight and accelerating body mass during walking. *Journal of Applied Physiology*. 98(2):579-583.

Griffin, T.M., Roberts, T.J., and Kram, R. (2003). Metabolic cost of generating muscular force in human walking: insights from load-carrying and speed experiments. *Journal of Applied Physiology*. 95(1):172-183.

Hair, J.F., Anderson, R.E., Tatham, R.L., and Black, W.C. (1998). *Multivariate data analysis*. Prentice-Hall International, Upper Saddle River, NJ.

Halsey, L.G., and White, C.R. (2017). A different angle: comparative analyses of whole-animal transport costs when running uphill. *Journal of Experimental Biology*. 220(2):161-166.

Heglund, N.C. (1979). *Size scaling, speed and the mechanics of locomotion*. (Doctoral dissertation). Harvard University.

Hellebrandt, F.A., Brogdon, E., and Tepper, R.H. (1940). Posture and its cost. *American Journal of Physiology - Legacy Content*. 129:773-781.

Hill, A.V. (1927). *Muscular Movement in Man: The Factors Governing Speed and Recovery from Fatigue*. McGraw-Hill, New York.

Holewijn, M. (1990). Physiological strain due to load carrying. *European Journal of Applied Physiology and Occupational Physiology*. 61(3-4):237-245.

Huang, T.P., and Kuo, A.D. (2014). Mechanics and energetics of load carriage during human walking. *Journal of Experimental Biology*. 217(4):605-613.

Jamnik, V., Gumienak, R., and Gledhill, N. (2013). Developing legally defensible physiological employment standards for prominent physically demanding public safety occupations: a Canadian perspective. *European Journal of Applied Physiology*. 113(10):2447-2457.

Jansson, M. (1985). A comparison of detransformed logarithmic regressions and power function regressions. *Geografiska Annaler: Series A, Physical Geography*. 67(1-2):61-70.

Johnson, A.T., Benjamin, M.B., and Silverman, N. (2002). Oxygen consumption, heat production, and muscular efficiency during uphill and downhill walking. *Applied Ergonomics*. 33(5):485-491.

Kim, H.Y. (2013). Statistical notes for clinical researchers: assessing normal distribution (2) using skewness and kurtosis. *Restorative Dentistry and Endodontics*. 38(1):52-54.

Kinoshita, H. (1985). Effects of different loads and carrying systems on selected biomechanical parameters describing walking gait. *Ergonomics*. 28(9):1347-1362.

Landers, G.J., Ong, K.B., Ackland, T.R., Blanksby, B.A., Main, L.C., and Smith, D. (2013). Kinanthropometric differences between 1997 World championship junior elite and 2011 national junior elite triathletes. *Journal of Science and Medicine in Sport*. 16(5):444-449.

Laursen, B., Ekner, D., Simonsen, E.B., Voigt, M., and Sjøgaard, G. (2000). Kinetics and energetics during uphill and downhill carrying of different weights. *Applied Ergonomics*. 31(2):159-166.

Lyons, J., Allsopp, A., and Bilzon, J. (2005). Influences of body composition upon the relative metabolic and cardiovascular demands of load-carriage. *Occupational Medicine*. 55(5):380-384.

Maloiy, G.M.O., Heglund, N.C., Prager, L.M., Cavagna, G.A., and Taylor, C.R. (1986). Energetic cost of carrying loads: have African women discovered an economic way? *Nature*. 319(6055):668-669.

Margaria, R. (1968). Positive and negative work performances and their efficiencies in human locomotion. *Internationale Zeitschrift für angewandte Physiologie einschließlich Arbeitsphysiologie*. 25(4):339-351.

Minetti, A.E., Ardigo, L.P., and Saibene, F. (1993). Mechanical determinants of gradient walking energetics in man. *The Journal of Physiology*. 472(1):725-735.

Nadel, E.R., Bergh, U., and Saltin, B. (1972). Body temperatures during negative work exercise. *Journal of Applied Physiology*. 33(5):553-558.

Newman, M.C. (1993). Regression analysis of log transformed data: Statistical bias and its correction. *Environmental Toxicology and Chemistry*. 12(6):1129-1133.

Pal, M.S., Majumdar, D., Pramanik, A., Chowdhury, B., and Majumdar, D. (2014). Optimum load for carriage by Indian soldiers on different uphill gradients at specified walking speed. *International Journal of Industrial Ergonomics*. 44(2):260-265.

Pandolf, K.B., Givoni, B., and Goldman, R.F. (1977). Predicting energy expenditure with loads while standing or walking very slowly. *Journal of Applied Physiology*. 43(4):577-581.

Peoples, G.E., Lee, D.S., Notley, S.R., and Taylor, N.A.S. (2016). The effects of thoracic load carriage on maximal ambulatory work tolerance and acceptable work durations. *European Journal of Applied Physiology*. 116(3):635-646.

Phillips, D.B., Ehnes, C.M., Stickland, M.K., and Petersen, S.R. (2016). The impact of thoracic load carriage up to 45 kg on the cardiopulmonary response to exercise. *European Journal of Applied Physiology*. 116(9):1725-1734.

Pierrynowski, M.R., Winter, D.A., and Norman, R.W. (1981). Metabolic measures to ascertain the optimal load to be carried by man. *Ergonomics*. 24(5):393-399.

Pimental, N.A., and Pandolf, K.B. (1979). Energy expenditure while standing or walking slowly uphill or downhill with loads. *Ergonomics*. 22(8):963-973.

Poole, M.A., and O'Farrell, P.N. (1971). The assumptions of the linear regression model. *Transactions of the Institute of British Geographers*. 52:145-158.

Ross, W.D., and Ward, R. (1985). *The O-scale system*. Rosscraft, Surrey, BC.

Ross, W.D., and Wilson, N.C. (1974). A stratagem for proportional growth assessment. *Acta Paediatrica Belgica*. 28:169-182.

Schertzer, E., and Riemer, R. (2014). Metabolic rate of carrying added mass: a function of walking speed, carried mass and mass location. *Applied Ergonomics*. 45(6):1422-1432.

Schiffman, J.M., Bensel, C.K., Hasselquist, L., Gregorczyk, K.N., and Piscitelle, L. (2006). Effects of carried weight on random motion and traditional measures of postural sway. *Applied Ergonomics*. 37(5):607-614.

Shapiro, S.S., and Wilk, M.B. (1965). An analysis of variance test for normality (complete samples). *Biometrika*. 52(3/4):591-611.

Sholl, D. (1948). The quantitative investigation of the vertebrate brain and the applicability of allometric formulae to its study. *Proceedings of the Royal Society of London B*. 135(879):243-258.

Silder, A., Delp, S.L., and Besier, T. (2013). Men and women adopt similar walking mechanics and muscle activation patterns during load carriage. *Journal of Biomechanics*. 46(14):2522-2528.

Soule, R.G., and Goldman, R.F. (1969). Energy cost of loads carried on the head, hands, or feet. *Journal of Applied Physiology*. 27(5):687-690.

Soule, R.G., Pandolf, K.B., and Goldman, R.F. (1978). Energy expenditure of heavy load carriage. *Ergonomics*. 21(5):373-381.

Taylor, C.R., Caldwell, S.L., and Rowntree, V.J. (1972). Running up and down hills: some consequences of size. *Science*. 178(4065):1096-1097.

Taylor, C.R., Heglund, N.C., and Maloiy, G.M.O. (1982). Energetics and mechanics of terrestrial locomotion. I. Metabolic energy consumption as a function of speed and body size in birds and mammals. *Journal of Experimental Biology*. 97(1):1-21.

Taylor, C.R., Heglund, N.C., McMahon, T.A., and Looney, T.R. (1980). Energetic cost of generating muscular force during running: a comparison of large and small animals. *Journal of Experimental Biology*. 86(1):9-18.

Taylor, C.R., Schmidt-Nielsen, K., and Raab, J.L. (1970). Scaling of energetic cost of running to body size in mammals. *American Journal of Physiology-Legacy Content*. 219(4):1104-1107.

Taylor, C.R., Shkolnik, A., Dmi'el, R., Baharav, D., and Borut, A. (1974). Running in cheetahs, gazelles, and goats: energy cost and limb configuration. *American Journal of Physiology-Legacy Content*. 227(4):848-850.

Taylor, N.A.S., Lewis, M.C., Notley, S.R., and Peoples, G.E. (2011). The Oxygen Cost of Wearing Firefighters' Personal Protective Equipment: Ralph Was Right. In: *ICEE 2011 XIV International Conference on Environmental Ergonomics: Book of Abstracts*. 236-239.

Taylor, N.A.S., Lewis, M.C., Notley, S.R., and Peoples, G.E. (2012). A fractionation of the physiological burden of the personal protective equipment worn by firefighters. *European Journal of Applied Physiology*. 112(8):2913-2921.

Taylor, N.A.S., Peoples, G.E., and Petersen, S.R. (2016). Load carriage, human performance, and employment standards. *Applied Physiology, Nutrition, and Metabolism*. 41(6):S131-S147.

Weisberg, S. (2014). *Applied Linear Regression*. Wiley, Minnesota.

Williams, D.A. (1987). Generalized linear model diagnostics using the deviance and single case deletions. *Applied Statistics*. 36(2):181-191.

Workman, J.M., and Armstrong, B.W. (1963). Oxygen cost of treadmill walking. *Journal of Applied Physiology*. 18(4):798-803.

Xiao, X., White, E.P., Hooten, M.B., and Durham, S.L. (2011). On the use of log transformation vs. nonlinear regression for analyzing biological power laws. *Ecology*. 92(10):1887-1894.

CHAPTER 6: THE EFFECT OF LOAD DISTRIBUTION WHEN SCALING STEADY-STATE, AMBULATORY OXYGEN CONSUMPTION

6.1 INTRODUCTION

The primary focus of this experiment was to determine whether a change in load position would modify the mass exponents[46] derived for unloaded (Chapters 3 and 4) and torso-loaded walking (Chapter 5). During torso-loaded walking (Chapter 5), the observed increase in oxygen consumption was mass dependent, and, at least with lighter loads (<30 kg), proportional to the mass change (Soule *et al.,* 1978; Taylor *et al.,* 1980; Phillips *et al.,* 2016). Accordingly, to carry the same fixed-mass, lighter individuals experience a greater relative increase in oxygen consumption. Compared with unloaded walking, that mass response to load carriage (25 kg) flattened the scaling regression, significantly reducing the body-mass exponent (unloaded: 0.80 [untransformed]; loaded: 0.66 [untransformed]; Chapter 5; $P<0.05$). As a result, different body-mass exponents were required to describe oxygen consumption during unloaded or loaded condition. Nevertheless, it proved possible to correct for that response by scaling data against total mass (body mass, clothing and all other external loads) rather than just against body mass. That outcome indicated that the increase in oxygen consumption associated with load carriage remained proportional to a similar increase in body mass. Consequently, both loading conditions could be described using the same total-mass exponent ($mass_{total}^{0.80}$ [untransformed]). However, since that outcome relied on a proportional relationship between load carriage and oxygen consumption, it remains uncertain whether load configurations that results in a non-proportional increases in oxygen consumption, such as loads carried on the head, hands and feet (Soule and Goldman, 1969; Kamon and Belding, 1971; Schertzer and Riemer, 2014), could also be described using that same universal mass exponent.

Load positioning has a direct effect on the metabolic burden of that load. Unbalanced torso loading disturbs both posture and gait by shifting the centre of gravity away from the body's centre of mass (Hellebrandt *et al.,* 1944; Kinoshita, 1985; Attwells *et*

[46] In non-linear, allometric regression ($y=ax^b$), the mass exponent (b) determines the steepness of the regression curve. That value can be used to normalise metabolic data for variations in body mass. In instances where the regression slope (exponent) differs significantly between metabolic intensities, unique mass exponents are required to describe each condition. Therefore the mass exponent was the primary measure evaluated within this Chapter.

al., 2006), increasing the work of walking and thereby increasing oxygen uptake (Datta and Ramanathan, 1971; Abe *et al.,* 2008). An even greater metabolic burden is observed when loads are carried distally (Soule and Goldman, 1969; Martin, 1985; Taylor *et al.,* 2012). For instance, a shift in load placement from the torso to the head, increases oxygen uptake by a factor of 1.2-1.3, almost proportional with torso loading, while loading at the hands and feet results in loading factors[47] of ~2 and 5.8-8.7 respectively (4.8 $km.h^{-1}$: Soule and Goldman, 1969; Taylor *et al.,* 2012). Oxygen uptake is greater during limb loading because the additional masses carried increase both rotational torque about the torso (Abe *et al.,* 2004) and swing-phase inertial work (Cavagna and Kaneko 1977; Browning *et al.,* 2007). Consequently, even light external loads, when placed distally, can significantly increase oxygen consumption. For that reason, within this final research phase, the effect of loading at the head, hands and feet on the on the mass exponent for the relationship between oxygen consumption and body mass was explored.

Distally carried loads of a fixed mass have the potential to modify the mass exponent by either of two ways: the proportional increase in oxygen consumption relative to the total mass change and the possibility that the loading factor is body-mass dependent. Firstly, as demonstrated in Chapter 5, the carriage of a fixed mass results in a mass-dependent response in nett oxygen uptake, whereby lighter individuals must work relatively harder to carry the same load. That response occurred despite a uniform nett increase in oxygen consumption per kilogram of added mass (~8.68 $mL.kg^{-1}.min^{-1}$ [level walking])[48]. Therefore, the reduction in mass-exponent value did not occur as a result of a non-uniform increase in oxygen consumption, but because that increase, relative to the unloaded condition, was proportionally different across the body-mass range. Consequently, a similar response would be expected with a change in the load position. However, the typically lighter loads carried at those locations (head, hands and feet) may not significantly increase oxygen consumption enough to observe that effect. Thus, the body-mass exponent would remain similar with the

[47] The term loading factor is used to define the multiplicative factor of metabolic burden during load carriage relative to the same mass carried on the torso.

[48] Mass-specific units have been used to describe the increase in oxygen consumption per kilogram of added mass, since the mass-specific burden remains similar with mass increase until very heavy loads are carried (>45 kg [standing]: Phillips *et al.,* 2016)

unloaded condition. Conversely, if that response were to be observed, it will most likely occur at load locations with a greater loading factor (hands and feet).

The second way in which load placement could effect the mass exponent is by altering the loading factor. In previous studies, where the size of the loading factor was explored across a range of mass (load) and load locations, the loading factor increased most dramatically for loads carried at the hands and feet (Soule and Goldman, 1969; Kamon and Belding, 1971; Schertzer and Riemer, 2014). However, since those studies were conducted using relatively small samples with a narrow body-mass range, it remains uncertain whether the same response will be observed when the same fixed mass is carried by individuals of widely variable body masses. If those loading factors vary with body mass, then it is presumed that, per kilogram of mass carried, oxygen consumption will increase by a greater amount in smaller people. As a result, a unique mass exponent may be required to describe oxygen consumption data during distally-loaded states.

The effect of load placement on the scaling relationship might be further modified by a change in gradient. During gradient walking, the rate of oxygen consumption is influenced by the relationship between the total mass carried and potential energy gain or loss (Taylor *et al.,* 1972; Borghols *et al.,* 1978). Accordingly, absolute oxygen consumption changes relative to the gradient direction (Chapters 4 and 5; Minetti *et al.,* 1993; Johnson *et al.,* 2002). Those changes in absolute oxygen consumption are further influenced during load-carriage states, for the increase in total mass correlates with a greater mechanical cost of movement (Soule *et al.,* 1978; Taylor *et al.,* 1980; Phillips *et al.,* 2016). Nevertheless, no significant effect of gradient on the mass exponent has been observed during unloaded (Chapter 4) or torso-loaded walking (25-kg weighted vest: Chapter 5). However, it is possible that distal load placement will magnify any underlying gradient relationship. For example, during uphill walking, the arm swing becomes more forceful to help transfer energy to the gait cycle (Pellegrini *et al.,* 2015), and during downhill walking, stride length increases to utilise the gravitational assistance to horizontal movement (Minetti *et al.,* 1993; Sheehan and Gottschall, 2012). Both of these responses increase the speed of limb movement, which, when loaded distally, is likely to exaggerate the metabolical

burden of load carriage: the loading factor. As previously discussed, such a disproportional increase in oxygen consumption per kilogram of mass carried may modify the mass exponent, providing that the mass-response to load carriage is statistically observable across the mass range. Accordingly, the effect of a gradient change was also evaluated within this experimental phase.

Therefore, to address those research questions, the effect of load placement at the head, hands and feet on the scaling relationship between oxygen consumption and body mass was explored. Specifically, conditions were compared to identify whether a change in load placement modified the mass exponents derived for both body and total mass during unloaded and torso-loaded walking. By using the same sample tested in Chapters 2-5 (unloaded and torso trials), it was possible to maintain a repeated-measures design to the project while comparing data against the unloaded (Chapters 3 and 4) and torso-loaded (Chapter 5) trials. To effectively assess those aims, four experimental hypotheses were developed, based on the assumption that the scaling regressions would remain nonlinear (allometric), thus, oxygen consumption would scale against an exponent of body mass.

Hypothesis Six-One: Compared with unloaded level walking, load carried on the head will not modify the mass exponent when scaled against either body mass or total mass

Hypothesis Six-Two: Compared with unloaded level walking, load carriage at the hands will significantly reduce the body-mass exponent.

Hypothesis Six-Three: Compared with unloaded level walking, load carriage at the feet will significantly reduce the body-mass exponent.

Hypothesis Six-Four: Compared with both unloaded and torso-loaded level walking, load carriage at both the hands and feet will significantly modify the total-mass exponent.

Hypothesis Six-Five: A change in walking gradient (-5%, 5%) will not significantly modify the scaling exponents observed during any load-carriage condition from that of level walking.

6.2 METHODS

6.2.1 Subjects

The sample used to explore the effect of load placement on the scaling relationship consisted of 72 healthy and physically-active men, recruited from the local university population and nearby sports teams. Within those 72 participants, there were 14 partial datasets (participants who had dropped out of the study before completing all the trials): identified using the red symbols in Figure 6.1. This was the same sample used in Chapters 2-5. Those participants had been evenly recruited across a two-fold mass range (56.0-117.1 kg: Figure 6.1) to permit scaling analyses. Furthermore, participants had been matched for physiological and morphological variables that could influence whole-body oxygen consumption (Section 2.2.1; Table 2.2; Figures 2.10 and 2.11).

Pre-test screening was used to eliminate subjects with a history of cardiovascular, respiratory or musculo-skeletal pathologiess contraindicative of participation in this experiment. Remaining participants were supplied with an information package and provided written, informed consent before commencing the trials. The procedures performed within this experimental phase were approved by the Human Research Ethics Committee (University of Wollongong; HE14/469).

6.2.2 Procedural overview

To explore the effect of load placement on the mass exponent, participants completed nine trials, across three laboratory visits. During each visit, participants walked (15-min stages; 4.8 $km.h^{-1}$) at one of three gradients (level, 5% uphill and -5% downhill) wearing loads placed at the head (Figure 6.2A), hands (Figure 6.2B) and feet (Figure 6.2C) during separate trials. Subjects had a 5-min rest between each load configuration. The gradient and load orders were balanced across participants using a Latin Square design. Data from those trials were compared with data from the previously-tested unloaded (Chapters 3 and 4) and torso-loaded (25-kg weighted vest; Chapter 5) trials. To increase test reliability, participants completed two familiarisation sessions before the main testing block (Jamnik *et al.,* 2013; Burdon *et al.,* 2018). In each session, participants walked for 10 min at each gradient wearing each load configuration. Ten minutes was a sufficient duration for participants' gait to

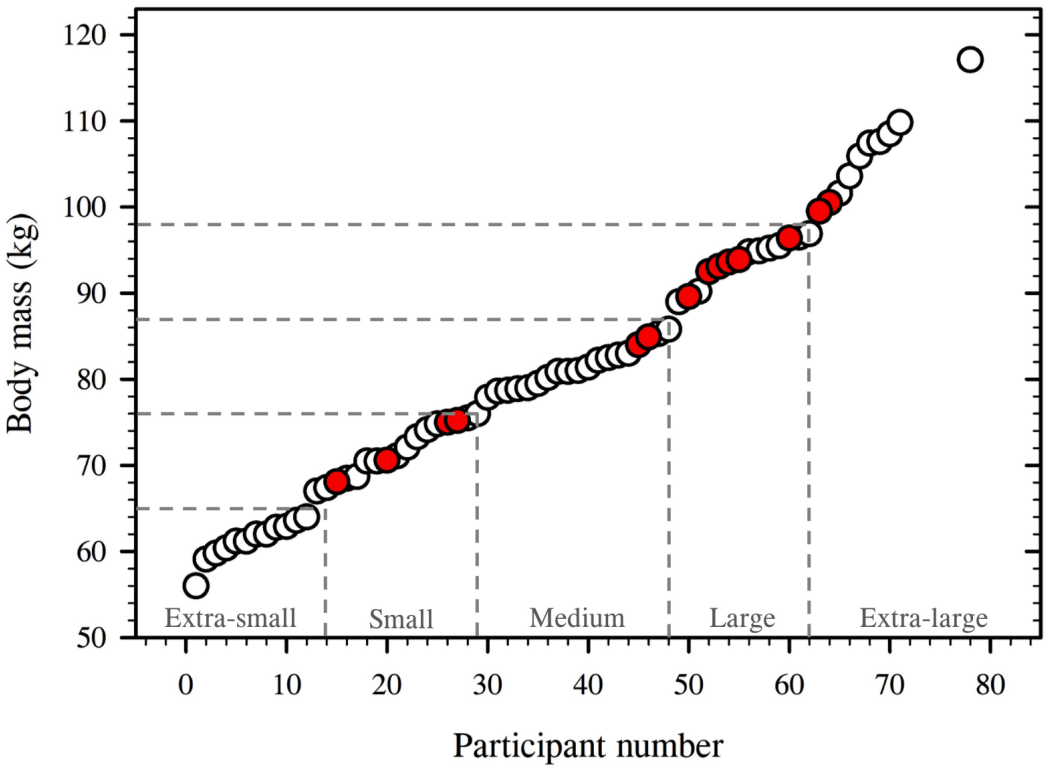

Figure 6.1: Scatter plot displaying the mass distribution of the sample, with participants arranged in ascending order of body mass. Data points are displayed for the full 72 participants who completed testing in the wider project (standing: $N=67$; level walking: $N=67$; uphill walking: $N=62$; downhill walking: $N=61$). Partial datasets are identified using the red symbols. A break down of the sample sizes is displayed in Figure 6.3. The drop-lines signify the borders separating each of the five body-mass groups and their sample sizes.

Figure 6.2: During these trials, participants wore one of three load configurations: 1.38-kg helmet (Figure 6.2A), a 2-kg weight on each wrist (4 kg total: Figure 6.2B) and 2-kg each foot comprised of work boots plus adjustable ankle weights to offset the mass difference (4 kg total: Figure 6.2C). Figure 6.2D represents the footwear configuration worn during all trials except during loading at the feet. To minimise the metabolic effect of loading at the feet (Soule and Goldman, 1969), adjustable ankle weights were worn to standardise individual shoe masses to 500 g. Garments (t-shirt and combat trousers) and loads were selected to correspond with those worn by Riflemen in the Australian Defence Force.[49]

[49] This project was funded by the Defence Science and Technology group, with the secondary aim of exploring the interactions between load carriage and body size in a military context.

stabilise (Wall and Charteris, 1981; Van de Putte *et al.*, 2006) and for them to reach a steady state metabolically (Åstrand and Saltin, 1961).

6.2.2.1 Experimental procedure

On arrival at the laboratory, both semi-nude and clothed (unshod) body masses were recorded. For these trials, participants wore the laboratory-provided clothing, a cardiac frequency monitor and an oronasal mask (Figure 2.4B). Each walking trial started with a 10-min, unloaded standing (stationary) baseline. Participants then commenced the treadmill walking stages (4.8 $km.h^{-1}$: Pulsar 3p Treadmill, H/P/Cosmos, Traunstein, Germany) at the respective gradient. That phase consisted of five, 15-min stages: the three trials tested within this phase (head, hands and feet loading) and the previously-reported unloaded (Chapters 3 and 4) and torso-loaded (Chapter 5) conditions.

6.2.3 Experimental standardisation

All testing was conducted in an air-conditioned laboratory ($\sim$23°C; $\sim$50% humidity). The trials commenced at the same time of day ($\pm$1 h) within participants, to minimise potential circadian effects. Prior to those tests, participants were instructed to refrain from drinking caffeine for 6 h and to consume a pre-experimental meal high in carbohydrates and low in fats $>$2 h before starting the test.

6.2.4 Experimental measures

Oxygen consumption (open-circuit respirometry: TrueOne 2400, ParvoMedics Inc., Utah, U.S.A.: Crouter *et al.,* 2006; see Section 2.2.4.1 for details) and cardiac frequency (ventricular depolarisation: Plug in receiver, Polar Electro, Kempele, Finland; see Section 2.2.4.3 for details) were measured continuously as 15-s averages (respiratory measures) and intervals (cardiac frequency), and sampled during the last 5 min of each testing stage. Body masses were measured each visit using digital scales (MS3200, Medical Scale, Charder, Taichung, Taiwan; see Section 2.2.4.4 for details). Anthropometric data were measured once, during the first visit at the laboratory (standing stretched-stature: Harpenden Stadiometer, Holtain Ltd.,

Crymych, UK; six-site sum of skinfolds[50]: Eiken skinfold calliper, Meikosha, Tokyo, Japan; see Section 2.2.4.4 for details). To minimise size-related morphometric differences, sum of skinfold and body mass data were normalised to a common standing height using Equation 2.5 (170.18 cm; Ross and Wilson, 1974). A criterion height-adjusted adiposity threshold of 88 mm was set for participant selection to control for variations in subcutaneous adiposity 88 mm (60th percentile: Ross and Ward, 1985; Landers *et al.,* 2013; Section 2.2.1).

6.2.5 Design and analysis

6.2.5.1 Experimental design

The effect of load placement was tested during three experimental conditions: level, uphill and downhill walking (Figure 6.3 [coloured cells]). When combined with the respective unloaded and torso-loaded trials (Chapters 3-5), this yielded an experiment that was based on a three-way, repeated-measures factorial design, with five levels of the first factor (body mass: extra-small, small, medium, large, extra-large), three levels for the second factor (metabolic intensity: level, uphill and downhill walking) and five levels of the third factor (load location: unloaded, torso, head, hands, feet). Together, this experimental design resulted in the investigation of nine new scaling regressions: head, hand and foot loading during three gradient conditions, level, uphill and downhill. Participants acted as their own controls. Data are presented as means with standard deviations (SD) used to describe data distributions and standard errors of the mean ($\pm$) used to provide information regarding the precision of the mean.

6.2.5.2 Data analysis

Each dataset was first evaluated using the regression decision-making flow chart (Figure 2.8) to confirm whether or not the scaling relationships remained non-linear (allometric). A non-linear relationship was confirmed providing that the model satisfied the assumptions of linear regression while $\log_{10}$ transformed. The $\log_{10}$ transformation resulted in a temporary linear regression (first-order polynomial: Figure 2.9) that could be used for statistical comparisons that assume linearity.

[50] Subcutaneous adiposity was measured at six sites on the body: triceps, subscapular, supraspinale, abdominal, anterior thigh and medial calf (see Figure 2.6 for details).

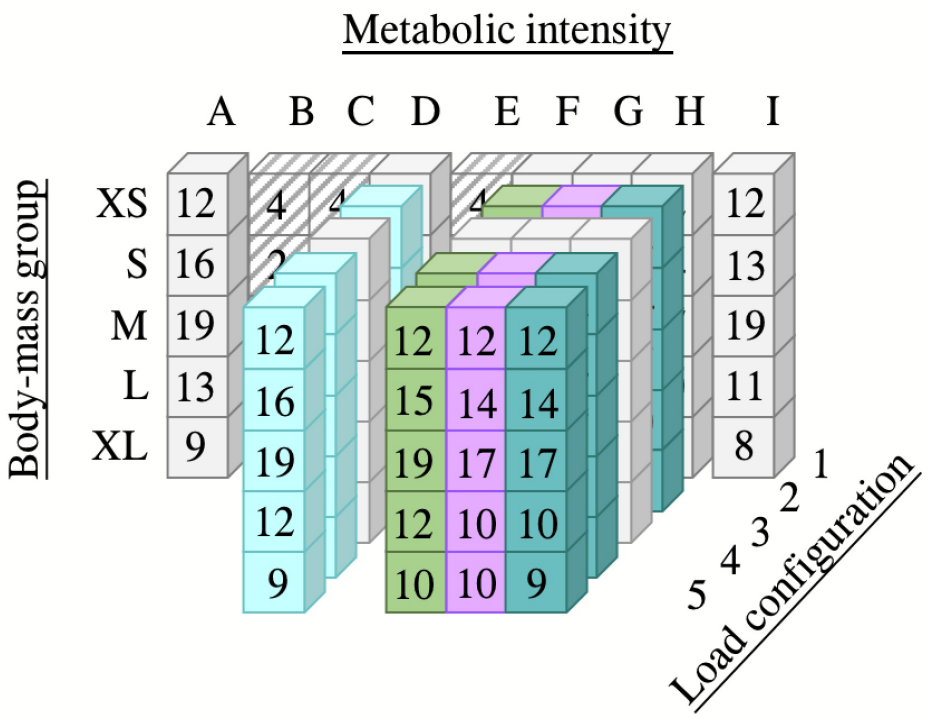

Figure 6.3: A schematic of the experimental design from Chapters 2 through to 6. Sample sizes are identified within each cell. Within the current experimental phase, a three-way factorial design was used, identified by the coloured cells. The first factor (body mass) had five levels: extra-small (XS: $<$65 kg); small (S: 66-76 kg); medium (M: 77-87 kg); large (L: 88-98 kg); and extra-large (XL: $>$99 kg). The second factor (metabolic intensity) had nine levels: supine (A: basal, rest); 100% mass-supported standing (B: exploratory investigation); 50% mass-supported standing (C: exploratory investigation); standing (D); 50% mass-supported walking (E: exploratory investigation); level walking (F); uphill walking (G); downhill walking (H); peak exercise (I). The third factor (load configuration) had five levels: unloaded (1), head loading (2: 1.38-kg helmet), torso loading (3: 25-kg weighted vest), hand loading (4: 2 kg each hand) and foot loading (5: 2 kg each foot).

However, due to the inherent error in applying log-linear regression coefficients to a non-transformed dataset (Jansson, 1985; Newman, 1993; Xiao *et al.,* 2011) it is recommended that the non-linear regression coefficients be used for predictive and normalisation purposes. For this reason, both raw (allometric) and $\log_{10}$-transformed (first-order polynomial) formats have been presented within this Chapter. For reference throughout the Chapter, the allometric exponents have been stated, unless specifically stated otherwise. Bootstrapping[51] (Efron, 1979; Fox and Weisberg, 2017) was performed on each regression equation to generate means and standard errors of the mean for each regression coefficient.

The differences between mass exponents were compared using analyses of covariance on the $\log_{10}$-transformed datasets, whereby a significant interaction effect indicated a difference between mass exponents at the 5% probability level. To determine whether or not those values could also be described using the exercise-specific mass exponent, the derived exponents were compared against $mass^{0.80}$ using null-hypothesis t-testing. As per previous Chapters, potential outliers were identified prior to scaling analyses, using scatter plots, box plots, the Bonferroni test (Cook and Weisberg, 1982; Williams, 1987; Fox, 1997) and Cook's distance (Cook, 1977; Fox, 1991; Hair *et al.,* 1998; see Section 2.2.5.2 for details).

The mean effect of loading on oxygen consumption and cardiac frequency was compared between body-mass groups using two-way factorial analysis of variance. To compare the loading factor among load positions, mass-specific nett oxygen consumption data have been presented. That is, the increase in absolute oxygen consumption per added kilogram of mass ($mL.kg^{-1}.min^{-1}$). Raw and height-adjusted morphometric and physiological differences were compared across body-mass groups using one-way analysis of variance. Analysis of covariance was performed when size-differences remained among height-adjusted measures. However, as no significant interaction effect was realised, the morphometric data were not included as variables within the scaling regressions.

[51] Each model was generated 1000 using a re-sampling approach from the original dataset.

6.3 RESULTS

6.3.1 Pre-experimental standardisation

Prior to performing any scaling analyses, it was necessary to assess two assumptions: that the sample were morphometrically homogeneous and that the scaling regressions remained non-linear during distal load carriage. The former minimised morphological differences, other than a proportional change in body size, that could influence oxygen consumption during these trials. The latter was tested to confirm that the new scaling regressions conformed to the statistical assumptions of analysis of covariance. Providing both assumptions were satisfied, the mass exponents obtained could be confidently compared with each other and applied to future metabolic datasets.

Between-group differences in morphometric data were compared to confirm whether or not the morphometric distribution of the sample was modified by the 17 partial datasets and the four identified outliers ($N=1$ [extra small]: level head, level hand and uphill hand; $N=1$ [large]: downhill head). Fortunately, those sample differences did not significantly change the sample characteristics for height-adjusted sum of skinfold and body mass measurements observed in Chapter 2 (Section 2.3.1.1). Accordingly, participants were considered proportionally similar, and any identified deviations in morphometric data (Section 2.3.1.1) did not significantly affect the scaling mass exponents generated within this Chapter ($P>0.05$).

Having established that the data could be scaled using just two variables (oxygen consumption and mass [body mass and total mass]), the decision-making flow chart (Figure 2.8) was used to evaluate whether or not the scaling relationship could be described using non-linear regression for the nine new metabolic intensities tested within this phase. However, first, the suitability of linear regression was tested. When least-squares, linear regression was applied to the untransformed datasets, a positive origin-intercept, significantly greater than zero was observed for every scaling relationship tested (Table 6.1; $P<0.05$). Thus, the biological assumption of an origin-intercept was violated for all nine regressions, and, as a result, linear regression was not considered a suitable method to describe any of the untransformed datasets.

Table 6.1: Regression equations for the least-squares linear regression models applied to the untransformed datasets. A significant non-zero intercept was observed for all scaling regressions ($P < 0.05$).

Load	Level	Uphill	Downhill
Head	$y = 0.01 \cdot x + 0.24$	$y = 0.02 \cdot x + 0.23$	$y = 0.01 \cdot x + 0.28$
Hands	$y = 0.01 \cdot x + 0.27$	$y = 0.01 \cdot x + 0.33$	$y = 0.01 \cdot x + 0.23$
Feet	$y = 0.01 \cdot x + 0.35$	$y = 0.02 \cdot x + 0.41$	$y = 0.01 \cdot x + 0.34$

In contrast, when $\log_{10}$ transformed , all datasets satisfied the assumptions of linear regression[52]. A linear relationship was observed for each model (Table 6.2), this meant that when data were untransformed they had an allometric (power) distribution. The residuals from those regressions were considered normally distributed when assessed using skewness and kurtosis z-scores ($< \pm 3.26$; Kim, 2013; $P > 0.05$) and the Shapiro-Wilk test (1965; $P > 0.05$). Moreover, no autocorrelation was observed in any dataset (Durbin-Watson test [1950, 1951]; $P > 0.05$). Since the $\log_{10}$-transformed datasets all satisfied the assumptions of linear regression, and when in a raw (allometric) format will also satisfy the origin-intercept requirement for the model, it was concluded that non-linear regression was a suitable method to describe those nine, load-placement scaling relationships.

6.3.2 Effect of load position

Loading at all four body locations significantly increased oxygen consumption and cardiac frequency compared with unloaded walking (Chapters 3 and 4; Table 6.3; $P < 0.05$), except during downhill walking while wearing the helmet ($P > 0.05$). This meant that even light load carriage, for example, at the head (1.38-kg helmet), was not expected to modify walking mechanics, resulted in an increase in metabolic intensity. Among those loading conditions, no difference in oxygen consumption was found between the head and hand loads, or between the torso and foot loads (Table 6.3; $P > 0.05$). However, both torso and foot loading significantly increased oxygen consumption compared with the other three load configurations (Table 6.3; $P < 0.05$). The fact that foot loading (2 kg each foot) resulted in a similar oxygen consumption to that of torso loading (25 kg) despite being less than one tenth of the mass, demonstrated the inefficiency of load carriage on the lower limbs. As a result, despite the differences in the absolute masses carried, the five load configurations could be separated into three statistically different metabolic intensities: unloaded, head and hand loading, torso and foot loading.

It was possible to compare the effect of load location by dividing the nett oxygen consumption by the additional mass carried ($mL.kg^{-1}.min^{-1}$; Table 6.3), this value

[52] The assumptions of linear regression: normal distribution of data, linearity, no autocorrelation and an equal variance of error among residuals.

Table 6.2: Least-squares linear regression equations and coefficient of determination (r^2) values for the $\log_{10}$-transformed datasets and allometric, power equations applied to the untransformed datasets. Oxygen consumption data are scaled against body mass (kg) to display the impact of load carriage on the mass exponent. Data presented for the unloaded and torso-loaded conditions are taken from Chapters 3-5 (C3-C5). Exponent values are highlighted in bold.

	Level		**Uphill**		**Downhill**	
Log_{10} transformed	**Equation**	r^2	**Equation**	r^2	**Equation**	r^2
Unloaded [C3,C4]	$\text{Log}_{10}(y) = \mathbf{0.85} \cdot \text{Log}_{10}(x) - 1.62$	0.81	$\text{Log}_{10}(y) = \mathbf{0.81} \cdot \text{Log}_{10}(x) - 1.39$	0.90	$\text{Log}_{10}(y) = \mathbf{0.71} \cdot \text{Log}_{10}(x) - 1.49$	0.60
Head	$\text{Log}_{10}(y) = \mathbf{0.76} \cdot \text{Log}_{10}(x) - 1.44$	0.77	$\text{Log}_{10}(y) = \mathbf{0.83} \cdot \text{Log}_{10}(x) - 1.42$	0.82	$\text{Log}_{10}(y) = \mathbf{0.63} \cdot \text{Log}_{10}(x) - 1.33$	0.63
Torso [C5]	$\text{Log}_{10}(y) = \mathbf{0.64} \cdot \text{Log}_{10}(x) - 1.14$	0.71	$\text{Log}_{10}(y) = \mathbf{0.69} \cdot \text{Log}_{10}(x) - 1.05$	0.82	$\text{Log}_{10}(y) = \mathbf{0.55} \cdot \text{Log}_{10}(x) - 1.09$	0.49
Hands	$\text{Log}_{10}(y) = \mathbf{0.74} \cdot \text{Log}_{10}(x) - 1.39$	0.76	$\text{Log}_{10}(y) = \mathbf{0.77} \cdot \text{Log}_{10}(x) - 1.29$	0.87	$\text{Log}_{10}(y) = \mathbf{0.69} \cdot \text{Log}_{10}(x) - 1.44$	0.69
Feet	$\text{Log}_{10}(y) = \mathbf{0.70} \cdot \text{Log}_{10}(x) - 1.25$	0.74	$\text{Log}_{10}(y) = \mathbf{0.75} \cdot \text{Log}_{10}(x) - 1.20$	0.85	$\text{Log}_{10}(y) = \mathbf{0.61} \cdot \text{Log}_{10}(x) - 1.23$	0.57
Untransformed	**Level**		**Uphill**		**Downhill**	
Unloaded [C3,C4]	$y = 0.02 \cdot x^{\mathbf{0.87}}$		$y = 0.05 \cdot x^{\mathbf{0.77}}$		$y = 0.05 \cdot x^{\mathbf{.63}}$	
Head	$y = 0.04 \cdot x^{\mathbf{0.76}}$		$y = 0.05 \cdot x^{\mathbf{0.76}}$		$y = 0.05 \cdot x^{\mathbf{0.65}}$	
Torso [C5]	$y = 0.07 \cdot x^{\mathbf{0.65}}$		$y = 0.11 \cdot x^{\mathbf{0.65}}$		$y = 0.10 \cdot x^{\mathbf{0.52}}$	
Hands	$y = 0.04 \cdot x^{\mathbf{0.74}}$		$y = 0.06 \cdot x^{\mathbf{0.74}}$		$y = 0.05 \cdot x^{\mathbf{0.64}}$	
Feet	$y = 0.06 \cdot x^{\mathbf{0.67}}$		$y = 0.08 \cdot x^{\mathbf{0.68}}$		$y = 0.06 \cdot x^{\mathbf{0.61}}$	

Table 6.3: Means and standard errors of those means (in parenthesis) for oxygen consumption and cardiac frequency data. Values presented for the unloaded and torso-loaded states have been taken from Chapters 3-5 (C3-C5). Within-gradient differences in load carriage are identified by symbols (*a*: different from unloaded; *b*: difference from head; *c*: difference from torso; *d*: different from hands; *e*: different from feet; $P < 0.05$).

Absolute oxygen consumption (L.min^{-1})	**Level**	**Uphill**	**Downhill**
Unloaded [C3, C4]	1.02 (0.02)^{ce}	1.46 (0.03)^{ce}	0.73 (0.02)^{ce}
Head	1.03 (0.02)^{ce}	1.47 (0.03)^{ce}	0.75 (0.01)^{ce}
Torso [C5]	1.23 (0.02)^{abd}	1.81 (0.03)^{abde}	0.89 (0.02)^{abd}
Hands	1.04 (0.02)^{ce}	1.53 (0.03)^{ce}	0.77 (0.02)^{ce}
Feet	1.20 (0.02)^{abd}	1.67 (0.03)^{abcd}	0.87 (0.02)^{abd}
Nett oxygen consumption (mL.kg^{-1}.min^{-1})	**Level**	**Uphill**	**Downhill**
Head	12.65 (4.47)	22.49 (4.11)	9.79 (5.04)
Torso [C5]	8.55 (0.29)	13.99 (0.38)	6.25 (0.28)
Hands	8.02 (1.36)	16.43 (1.81)	8.98 (1.44)
Feet	60.10 (2.59)^{cde}	70.95 (2.99)^{cde}	46.08 (3.00)^{cde}
Cardiac frequency (b.min^{-1})	**Level**	**Uphill**	**Downhill**
Unloaded [C3,C4]	97 (2)^{ce}	115 (2)^{ce}	90 (1)^{c}
Head	98 (2)^{ce}	118 (2)^{ce}	91 (1)^{c}
Torso [C5]	108 (2)^{ab}	135 (2)^{abde}	99 (2)^{abd}
Hands	99 (2)	120 (2)^{c}	91 (1)^{c}
Feet	104 (2)^{ab}	126 (2)^{abc}	95 (2)

would be relatively consistent due to the proportional relationship between the mechanical cost of movement and the load carried (Heglund, 1979; Heglund and Taylor, 1988). In this format, locations with a greater mass-specific value displayed a greater loading factor. During level walking, as anticipated, loading at the feet represented the load location with the greatest metabolic burden and was significantly greater than all other loads tested (Table 6.3; $P<0.05$). However, there were no other between-group comparisons, at any gradient ($P>0.05$).

A significant effect of gradient was observed when loads were carried at three locations on the body. When carrying loads at the hands, mass-specific oxygen consumption was significantly greater during uphill walking compared with both other gradient trials (Table 6.3; $P<0.05$). During torso and foot loading conditions, a significant difference was realised among all three gradient trials, with mass-specific oxygen consumption changing in relation to gradient direction (Table 6.3; $P<0.05$). As a result, nett oxygen consumption displayed a gradient relationship with loads that are carried at the torso, hands and feet. Moreover, it is possible that a similar response might occur the among mass exponents observed for those trials.

To evaluate whether or not the effect of load placement on oxygen consumption was influenced by body mass, mass-specific nett data were compared between the 10 lightest and 10 heaviest individuals for each load condition. A body-mass effect was only realised in two datasets, uphill and downhill walking while participants wore a helmet. During those conditions, heavier people experienced a greater loading effect while walking uphill (extra small: 13.11 $mL.kg^{-1}.min^{-1}$; extra large: 35.71 $mL.kg^{-1}.min^{-1}$; $P<0.05$), yet an energy-saving effect of loading during downhill walking (extra small: 15.81 $mL.kg^{-1}.min^{-1}$; extra large: -26.81 $mL.kg^{-1}.min^{-1}$; $P<0.05$). It is possible that the mass-response to head loading was an effect of participant standing height and the associated postural changes with high load placement (Hellebrandt *et al.,* 1944; Attwells *et al.,* 2006; Qu and Yeo, 2011).

6.3.2.1 The effect of load placement on the scaling regressions

Since the three load configurations (head, hands and feet) resulted in unique metabolic intensities during each walking gradient, it was possible that the body-mass exponents

might differ in accordance with those outcomes. However, only four between-load differences were realised. Unloaded level walking (Chapter 3) was significantly greater than the exponents for both torso (Chapter 5) and foot loading (Table 6.4; Figure 6.4; $P<0.05$). During uphill walking, the mass exponent for torso loading was significantly lower than both the unloaded (Chapter 5) and head-loaded conditions (Table 6.4; Figure 6.4; $P<0.05$). That outcome led to the acceptance of Hypotheses Six-One and Six-Three, however, the rejection of Hypothesis Six-Two. Whereas, no between-load differences were realised among the mass exponents during the downhill trials (Table 6.4; Figure 6.4; $P>0.05$). The fact that foot loading only modified the body-mass exponent during level walking but not uphill as observed with torso loading may indicate some interaction between body size and walking efficiency occurring at that location. Specifically, it may signify that the differences in relative oxygen increase associated with fixed-mass load carriage may be minimised during uphill walking when loads are carried at the feet, indicating that the metabolic response is more uniform across the mass range.

While scaling against body mass provides an effective method to explore the body-mass response to absolute load carriage, as demonstrated within Chapter 5, scaling against total mass is the more appropriate method of normalising oxygen consumption data for variations in body mass and torso-load carriage. An aim within this research phase was to identify whether or not that same scaling approach could also be adopted when loads where carried distally on the body. To evaluate that aim, oxygen consumption data from all nine trials were scaled against total mass (body mass, clothing and all other external loads) to generate new mass exponents (Table 6.4). Analysis of covariance was first used to compare these regressions against each other and the previously-established walking exponents: unloaded (Chapters 3 and 4) and the torso-loaded (Chapter 5). No between-load differences were realised among those fifteen total-mass exponents (Figure 6.4; Table 6.4; $P>0.05$).

Null-hypothesis t-testing was then used to identify whether or not metabolic data from the nine new metabolic intensities could also be described using the single exercise-specific exponent ($mass_{total}^{0.80}$: Chapters 3-5). The total-mass exponents for all but two conditions were considered statistically similar to 0.80 ($P>0.05$), with the exceptions

Table 6.4: Least-squares, linear regression equations and coefficients of determination (r^2) for the $\log_{10}$-transformed datasets and allometric, power equations applied to the untransformed datasets. Oxygen consumption data are scaled against total mass (kg: body mass, clothing and all external loads). Data presented for the unloaded and torso-loaded conditions are taken from Chapters 3-5 (C3-C5). Exponent values are highlighted in bold.

Log_{10} transformed	**Level**		**Uphill**		**Downhill**	
	Equation	r^2	**Equation**	r^2	**Equation**	r^2
Unloaded [C3,C4]	$\text{Log}_{10}(y) = \mathbf{0.87} \cdot \text{Log}_{10}(x) - 1.66$	0.81	$\text{Log}_{10}(y) = \mathbf{0.83} \cdot \text{Log}_{10}(x) - 1.43$	0.90	$\text{Log}_{10}(y) = \mathbf{0.72} \cdot \text{Log}_{10}(x) - 1.52$	0.60
Head	$\text{Log}_{10}(y) = \mathbf{0.79} \cdot \text{Log}_{10}(x) - 1.51$	0.77	$\text{Log}_{10}(y) = \mathbf{0.87} \cdot \text{Log}_{10}(x) - 1.50$	0.94	$\text{Log}_{10}(y) = \mathbf{0.66} \cdot \text{Log}_{10}(x) - 1.40$	0.64
Torso [C5]	$\text{Log}_{10}(y) = \mathbf{0.86} \cdot \text{Log}_{10}(x) - 1.67$	0.71	$\text{Log}_{10}(y) = \mathbf{0.92} \cdot \text{Log}_{10}(x) - 1.62$	0.82	$\text{Log}_{10}(y) = \mathbf{0.73} \cdot \text{Log}_{10}(x) - 1.54$	0.49
Hands	$\text{Log}_{10}(y) = \mathbf{0.79} \cdot \text{Log}_{10}(x) - 1.51$	0.76	$\text{Log}_{10}(y) = \mathbf{0.83} \cdot \text{Log}_{10}(x) - 1.43$	0.87	$\text{Log}_{10}(y) = \mathbf{0.74} \cdot \text{Log}_{10}(x) - 1.56$	0.69
Feet	$\text{Log}_{10}(y) = \mathbf{0.74} \cdot \text{Log}_{10}(x) - 1.36$	0.75	$\text{Log}_{10}(y) = \mathbf{0.79} \cdot \text{Log}_{10}(x) - 1.31$	0.85	$\text{Log}_{10}(y) = \mathbf{0.66} \cdot \text{Log}_{10}(x) - 1.33$	0.57
Untransformed	**Level**		**Uphill**		**Downhill**	
Unloaded [C3,C4]	$y = 0.02 \cdot x^{\mathbf{0.88}}$		$y = 0.04 \cdot x^{\mathbf{0.80}}$		$y = 0.04 \cdot x^{\mathbf{0.65}}$	
Head	$y = 0.03 \cdot x^{\mathbf{0.80}}$		$y = 0.04 \cdot x^{\mathbf{0.80}}$		$y = 0.04 \cdot x^{\mathbf{0.68}}$	
Torso [C5]	$y = 0.02 \cdot x^{\mathbf{0.88}}$		$y = 0.03 \cdot x^{\mathbf{0.88}}$		$y = 0.04 \cdot x^{\mathbf{0.71}}$	
Hands	$y = 0.03 \cdot x^{\mathbf{0.80}}$		$y = 0.04 \cdot x^{\mathbf{0.80}}$		$y = 0.04 \cdot x^{\mathbf{0.70}}$	
Feet	$y = 0.05 \cdot x^{\mathbf{0.71}}$		$y = 0.07 \cdot x^{\mathbf{0.72}}$		$y = 0.05 \cdot x^{\mathbf{0.66}}$	

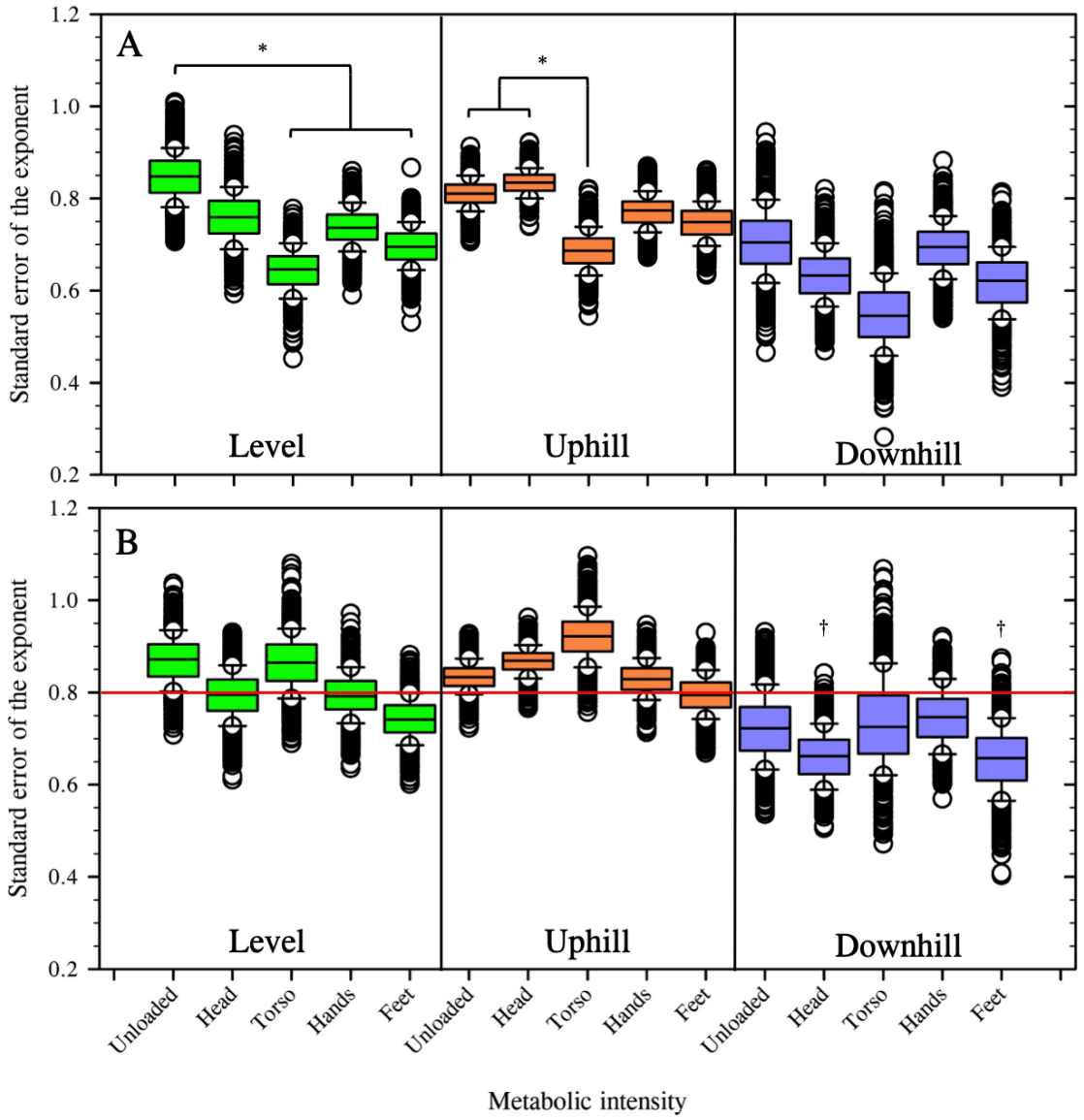

Figure 6.4: Box plots displaying the mean and standard errors of the mean for each trial when oxygen consumption data were scaled against body mass (Figure 6.4A) and total mass (Figure 6.4B). Bootstrapping (repeated sampling 1000 times) was used to obtain those values for each regression equation. Mass exponents are coloured according to walking gradient (level: green; uphill: orange; downhill: purple) and are identified with each load position. The red line in Figure 6.4B indicates the total-mass exponent obtained in Chapter 5 ($mass_{total}^{0.80}$). Significant differences are identified by the symbols (*: within-intensity differences; †: total-mass exponents different from $mass_{total}^{0.80}$; $P<0.05$). No between-gradient differences were realised ($P>0.05$).

being head- and foot-loaded downhill walking ($P<0.05$; Figure 6.4), which both scaled by the same exponent ($mass_{total}^{0.66}$; Table 6.4; $P>0.05$). Otherwise, there was no effect of gradient nor load position (leading to the partial acceptance of Hypotheses Six-Four and Six-Five). Consequently, providing that participants are supporting their own body mass, as well as the carried masses (see Section 3.3.3.1 for details on mass-supported scaling), oxygen consumption data during all exercise intensities can be scaled and normalised using either of two mass exponents: for downhill walking while loaded at the head or feet, $mass_{total}^{0.66}$, and for all other conditions tested, $mass_{total}^{0.80}$ (untransformed exponents; Figure 6.4; Table 6.4; Table 6.5).

6.4 DISCUSSION

In this Chapter the effects of distal load placement were explored on the scaling relationship between oxygen consumption and body mass, this is the first investigation found where this has been performed using human data. It is well known that loads placed away from the body's centre of mass result in a greater metabolic cost per kilogram of carried mass (Soule and Goldman, 1969; Martin, 1985; Taylor *et al.,* 2012). However, how body size interacts with that relationship remained unknown. As previously demonstrated (Chapter 5; Taylor *et al.,* 1980), fixed-mass load carriage results in a non-uniform, relative increase in oxygen consumption. There is also evidence that a body-mass response might be observable for the loading factor when loads are carried at the hands and head (Soule and Goldman, 1969; Kamon and Belding, 1971). Together, those relationships could result in a modified body- and total-mass exponent during walking, at any gradient, compared with that of torso loading. The purpose of this experiment was therefore to determine the most appropriate mass exponent to describe oxygen consumption during level and gradient walking while carrying distally placed loads.

All load configurations significantly increased oxygen consumption compared with unloaded walking (Table 6.3; $P<0.05$), resulting in three distinct metabolic intensities at each gradient (5%, 0%, -5%; Table 6.3; $P<0.05$): unloaded, head and hands, torso and feet. Foot loading resulted in a similar metabolic intensity to torso load carriage, despite being almost one-tenth of the carried mass, due to a significantly greater loading factor (Table 6.3; $P<0.05$). However, no difference in

Table 6.5: Steady-state level walking, oxygen consumption data ($L.min^{-1}$) for the five load configurations: unloaded, head (1.38-kg helmet), torso (25-kg weighted vest), hands (2-kg wrist weights [each hand]) and feet (2 kg each foot). Data are presented as normalised residuals with standard errors or the mean in parentheses for three normalisation methods: $mass_{total}^{0.80}$, $mass_{body}^{0.80}$ and $mass^{-1}$ (ratiometric). No within- or between-group differences were observed when data were normalised using $mass_{total}^{0.80}$ ($P > 0.05$). When data were normalised using $mass_{body}^{0.80}$, residuals for the foot and torso loads were significantly higher than the other three conditions ($P < 0.05$), but there were no within condition body-mass differences ($P > 0.05$). Significant within and between group differences were observed when data were normalised using the ratiometric approach, identified by the symbol (*; $P < 0.05$).

$Mass_{total}^{0.80}$	**Unloa ded ($N=68$)**	**Head ($N=68$)**	**Torso ($N=67$)**	**Hands ($N=68$)**	**Feet ($N=68$)**
Full sample	0.03 ($\pm < 0.01$)	0.03 ($\pm < 0.01$)	0.03 ($\pm < 0.01$)	0.03 ($\pm < 0.01$)	0.03 ($\pm < 0.01$)
Lightest ($N=10$)	0.03 ($\pm < 0.01$)	0.03 ($\pm < 0.01$)	0.03 ($\pm < 0.01$)	0.03 ($\pm < 0.01$)	0.03 ($\pm < 0.01$)
Heaviest ($N=10$)	0.03 ($\pm < 0.01$)	0.03 ($\pm < 0.01$)	0.03 ($\pm < 0.01$)	0.03 ($\pm < 0.01$)	0.03 ($\pm < 0.01$)
$Mass_{body}^{0.80}$	**Unloa ded ($N=68$)**	**Head ($N=68$)**	**Torso ($N=67$)**	**Hands ($N=68$)**	**Feet ($N=68$)**
Full sample	0.03 ($\pm < 0.01$)	0.03 ($\pm < 0.01$)	0.04 ($\pm < 0.01$)	0.03 ($\pm < 0.01$)	0.04 ($\pm < 0.01$)
Lightest ($N=10$)	0.03 ($\pm < 0.01$)	0.03 ($\pm < 0.01$)	0.04 ($\pm < 0.01$)	0.03 ($\pm < 0.01$)	0.04 ($\pm < 0.01$)
Heaviest ($N=10$)	0.03 ($\pm < 0.01$)	0.03 ($\pm < 0.01$)	0.04 ($\pm < 0.01$)	0.03 ($\pm < 0.01$)	0.04 ($\pm < 0.01$)
$Mass^{-1}$	**Unloa ded ($N=68$)**	**Head ($N=68$)**	**Torso ($N=67$)**	**Hands ($N=68$)**	**Feet ($N=68$)**
Full sample	0.01 ($\pm < 0.01$)	0.01 ($\pm < 0.01$)	0.02 ($\pm < 0.01$)*	0.01 ($\pm < 0.01$)	0.01 ($\pm < 0.01$)
Lightest ($N=10$)	0.01 ($\pm < 0.01$)	0.01 ($\pm < 0.01$)	0.02 ($\pm < 0.01$)*	0.01 ($\pm < 0.01$)	0.02 ($\pm < 0.01$)*
Heaviest ($N=10$)	0.01 ($\pm < 0.01$)	0.01 ($\pm < 0.01$)	0.01 ($\pm < 0.01$)	0.01 ($\pm < 0.01$)	0.01 ($\pm < 0.01$)

loading factor was observed among and of the other three load locations (Table 6.3; $P > 0.05$). This meant that, at least for the masses carried, loading at the head and hands scales proportionally with torso loading.

The effect of load carriage on the body-mass exponent was only realised during torso (Chapter 5) and foot load carriage, whereby it was significantly reduced (Table 6.3; Figure 6.4; $P < 0.05$). Thus, Hypotheses Six-One [body-mass exponent section] and Six-Three were accepted, but Hypothesis Six-Two was rejected. Therefore, the mass exponent was only modified during load locations that resulted in a significantly greater metabolic burden (Table 6.3): the product of load location (loading factor) and the mass carried. That increase in absolute oxygen consumption would result in a mass-dependent change in relative oxygen consumption, which would be greater with a decrease in body mass, thus, flattening the regression slope (smaller mass exponent). As a result, it is possible to observe this response at any load location, providing that metabolic burden is sufficiently increased. However, the minimum stimulus required to observe this response remains uncertain and it is also unknown whether heavier loads will result in an even smaller body-mass exponent. This uncertainty means that caution must be used when scaling loaded states using body-mass. Therefore, an alternative method was explored: total mass.

In Chapter 5, the effect of torso loading on the mass exponent could be minimised if data were scaled against total mass, rather than body mass. This same scaling approach was evaluated for the datasets tested in this research phase. Analysis of covariance revealed no between-group differences among the total-mass exponents (Table 6.4; Figure 6.4; $P > 0.05$). However, when those exponents were compared against the exercise-specific exponent ($mass_{total}^{0.80}$), two conditions deviated from that response: head- and foot-loaded downhill walking (both: $mass_{total}^{0.66}$; Figure 6.4; $P < 0.05$). That outcome highlighted the presence of an energy-saving mechanism that becomes more effective as body mass increases during downhill walking. Accordingly, it appears that a proportional relationship exists between oxygen consumption and the total mass (growth or external load) carried during almost all steady-state walking conditions. This response occurred regardless of the significantly greater loading factor observed for load carriage at the feet (Table 6.3; $P < 0.05$).

Therefore, it is anticipated that this outcome will remain possible for metabolic burdens up to 70 mL.kg^{-1}.min^{-1} (uphill walking with loads carried at the feet: Table 6.3).

6.4.1 The effect of carrying loads on the head

Load carriage on the head is considered somewhat more economical than carrying loads elsewhere on the body such as the hands and feet (Soule and Goldman, 1969; Kamon and Belding, 1971; Schertzer and Riemer, 2014), and economically is considered second only to the torso (Soule and Goldman, 1969; Minetti *et al.,* 2006). That is because, if the load is balanced centrally, minimal disturbances occur to the body's centre of gravity. However, since there is an increase in the total mass carried, the metabolic cost of walking is still increased. As a result, there remains the possibility that oxygen consumption will scale by a different mass exponent when loads are carried on the head compared with unloaded, level walking.

Within the present investigation, load carriage on the head (1.38-kg helmet) increased mean oxygen consumption by $\sim$1% during level walking (unloaded: 1.02 L.min^{-1}; head: 1.03 L.min^{-1}; $P<0.05$). Nett mass-specific oxygen consumption was similar to previously reported loaded and unloaded values (unloaded: 12.64 mL.kg^{-1}.min^{-1} [current investigation]; 12.94 mL.kg^{-1}.min^{-1} [Soule and Goldman, 1969]; 12.80 mL.kg^{-1}.min^{-1} [Taylor *et al.,* 2012]; head: 12.44 mL.kg^{-1}.min^{-1} [current investigation]; 13.67 mL.kg^{-1}.min^{-1} [Soule and Goldman, 1969]; 13.40 mL.kg^{-1}.min^{-1} [Taylor *et al.,* 2012]), despite having sampled a wide participant mass range within this experiment and variable load masses being used within each study (1.38 kg [current study]; 1.40 kg [Taylor *et al.,* 2012]; 14 kg [Soule and Goldman, 1969]). Thus, the loading factor and scaling responses observed within this experiment should remain consistent up to head loads of at least 14 kg.

Loading on the head was the only load configuration where a body-mass response was observed among the mass-specific nett data. That is, heavier people experienced a greater loading effect while walking uphill (extra small: 13.11 mL.kg^{-1}.min^{-1}; extra large: 35.71 mL.kg^{-1}.min^{-1}; $P<0.05$), but an energy-saving effect of loading during downhill walking (extra small: 15.81 mL.kg^{-1}.min^{-1}; extra large: -26.81

$mL.kg^{-1}.min^{-1}$; $P < 0.05$). Those variable within-gradient differences meant that the gradient-specific changes to mass-specific nett oxygen consumption were non-significant ($P > 0.05$). It is hypothesised that this response was due to the postural changes associated with gradient walking. During uphill walking, a greater forwards lean is observed to help maintain postural balance (Leroux *et al.,* 2002; Kimel-Naor *et al.,* 2017) and is thought to facilitate power generation and absorption during walking (Leroux *et al.,* 2002). However, when loads are carried at the head, it is possible that taller (generally larger) participants would require greater postural stabilisation (Hellebrandt *et al.,* 1944) to counter the increased gravitational forces pulling the body's centre of mass away from the centre of gravity. In contrast, during downhill walking, an increase in hip extension is observed (Leroux *et al.,* 2002; Kimel-Naor *et al.,* 2017) resulting in a backwards lean that would maintain a more upright posture. As a result, the head load can be carried relatively passively through the support of the skeletal structure, and thus would reduce the metabolic impact of load carriage. In summary, the mass-dependent loading factor observed for head loading during gradient walking is believed to be a product of the impact of the gravitational forces applied to the body. That effect is most prominent during uphill walking, where an increased forwards lean is adopted, thereby increasing the magnitude of forces destabilising the body.

Despite the increase in absolute oxygen consumption, and the mass-dependent response to load carriage during gradient walking (Table 6.3), head loading did not modify the body-mass exponent at any gradient (Table 6.2; Figure 6.4; $P > 0.05$). Although the loading factor was similar to that of torso loading (Table 6.3), it appears that a greater mass change is required before the body-mass exponent will be modified. Therefore, it is possible that, if heavier loads are placed at the head, the body-mass exponent may still be reduced.

In contrast, when scaled using total mass, although not statically different from the other conditions tested (Hypothesis Six-One accepted: *ANCOVA*: $P > 0.05$), the exponent for head-loaded downhill walking was statistically smaller than $mass_{total}^{0.80}$ ($mass_{total}^{0.66}$; Figure 6.4; Table 6.4; $P < 0.05$). In support of the mass-specific nett oxygen consumption data, this highlighted a biologically meaningful difference

undetected by the analysis of covariance (head-loading element of Hypothesis Six-Five rejected; Table 6.3). That is, compared with the level walking condition, while downhill walking and carrying a load on the head, larger participants used proportionally less oxygen consumption than the lighter individuals. As discussed previously, it is anticipated that this trial configuration might modify the body's angle (Leroux *et al.,* 2002; Kimel-Naor *et al.,* 2017), increasing walking efficiency relative to the total mass carried, and by building upon the mass-dependent response observed during unloaded walking (Chapter 4), reduce the total-mass exponent.

Nevertheless, as that response to total-mass scaling was only observed during the downhill trial when loaded at the head (Table 6.4; Figure 6.4), both level and uphill walking could still be scaled using that single exponent ($mass_{total}^{0.80}$). Since the loading factors for this load configuration were similar to previously-reported values, it is anticipated that oxygen consumption should scale by that same total-mass exponent for masses up to 14 kg at the head during level and uphill walking.

6.4.2 The effect of carrying loads at the hands

Loads are regularly carried in the hands and around the forearm, both in daily life and for occupational tasks. As a result, the metabolic impact of load carriage at this location has been widely studied. However, this was the first study where the effect of hand (wrist) loading on the scaling relationship was explored.

Loading the hands resulted in a similar absolute and mass-specific metabolic intensity as head loading, even though the load at the hands was more than double the mass carried on the head (head: 1.38 kg; hands: 4 kg total; Table 6.3; $P > 0.05$). Accordingly, per kilogram of added mass, loads carried at the both head and hands increased oxygen consumption at the same rate as torso load carriage. That outcome was atypical from those reported in literature, whereby a greater loading factor is normally observed for the hands (Soule and Goldman, 1969; Kamon and Belding, 1971; Abe *et al.,* 2004). The main difference between those studies and the current investigation is the method of load carriage: carried hand weights versus wrist weights (Figure 6.2B). As such, it is probable that the action of holding the weight, rather than passively carrying it about the wrist, increases the metabolic burden.

However, at light loads, no difference in oxygen consumption has been observed between both load-carriage methods (Graves *et al.,* 1988). An alternative theory is that light load carriage (<9 kg: Abe *et al.,* 2004) may actually increase walking efficiency, by increasing the amount of potential energy transferred into the gait cycle.

Nevertheless, that same relationship between load location and mass-specific loading factor was not observed during uphill walking, where the mass-specific cost of load carriage doubled (level: 8.02 $mL.kg^{-1}.min^{-1}$; uphill: 16.43 $mL.kg^{-1}.min^{-1}$; $P<0.05$). In fact, that was the greatest relative increase in loading factor among all four load conditions (Table 6.3). During uphill walking, while the arm swing is still used to transfer energy into the gait cycle, the swing is no longer mostly passive (Pellegrini *et al.,* 2015). Therefore, the associated metabolic cost of a forceful arm swing will be increased with distal load placement (Cavagna and Kaneko 1977) in a similar way to that observed at faster walking speeds (Soule and Goldman, 1969; Abe *et al.,* 2004). In contrast, no change to the loading factor was observed during downhill walking (Table 6.3; $P>0.05$). Therefore, it was assumed that the arm swing remained relatively passive during load carriage during the decent.

Since the metabolic increases observed while loads were carried at the hands were relatively small (Table 6.3; $P<0.05$), the change in oxygen consumption was not sufficient to modify the mass exponent when scaling against body mass or total mass (Table 6.2; Table 6.4; Figure 6.4; $P>0.05$). Thus, Hypotheses Six-Two and the hand-loading element of Six-Four were rejected. The total-mass exponent was also statistically similar to the previously derived value for exercise intensities, $mass_{total}^{0.80}$ (Chapters 3-5; $P>0.05$). Consequently, hand loading while walking at the velocity of 4.8 $km.h^{-1}$, and at any ambulatory gradient, can be scaled using that same exponent ($mass_{total}^{0.80}$). However, as relatively light increases in the load carried at the hands can significantly increase the loading factor (7 kg: Soule and Goldman, 1969), it is recommended that, during heavier load carriage, the scaling factor be assessed before applying this approach.

6.4.3 The effect of carrying loads on the feet

Foot load carriage was the final load location explored within this experimental phase. Loading at this location had been previously shown to have the greatest loading factor (Soule and Goldman, 1969; Kamon and Belding, 1971; Schertzer and Riemer, 2014, and thus metabolic burden per kilogram of added mass carried. However, it was unknown whether or not that increase in oxygen consumption would be modified by differences in body mass, and therefore influence the shape of the scaling relationship compared with other load configurations.

Foot loading resulted in the greatest nett mass-specific oxygen consumption at all three gradients by 4.7-7.8 fold (Table 6.3; $P<0.05$). As a result, absolute oxygen consumption was equivalent to torso load carriage (Table 6.3; $P>0.05$), despite the foot load being almost one-tenth of the mass. However, the mass-specific value observed for the foot loading was a little lower than those reported by other authors: 60.10 $mL.kg^{-1}.min^{-1}$ (4 kg: current study) versus 73.60 $mL.kg^{-1}.min^{-1}$ (12 kg: Soule and Goldman, 1969) and 88.75 $mL.kg^{-1}.min^{-1}$ (2.44 kg: Taylor *et al*, 2012). It is possible that this was a result of having some of the load distributed about the ankle (Figure 6.2C), thereby reducing the kinematic and metabolic responses to load carriage as the load is place closer to the body (Browning *et al.,* 2007).

The increase in oxygen consumption associated with loading the feet resulted in a significant reduction to the body-mass exponent during level walking (Table 6.2; Figure 6.4; $P<0.05$), similar to that of torso loading (Table 6.2; Figure 6.4; $P>0.05$). Therefore, Hypothesis Six-Three was accepted. That response confirmed the assumption that, for load carriage to modify the body-mass exponent, it is dependent upon the absolute increase in oxygen consumption, the product of the loading factor and mass carried, rather than either factor individually. However, during uphill walking, similar responses were not observed between torso and foot loading locations (Table 6.2; Figure 6.4; $P<0.05$). While the body-mass exponent was decreased during torso loading (Chapter 5), the same outcome was not realised during foot-load carriage. That outcome was unexpected, as both load locations also displayed similar metabolic intensities during uphill walking (Table 6.3; $P>0.05$). However, a significant body-mass response was not observed during gradient

walking. Therefore, oxygen consumption during that condition might also be influenced by an additional independent variable. For example, there may be a reduction in stored potential energy during the landing phase of the gait cycle relative to the total mass increase. Since the increase in mass occurs at the foot, a location below the structures that store the compressive forces, there will be no increase in landing forces applied to those structures. That outcome will be independent of body size, and thus, the increase in mechanical energy required to move the external mass will remain constant across the mass range.

Despite the significantly greater loading factor observed during load carriage at the feet, the total-mass exponents for level and uphill walking were statistically similar to those of other conditions, as well as the exercise-intensity exponent ($mass_{total}^{0.80}$; $P > 0.05$). Thus, Hypothesis Six-Four was rejected. This meant that, as with loading at other conditions, the increase in oxygen consumption was considered proportional to a change in the total mass carried. Moreover, that outcome raised the question of whether or not during level and uphill walking a similar response would be observed with loading factors up to ~ 70 mL.min^{-1}.kg^{-1} (foot loading during uphill walking) regardless of the load placement. This could mean that even heavy loads carried at the hands, where an increase in loading factor is anticipated, might still scale against the same total-mass exponent: $mass_{total}^{0.80}$. Such an outcome warrants future testing, as it has a practical application to realistic load carriage, for example, when generating task-specific metabolic cut scores.

Nevertheless, the same scaling response was not observed during foot-loaded downhill walking. While the total-mass exponent was statistically similar to the others tested (*ANCOVA*: $P > 0.05$), oxygen consumption scaled by a significantly smaller total-mass exponent than $mass_{total}^{0.80}$ (Chapters 3-5; $mass_{total}^{0.66}$; $P < 0.05$). Thus, Hypothesis Six-Five was only partially accepted. Like the head loading condition, this response highlighted a disproportionately greater decrease in oxygen consumption from the level-walking values as the total mass increased (ten lightest: 24%; ten heaviest: 31%). A similar response was observed during unloaded walking (Chapter 4); however, this had no significant impact on the scaling relationship. While the mechanism behind this relationship is not yet known, it cannot be solely related to the

greater eccentric loading associated with an increase in the total mass carried, for it was only observed in some loading conditions (head and feet) and not during torso-load carriage, the heaviest external mass tested. Thus, an additional underlying relationship between body size and load location must have an impact on this scaling response.

Unlike the other load configurations, during the stance phase of walking load placement at the foot is supported by the ground, reducing the cost of oxygen per kilogram of total mass. However, this reduction in oxygen consumption is typically offset by the increase in energy required to initiate and stop the leg swing when the load is carried distally (Cavagna and Kaneko 1977; Browning *et al.,* 2007), particularly when loaded (Soule and Goldman, 1969; Martin, 1985; Taylor *et al.,* 2012). Accordingly, a greater metabolic cost per unit of total mass should be expected, and can be observed during foot-loaded level and uphill walking (Table 6.3). In contrast, once initiated, the swing phase is relatively passive during downhill walking (Garcia *et al.,* 1998; Hunter *et al.,* 2010): assisted by the release of potential energy. In this way, gravity assists both the leg swing and the forwards momentum of the body during downhill walking, reducing the oxygen cost of walking per step relative to level and uphill conditions. Therefore, it is possible that participants increased their stride length and reduced their step frequency to capitalise on this energy-saving mechanism, as has been previously observed during unloaded conditions (Minetti *et al.,* 1993; Sheehan and Gottschall, 2012). Moreover, since the capacity to lengthen the stride increases with body size, this relationship may help to explain the greater walking efficiency observed as body mass increased during this condition. Consequently, when these metabolic data are then scaled against the total mass carried, this saving in oxygen consumption may produce the flatter scaling regression observed and thus the smaller mass exponent.

6.5 CONCLUSION

This is the first investigation wherein the effect of load placement on the scaling relationship between oxygen consumption and body mass has been explored. Previously, it was unclear whether the loading factors associated with distal load placements would modify the mass exponents (body and total mass), and whether

those factors would be further influenced by variations in body mass among individuals carrying those loads. However, despite the five load configurations resulting in three distinct metabolic intensities, only loads carried at the torso and feet significantly reduced the body-mass exponent. Since those loads varied significantly in mass, yet produced similar absolute rates of oxygen consumption, it was concluded that a change to the body-mass exponent is determined by the size of the increase in oxygen consumption, as opposed to load carriage in a specific location: the product of the external mass carried and its configuration-specific loading factor.

Despite the variations in walking gradient and loading factors observed, the metabolic changes associated with distal load placement remained proportional to the change in total mass for all but two conditions. Accordingly, it was possible to describe and normalise those oxygen consumption data using a single mass exponent: $mass_{total}^{0.80}$. For the two conditions that deviated from this response, head- and foot-loaded downhill walking, a greater reduction in oxygen consumption was observed as body mass increased, resulting in a reduced mass exponent ($mass_{total}^{0.66}$). It is hypothesised that this scaling response was due to a greater load-specific release in potential energy that could be capitalised by adopting a longer stride, thus favouring larger individuals. In summary, it was possible to describe all fifteen load configurations tested during steady-state walking across Chapters 3 to 6 using either of two mass exponents: $mass_{total}^{0.66}$ during downhill walking loaded at either the head or feet and $mass_{total}^{0.80}$ for all other conditions.

6.6 REFERENCES

Abe, D., Muraki, S., and Yasukouchi, A. (2008). Ergonomic effects of load carriage on the upper and lower back on metabolic energy cost of walking. *Applied Ergonomics*. 39(3):392-398.

Abe, D., Yanagawa, K., and Niihata, S. (2004). Effects of load carriage, load position, and walking speed on energy cost of walking. *Applied Ergonomics*. 35(4):329-335.

Åstrand, P.O., and Saltin, B. (1961). Oxygen uptake during the first minutes of heavy muscular exercise. *Journal of Applied Physiology*. 16(6):971-976.

Attwells, R.L., Birrell, S.A., Hooper, R.H., and Mansfield, N.J. (2006). Influence of carrying heavy loads on soldiers' posture, movements and gait. *Ergonomics*. 49(14):1527-1537.

Borghols, E.A.M., Dresen, M.H.W., and Hollander, A.P. (1978). Influence of heavy weight carrying on the cardiorespiratory system during exercise. *European Journal of Applied Physiology and Occupational Physiology*. 38(3):161-169.

Browning, R.C., Modica, J.R., Kram, R., and Goswami, A. (2007). The effects of adding mass to the legs on the energetics and biomechanics of walking. *Medicine and Science in Sports and Exercise*. 39(3):515-525.

Burdon, C.A., Park, J., Tagami, K., Groeller, H., and Sampson, J.A. (2018). Effect of Practice on Performance and Pacing Strategies During an Exercise Circuit Involving Load Carriage. *The Journal of Strength and Conditioning Research*. 32(3):700-707.

Cavagna, G.A., and Kaneko, M. (1977). Mechanical work and efficiency in level walking and running. *The Journal of Physiology*. 268(2):467-481.

Cook, R.D. (1977). Detection of influential observation in linear regression. *Technometrics*. 19(1):15-18.

Cook, R.D., and Weisberg, S. (1982). *Residuals and influence in regression*. Chapman and Hall, New York.

Datta, SR., a nd Ramanathan, N.L. (1971). Ergonomic comparison of seven modes of carrying loads on the horizontal plane. *Ergonomics*. 14(2):269-278.

Durbin, J., and Watson, G.S. (1950). Testing for serial correlation in least squares regression: I. *Biometrika*. 37(3/4):409-428.

Durbin, J., and Watson, G.S. (1951). Testing for serial correlation in least squares regression. II. *Biometrika*. 38(1/2):159-177.

Efron, B. (1979). Computers and the theory of statistics: thinking the unthinkable. *SIAM review*. 21(4):460-480.

Fox, J. (1991). *Regression diagnostics: An introduction*. Volume 79. Sage, London.

Fox, J. (1997). *Applied regression analysis, linear models, and related methods*. Sage, London.

Fox, J., and Weisberg, S. (2017). *An R Companion to Applied Regression.* Sage, London.

Garcia, M., Chatterjee, A., Ruina, A., and Coleman, M. (1998). The simplest walking model: stability, complexity and scaling. *Journal of Biomechanical Engineering*. 120(2): 281-288.

Graves, J.E., Martin, A.D., Miltenberger, L.A., and Pollock, M.L. (1988). Physiological responses to walking with hand weights, wrist weights, and ankle weights. *Medicine and Science in Sports and Exercise*. 20(3):265-271.

Hair, J.F., Anderson, R.E., Tatham, R.L., and Black, W.C. (1998). *Multivariate data analysis*. Prentice-Hall International, Upper Saddle River, NJ.

Heglund, N.C. (1979). *Size scaling, speed and the mechanics of locomotion*. (Doctoral dissertation). Harvard University.

Heglund, N.C., and Taylor, C.R. (1988). Speed, stride frequency and energy cost per stride: how do they change with body size and gait? *Journal of Experimental Biology*. 138(1):301-318.

Hellebrandt, F.A., Fries, E.C., Larsen, E.M., and Kelso, L.E.A. (1944). The influence of the Army pack on postural stability and stance mechanics. *American Journal of Physiology - Legacy Content*. 140(5):645-655.

Hunter, L.C., Hendrix, E.C., and Dean, J.C. (2010). The cost of walking downhill: Is the preferred gait energetically optimal? *Journal of Biomechanics*. 43(10):1910-1915.

Jamnik, V., Gumienak, R., and Gledhill, N. (2013). Developing legally defensible physiological employment standards for prominent physically demanding public safety occupations: a Canadian perspective. *European Journal of Applied Physiology*. 113(10):2447-2457.

Jansson, M. (1985). A comparison of detransformed logarithmic regressions and power function regressions. *Geografiska Annaler: Series A, Physical Geography*. 67(1-2):61-70.

Johnson, A.T., Benjamin, M.B., and Silverman, N. (2002). Oxygen consumption, heat production, and muscular efficiency during uphill and downhill walking. *Applied Ergonomics*. 33(5):485-491.

Kamon, E., and Belding, H.S. (1971). The physiological cost of carrying loads in temperate and hot environments. *Human Factors*. 13(2):153-161.

Kim, H.Y. (2013). Statistical notes for clinical researchers: assessing normal distribution (2) using skewness and kurtosis. *Restorative Dentistry and Endodontics*. 38(1):52-54.

Kimel-Naor, S., Gottlieb, A., and Plotnik, M. (2017). The effect of uphill and downhill walking on gait parameters: a self-paced treadmill study. *Journal of Biomechanics*. 60:142-149.

Kinoshita, H. (1985). Effects of different loads and carrying systems on selected biomechanical parameters describing walking gait. *Ergonomics*. 28(9):1347-1362.

Landers, G.J., Ong, K.B., Ackland, T.R., Blanksby, B.A., Main, L.C., and Smith, D. (2013). Kinanthropometric differences between 1997 World championship junior elite and 2011 national junior elite triathletes. *Journal of Science and Medicine in Sport*. 16(5):444-449.

Leroux, A., Fung, J., and Barbeau, H. (2002). Postural adaptation to walking on inclined surfaces: I. Normal strategies. *Gait and Posture*. 15(1):64-74.

Martin, P.E. (1985). Mechanical and physiological responses to lower extremity loading during running. *Medicine and Science in Sports and Exercise*. 17(4):427-433.

Minetti, A.E., Ardigo, L.P., and Saibene, F. (1993). Mechanical determinants of gradient walking energetics in man. *The Journal of Physiology*. 472(1):725-735.

Minetti, A.E., Formenti, F., and Ardigo, L.P. (2006). Himalayan porter's specialization: metabolic power, economy, efficiency and skill. *Proceedings of the Royal Society of London B: Biological Sciences*. 273(1602):2791-2797.

Newman, M.C. (1993). Regression analysis of log transformed data: Statistical bias and its correction. *Environmental Toxicology and Chemistry*. 12(6):1129-1133.

Pellegrini, B., Peyré-Tartaruga, L.A., Zoppirolli, C., Bortolan, L., Bacchi, E., Figard-Fabre, H., and Schena, F. (2015). Exploring muscle activation during nordic walking: a comparison between conventional and uphill walking. *PloS one*. 10(9):e0138906.

Phillips, D.B., Stickland, M.K., and Petersen, S.R. (2016). Ventilatory responses to prolonged exercise with heavy load carriage. *European Journal of Applied Physiology*. 116(1):19-27.

Qu, X., and Yeo, J.C. (2011). Effects of load carriage and fatigue on gait characteristics. *Journal of Biomechanics*. 44(7):1259-1263.

Ross, W.D., and Ward, R. (1985). *The O-scale system*. Rosscraft, Surrey, BC.

Ross, W.D., and Wilson, N.C. (1974). A stratagem for proportional growth assessment. *Acta Paediatrica Belgica*. 28:169-182.

Schertzer, E., and Riemer, R. (2014). Metabolic rate of carrying added mass: a function of walking speed, carried mass and mass location. *Applied Ergonomics*. 45(6):1422-1432.

Shapiro, S.S., and Wilk, M.B. (1965). An analysis of variance test for normality (complete samples). *Biometrika*. 52(3/4):591-611.

Sheehan, R.C., and Gottschall, J.S. (2012). At similar angles, slope walking has a greater fall risk than stair walking. *Applied Ergonomics*. 43(3):473-478.

Soule, R.G., and Goldman, R.F. (1969). Energy cost of loads carried on the head, hands, or feet. *Journal of Applied Physiology*. 27(5):687-690.

Soule, R.G., Pandolf, K.B., and Goldman, R.F. (1978). Energy expenditure of heavy load carriage. *Ergonomics*. 21(5):373-381.

Taylor, C.R., Caldwell, S.L., and Rowntree, V.J. (1972). Running up and down hills: some consequences of size. *Science*. 178(4065):1096-1097.

Taylor, C.R., Heglund, N.C., McMahon, T.A., and Looney, T.R. (1980). Energetic cost of generating muscular force during running: a comparison of large and small animals. *Journal of Experimental Biology*. 86(1):9-18.

Taylor, N.A.S., Lewis, M.C., Notley, S.R., and Peoples, G.E. (2012). A fractionation of the physiological burden of the personal protective equipment worn by firefighters. *European Journal of Applied Physiology*. 112(8):2913-2921.

Van de Putte, M., Hagemeister, N., St-Onge, N., Parent, G., and de Guise, J.A. (2006). Habituation to treadmill walking. *Bio-Medical Materials and Engineering*. 16(1):43-52.

Wall, J.C., and Charteris, J. (1981). A kinematic study of long-term habituation to treadmill walking. *Ergonomics*. 24(7):531-542.

Williams, D.A. (1987). Generalized linear model diagnostics using the deviance and single case deletions. *Applied Statistics*. 36(2):181-191.

Xiao, X., White, E.P., Hooten, M.B., and Durham, S.L. (2011). On the use of log transformation vs. nonlinear regression for analyzing biological power laws. *Ecology*. 92(10):1887-1894.

CHAPTER 7: CONCLUSIONS AND RECOMMENDATIONS

7.1 CONCLUSIONS

The purpose of this experimental series was to establish whether a linear (first-order polynomial) or non-linear (allometric) approach is more appropriate to describe the scaling relationship[53] between oxygen consumption and body mass in adult humans. Although both scaling methods have previously been used to describe human metabolic data, a systematic difference exists between those methods, with that difference increasing as the mass range of interest is expanded (Figure 2.14). This indicates that only one approach could be appropriate to faithfully describe and model such data. However, until now, a direct comparison between those scaling methods had not been comprehensively performed on human data. Accordingly, this is the first series of investigations to directly compare those scaling models against human metabolic data. To ensure that the outcomes from those investigations were robust, metabolic data were assessed systematically (Figure 2.8), using a strictly controlled population sample and a statistically-appropriate sample size. The overall project was split into five, repeated-measures experimental phases, permitting model comparisons across a broad range of metabolic intensities. The first experiment (Chapter 2) was aimed at determining the appropriate scaling model for resting intensities (basal and standing). In the second experiment (Chapter 3), the scaling models for unloaded, steady-state walking (4.8 $km.h^{-1}$) and peak exercise (running) were explored. By combining Chapters 2 and 3, the entire physiological range of metabolic intensities had been tested. The subsequent experiments (Chapters 4-6) were an extension of the walking intensity, whereby the impact of variations in ambulatory gradient (Chapter 4), load carriage (Chapter 5) and load distribution (Chapter 6) on oxygen consumption were described.

Before conducting any experimental work, it was necessary to address two sample requirements: the population selected and the sample size. This step is sometimes overlooked within scaling research. However, it is essential to ensure that uncorrected inter-individual variations, and the associated noise, are not introduced. It was

[53] The term scaling relationship has been used solely to refer to the relationship between oxygen consumption and body mass, independently from inferring to whether that relationship is linear or non-linear.

important that a wide body-mass range was sampled, and that the physiological and morphological differences between participants were minimised so that variations in oxygen consumption were a direct result of a proportional change in body mass. Only adult (18-34 y) males were tested, due to the non-mass-dependent differences in metabolism between genders (Solomon *et al.,* 1982; Webb, 1986; Buchholz *et al.,* 2001) and to reduce the possible influence of age (Harris and Benedict, 1919; Mitchell, 1962; Tzankoff and Norris, 1977). Within that population, the sample recruited exceeded the 5^{th} and 95^{th} percentiles of the specified population normative data (Australian Bureau of Statistics, 2012), with participants evenly distributed between 56 kg and 117 kg.

Since absolute skinfold thickness changes relative to body mass (Clarys *et al.,* 1987), a more complex method was required to control for variations the morphological variables. This task was successfully achieved by adjusting morphological data for variations in standing height (Equation 2.3; Ross and Wilson, 1974), which meant that non-proportional variations could be identified, and removed if required. As the morphology of the sample was strictly controlled, this was the first investigation where the scaling regression obtained for oxygen consumption could be confidently attributed to proportional changes in body mass.

The final requirement was to determine the estimated sample size. As both linear and non-linear models were assessed, it was important to consider the requirements for each model. Based on the literature for the linear regression (Harris, 1985; Green, 1991; van Voorhis and Morgan, 2007) and an *a priori* test for the non-linear regression (Figure 2.2), a sample size between 50 and 75 was sought to minimise the standard error of the mean for the regression coefficients generated. Utilising a repeated-measures approach, a total sample of 72 participants was tested across all experimental Chapters, with at least 10 participants recruited in each body-mass group. The sample size, therefore, exceeded the minimum values required for both linear and non-linear regression modelling, and the number previously shown to stabilise a power exponent within a human mass range (>30: Jensen *et al.,* 2001). Bootstrapping was then performed on those regressions, whereby each regression was generated 1000 times using a unique selection of data points from each sample

provided, to obtain a mean and standard error of the mean for each regression coefficient. Together, these methods maximised confidence in the scaling models obtained.

It was hypothesised that, throughout the physiological range of metabolic intensity, oxygen consumption would scale non-linearly (allometrically) against body mass. Moreover, due to the plethora of metabolic scaling models for animals all adhering to a simple allometric regression (an origin intercept) within the literature (*e.g.* Sarrus and Rameaux, 1839; White and Seymour, 2003, 2004; Sieg *et al.,* 2009) the assumption was made that human data, if also non-linear, would follow this same relationship.

However, within that range, it was deemed likely that the shape of that relationship, specifically, the mass exponent[54], would change with metabolic intensity (allometric cascade theory[55]: Darveau *et al.,* 2002). As a result, there was the potential need for unique, intensity-specific scaling models. Therefore, each intensity-specific regression was first individually assessed before comparing it with the other conditions. Those two hypotheses (non-linear model: Hypotheses Two-One [basal] and Two-Three [standing]; effect of metabolic intensity: Hypothesis Two-Four) were first tested during two resting states: basal and standing (stationary: Chapter 2).

Due to the strict experimental standardisation required to achieve a truly basal state (Section 2.2.1) those data could be used to establish a baseline for the scaling relationship, from which the effect of intensity could be compared. The Weir formula

---

[54] Within an allometric (power) regression ($y = ax^b$) the mass exponent "b" determines the shape of the regression curve. Consequently, differences in this value can be used to identify changes in the scaling relationship between conditions. More importantly, it can also be used to normalise the effect of body mass when comparing the oxygen cost of various metabolic demands.

[55] Within the allometric cascade theory, it is argued that the rate of oxygen consumption is limited by different factors throughout the metabolic range. At rest, oxygen consumption meets the demand of cellular respiration, while an increase in metabolic intensity shifts the metabolic pathways, and therefore potential rate of metabolism, until the body is at peak metabolic intensity. During that stage, oxygen consumption is limited by its rate of delivery. As a result, it was expected that the mass exponent will change relative to the metabolic intensity.

(1949; Equation 2.1) was used to estimate basal metabolic rate from steady-state oxygen consumption data, collected using open-circuit, indirect respirometry. While statistically, both the linear and non-linear models both fit the mass range tested, only the non-linear regression displayed realistic, predicted values outside of the mass range investigated. In the linear model, this was most clearly demonstrated by a significant, positive ordinate intercept at zero mass (3569.07 kJ.day^{-1}; Figure 2.14; $P<0.05$), a physiologically impossible outcome. In contrast, the allometric regression satisfied all model requirements (Figures 2.8 and 2.14) and was thus considered the more appropriate model choice. Moreover, the applicability of this model choice for scaling human data beyond the mass range tested was demonstrated in Figure 2.24, depicting the scaling relationship for males from 2.7 to 117.1 kg (Schofield, 1985; Chapter 2 [basal data]). The basal exponent from Chapter 2 was similar to that applied to the combined dataset (Chapter 2: mass$^{0.54}$; combined exponent: mass$^{0.52}$) as well as that of a heterogeneous adult-human population (males and females, $N=262$, mass$^{0.59}$: Müller *et al.,* 2011). This confirmed that, at its baseline, human metabolism scales non-linearly against body mass, and this implied that the entire metabolic range was likely to be non-linear.

Unlike animal data, where adjusting metabolic data to a common deep-body temperature unified the global scaling exponent observed across species (White and Seymour, 2003, 2004), the same process did not modify the human mass exponent (Figure 2.17; Table 2.7; $P>0.05$). There were two reasons for this. Firstly, during rest, human deep-body temperature has a range of only 1-2°C (Darowski, 1991; Sund Levander *et al.,* 2002; Taylor *et al.,* 2014), therefore any within-species differences in Q_{10} reaction rates[56] will be minimal. Secondly, the mean deep-body temperature for the sample (36.3°C) was similar to the adjusted value used for animals (36.2°C). Accordingly, adjusting data for variations in deep-body temperature in those human data did not modify the regression model, it only lowered the mean metabolic rate (unadjusted: 8112.2 kJ.day^{-1} [±117.8]; temperature adjusted: 7943.6 kJ.day^{-1} [±118.0]; $P<0.05$). As a result, when testing healthy adult humans in a

[56]A Q_{10} classification defines the relationship between an enzyme's rate of reaction and its temperature. For example, a $Q10$ of 2 means the reaction rate will double with every 10°C elevation in temperature.

normothermic environment, it is not necessary to adjust human basal data for variations in deep-body temperature before comparing data within or across species.

The mass exponent derived for human basal metabolism was statistically smaller than that observed for the animal kingdom ($mass^{0.57}$ [present investigation; log_{10}-transformed exponent]; $mass^{0.67}$ [animal literature]: Sarrus and Rameaux, 1839; White and Seymour, 2003). This means that it is statistically inappropriate to scale human basal data against the same value used in comparative physiology. It may also highlight why some early researchers advocated against using non-linear scaling and the surface law to describe human metabolic data (Harris and Benedict, 1919), since they applied $mass^{0.67}$ but did not evaluate those data for a more appropriate non-linear exponent. It is suspected that there is no universal mass exponent to describe all basal metabolic datasets across animal species (Dodds *et al.,* 2001; Savage *et al.,* 2004; White *et al.,* 2007), but rather phylogenic-specific values (White *et al.,* 2007, 2009; Sieg *et al.,* 2009), that vary depending upon both the number of species tested and the mass range sampled.

The second part of the experimental phase (Chapter 2) was aimed at identifying whether the resulting metabolic increase from a change in posture (supine to standing), would significantly modify the basal scaling relationship. Until this investigation, no scaling relationships had been reported for a metabolic intensity between basal and steady-state walking. As a result, it was unclear whether a change in metabolic intensity would warrant a unique scaling approach. Using the same sample, immediately after the basal condition, participants completed a 10-min standing (stationary) stage. The change in posture significantly increased oxygen consumption (supine: 0.27 $L.min^{-1}$ [$\pm < 0.01$]; standing: 0.33 $L.min^{-1}$ [± 0.01]; $P < 0.05$), however, the mass exponent did not differ from the basal value (Figure 2.23; $P > 0.05$). As the work performed during standing is relatively passive, with the body supported mainly by its skeletal structure, and the small increase in oxygen consumption remained proportional with body mass. Consequently, a single mass exponent (supine: $mass^{0.54}$ [allometric]) could be used to describe metabolic data across a range of resting states: between basal and standing. However, it remained unclear whether that same mass exponent could be applied during greater metabolic

intensities (exercise states).

During exercise, the increase in oxygen consumption is primarily driven by the skeletal muscles (~40% body mass). The magnitude of that increase varies with exercise mode, and is primally determined by whether or not the body mass is supported. In this, and all subsequent research phases, an upright posture was used with the body mass wholly supported by each participant. This changes the dynamic of the scaling relationship, which, during resting states, is predominately determined by the organs (~6% body mass). To explore the impact of exercise on the scaling relationship, participants were tested during steady-state walking (15 min; 4.8km.h^{-1}; 0% gradient) and peak-exercise (ramp treadmill test to volitional exhaustion) conditions (Chapter 3). Besides a difference in metabolic intensity, those two states presented an additional variable that might have affected the scaling relationship. Since it was possible that a size relationship would be evident during the fixed-velocity walking, whereby smaller individuals would have to work at a higher relative intensity to maintain the same walking pace. While some studies have explored scaling during both of these intensities (Rogers *et al.,* 1995; Markovic *et al.,* 2007), they suffered due to both sample size and standardisation limitations. Therefore, it was uncertain how the scaling relationship would be effected by those two exercise states.

As predicted, both regressions remained significantly non-linear and scaled by a greater mass exponent than those observed during the resting states (Chapter 2). Thus, it was confirmed that human metabolism can be scaled by a non-linear power regression throughout the physiological range of metabolic intensities. However, there was no significant difference in the mass exponent between the two exercise conditions, neither was there any evidence of a size-dependent interaction during the fixed-velocity walking. Since those two states were considered to lie at either end of the exercise-intensity range, it was concluded that a uniform mass exponent could be used to scale oxygen consumption during all ambulatory exercise. Of the two exponents observed, the peak-exercise value was selected for this purpose (mass$^{0.80}$). That value was chosen as it represented the maximal metabolic rate, and thus the upper limit for human scaling without the influence of an additional variable. It

appears that, while skeletal muscle recruitment (resting to exercise) results in a modified mass exponent, once exercising, additional recruitment of motor units does not significantly change the mass exponent. This outcome meant that the entire physiological range of metabolic intensity could be described using two mass exponents: $mass^{0.54}$ for resting states and $mass^{0.80}$ for exercising states.

In the next experimental phase (Chapter 4), the fixed-velocity theme was extended to encompass gradient walking (5% and -5%; 4.8 $km.h^{-1}$; 15-min stages) as both are known to modify oxygen consumption and in opposite directions (Minetti *et al.,* 1993; Johnson *et al.,* 2002). It was anticipated that the effect of gravity on absolute oxygen consumption would result in a metabolic-intensity-specific change to the mass exponent: increasing during uphill walking and decreasing during downhill walking. Nevertheless, no change to the mass exponent was observed with a change in ambulatory gradient. Despite that outcome, a relationship between body mass and downhill walking energy expenditure was still observed. Between level and downhill gradients, oxygen consumption decreased by a significantly greater percentage among the heavier individuals. This was an unanticipated novel finding, and was postulated to be a passive response related to a greater eccentric pre-stretch due to heavier impact forces among the larger individuals (Abe *et al.,* 2008). This theme was further explored with load carriage in Chapter 5, however, a 25-kg increase in total mass (body mass or load carriage) was not sufficient to induce the same response (Figure 5.8), and it remains unknown whether the carriage of heavier loads would demonstrate the same pre-stretch response.

The effect of an overall body-mass change (load carriage) on the scaling relationship was next explored (Chapters 5 and 6). It was anticipated that the mass exponent was more likely to change from loading with a fixed-mass than a relative load (*i.e.,* 10% body mass), and the former option was tested to determine the greater possible impact of load carriage on the scaling model. Since oxygen consumption increases proportionally with the mass change during load carriage (Taylor *et al.,* 1980), it was expected that lighter individuals would experience a greater relative metabolic strain, resulting in a reduced mass exponent, a flatter regression slope, and thus the requirement for a unique mass exponent during load-carriage states.

This relationship was explored during torso (25-kg weighted vest: Chapter 5) and distally-placed loads (1.38-kg helmet; 2-kg wrist weights [each arm]; 2-kg boots and ankle weights [each foot]: Chapter 6). Due to the greater postural demands (Hellebrandt *et al.,* 1944; Kinoshita, 1985; Attwells *et al.,* 2006) and an increased moment of inertia of distal load carriage (Cavagna and Kaneko 1977; Browning *et al.,* 2007), a greater metabolic response per kilogram of load carried was expected at those locations (Soule and Goldman, 1969; Martin, 1985; Taylor *et al.,* 2012). Since, this would increase oxygen consumption disproportionately from that of the unloaded or torso-loaded conditions, there was the potential for each load location to scale by a unique regression equation, and thus different mass exponents. To test those hypotheses, oxygen consumption data were collected for each load condition during a 15-min steady-state walking stage at 4.8 $km.h^{-1}$ at three walking gradients (5%, 0%, -5%).

Load carriage significantly decreased the body-mass exponent when participants were loaded at the torso and feet (Figure 5.6; Table 6.2; Figure 6.4; $P<0.05$), but not for the other two locations. That was most likely because the lighter masses carried at those locations (head: 1.38 kg; hands: 4 kg total) did not generate a significant mass-dependent change in nett oxygen consumption. The reduced body-mass exponents observed during torso and foot loading did not differ between those two locations (Table 6.2; Figure 6.4; $P>0.05$), highlighting the increased metabolic loading with distally carried loads. However, this indicated a potential for a variable effect of loading per kilogram of mass added depending upon the load location and potentially its mass. It would be of interest to retest the effect of distal loading carrying greater and uniform-mass loads.

A successful method used to overcome the effect of load carriage on the scaling relationship was to scale those data against total mass (body mass and all external loads), rather than body mass alone. As a result, the physiological strain associated with supporting and carrying that total mass was accounted for during the scaling process. Indeed, when scaling against total mass, a statistically uniform mass exponent was observed for all but two testing conditions ($mass_{total}^{0.80}$; Figure 6.4), where downhill walking with loads carried on the head or feet scaled against a

significantly smaller exponent ($mass_{total}^{0.66}$; $P < 0.05$). This meant that within the mass ranges tested, a proportional relationship between oxygen consumption and the change in total mass was observed for most conditions (whether from growth [an increase in body mass] or external load carriage). It was anticipated that during downhill walking, loading at the head and feet may promote size-dependent changes to the gait cycle *i.e.* a greater hip extension (Leroux *et al.,* 2002; Kimel-Noar *et al.,* 2017) and stride length (Minetti *et al.,* 1993; Sheehan and Gottschall, 2012), that could have resulted in the improved walking economy observed among the larger participants, and thus, the smaller mass exponent. Consequently, oxygen consumption collected during exercise states could be scaled and normalised using either of two mass exponents providing that the morphometric scaling variable is total mass. It is important to consider that this relationship is dependent on a proportional increase in nett oxygen consumption with the load carried, and therefore may not be appropriate during heavier load carriage at those locations and has been demonstrated to change in some downhill walking conditions.

An exception to using that bipedal, total-mass exponent would be during peak exercise (running), whether unloaded or loaded. While load carriage limits physical performance, reducing both time to exhaustion, running velocity and maximal acceptable work duration, it does not change the maximal rate of oxygen consumption within the body (Taylor *et al.,* 2012; Lee *et al.*, 2013; Peoples *et al.,* 2016; Hingley *et al.,* 2017). For this reason, the additional load being carried by the body does not need to be considered during the scaling process, for the rate of oxygen consumption is determined internally by the cardio-respiratory system (Saltin and Strange, 1992). Accordingly, $mass_{body}^{0.80}$, rather than $mass_{total}^{0.80}$, should be used to scale peak oxygen consumption, regardless of the external loads carried.

In summary, the scaling relationship between oxygen consumption and body mass in humans is non-linear across the physiological range of metabolic intensity. The value of that exponent is intensity and load specific. However, it is possible to scale metabolic data against one of four mass exponents: $mass_{body}^{0.54}$ (rest), $mass_{total}^{0.80}$ (steady-state exercise), $mass_{total}^{0.66}$ (head- or foot-loaded downhill walking) and $mass_{body}^{0.80}$ (peak exercise).

7.1.1 CONCLUDING REMARKS

From this series of experiments, seven novel conclusions have emerged:

(i) In adult men, absolute oxygen consumption scales by a non-linear, allometric regression against body mass throughout the physiological range of unloaded metabolic intensity (basal to peak exercise: $mass_{body}^{exponent}$).

(ii) During unloaded and loaded resting states, from basal (supine) through to standing (rest), the relationship between oxygen consumption and body mass in adult men can be described using a single scaling exponent: $mass_{body}^{0.54}$.

(iii) During level and uphill steady-state walking, the relationship between oxygen consumption and body mass in adult men can be described using a single scaling exponent: $mass_{total}^{0.80}$. That total-mass exponent is applicable during both unloaded and loaded states (1.38-kg helmet; 25-kg weighted vest; 2-kg wrist weights [each wrist]; 2 kg each foot) and is anticipated to remain suitable to scale oxygen consumption during all loading conditions, providing that the relationship between oxygen consumption and total mass change remains proportional.

(iv) During downhill steady-state walking, the relationship between oxygen consumption and body mass in adult men can be described using either of two scaling exponent: $mass_{total}^{0.80}$ or $mass_{total}^{0.66}$. The former is applicable during walking while unloaded and loaded at the hands (2 kg each wrist) or torso (25-kg weighted vest), where the increase in oxygen consumption remains proportional to the total mass change. The latter is applicable during head- (1.38-kg helmet) and foot-loaded (2 kg each foot) walking, and indicates the presence of an energy-saving mechanism with an increase in total mass. It is yet to be determined how these responses may change with a greater increase in the total mass carried (heavier loads).

(v) During level and uphill walking, there was no difference in the increase in oxygen consumption with an increase in total mass, whether that was from growth or external loading. Accordingly, by scaling oxygen consumption against total mass, both unloaded and loaded conditions could be described using the same exponent:

$mass_{total}^{0.80}$. This confirmed two underlying principles: that oxygen consumption increases proportionally with a change in total mass and that the cost of mechanical work remains constant with an increase in mass, regardless of its composition.

(vi) During unloaded and loaded peak exercise, the relationship between oxygen consumption and body mass in adult men can be described using a single scaling exponent: $mass_{body}^{0.80}$. A body-mass exponent should be used for this metabolic intensity, as peak oxygen consumption is not modified by an increase in total mass, but by the cardio-respiratory system.

(vii) Per kilogram of added mass, the metabolic cost of load carriage (loaded less unloaded, divided by the mass of the load) remained constant with a change in body mass for all load locations tested (torso, hands and feet) except for the head, within which a gradient effect was observed.

7.2 FUTURE RESEARCH RECOMMENDATIONS

7.2.1 The effect of heavy load carriage on the scaling relationship between oxygen consumption and body mass in adult humans

Throughout this series of investigations (Chapters 2-6) it was established that in humans oxygen consumption scales by a non-linear, allometric regression against body mass. During steady-state ambulation, the shape (mass exponent) of that scaling relationship was significantly modified by fixed-mass load carriage (25-kg weighted vest: Chapter 5; $P < 0.05$), whereby oxygen consumption increased relative to the change in total mass: reducing the body-mass exponent compared with unloaded walking. Thus, supporting the observations of previous researchers and applying those findings to a human scaling context (Goldman and Iampietro, 1962; Taylor *et al.,* 1980; Taylor *et al.,* 2016). However, that scaling outcome highlighted the requirement for a unique body-mass exponent to describe oxygen consumption during loaded ambulation ($mass_{body}^{0.64}$: Chapter 5).

Fortunately, it was possible to minimise the effect of load carriage on the scaling relationship by changing the morphometric scaling variable used from body mass to

the total mass carried (body mass and all external loads), in this way both unloaded and loaded ambulation could be described using the same mass exponent ($mass_{total}^{0.80}$: Chapter 5). This finding confirmed the underlying principle that the mechanical cost of work remained constant per kilogram of mass carried, regardless of its composition, as has also been observed by others (Heglund, 1979; Taylor *et al.,* 1980; Halsey and White, 2017).

Nevertheless, during heavy, military-specific load carriage, oxygen consumption increases at a disproportionately faster rate. This has been reported with loads greater than 45 kg during standing (Phillips *et al.,* 2016) and is estimated to occur once loads reach 40-50% of body mass during walking (Renbourn, 1954; Schoenfeld *et al.,* 1978; Maloiy *et al.,* 1986), ~30 kg assuming a mean body mass of 81.2 kg (present sample mean). Accordingly, it is possible to extend the findings from this experimental series to determine whether or not heavier load carriage can be scaled using the same total-mass exponent as established for unloaded and loaded walking tested within this project ($mass_{total}^{0.80}$: Chapters 5). It is important to determine whether or not this inflexion point exists within a useable load range, for, if it does, then loads above that value will scale against a unique mass exponent. This is an important consideration for occupational testing, for example in a military setting, where such values could be used to determine cut scores for physical employment standards and the application of an incorrect scaling exponent could lead to spurious results.

To perform such an evaluation, participants would complete five experimental trials split across two laboratory visits. In the first laboratory visit, subjects would complete four, 15-min steady-state walks on a treadmill at 4.8 $km.h^{-1}$ (0%), with 5-min rest between stages. During each stage, subjects would wear a balanced, weighted vest at one of five masses: 25 kg, 35 kg, 40 kg, 45 kg and 50 kg. This mass range would increase the load carriage starting at ~50% body mass of the smallest individual through to ~50% body mass of the heaviest individual. The lightest mass (25 kg) would act as a control, to confirm whether or not the exponent established matched that observed in Chapter 5 ($mass_{total}^{0.80}$). All load and visit orders would be balanced using a Latin Square Design. Oxygen consumption (open-circuit, indirect

respirometry) and cardiac frequency (ventricular depolarisation) would be assessed during steady-state walking, wearing the range of heavy, external loads. To maintain consistency when establishing a new mass exponent, the sample tested must satisfy the same inclusion criteria applied in the current project (Section 2.2.1): sample size between 50 and 75, male, 18-30 y, 2-fold mass range, physically active, relative adiposity less than 88 mm. In addition, the regression shape should be systematically evaluated using the steps outlined in the decision-making flow chart (Figure 2.8) to ensure that it is appropriately assessed. It is expected that the total-mass exponent will significantly decrease during heavy-load carriage, similar to the effect of load carriage on the body-mass exponent (Chapter 5).

7.2.2 The effect of steep gradients on the scaling relationship during unloaded and loaded steady-state walking

The outcomes in Chapters 4 and 5 revealed no covariant effect of gradient for the non-linear scaling relationship between oxygen consumption and body mass in adult men. Accordingly, within a $\pm 5\%$ gradient range, ambulatory oxygen consumption could be scaled using the same mass exponent for both unloaded (Chapter 4) and loaded conditions (Chapter 5; $mass_{total}^{0.80}$). Thus, the increase in oxygen consumption remained proportional with a change in total mass regardless of the tissue type; demonstrating a constant mechanical cost of walking and purely vertical movement (unloaded [Chapter 4]: 1.40 $mL.kg^{-1}.m^{-1}$ [± 0.03]; loaded [Chapter 5]: 1.37 $mL.kg^{-1}.m^{-1}$ [± 0.03]; $P > 0.05$), per kilogram of total mass. These observations were consistent with those of previous researchers (constant mechanical cost of walking: Goldman and Iampietro, 1962; Heglund, 1979; Taylor *et al.,* 1980; constant cost of purely vertical movement: Dill, 1965; Taylor *et al.,* 1970; Cohen *et al.,* 1978).

Based on these observations, a logical follow-up study would be to explore the effect of a steeper ambulatory gradient on the scaling exponent, as the relationship between oxygen consumption and the gradient slope is not constant (Minetti *et al.,* 1993; Johnson *et al.,* 2002). In a similar way that fixed-mass load carriage resulted in a mass-dependent change in relative oxygen consumption in Chapter 5, across an animal mass range (30-g mouse to 1000-kg horse), Taylor and his colleagues (1970)

observed that the metabolic response to uphill ambulation produces a similar mass-dependent response: where oxygen consumption was significantly increased in the (large) horse but not the (small) mouse ($P<0.05$). Accordingly, it is possible that within the human mass range, providing the stimulus was sufficient (for example, a steeper ambulatory gradient), a similar response might be observed, thus changing the scaling exponent. Understanding this relationship and the potential impact on the mass exponent will inform how metabolic data are scaled beyond a $\pm 5\%$ ambulatory gradient range.

Furthermore, in Chapter 4, between level and downhill walking, oxygen consumption decreased by a greater amount in the heaviest individuals, compared with the lightest (Figure 4.3; $P<0.05$). This was, at least in part, attributed to a greater pre-stretch load among the heavier individuals, that in turn, increased the energy transferred after the eccentric muscle activation during the gait cycle. While that response was not reproducible across a 25-kg mass range during walking at a -5% gradient (Chapter 5), it is possible that the increased effect of gravity during a steeper descent might generate a similar pre-stretch stimulus to a wider mass range at a shallower grade. By further exploring this research theme, it would be possible to determine a threshold mass range for the onset of this mass-dependent response during downhill walking. Such information could be used to generate work rates during a prescriptive downhill rehabilitation or when predicting work tolerance times during downhill ambulation.

To explore these relationships, a controlled sample suitable for scaling analyses should be used (Section 2.2.1). Participants would complete six, 15-min unloaded treadmill walks, with 5-min rest between gradient conditions: -15%, -10%, -5%, 5%, 10% and 15%. Beyond a $\pm 15\%$ gradient, the relationship between that positive and negative work of walking does not change (Minetti *et al.,* 1993). Oxygen consumption would be measured continuously throughout all tests using open-circuit respirometry and sampled in the last 5-min of each stage. In this way, the relationship between body mass and the effect of gravity can be explored across a realistic gradient range. Following the analyses steps outlined in Figure 2.8, the shape of each regression would be established before comparing the effect of a gradient change on the mass exponent using analysis of covariance.

A sub-sample of participants would also complete a secondary (loaded) investigation on a separate laboratory visit, whereby the 10 lightest and 10 heaviest participants would complete two downhill walks at each gradient, wearing a 35-kg and 45-kg weighted vest. Those data would also be compared against two matched, mass-range samples (each 10 participants). Using two-way factorial analysis of variance, it would be possible to determine whether or not a threshold for that metabolic mass response during downhill walking exists within that total mass range.

7.2.3 The effect of non-locomotive exercise on the scaling relationship between oxygen consumption and body mass

From this series of investigations (Chapters 2-6) three scaling models have been established to describe the relationship between oxygen consumption and body mass throughout the physiological range of metabolic intensity (basal [supine] to peak exercise [running]): $mass_{body}^{0.54}$ (rest: Chapter 2), $mass_{total}^{0.80}$ (steady-state walking: Chapters 3-6), $mass_{body}^{0.80}$ (peak exercise: Chapter 3). Accordingly, the scaling relationship during resting and bipedal exercising states has been thoroughly explored.

Based on these findings, the next logical progression would be to explore the scaling relationship during non-weight-bearing exercise. During such conditions, the effect of mass carriage is removed from the scaling outcome, thus modifying the nature of the work performed. While, it has been suggested that a scaling exponent of $mass_{body}^{0.67}$ should be used to scale such data (Vanderburgh *et al.,* 1998; Markovic and Jaric, 2004), this is an arbitrary number selected based on the relationship between cross-sectional area and power (Maughan *et al.,* 1983) that has not been directly validated for scaling purposes. Moreover, it is important to consider the possibility that scaling any submaximal work using a unit that describes potential power output is similar to describing metabolic rate against lean body mass (Chapter 3). Using that method, only the active tissues are considered and they are assumed to be working at their full capacity during all metabolic intensities. Therefore, this unit might not be appropriate to describe oxygen consumption during non-weight-bearing exercise. The importance of using the appropriate scaling exponent has been demonstrated within this series of

investigations (Chapters 2-6), whereby a small change to the scaling exponent value can result in spurious results when predicting and normalising metabolic data. As non-weight-bearing exercise modalities are commonly used during metabolic testing in a research and athletic setting, it would now be important to extend this research theme to such exercise modalities.

Accordingly, to explore this research theme, steady-state oxygen consumption would be collected in participants spanning a wide body-mass range, but who were otherwise controlled for morphological and physiological variables that might influence oxygen consumption (see Section 2.2.1). Across two laboratory visits, subjects would be tested while exercising during five exercise modes: level treadmill walking, zero-gravity treadmill, cycle (ergometer), rowing (ergometer) and a swimming (flume). Within each condition, participants would complete two, 15-min steady-state trials. The first matched for relative intensity (percentage peak oxygen consumption) across the three exercise modes, the second matched for external work rate. By using the level walking trial as a control condition that could be validated against the scaling outcome in Chapter 3, it would be possible to identify whether or not a uniform mass exponent is appropriate for both relative and fixed work rate metabolic intensities, and whether or not it is influenced by a change in exercise mode. Due to the observed relationships between total mass and oxygen consumption, whereby the mass exponent was elevated during weight bearing conditions, it is anticipated that, compared with the present investigations (Chapters 2-6), during non-weight bearing exercise a mass exponent between basal and exercising conditions will be most appropriate.

Accordingly, during this experimental series (Chapters 2-6), it has been established that oxygen consumption scales by a non-linear, allometric regression against body mass in adult men. This relationship has been investigated across the physiological range of resting and bipedal metabolic intensity, from basal (supine) through to peak exercise (running). Across that range of metabolic intensity, it is possible to describe oxygen consumption measured during the 18 separate trials (Figure 1.2 [p.9]) using just three scaling exponents: for unloaded and loaded resting states between basal (supine) and standing (rest), $mass_{body}^{0.54}$; during unloaded and loaded steady-state

walking, across a $\pm 5\%$ gradient range, $mass_{total}^{0.80}$; and during peak exercise (running), $mass_{body}^{0.80}$. With these three proposed studies, it would be possible to confidently include the application of this work to steady-state walking while carrying a heavy load (>30 kg), at steep ambulatory gradients ($\leq \pm 15\%$) and during a range of non-weight-bearing exercise modes.

7.3 REFERENCES

Abe, D., Muraki, S., and Yasukouchi, A. (2008). Ergonomic effects of load carriage on the upper and lower back on metabolic energy cost of walking. *Applied Ergonomics*. 39(3):392-398.

Attwells, R.L., Birrell, S.A., Hooper, R.H., and Mansfield, N.J. (2006). Influence of carrying heavy loads on soldiers' posture, movements and gait. *Ergonomics*. 49(14):1527-1537.

Australian Bureau of Statistics. (2012). *4338.0 - Profiles of Health, Australia: Physical Measurements*. Australian Bureau of Statistics, Canberra.

Browning, R.C., Modica, J.R., Kram, R., and Goswami, A. (2007). The effects of adding mass to the legs on the energetics and biomechanics of walking. *Medicine and Science in Sports and Exercise*. 39(3):515-525.

Buchholz, A.C., Rafii, M., and Pencharz, P.B. (2001). Is resting metabolic rate different between men and women? *British Journal of Nutrition*. 86(6):641-646.

Cavagna, G.A., and Kaneko, M. (1977). Mechanical work and efficiency in level walking and running. *The Journal of Physiology*. 268(2):467-481.

Clarys, J.P., Martin, A.D., Drinkwater, D.T., and Marfell-Jones, M.J. (1987). The skinfold: Myth and reality. *Journal of Sports Sciences*. 5(1):3-33.

Cohen, Y., Robbins, C.T., and Davitt, B.B. (1978). Oxygen utilization by elk calves during horizontal and vertical locomotion compared to other species. *Comparative Biochemistry and Physiology--Part A: Physiology*. 61(1):43-48.

Darowski, A., Weinberg, J.R., and Guz, A. (1991). Normal rectal, auditory canal, sublingual and axillary temperatures in elderly afebrile patients in a warm environment. *Age and Ageing*. 20(2):113-119.

Darveau, C.A., Suarez, R.K., Andrews, R.D., and Hochachka, P.W. (2002). Allometric cascade as a unifying principle of body mass effects on metabolism. *Nature*. 417(6885):166-170.

Dill, D.B. (1965). Oxygen used in horizontal and grade walking and running on the treadmill. *Journal of Applied Physiology*. 20(1):19-22.

Dodds, P.S., Rothman, D.H., and Weitz, J.S. (2000). Re-examination of the" 3/4-law" of metabolism. *Journal of Thermal Biology*. 209:9-27.

Goldman, R.F., and Iampietro, P.F. (1962). Energy cost of load carriage. *Journal of Applied Physiology*. 17(4):675-676.

Green, S.B. (1991). How many subjects does it take to do a regression analysis. *Multivariate Behavioral Research*. 26(3):499-510.

Halsey, L.G., and White, C.R. (2017). A different angle: comparative analyses of whole-animal transport costs when running uphill. *Journal of Experimental Biology*. 220(2):161-166.

Harris, J.A., and Benedict, F.G. (1919). *A Biometric Study of Basal Metabolism in Man*. Carnegie Institution, Washington.

Harris, R.J. (1985). *A primer of multivariate statistics*. Academic Press, New York.

Heglund, N.C. (1979). *Size scaling, speed and the mechanics of locomotion*. (Doctoral dissertation). Harvard University.

Hellebrandt, F.A., Brogdon, E., and Tepper, R.H. (1940). Posture and its cost. *American Journal of Physiology - Legacy Content*. 129:773-781.

Hingley, L., Caldwell, J.N., Taylor, N.A.S., and Peoples, G.E. (2017). Thoraco-pulmonary mechanical perturbations accompanying thoracic loading. *Proceedings of the Australian Physiological Society*. 48:114P

Jensen, K., Johansen, L., and Secher, N.H. (2001). Influence of body mass on maximal oxygen uptake: effect of sample size. *European Journal of Applied Physiology*. 84(3):201-205.

Johnson, A.T., Benjamin, M.B., and Silverman, N. (2002). Oxygen consumption, heat production, and muscular efficiency during uphill and downhill walking. *Applied Ergonomics*. 33(5):485-491.

Kimel-Naor, S., Gottlieb, A., and Plotnik, M. (2017). The effect of uphill and downhill walking on gait parameters: a self-paced treadmill study. *Journal of Biomechanics*. 60:142-149.

Kinoshita, H. (1985). Effects of different loads and carrying systems on selected biomechanical parameters describing walking gait. *Ergonomics*. 28(9):1347-1362.

Lee, J.Y., Bakri, I., Kim, J.H., Son, S.Y., and Tochihara, Y. (2013). The impact of firefighter personal protective equipment and treadmill protocol on maximal oxygen uptake. *Journal of Occupational and Environmental Hygiene*. 10(7):397-407.

Leroux, A., Fung, J., and Barbeau, H. (2002). Postural adaptation to walking on inclined surfaces: I. Normal strategies. *Gait and Posture*. 15(1):64-74.

Maloiy, G.M.O., Heglund, N.C., Prager, L.M., Cavagna, G.A., and Taylor, C.R. (1986). Energetic cost of carrying loads: have African women discovered an economic way? *Nature*. 319(6055):668-669.

Markovic, G., and Jaric, S. (2004). Movement performance and body size: the relationship for different groups of tests. *European Journal of Applied Physiology*. 92(1-2):139-149.

Markovic, G., Vucetic, V., and Nevill, A.M. (2007). Scaling behaviour of in athletes and untrained individuals. *Annals of Human Biology*. 34(3):315-328.

Maughan, R.J., Watson, J.S., and Weir, J.D.V. (1983). Strength and cross sectional area of human skeletal muscle. *The Journal of Physiology*. 338(1):37-49.

Martin, A.D., Ross, W.D., Drinkwater, D.T., and Clarys, J.P. (1985). Prediction of body fat by skinfold caliper: assumptions and cadaver evidence. *International Journal of Obesity*. 9:31-39.

Minetti, A.E., Ardigo, L.P., and Saibene, F. (1993). Mechanical determinants of gradient walking energetics in man. *The Journal of Physiology*. 472(1):725-35.

Mitchell, H.H. (1962). *Comparative Nutrition of Man and Domestic Animals*. Volume 1. Academic Press, New York. Pp. 3–90.

Müller, M.J., Langemann, D., Gehrke, I., Later, W., Heller, M., Glüer, C.C., Heymsfield, S.B., and Bosy-Westphal, A. (2011). Effect of constitution on mass of individual organs and their association with metabolic rate in humans—a detailed view on allometric scaling. *PloS one*. 6(7):e22732.

Peoples, G.E., Lee, D.S., Notley, S.R., and Taylor, N.A.S. (2016). The effects of thoracic load carriage on maximal ambulatory work tolerance and acceptable work durations. *European Journal of Applied Physiology*. 116(3):635-646.

Phillips, D.B., Ehnes, C.M., Stickland, M.K., and Petersen, S.R. (2016). The impact of thoracic load carriage up to 45 kg on the cardiopulmonary response to exercise. *European Journal of Applied Physiology*. 116(9):1725-1734.

Renbourn, E.T. (1954). The knapsack and pack: an historical and physiological survey with particular reference to the British soldier. *Journal of the Royal Army Medical Corps*. 100(2):77-88.

Rogers, D.M., Olson, B.L., and Wilmore, J.H. (1995). Scaling for the $\dot{V}O_2$-to-body size relationship among children and adults. *Journal of Applied Physiology*. 79(3):958-967.

Ross, W.D., and Wilson, N.C. (1974). A stratagem for proportional growth assessment. *Acta Paediatrica Belgica.* 28, 169-182.

Saltin, B., and Strange, S. (1992). Maximal oxygen uptake:" old" and" new" arguments for a cardiovascular limitation. *Medicine and Science in Sports and Exercise*. 24(1):30-37.

Sarrus, F., and Rameaux, J.F. (1839). Mathématique appliquée à la physiologie. *Bulletin de l'Academie Royale de Medicine de Paris*. 3:1094-100.

Savage, V.M., Gillooly, J.F., Woodruff, W.H., West, G.B., Allen, A.P., Enquist, B. J., and Brown, J.H. (2004). The predominance of quarter power scaling in biology. *Functional Ecology*. 18(2):257-282.

Schofield, W.N. (1985). Predicting basal metabolic rate, new standards and review of previous work. *Human Nutrition. Clinical Nutrition*. 39C(S1):5-41.

Sheehan, R.C., and Gottschall, J.S. (2012). At similar angles, slope walking has a greater fall risk than stair walking. *Applied Ergonomics*. 43(3):473-478.

Sieg, A.E., O'Connor, M.P., McNair, J.N., Grant, B.W., Agosta, S.J., and Dunham, A.E. (2009). Mammalian metabolic allometry: do intraspecific variation, phylogeny, and regression models matter? *The American Naturalist*. 174(5):720-733.

Solomon, S.J., Kurzer, M.S., and Calloway, D.H. (1982). Menstrual cycle and basal metabolic rate in women. *The American Journal of Clinical Nutrition*. 36(4):611-616.

Soule, R.G., and Goldman, R.F. (1969). Energy cost of loads carried on the head, hands, or feet. *Journal of Applied Physiology*. 27(5):687-690.

Sund Levander, M., Forsberg, C., and Wahren, L.K. (2002). Normal oral, rectal, tympanic and axillary body temperature in adult men and women: a systematic literature review. *Scandinavian Journal of Caring Sciences*. 16(2):122-128.

Taylor, C.R., Heglund, N.C., McMahon, T.A., and Looney, T.R. (1980). Energetic cost of generating muscular force during running. *Journal of Experimental Biology*. 86(1):9-18.

Taylor, C.R., Schmidt-Nielsen, K., and Raab, J.L. (1970). Scaling of energetic cost of running to body size in mammals. *American Journal of Physiology*. 219(4):1104-1107.

Taylor, N.A.S, Lewis, M.C., Notley, S.R., and Peoples, G.E. (2012). A fractionation of the physiological burden of the personal protective equipment worn by firefighters. *European Journal of Applied Physiology*. 112(8):2913-2921.

Taylor, N.A.S., Peoples, G.E., and Petersen, S.R. (2016). Load carriage, human performance, and employment standards. *Applied Physiology, Nutrition, and Metabolism*. 41(6):S131-S147.

Taylor, N.A.S., Tipton, M.J., and Kenny, G.P. (2014). Considerations for the measurement of core, skin and mean body temperatures. *Journal of Thermal Biology*. 46:72-101.

Tzankoff, S.P., and Norris, A.H. (1977). Effect of muscle mass decrease on age-related BMR changes. *Journal of Applied Physiology: Respiratory, Environmental and Exercise Physiology*. 43(6):1001-1006.

Vanderburgh, P.M. (1998). Two important cautions in the use of allometric scaling: the common exponent and group difference principles. *Measurement in Physical Education and Exercise Science*. 2(3):153-163.

Van Voorhis, C.W., and Morgan, B.L. (2007). Understanding power and rules of thumb for determining sample sizes. *Tutorials in Quantitative Methods for Psychology*. 3(2):43-50.

Webb, P. (1986). 24-hour energy expenditure and the menstrual cycle. *American Journal of Clinical Nutrition*. 44(5):614-619.

Weir, J.D.V. (1949). New methods for calculating metabolic rate with special reference to protein metabolism. *The Journal of Physiology*. 109(1-2):1-9.

White, C.R., Blackburn, T.M., and Seymour, R.S. (2009). Phylogenetically informed analysis of the allometry of mammalian basal metabolic rate supports neither geometric nor quarter power scaling. *Evolution: International Journal of Organic Evolution*. 63(10):2658-2667.

White, C.R., Cassey, P., and Blackburn, T.M. (2007). Allometric exponents do not support a universal metabolic allometry. *Ecology*. 88(2):315-323.

White, C.R., and Seymour, R.S. (2003). Mammalian basal metabolic rate is proportional to body mass$^{2/3}$. *Proceedings of the National Academy of Sciences*. 100(7):4046-4049.

White, C.R., and Seymour, R.S. (2004). Does basal metabolic rate contain a useful signal? Mammalian BMR allometry and correlations with a selection of physiological, ecological, and life-history variables. *Physiological and Biochemical Zoology*. 77(6):929-941.